Understanding the kinetic profile of phosphatidylinositol-specific phospholipase C from Listeria monocytogenes

Author: Wei Chen

Boston College

The Graduate School of Arts and Sciences

Department of Chemistry

UNDERSTANDING THE KINETIC PROFILE OF PHOSPHATIDYLINOSITOL-SPECIFIC PHOSPHOLIPASE C FROM *LISTERIA MONOCYTOGENES*

a dissertation

by

WEI CHEN

submitted in partial fulfillment of the requirements

for the degree of

Doctor of Philosophy

September, 2008

Understanding the kinetic profile of phosphatidylinositol-specific phospholipase C from *Listeria monocytogenes*

by Wei Chen

Under the direction of Dr. Mary F. Roberts

Abstract

The phosphatidylinositol-specific phospholipase C (PI-PLC) from *Listeria monocytogenes* (a monomer in solution) shows unusual kinetic properties compared to other well-studied phospholipases: (i) increased specific activity with decreasing protein concentration, (ii) activation of the phosphotransferase step by salts, and (iii) activation of both the interfacial phosphotransferase and water-soluble phosphodiesterase steps by zwitterionic and neutral amphiphiles. A variety of biophysical studies (fluorescence, NMR, monolayer, vesicle binding) of enzyme/lipid complexes coupled with kinetics have allowed us to propose a model that accounts for these features. The enzyme binds tightly to anionic surfaces and much more weakly to a zwitterionic interface. The tight binding can be reduced by adding KCl at concentrations that activate the enzyme. In the crystal structure of the enzyme, many basic residues are clustered on the sides and bottom of TIM-barrel far away from the opening to the active site. These cause the enzyme to adopt

a non-productive orientation on negatively charged membranes that leads to a reversible clustering of anionic lipids and vesicle aggregation. An increased surface concentration of zwitterionic / neutral amphiphiles along with the salt disperses the anionic substrate, shields charges on the protein, and enhances productive encounters of the protein with substrate molecules. This model has been tested by examining the behavior of enzyme with citraconylated lysines and mutants of neutral surface residues at the rim of the active site. The unusual kinetic behavior of this PI-PLC also appears to contribute to the escape of *L. monocytogenes* from vacuoles during infection.

this dissertation is dedicated to

my husband: Zhenhua Sun and my son: Herbert Chen Sun

Acknowledgements

First and foremost, I would like to thank my advisor, Prof. Mary F. Roberts, for her guidance and support throughout my Ph.D. research. Her constant encouragement and great confidences in me have advanced my research progress. Her extraordinary personality made my graduate studies enjoyable and memorable.

I would like to thank the following for their contribution in this work. Prof. Howard Goldfine at University of Pennsylvania generously provided me with pDP1462 and pBS1462 plasmids and checked the infectivity of the F237W by plaque formation assay. Prof. Wonhwa Cho at University of Illinois checked binding of *L. monocytogens* PI-PLC with SUVs by monolayer study.

I would like to thank all members of the Prof. Roberts' group, the present and the past, for their friendship and helpful discussions. I would like to give special thanks to Dr. Hongying Yang and Dr. Jianwen Feng for their guidance in my research.

I would like to thank Prof. Evan Kantrowitz, Prof. Larry McLaughlin, Prof. Shana O. Kelley, and their group members for their generously letting me use many of their laboratory equipments and their kind help. I would like to thank Dr. John Boylan for the help on NMR.

Finally, I am grateful to my parents, my brother, especially to my husband for the love, understanding, encouragement and support. My son, although only 4 months, does bring me lots happiness, and I would like to thank him too.

Abbreviations

β-BODIPY FL C_5-HPC	2-(4,4-difluoro-5,7-dimethyl-4-bora-3a,4a-diaza-s-indacene-3-pentanoyl)-1-hexadecanoyl-*sn*-glycero-3-phosphocholine
β-Pyr-C_{10}-PG	1-hexadecanoyl-2-(1-pyrenedecanoyl)-*sn*-glycero-3-phosphoglycerol
APG	p-azidophenyl glyoxal monohydrate
B. cereus	*Bacillus cereus*
B. thuringiensis	*Bacillus thuringiensis*
BSA	bovine serum albumin
C2	protein kinase C conserved region 2
CBD	chitin binding domain
CD	circular dichroism
CDC	cell division cycle
cIP	D-*myo*-inositol 1,2-cyclic phosphate
CMC	critical micelle concentration
$cPLA_2$	cytosolic phospholipase A_2
CPM	7-diethylamino-3-(4'-maleimidylphenyl)-4-methylcoumarin
CPP	critical packing parameter
DAG	diacylglycerol
dam	DNA-[N^6-adenine] methyltransferase
DC	dendritic cell
diC_4PI	dibutyroylphosphatidylinositol
diC_6PC	dihexanoylphosphatidylcholine
diC_7PC	diheptanoylphosphatidylcholine
DMS	dimethyl suberimidate·2HCl)
DMSO	dimethyl sulfoxide

DOPMe	1,2-dioleoyl-*sn*-glycero-3-phosphatidylmethanol
DTT	dithiothreitol
E. coli	*Escherichia coli*
EDC	1-ethyl-3-[3-dimethylaminopropyl]carbodiimide hydrochloride
EF	elongation factor
excimer	excited-state dimer
FCS	fluorescence correlation spectroscopy
FRET	fluorescence resonance energy transfer
GAP	GTPase-activating protein
GEF	guanine nucleotide exchange factor
GLV	giant unilamellar vesicles
GPI	glycosylphosphatidylinositol
HEPES	4-(2-hydroxyethyl)-1-piperazineethanesulfonic acid
I-1-P	D-*myo*-inositol 1-phosphate
IEF	isoelectric focusing
IP_3	inositol-1,4,5-triphosphate
IPG-Dalt	immobilized pH gradients
$iPLA_2$	Ca^{2+}-independent phospholipase A_2
IPTG	isopropyl-β-D-thiogalactopyranoside
L. monocytogenes	*Listeria monocytogenes*
LAB	lactic acid bacteria
LLO	listeriolysin O
LS	light scattering
LUV	large unilamellar vesicle
MLV	multilamellar vesicle
NMR	nuclear magnetic resonance
PA	phosphatidic acid

PAGE	polyacrylamide gel electrophoresis
PAP	phosphatidic acid phosphohydrolase
PC	phosphatidylcholine
PCR	polymerase chain reaction
PDZ	post synaptic density protein, drosophila disc large tumor suppressor, and zonula occludens-1 protein
PE	phosphatidylethanolamine
PG	phosphatidylglycerol
PH	pleckstrin homology
Pi	inorganic phosphate
PI	phosphatidylinositol
PI3K	phosphatidylinositol 3-kinase
PIKE	PI-3-OH kinase enhancer
PI-PLC	phosphatidylinositol-specific phospholipase C
PKC	protein kinase C
PLA	phospholipase A
PLB	phospholipase B
PLC	phospholipase C
PLD	phospholipase D
PMe	phosphatidylmethanol
POPA	1-palmitoyl-2-oleoyl-phosphatidic acid
POPC	1-palmitoyl-2-oleoyl-phosphatidylcholine
POPG	1-palmitoyl-2-oleoyl-phosphatidylglycerol
POPS	1-palmitoyl-2-oleoyl-phosphatidylserine
PRIP	phospholipase C-related, catalytically inactive proteins
PS	phosphatidylserine
RA	ras-association
RI	refractive index

RTK	receptor tyrosine kinases
SDS	sodium dodecyl sulfate
SEC	size exclusion chromatography
SH2	Src homology 2
SPases	signal peptidase
SUV	small unilamellar vesicle
TEMED	N,N,N',N'-tetramethylethylenediamine
TIM	triose phosphate isomerase
TX-100	Triton X-100
WT	wild type
X_{det}	mole fraction of detergent

Table of Contents

List of Figures

List of Tables

Chapter 1:

Introduction

I. Phospholipids

A. Structure of phospholipids

Phospholipids are amphiphilic molecules with one variable phosphate-containing polar / charged group and two long, hydrophobic chains covalently linked to a glycerol backbone (Figure 1-1). Phospholipids may contain different hydrophobic tails but are classified according to their polar head group. With different phosphate-containing groups attached, the net charge of phospholipid varies from 0 to -2 under physiological conditions as shown in Figure 1-1. For bacteria and eukaryotes, two fatty acid chains, each typically having an even number of carbon atoms between 14 and 24, are attached to the first and second carbons of the glycerol molecule via a dual esterification (denoted as sn-1 and sn-2 chains, respectively) (Figure 1-1A). The configuration of groups on the second carbon of the glycerol backbone defines naturally occurring phospholipids as the L-configuration. Fatty acids can be saturated or unsaturated with preference for the *cis* configuration of the double bond. Both the number and positions of unsaturated bonds along with the number of carbon atoms of fatty acyl chains have profound effects on membranes fluidity. Typical phospholipids usually have a saturated fatty acid, such as palmitic or stearic acid, at the sn-1 position with an unsaturated fatty acid, like oleic or arachidonic acid, at the sn-2 position. For archaeal phospholipids, two isoprenoid chains are ether-linked to sn-1 and sn-2 positions of the D-glycerol backbone (Figure 1-1B). Because isoprene is used, the sn-1 and sn-2 chains have methyl branches along the chain which create some unique properties of archaeal phospholipids. Archaeal phospholipids

can also have two headgroups joined via two very long chains forming a ring that can span the thickness of a typical bilayer with headgroups oriented on each side (Gliozzi et al., 2002).

B. Aggregation of phospholipids

Due to their amphiphilic properties, phospholipids self-assemble into various aggregates in aqueous solution (Figure 1-2), favored by the hydrophobic effect (Chandler, 2005), to minimize the contact of hydrophobic tails with solvent and keep the contact of polar headgroup with water. The structures and sizes of these aggregates are determined by thermodynamic laws (Horváth et al., 1976) and intermolecular forces. When dispersed in the aqueous solution, phospholipids at the air-water interface always form monolayers with their polar headgroups solvated in water and hydrophobic tails sticking into the air, whereas in the solution phospholipids are presented as monomers as well as aggregates if above their critical aggregation concentrations. The structure of the aggregate in solution can be predicted in terms of a 'critical packing parameter' (CPP) (Cullis and de Kruijff, 1979; Israelachvili et al., 1980), v/a_0l_c, where v represents the volume of the hydrophobic chains per molecule, a_0 the optimal surface area per amphiphile, l_c the maximum length of the chains (meaning completely extended, all *trans* conformation chains). Phospholipids will form spherical micelles if CPC<1/3, globular or rod-shaped micelles if 1/3<CPC<1/2, vesicles if 1/2<CPC<1, and inverse micelle if CPC>1 (Goldfine, 1984; Cevc and Marsh, 1987; Gennis, 1989). The surface curvature of aggregates, closely related to the type of aggregates, can affect catalytic efficiency of many lipolytic enzymes such as phospholipases.

Figure 1-1 General structure of phospholipids in (A) bacteria and eukaryotes, and (B) archaea. With different polar head groups attached, the net charge of a phospholipid can vary from 0 to -2 under physiological conditions

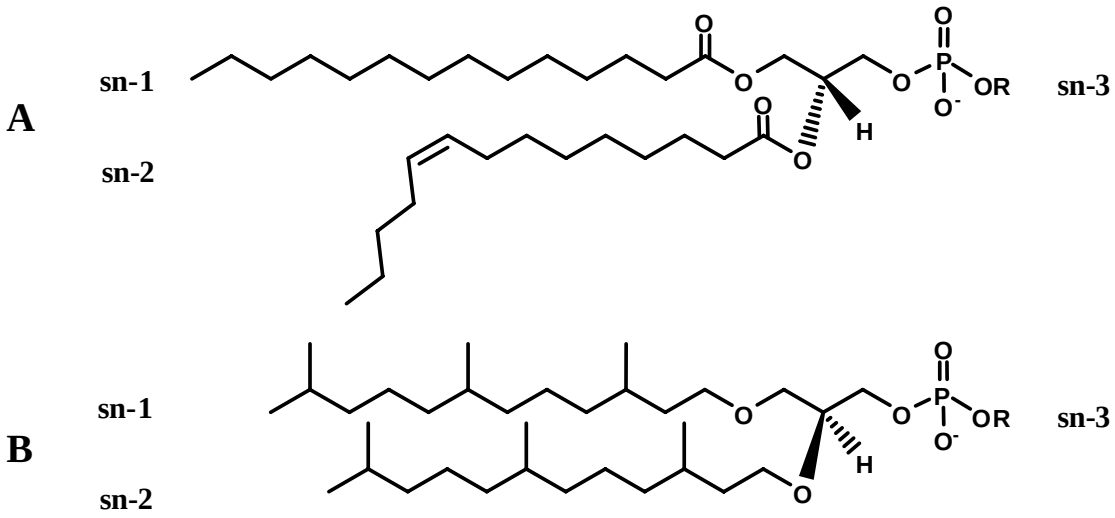

Lipid Name	R	Net Charge at physiological pH
Phosphatidic Acid (PA)	—H	-2
Phosphatidylmethanol (PMe)	—CH_3	-1
Phosphatidylserine (PS)	—$CH_2CH(NH_3^+)COO^-$	-1
Phosphatidylglycerol (PG)	—$CH_2CH(OH)CH_2OH$	-1
Phosphatidylinositol (PI)	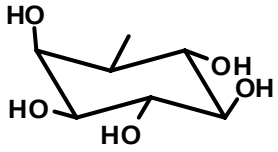	-1
Phosphatidylethanolamine (PE)	—$CH_2CH_2NH_3^+$	0
Phosphatidylcholine (PC)	—$CH_2CH_2N^+(CH_3)_3$	0

Figure 1-2 Various physical states of phospholipids in aqueous solution. At the air-water interface, phospholipids always form monolayers with polar headgroups solvated in water and hydrophobic tails sticking into the air. In the aqueous solution, phospholipid molecules are present as monomers as well as aggregates (micelles or vesicles) if above their critical aggregation concentrations.

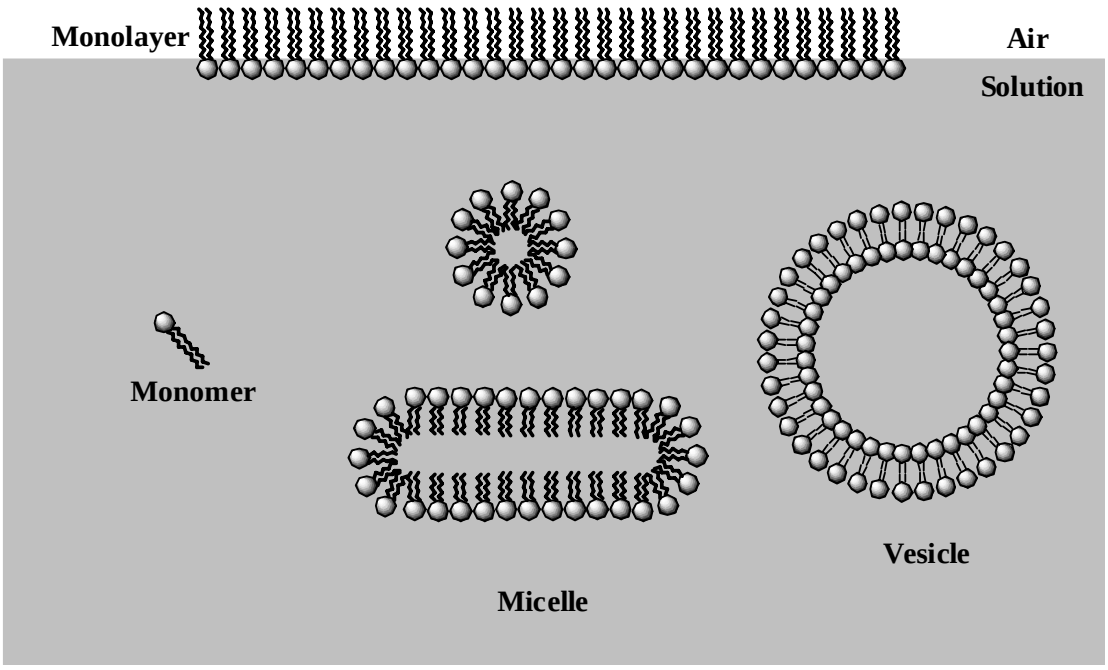

In general, synthetic short chain phospholipids with chain length no longer than 8 carbons form micelles containing 5 to 500 amphiphilic lipid molecules where the shape of micelles varies with the length of chain, the concentration of lipid and the surface area of the headgroup (Gennis, 1989). For instance, diC_6PC (dihexanoylphosphatidylcholine) forms nearly spherical small micelles that only grow slightly as the diC_6PC concentration increases; diC_7PC forms larger rod-shaped micelles that grow considerably as the diC_7PC concentration increases; while diC_8PC forms extended rods or branched networks (Lin et al., 1986; Roberts, 1991).

Naturally occurring phospholipids can form aggregates of different types depending on the preparation method used. When dispersed in aqueous solution, a dried phospholipid film spontaneously forms multilamellar vesicles (MLVs) consisting of concentric multiple alternating lipid bilayers and aqueous layers in an onion skin arrangement with a diameter of 1-5 μm (Bangham et al., 1965). These multilamellar liposomes can be further processed by other techniques to form other aggregate structures. Upon the addition of detergents, phospholipid MLVs can be solubilized and transformed into mixed micelles (Lichtenberg et al., 1983). If the detergent used has a high critical micelle concentration (CMC), and if it is subsequently removed by dialysis or column chromatography, large unilamellar vesicles (LUVs) can be generated (Brunner et al., 1976). By sonication under an inert atmosphere, MLVs can be converted to small unilamellar vesicles (SUVs) with a diameter 20-50 nm (Johnson et al., 1971). Multiple extrusion of MLVs through membrane filters with appropriate pore sizes, will generate SUVs or LUVs (Olson et al., 1979; Mayer et al., 1986; Nayar et al., 1989). Other

techniques, such as pH-induced vesiculation (Hauser and Gains, 1982), fusion of vesicles by repeated freezing and thawing (Uhumwangho and Okor, 2005), or fusion of vesicles containing anionic phospholipids by Ca^{2+} mediated aggregation followed with EDTA treatment (Szoka and Papahadjopoulos, 1980), have also been used to transform the structure of lipid aggregates. Giant unilamellar vesicles (GLVs) with diameters between 5 and 200 μm (Menger and Keiper, 1998), which are the same size as cells, have been prepared by several methods including gentle hydration, solvent evaporation, and electroformation (Bagatolli et al., 2000). Aside from micelles and vesicles, planar lipid bilayers (black lipid membranes) serve as a useful tool for biomembrane research and biosensor applications (Sackmann, 1996). These can be prepared on solid supports by classical Langmuir-Blodgett techniques (Kuhner et al., 1994; Beyer et al., 1996), liposome fusion techniques (Brian and McConnell, 1984), and a hybrid of those two methods (Kalb et al., 1992; Wenzl et al., 1994).

C. Dynamic movement of phospholipids

The modern view of biomembranes is loosely based on the "fluid mosaic" model in which cell membranes are considered as two-dimensional solutions of oriented proteins and lipids (Singer and Nicolson, 1972). Phospholipids in the membranes undergo several types of movements: lateral diffusion in the plane of membrane, flexing of acyl chains, rotational diffusion, and transverse diffusion (flip-fop) between the two sides of a bilayer. Those motions within the same leaflet occur at a very fast rate. The diffusion coefficient for lateral diffusion can range from 10^{-6} to 10^{-9} cm^2/s (Jones and Chapman, 1995). In contrast, spontaneous "flip-flop" motion, where it is

thermodynamically unfavorable to pass the hydrated, polar headgroup of the lipid through the hydrophobic core of the bilayer, is extremely slow with half-life for the process ranging from several hours to days (Jones and Chapman, 1995). The rare occurrence of spontaneous transverse diffusion of lipids enables the asymmetry of a membrane to be maintained.

D. Function of phospholipids

It is widely recognized that phospholipids are involved at multiple levels of cellular organization and function. They function primarily as biological membrane structural elements in defining the permeability barrier of cells and organelles by forming a phospholipid bilayer. The hydrophobic core of the bilayer allows the passage of only small non-polar molecules but not charged ones, a prerequisite for the generation of electrochemical potentials used for ATP synthesis or active transport. By providing a bilayer as the matrix for the organization of various membrane proteins, phospholipids directly affect membrane protein structure and function (van Klompenburg et al., 1997; Bogdanov et al., 2002; Zhang et al., 2003; Dowhan et al., 2004; Zhang et al., 2005). Phospholipids were also reported to serve as molecular chaperones (Bogdanov et al., 1996; Bogdanov and Dowhan, 1999), precursors for various second messengers (Exton, 1994; Lennartz, 1999), donors to the synthesis of macromolecules (Becker and Lester, 1980; Menon and Stevens, 1992; Fankhauser et al., 1993; Lester and Dickson, 1993; Bishop et al., 2000), surfactants (Batenburg, 1992), essential components of bile (van Erpecum et al., 2007), and donors in protein lipidation (Ichimura et al., 2000).

II. Phospholipases

Phospholipases constitute a heterogeneous group of enzymes that hydrolyze the various ester linkages in glycerophospholipids. As shown in Figure 1-3, Phospholipases are classified into A_1 (PLA_1), A_2 (PLA_2), B (PLB), C (PLC), and D (PLD) based on their site of attack on phospholipids. PLA_1 and PLA_2 specifically hydrolyze the fatty acyl ester bond at the sn-1 and sn-2 position of the glycerol moiety, respectively, to generate fatty acid and corresponding lysophospholipid. In addition to the PLA activity, several PLA enzymes, such as PA-PLA_1 (specific for phosphatidic acid, PA), PS-PLA_1 (specific for phosphatidylserine, PS), $cPLA_2$ (cytosolic PLA_2), and $iPLA_2$ (Ca^{2+}-independent PLA_2) also display lysophospholipase activity to remove the fatty acid from lysophospholipids (Wang and Dennis, 1999). PLB enzymes usually possess three kinds of activities in that they act as a phospholipase A to sequentially remove both the sn-1 and sn-2 acyl ester bonds, lysophospholipase to remove the remaining fatty acid from lysophospholipids, and lysophospholipase-transacylase to transfer free fatty acid to lysophospholipid to produce phospholipid. PLC catalyzes the cleavage of glycerophosphate ester bond to diacylglycerol (DAG) and phosphorylated headgroup. PLD cleaves the terminal phosphodiester bond to liberate phosphatidic acid (PA) and free headgroup.

Phospholipases are ubiquitous and play important roles in a number of physiological processes. As phospholipids provide matrix for biomembranes, it is conceivable that degradation of phospholipids by phospholipases alters membrane composition (i.e. depletion of PC, accumulation of PA, DAG, and lysophospholipids) and therefore membrane physical properties (Shoemaker and Vanderlick, 2002; Larijani and

Dufourc, 2006). With lipolytic activities, phospholipases play roles in lipid catabolism and membrane remodeling during cell differentiation, cell growth and development, senescence, aging, and in response to stresses (Wang, 2001). Phospholipases also generate several important second messengers involved in cellular regulation. Of particular interest in signal transduction pathways are the following: (1) the unsaturated fatty acid generated by PLA_2, arachidonic acid, is an important precursor of the eicosanoid family of inflammatory mediators including prostaglandins, thromboxanes, lipoxins, and leukotrienes (Balsinde et al., 2002); (2) DAG, either released directly via PLC or indirectly by the sequential action of PLD and phosphatidic acid phosphohydrolase (PAP-1), can activate protein kinase C (PKC) enzymes and play roles in cell proliferation, apoptosis, survival and migration, and perhaps tumorigenesis (Griner and Kazanietz, 2007); (3) inositol-1,4,5-triphosphate (IP_3), generated by phosphatidylinositol-specific phospholipase C (PI-PLC), can mobilize the interior Ca^{2+} stores and trigger a series of calcium-sensitive activators and repressors (Berridge, 1993; Duncan et al., 2007); (4) PA, a product of PLD, has been implicated in a series of biological cellular responses regulating cell growth, proliferation, reproduction, vesicle trafficking, secretion, and endocytosis (Jenkins and Frohman, 2005; Wang et al., 2006). Besides those diverse intracellular roles, extracellular phospholipids have been implicated as virulence factors for bacteria and pathogenic fungi (Songer, 1997; Ghannoum, 2000). PLA enzymes from some protozoan species facilitates host cell penetration (Ghannoum, 2000).

Figure 1-3 Action sites of phospholipases. PLA_1 and PLA_2 specifically hydrolyze the fatty acyl ester bond at the sn-1 and sn-2 position of the glycerol moiety, respectively; PLB enzymes can remove both the sn-1 and sn-2 acyl ester bonds; PLC catalyzes the cleavage of glycerophosphate ester bond; and PLD cleaves the terminal phosphodiester bond.

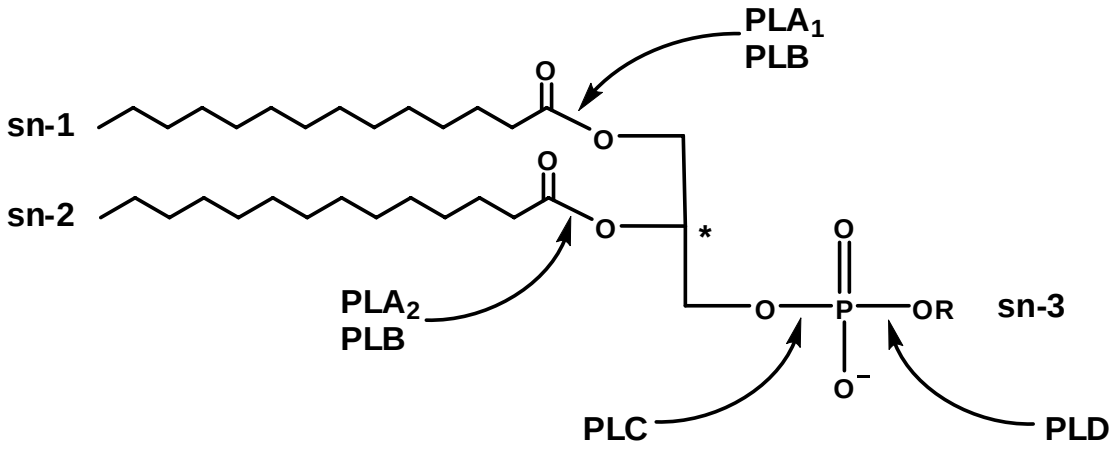

III. Interfacial enzyme kinetics

The fact that phospholipases are water-soluble while naturally occurring phospholipids are amphiphilic and aggregated in biological membranes (Jain, 1988) complicates the kinetic behavior of phospholipases in that binding of enzymes to the interface is required to access their substrates. The model shown in Figure 1-4 (Jain and Berg, 1989; Berg et al., 1991), simplifying the analysis of interfacial kinetics by separating the contribution of the interfacial binding from the interfacial catalytic steps, is widely adapted to represent the Michaelis-Menten kinetics of enzyme at interfaces. Here, the overall catalytic process occurs in two discrete steps: the enzyme in the aqueous phase (E) initially binds to the interface of the aggregated substrate where the interfacial-associated enzyme (E*) further undergoes a series of catalytic steps at the interface including binding and catalyzing the hydrolysis of substrate, releasing the product to regenerate free E* which either goes back to the aqueous phase (E) in the hopping mode or stays in the same interface to carry out another round of interfacial catalysis in the scooting mode. The overall rate of catalytic turnover is thus affected not only by the kinetics of those interfacial catalytic steps but also by the kinetics of binding and desorption of the enzyme at the interface. The relative contribution of these two factors clearly depends on the processivity of the reaction progress. For enzymes working in pure scooting mode (achieved with a suitable assay system), the enzyme always remains bound at the membrane interface and exhibits negligible inter-aggregate fusion or exchange on the time scale of the reaction progress. Scooting mode kinetics provide near ideal conditions for the characterization and analysis of the events of the interfacial

turnover cycle. Assays in pure hopping mode or with rate-limiting inter-aggregate exchange of substrates and products provide insights into the contribution of the kinetics of binding and desorption of the enzyme at the interface.

Interfacial activation, defined as "binding of the enzyme to the membrane that may cause an allosteric activation that makes the enzyme a more efficient catalyst (larger k_{cat}/K_m for a particular substrate)" (Gelb et al., 2000), is observed for many interfacial enzymes. Phospholipases exhibit interfacial activation as the preference of aggregated versus monomeric substrates (Verheij et al., 1981). Comparing the activities of a phospholipase toward the same substrate in aggregated versus monomeric form, usually synthetic short chain phospholipids with a CMC in the mM range (i.e. diC_6- or diC_7-), is the way to check for interfacial activation behavior of phospholipases. The observed kinetic activation upon forming aggregated substrate, varies from 2- to 3- fold (Zhou et al., 1997b) to 10,000-fold (Verger et al., 1973), depending on the properties of enzyme and the structure and dynamics of the interface. The understanding of interfacial activation is mostly derived from investigating the kinetic and mechanistic bases of two well structurally characterized groups of interfacial enzymes: triglyceride hydrolases and PLA_2 enzymes (Derewenda et al., 1992; Jain and Berg, 2006). Various explanations have been proposed to account for the interfacial activation, including an increased binding of the enzyme to the interface, facilitated replenishment of the substrate, opening of the lid on the active site, and the K_s*- and k_{cat}*-allosteric activation (Derewenda et al., 1992; Berg et al., 1997; Carrière et al., 1997).

Figure 1-4 Scheme for interfacial catalysis (adapted from Berg et al., 1991). The species shown in the box are embedded in or bound to the interface.

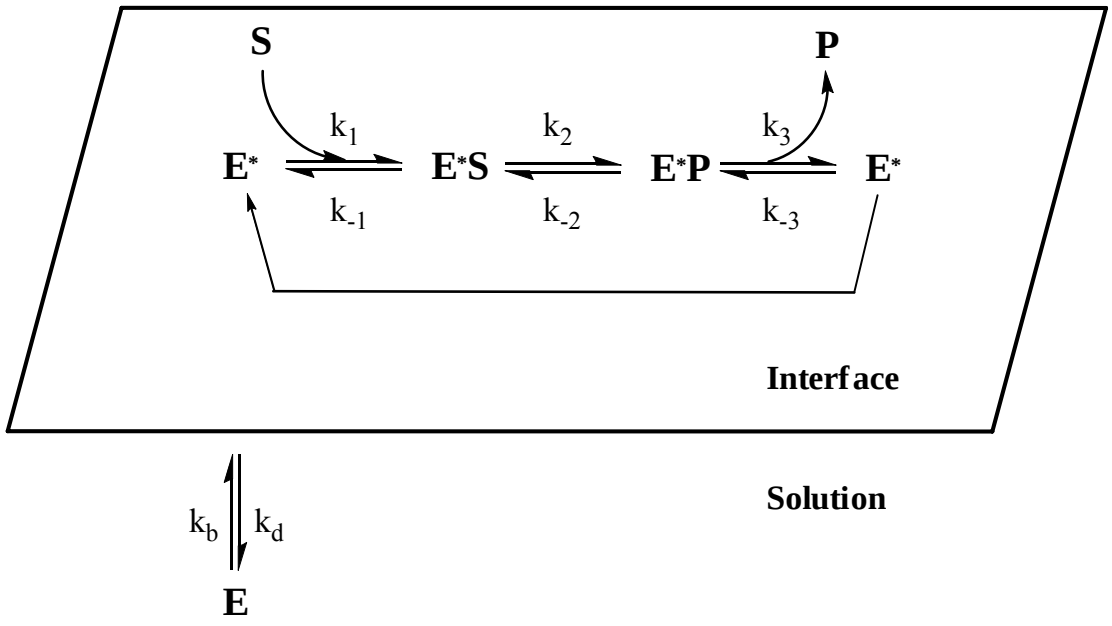

E - enzyme in the aqueous phase

E* - enzyme in the interface

S - substrate

P - product

Concentration is defined as “a thermodynamic term that is related to the statistical probability of random encounter of the reactant molecules in thermal motion” (Berg and Jain, 2002). It is reasonable that in a heterogeneous system, like interfacial reaction progress, the local concentration instead of bulk concentration is important for the overall kinetic rate. In diluting the substrate at the interface by adding more detergents or nonsubstrate lipids while keeping the total concentration of substrate constant, many phospholipases exhibit a lower specific activity, a phenomenon called “surface dilution”. Except for the decrease in surface concentration of the substrate, increase in the surface concentration of possible competitive lipophilic inhibitor may also account for the reduction in activity (Dennis, 1973; Carman et al., 1995).

IV. Phosphatidylinositol-specific phospholipase C

Phosphatidylinositol-specific phospholipase C (PI-PLC) enzymes are a large family of closely related enzymes that specifically hydrolyze phosphoinositide substrates (bacteria enzymes prefer PI and glycosyl-PI (GPI), while most mammalian enzymes prefer PI(4,5)P_2 > PI(4)P, PI(5)P > PI), a minor but important class of regulatory phospholipids (Cockcroft and De Matteis, 2001; Martin, 2001; Stossel et al., 2001; Clapham, 2003; Irvine, 2003). PI-PLC activity was first identified in rat liver (Kemp et al., 1959). From then on, PI-PLCs have been isolated from many bacterial and eukaryotic sources (Flick and Thorner, 1993; Bennett et al., 1998; Griffith and Ryan, 1999; Nozaki et al., 1999; Katan, 2005; Pan et al., 2005).

A. Mammalian PI-PLC

So far, thirteen mammalian PI-PLC isozymes have been identified and classified into six families based on their structure, PLC-β(1-4), PLC-γ(1,2), PLC-δ(1,3,4), PLC-ε(1), PLC-ζ(1), and PLC-η(1,2) (Figure 1-5 and Figure 1-6) (Rhee and Bae, 1997; Saunders et al., 2002; Wing et al., 2003; Irino et al., 2004; Hwang et al., 2005; Nakahara et al., 2005; Stewart et al., 2005; Zhou et al., 2005).

As shown in Figure 1-5, the typical PLC-δ family member is composed of a string of modular domains including PH (pleckstrin homology) domain, EF (elongation factor)-hand domains, catalytic X and Y regions, and a C2 (protein kinase C conserved region 2) domain. Among the PLC family isozymes, PLC-δ is considered as evolutionally conserved (Rebecchi and Pentyala, 2000), and these four domains represent the common core structure of all mammalian PI-PLC isozymes, with the exception of sperm-specific PLC-ζ which lacks the PH domain. The X and Y regions are highly conserved with 40-60% amino acid sequence similarity among all mammalian isozymes (Zhou et al., 2005) and associate tightly to form the catalytic domain (Essen et al., 1996; Essen et al., 1997). Two additional PLC-like proteins, PLC-L1 and –L2, or named as PRIPs (Phospholipase C-Related, catalytically Inactive Proteins), have been identified by searching databases with conserved sequences between β, γ, and δ isoforms. Despite sharing the common regions, PLC-Ls do not have PI-PLC activity because they lack critical catalytic residues (Uji et al., 2002). PH domains are found in many other proteins as adaptors or tethers to link their host proteins to the membrane surface (Ferguson et al., 1995; Rebecchi and Scarlata, 1998), mostly to phosphoinositides and βγ-subunits of heterotrimeric G proteins.

Figure 1-5 Domain organization of mammalian PI-PLC isoforms (adapted from Weerninka et al., 2007). The four domains (PH, EF-hand, catalytic, and C2) represent the common core structure of all mammalian PI-PLC isozymes (except sperm-specific PLC-ζ). Other subtype-specific domains contribute to their specific regulatory mechanisms. The structure of bacterial PI-PLC is similar to the catalytic core of mammalian PLC-δ1.

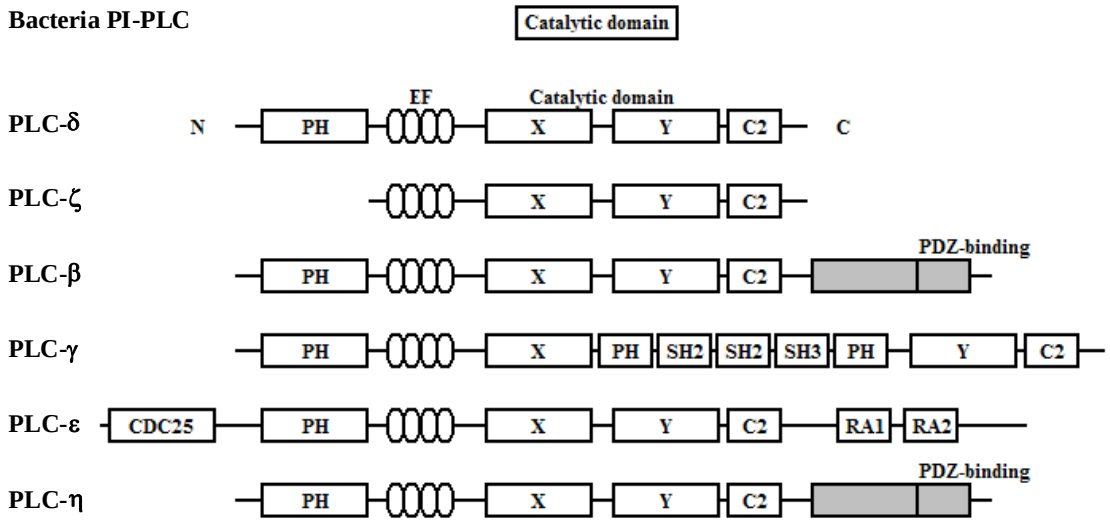

Figure 1-6 Dendrogram of mammalian PI-PLC isoforms (adapted from Katan, 2005). Although sharing the common core structure, two PLC-like proteins (PLC-L1 and –L2) do not have PI-PLC activity for lack of critical catalytic residues.

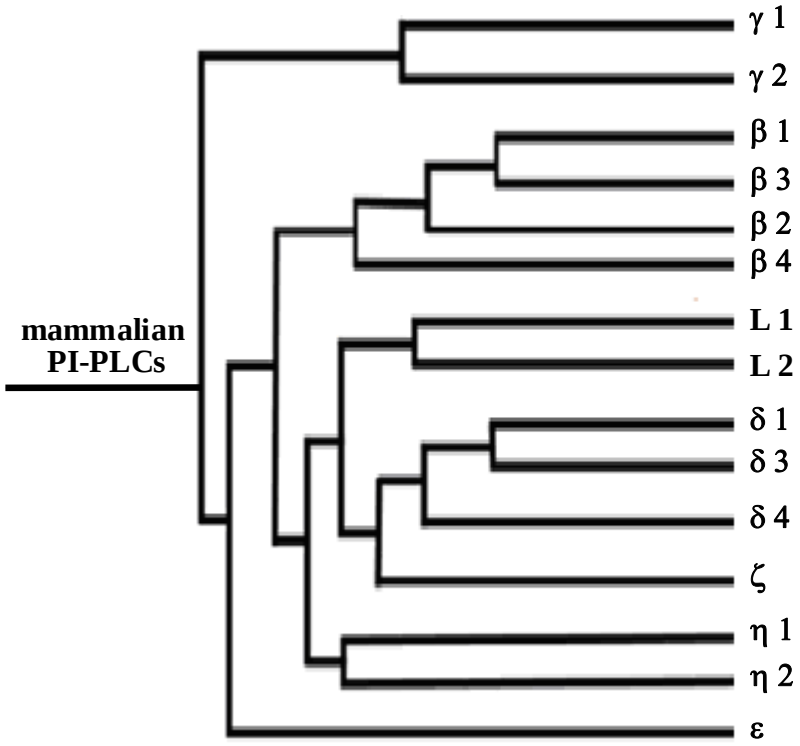

Sequence diversity of PH domains among PLC isoforms indicates that PH domains are involved in subtype-specific regulation. The PLC-δ PH domain binds with high affinity and stereospecificity to the polar head group of $PI(4,5)P_2$ (Garcia et al., 1995), an event that is essential for processive hydrolysis of substrates (Lomasney et al., 1996). PLC-γ N-terminal PH domains bind the triply phosphorylated phosphoinositide, $PI(3,4,5)P_3$ (Bae et al., 1998; Falasca et al., 1998), while PLC-β isoforms bind artificial bilayers with relatively little specificity for phospholipid head group (Wang et al., 1999). All mammalian PLC isoforms have up to four helix-loop-helix EF-hand motifs. Although EF-hand motifs usually bind calcium ions, some of them do not have the critical residues for calcium binding. The first two EF-hands of PLC-δ1 are able to bind calcium or magnesium ions, whereas EF3 and EF4 do not (Rebecchi and Pentyala, 2000). Recently, the role of EF-hands of PLC-ζ, an isozyme with high Ca^{2+} sensitivity of the $PI(4,5)P_2$-hydrolyzing activity, has been explored (Kouchi et al., 2005). EF1 and EF2 function primarily in a structural role to form the active conformation rather than Ca^{2+} binding sites for activation of the catalytic activity. EF3 is required for the high Ca^{2+} sensitivity of PLC-ζ although it seems the highly coordinated structure of the EF-hand region instead of the primary sequence in the Ca^{2+} binding loop accounts for the high Ca^{2+} sensitivity. All four EF-hands are prerequisites for the activity since deletion of these EF-hands abolished PLC-ζ activity completely. C2 domains usually play a role in calcium-dependent membrane targeting processes (Davletov and Südhof, 1993) and are unique among membrane targeting domains in that they show wide range of lipid selectivity for the major components of cell membranes, including PS and PC. The C2 domain of PLC-

δ1 contains three to four Ca^{2+} binding sites (Grobler and Hurley, 1998) and is important for activity by forming an enzyme-PS-Ca^{2+} ternary complex upon binding of calcium ions (Lomasney et al., 1999). For PLC-ζ, the C2 domain is a prerequisite for the activity. The C2 domain also has affinity for PI(3)P and PI(5)P, but not PI(4,5)P_2 or acidic phospholipids, and thus negatively regulates PLC-ζ (Kouchi et al., 2005). However, the key calcium-binding residues are not conserved in all C2 domains among PLC isozymes (e.g. PLC-β and -γ). The C2 domains of PLC-β isozymes are unable to bind calcium; instead, they do interact strongly and specifically with their activator, activated α subunits of Gq proteins (Wang et al., 1999).

In addition to these canonical domains, other subtype-specific domains (Figure 1-5) contribute to specific regulatory mechanisms. PLC-β isozymes are distinguished from other PLCs by a ~400 residue C-terminal extension downstream of their Y domain. This region interacts with GTP-bound α subunits of Gq proteins (Zhang and Neer, 2001; Ilkaeva et al., 2002; Singer et al., 2002) and PDZ (combination of the first letters of post synaptic density protein, Drosophila disc large tumor suppressor, and zonula occludens-1 protein) domain-containing scaffold proteins (Suh et al., 2001). It bears selective GTPase-activating protein (GAP) activity to enhance the hydrolysis of GTP by Gq protein up to 50-fold (Ross and Wilkie, 2000), and triggers membrane association and nuclear localization (Kim et al., 1996). The unique region of PLC-γ is inserted within the Z region, a flexible loop linking the X- and Y- catalytic regions, and includes a second split PH domain, two Src homology 2 (SH2) domains and one SH3 domain. The second split PH domain interacts with EF-1α, a PI-4 kinase activator in mammalian cells (Chang

et al., 2002). SH2 domains mediate the association of PLC-γ with tyrosine-phosphorylated proteins and promote the regulation of enzyme by nonreceptor and receptor tyrosine kinases (RTK) (Rebecchi and Pentyala, 2000). The SH3 domain contributes to the mitogenic properties of PLC-γ by exhibiting guanine nucleotide exchange factor (GEF) activity towards PIKE (PI-3-OH kinase enhancer), a nuclear GTPase regulating the nuclear PI3K activity (Ye et al., 2002). The SH3 domain also interacts with PLD2 and may couple the activity of PLC with that of PLD (Jang et al., 2003). PLC-ε contains a N-terminal CDC25 (cell division cycle) domain with GEF (guanyl-nucleotide exchange factor) activity for Ras GTPases as well as two C-terminal Ras-association (RA) domains to bind activated Ras GTPases for upstream and downstream interactions of PLC-ε with Ras GTPases (Kelley et al., 2001; Lopez et al., 2001; Song et al., 2001). PLC-η isozymes, neuron-specific enzymes identified most recently (Hwang et al., 2005; Nakahara et al., 2005; Stewart et al., 2005; Zhou et al., 2005), bear a long C-terminal sequence ending with a PDZ-binding motif. Splice variants of PLC-η that differ at the C-terminus have been reported (Zhou et al., 2005) and further investigation is need to understand the roles of PLC-η C-terminal sequence.

B. Bacterial PI-PLC

The smallest PI-PLCs, about 35 kDa in size, are secreted by a variety of bacteria, including the pathogens *Bacillus cereus*, *B. thuringiensis*, *B. anthracis*, *Listeria monocytogenes*, *L. ivanovii*, *Staphylococcus aureus*, *Clostridium novyi*, *Rhodococcus equii*, and also non-pathogenic species *L. seeligeri*, *Streptomyces antibioticus*, *Cytophaga* sp., and some strains of lactic acid bacteria (LAB) such as *Lactobacillus rhamnosus*

(Griffith and Ryan, 1999; Rodriguez et al., 2001; Klichko et al., 2003; Read et al., 2003). While they all prefer nonphosphorylated PI as the substrate, some of these enzymes also have high activity towards GPI-anchors. The interest in bacterial PI-PLC arises from (1) their role in bacterial virulence, (2) their use as tools to investigate GPI-linked proteins, and (3) their structural similarity to the mammalian catalytic domain and use as a simple model system. PI-PLC enzymes are potential virulence factors for a number of pathogenic bacteria (Mengaud et al., 1991; Daugherty and Low, 1993). *L. monocytogenes* PI-PLC plays roles in the escape of bacteria from phagolysosomes (Smith et al., 1995; Portnoy et al., 2002) and modulation of host cell signaling pathways including Ca^{2+} signaling in macrophages (Goldfine and Wadsworth, 2002) and PI metabolism in endothelial cells and macrophages (Sibelius et al., 1996b; Goldfine and Wadsworth, 2002). *B. anthracis* PI-PLC down-modulates dendritic cell (DC) function and T cell responses, possibly by cleaving GPI-anchored proteins important for TLR-mediated DC activation (Zenewicz et al., 2005). Without PI-PLC, *B. cereus* is less able to cause disease, although the mechanism is unclear (Callegan et al., 2002). The role for PI-PLC in other pathogenic bacteria has not been examined. It has been reported that PI-PLC of *Lactobacillus rhamnosus* has the ability to translocate the bacteria (Rodriguez et al., 2001) which could be associated with potential bacterial infectivity and pathogenic degree (Zhou et al., 2000). Bacterial PI-PLC enzymes also serve as useful tools for research on GPI-anchored proteins (Ikezawa, 2004). With the ability to cleave GPI-anchors, bacterial PI-PLCs can act as membrane-attacking agents to release proteins tethered to the cell membrane via GPI anchors. Of particular interest to our group has been the use of

bacterial PI-PLC enzymes as a model system for understanding the more complex and highly regulated eukaryotic PI-PLC. This is based on the structural similarities between bacterial PI-PLC and catalytic core of mammalian PLC-δ1 (Heinz et al., 1998).

Bacterial PI-PLCs have been shown to catalyze a two-step reaction, as shown in Figure 1-7, that is independent of Ca^{2+}. The first step is a phosphotransferase reaction to cleave phosphatidylinositol and produce DAG and D-*myo*-inositol 1,2-cyclic phosphate, (cIP). This is followed by a cyclic phosphodiesterase reaction that converts cIP to D-*myo*-inositol 1-phosphate, I-1-P. For most of these enzymes the water-soluble intermediate product cIP accumulates because the second step is about 10^3-times slower than the first one (Volwerk et al., 1990). Bacterial PI-PLCs are extremely sensitive to the conformation of substrate head group which should be *myo*-inositol in D-configuration (Leigh et al., 1992; Lewis et al., 1993) with a free, axial 2-OH group (Lewis et al., 1993) and free, equatorial 3-, 4-, and 5-OH groups (Volwerk et al., 1989). The activity of PI-PLC toward *chiro*-inositol with an axial 3-OH, which is the only allowed conformational change reported, reduces the rate by a factor of 10^3 (Bruzik et al., 1994). The GPI anchor, where the *myo*-inositol is linked via a glycosidic bond of its 6-OH group to a linear oligosaccharide, can also be hydrolyzed by bacterial PI-PLC. The strict conformation requirements also hold in the second step (Volwerk et al., 1990). In contrast to the head group specificity, bacterial PI-PLCs are insensitive to the conformation of the lipid portion of the substrate. Variations, around either the glycerol sn-2 carbon or chain linkages (ether- or ester-linked, saturated or unsaturated, lyso-), produce molecules that

Figure 1-7 Two reactions catalyzed sequentially by bacterial PI-PLC enzymes (adapted from Griffith and Ryan, 1999).

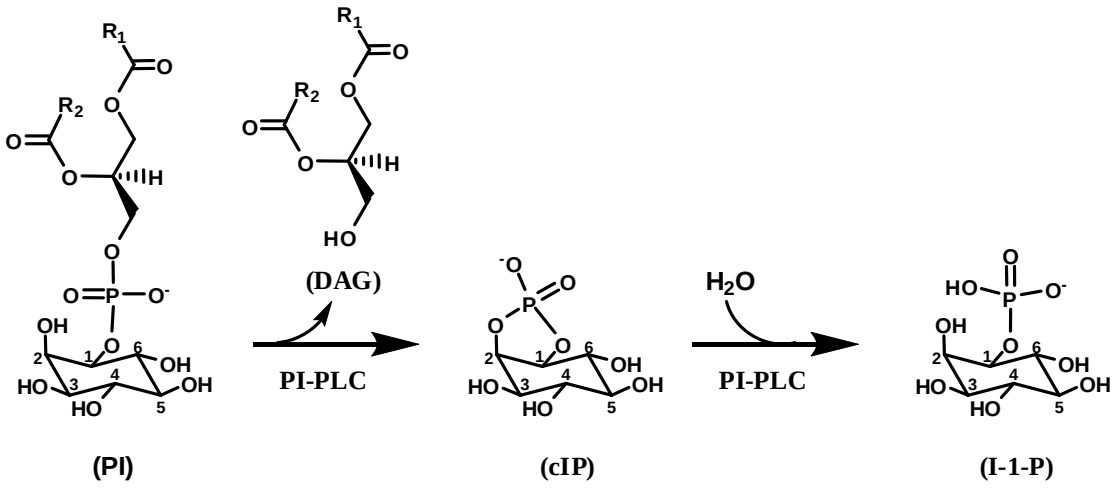

are usually good substrates (Bruzik et al., 1992; Bruzik and Tsai, 1994; Guther et al., 1994).

Several crystal structures of bacterial PI-PLCs have been reported (Heinz et al., 1995; Heinz et al., 1996; Moser et al., 1997). These enzymes are folded as a single, distorted $(\beta\alpha)_8$-barrel or TIM (triose phosphate isomerase)-barrel (Figure 1-8) with the active site at the C-terminal end of the β-strands. In *B. cereus* PI-PLC, the α-helices between β-strands IV/V and V/VI are missing and replaced with a loop and an anti-parallel strand Vb, respectively. Reduced main chain hydrogen bonds between strands V and VI keeps this region open compared to that of regular TIM barrels. The active site pocket was identified by co-crystallization with *myo*-inositol (Heinz et al., 1995) as well as with the core region of a GPI-anchor (Heinz et al., 1995; Heinz et al., 1996). As shown in Figure 1-9, the inositol ring binds in an edge-on orientation with the 2-, 3-, 4-, and 5-OH groups of the ring strongly coordinated with a network of hydrogen bonds. One or more hydrogen bond interactions are formed between those hydroxyl groups and the side chains of several residues which themselves are held in position by other residues via hydrogen bonds. There is also a planar stacking interaction between the apolar side of the *myo*-inositol ring and the phenol ring of Tyr-200 to position the *myo*-inositol ring. No close contact is found between the protein and O1 or O6 of the *myo*-inositol moiety. These binding patterns of *myo*-inositol in the active site are consistent with the exquisite sensitivity of enzyme to the conformation of inositol.

Alignment of all published sequence of PI-PLCs revealed two histidines, His-32 and His-82 in *B. cereus*, which are conserved in bacterial PI-PLCs and the mammalian X-

Figure 1-8 Side by side view of the topologies of *B. cereus* PI-PLC and *L. monocytogenes* PI-PLC with *myo*-inositol (labeled Ins in yellow) bound in the active site pocket (adapted from Moser et al., 1997).

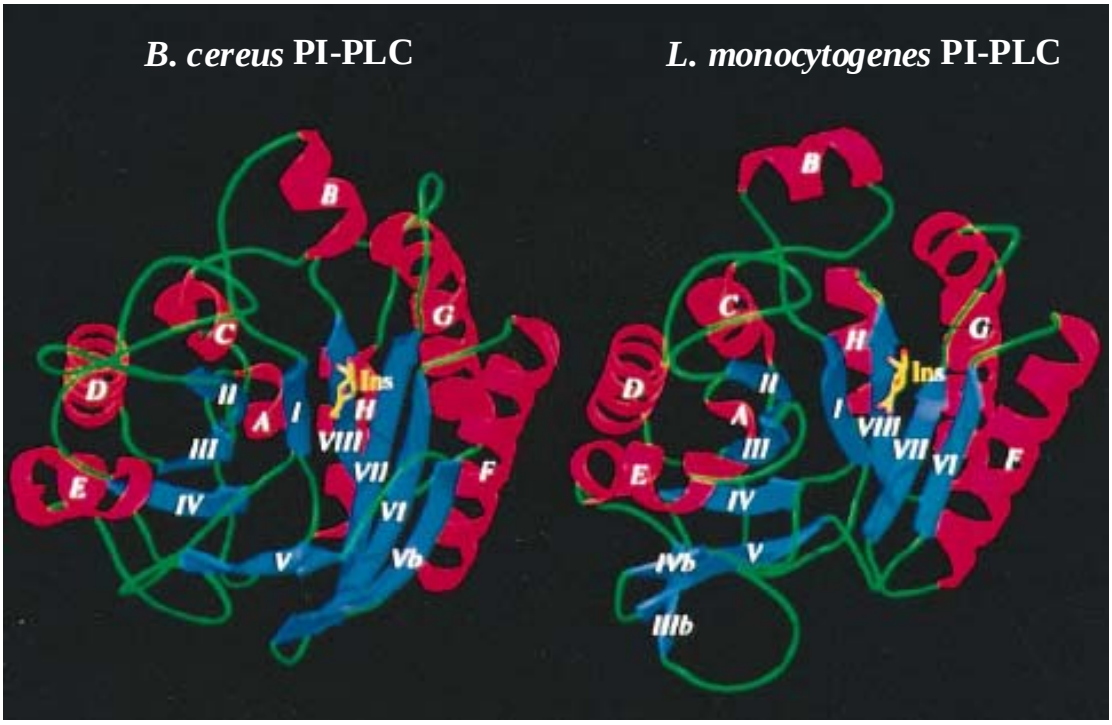

Figure 1-9 Binding of (A) *myo*-inositol (labeled Ins, headgroup of PI substrate) and (B) glucosaminyl(α1→6)-D-*myo*-inositol (labeled GlcNIns, the central portion of a GPI anchor substrate) at the active site of *B. cereus* PI-PLC (adapted from Griffith and Ryan, 1999).

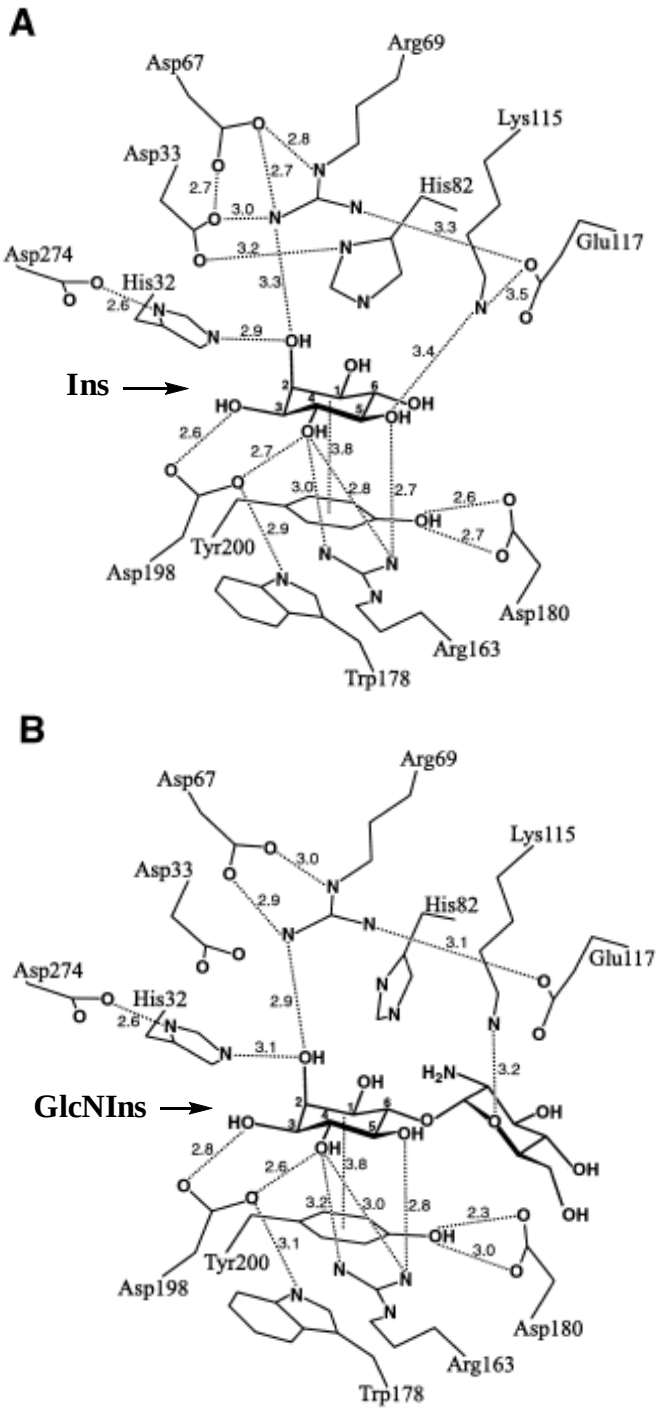

Figure 1-10 The catalytic mechanism for the hydrolysis of (A) PI and (B) cIP by *B. cereus* PI-PLC. His32-Asp274-inositol-2-OH and His82-Asp33-Arg69 form the catalytic triad (Kubiak et al., 2001; Ryan et al., 2001).

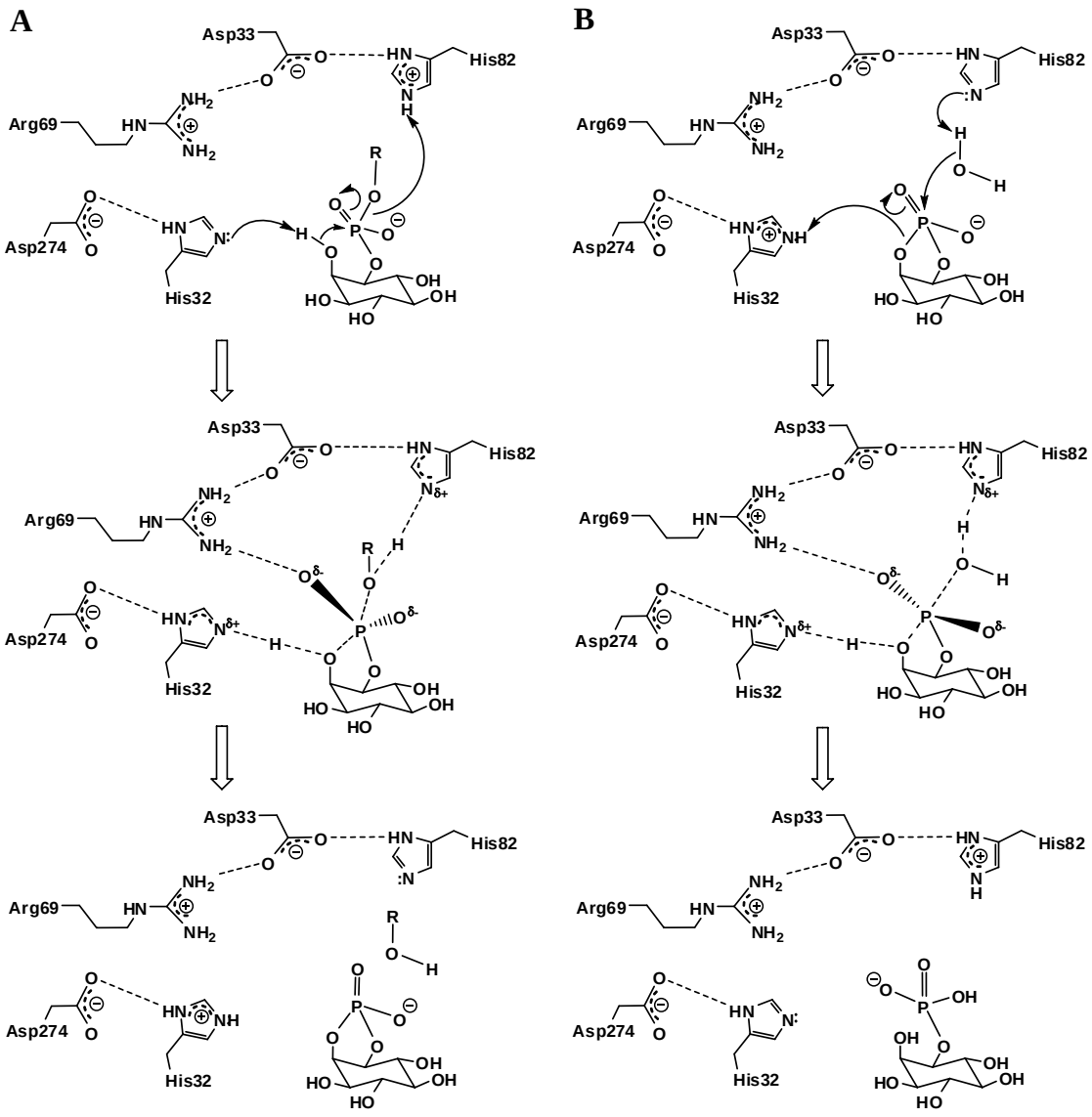

region and may be good candidate residues for catalysis. Combining the results of stereochemical approaches (Lin et al., 1990; Bruzik et al., 1992) and the solved crystal structures, researchers suggested that the catalysis of PI-PLC occurs via an in-line SN2 displacement using His-32 and His-82 as general base and general acid (Heinz et al., 1995). The importance of these residues has been confirmed by mutagenesis studies (Gässler et al., 1997). More recent studies have suggested that H32-D274-inositol-2-OH and H82-D33-R69 form the complex catalytic triad as general base and acid as shown in Figure 1-10 (Ryan et al., 2001; Kubiak et al., 2001).

As interfacial enzymes, the interfacial binding region of bacterial PI-PLCs is important to regulate its activity. Both interfacial activation and surface dilution inhibition were observed for *Bacillus* PI-PLC enzymes (Zhou et al., 1997b). The crystal structure of *B. cereus* PI-PLC has revealed several solvent accessible hydrophobic amino acid residues, arranged in a semicircle around the active site cleft, that form a hydrophobic ridge to contact with lipid surfaces via hydrophobic interactions. These residues are from the short α-helix B, a loop between strand II and helix D, and the loop between strand VII and helix G.

V. *Listeria monocytogenes*

Listeria monocytogenes, first described by Murray and coworkers (1926) based on six cases of sudden death of young rabbits, is a widespread, rapidly growing Gram-positive bacterial pathogen and the causative agent of human and animal listeriosis. *Listeriae* are acquired primarily through the consumption of contaminated foods. Although *L. monocytogenes* infection is usually limited to pregnant women, newborns,

and immunocompromised individuals, the high mortality rate associated with human listeriosis make *L. monocytogenes* the leading cause of death amongst foodborne bacterial pathogens (Paoli et al., 2005).

L. monocytogenes has served as a model for the study of intracellular pathogenesis for decades, and many aspects of the pathogenic process are well understood (Portnoy et al., 2002; Pamer, 2004). As shown in Figure 1-11, the infection process of *L. monocytogenes* can be separated into the following steps. (1) The first step is the association of this microorganism with the host cell and internalization into a phagosome formed by fusing with early endosomal compartments of the host cell. *L. monocytogenes* enters almost all adherent cells but has a 10,000-fold higher efficiency of uptake by macrophages and macrophage-like cell lines compared to fibroblast cell lines (Camilli et al., 1993). (2) The next step is the escape from the primary vacuole into the cytosol of host cell. (3) Once free from the vacuole, the bacteria start intracytosolic replication. (4) The bacteria then gain propulsion from the rapid polar polymerization of host actin. (5) With a pseudopod-like structure, the bacteria are then able to reach into the neighbouring cell and spread cell-to-cell by forming an intermediate double-membraned vacuole. (6) The bacteria can then escape the secondary vacuole and continue the replication.

The virulence of *L. monocytogenes* is directly related to its ability for intracellular growth and spread. Several genes encoding determinants of pathogenesis have been identified and found to be clustered on the chromosome (Goldfine et al., 1995). Among these are *hly*, encoding the pore-forming cytolysin listeriolysin O (LLO); *plcA*, encoding

PI-PLC; and *plcB*, encoding broad-range, PC-preferring PLC (PC-PLC). LLO is an essential determinant of pathogenicity and largely responsible for mediating escape of bacteria from both vacuoles (Vazquez-Boland et al., 2001). Mutants lacking LLO failed to escape from vacuoles in most cells, but they regain the ability to escape from a vacuole with the help of LLO from other organisms (Bielecki et al., 1990). The pores formed by LLO are too small for bacteria to cross the membrane (Palmer, 2001), instead they allow the bidirectional diffusion of electrolytes between the cytoplasm and the phagosome (Higgins et al., 1999; Repp et al., 2002). *L. monocytogenes* PI-PLC and PC-PLC have overlapping roles in the escape of bacteria from phagolysosomes (Smith et al., 1995; Portnoy et al., 2002) and modulation of host cell signaling pathways including Ca^{2+} signaling in macrophages (Goldfine and Wadsworth, 2002) and PI metabolism in endothelial cells and macrophages (Sibelius et al., 1996b; Goldfine and Wadsworth, 2002). PI-PLC helps the bacteria to escape from the primary vacuole of macrophages (Camilli et al., 1993). The loss of *L. monocytogenes* PI-PLC by an in-frame *plcA* deletion mutation or by mutagenesis of active site histidines resulted in a significant defect in the ability of *L. monocytogenes* to escape from the primary vacuole, a slight defect in cell-to-cell spread, and a large decrease in growth in the liver of a mouse after infection (Camilli et al., 1993; Smith et al., 1995; Bannam and Goldfine, 1999). The role of PI-PLC as virulence factor recently has been shown to be closely related to its weak GPI cleavage activity (Wei et al., 2005). There are other virulence factors involved in different infection steps, such as mediation of the internalization of bacteria by nonprofessional

Figure 1-11 Stages in the intracellular life-cycle of *Listeria monocytogenes* (adapted from Portnoy et al., 2002). The entry, escape from a vacuole, actin nucleation, actin-based motility, and cell-to-cell spread of this bacteria are shown with both cartoon in the center and electron micrographs outside.

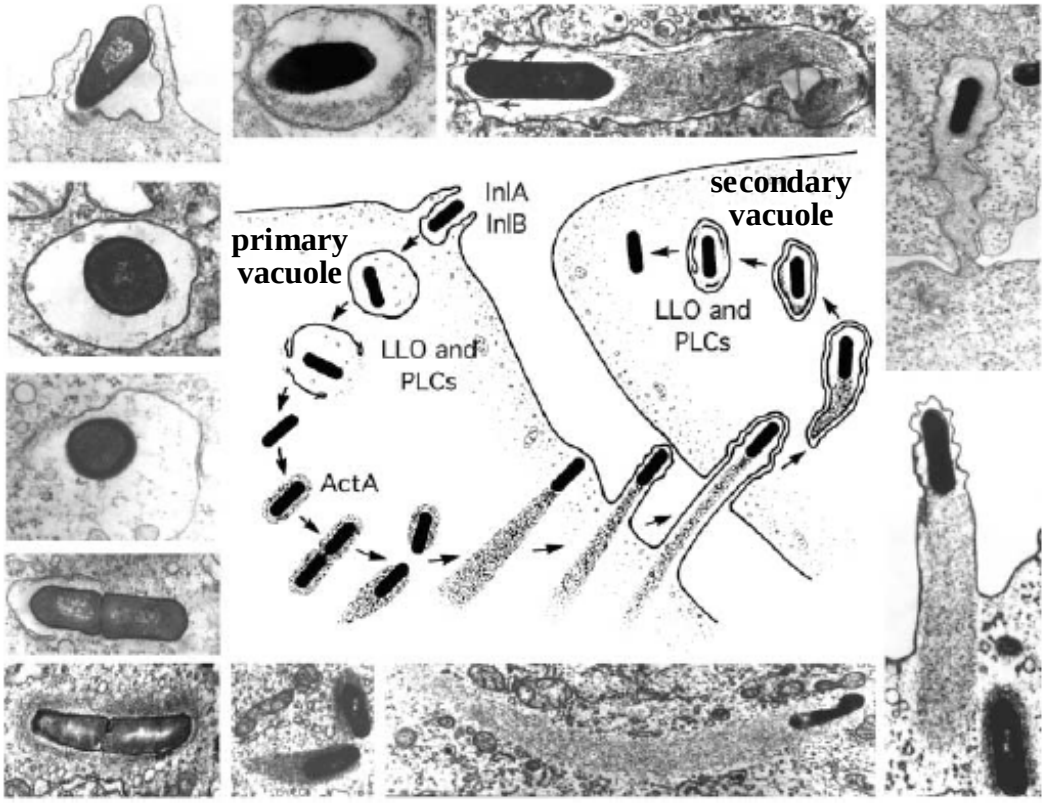

phagocytic cells (Braun and Cossart, 2000; Cossart, 2001), ActA to mediate actin nucleation and actin-based motility (Cameron et al., 2000).

VI. *L. monocytogenes* PI-PLC

PI-PLC from *L. monocytogenes* is a small 33 kDa protein. It is the most basic among the bacterial PI-PLC, with a pI above 9. This enzyme can be activated by salts and has relatively weak activity on GPI anchors, which is differ from the other well studied *Bacillus* sp. PI-PLC counterpart (Goldfine and Knob, 1992).

The crystal structure of *L. monocytogenes* PI-PLC has been solved using molecular replacement and single isomorphous replacement with *B. cereus* PI-PLC as model despite the relative low sequence homology (~24%) between them (Moser et al., 1997). Similar to *B. cereus* PI-PLC, the *L. monocytogenes* enzyme folds as a TIM-barrel with dimensions of about 40 Ǻ × 40 Ǻ × 50 Ǻ. The TIM-barrel is also disordered due to missing two α-helices between strands IV and V, strands V and VI, respectively. The β-barrel is also open between β-strands V and VI because of the lack of main-chain hydrogen bonding interactions. As shown in Figure 1-8 and Figure 1-12, most secondary structures of *L. monocytogenes* PI-PLC and *B. cereus* enzymes superimpose well except for the regions between strand V and VI. The strand Vb of *B. cereus* PI-PLC is missing in the *L. monocytogenes* enzyme, resulting in a more open active site groove and unfavorable binding of the oligosaccharide portion of GPI anchors (Wei et al., 2005). In compensation, two short strands, IIIb and IVB, are present in *L. monocytogenes* PI-PLC to stabilize this area. The α-helix B of *L. monocytogenes* PI-PLC, part of the expected interfacial region, is tilted by approximately 70˚. The regions dominated by amino acid

Figure 1-12 Structure-based sequence alignment of *B. cereus* PI-PLC (labeled BPI-PLC) and *L. monocytogenes* PI-PLC (labeled LPI-PLC) (adapted from Moser et al., 1997). *L. monocytogenes* PI-PLC is numbered from Tyr-30 of the PI-PLC precursor. Residues disordered in crystals are replaced by stars. α-helices, β-strands, and loops are symbolized by barrels, arrows, and lines, respectively. Conserved residues are in bold letters.

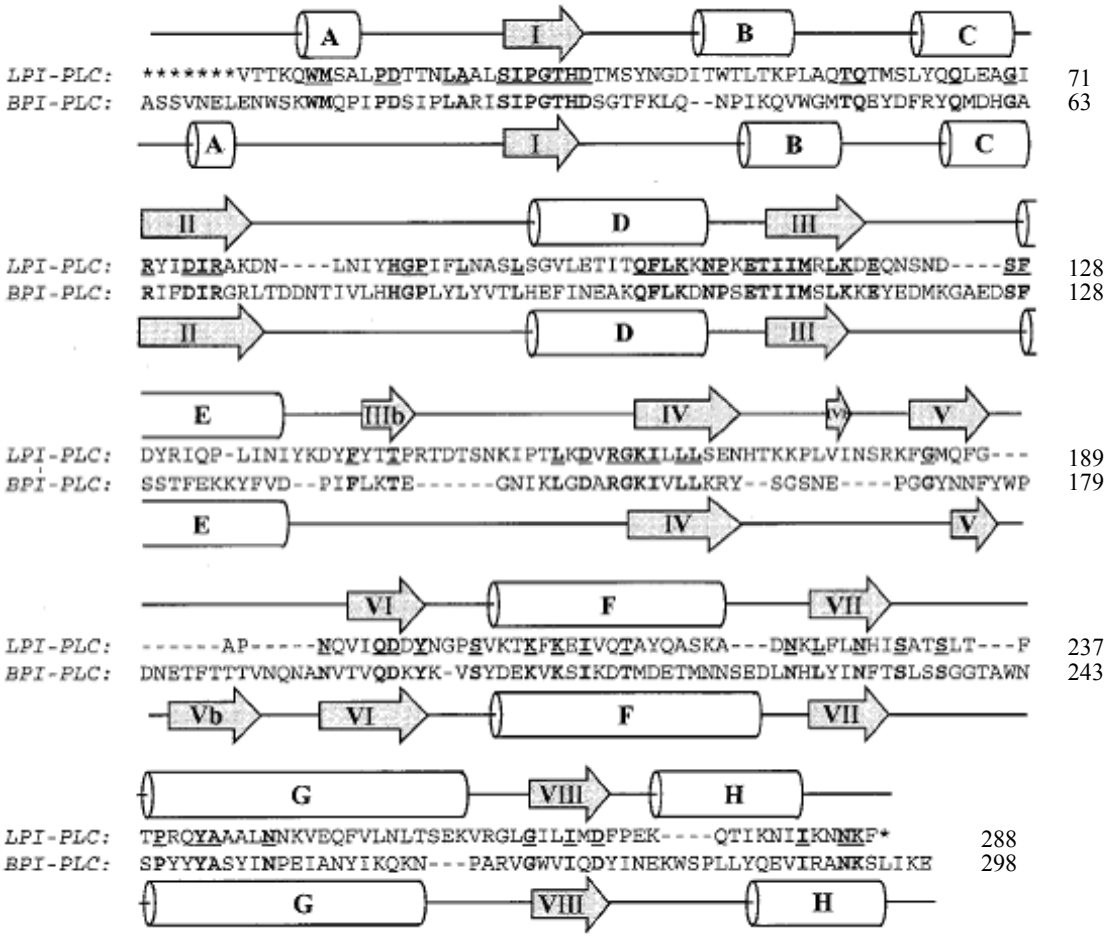

Figure 1-13 Side by side view of the active sites of *B. cereus* PI-PLC and *L. monocytogenes* PI-PLC with *myo*-inositol (labeled Ins in yellow) bound (adapted from Moser et al., 1997).

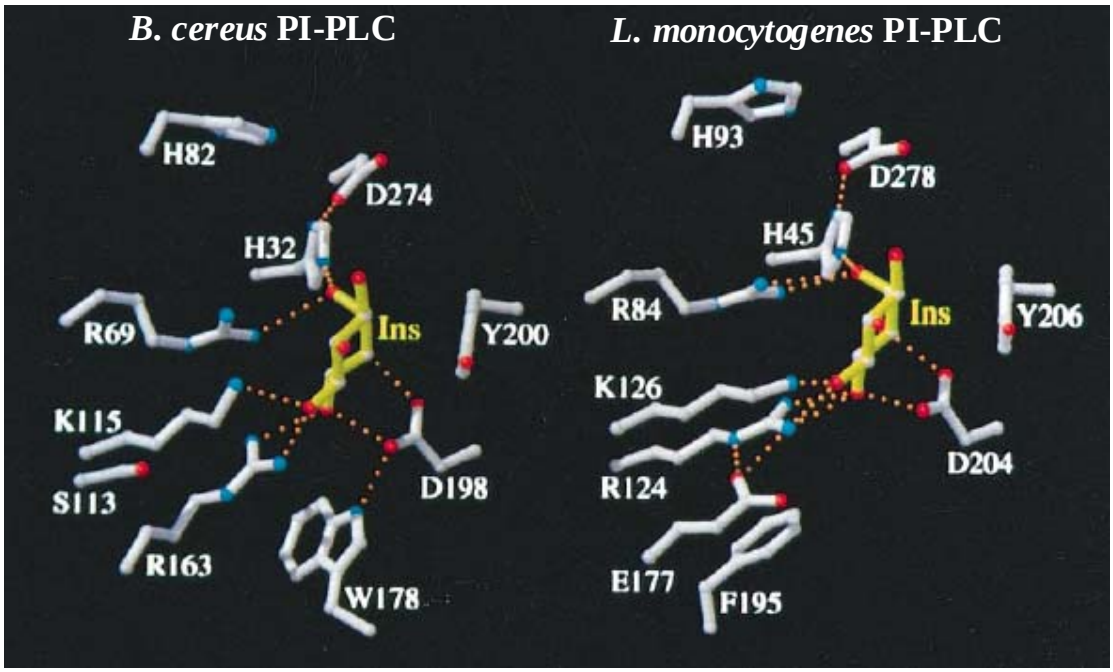

Figure 1-14 Molecular surfaces of *B. cereus* PI-PLC and *L. monocytogenes* PI-PLC viewing from the C-terminal face of the TIM-barrel (adapted from Moser et al., 1997). The active site pockets with bound *myo*-inositol (in yellow) are placed in the center. The hydrophobic ridge and the extended GPI-binding site are designated by A and B, respectively. The charges on the surface are shaded in red for negative potentials and blue for positive potentials.

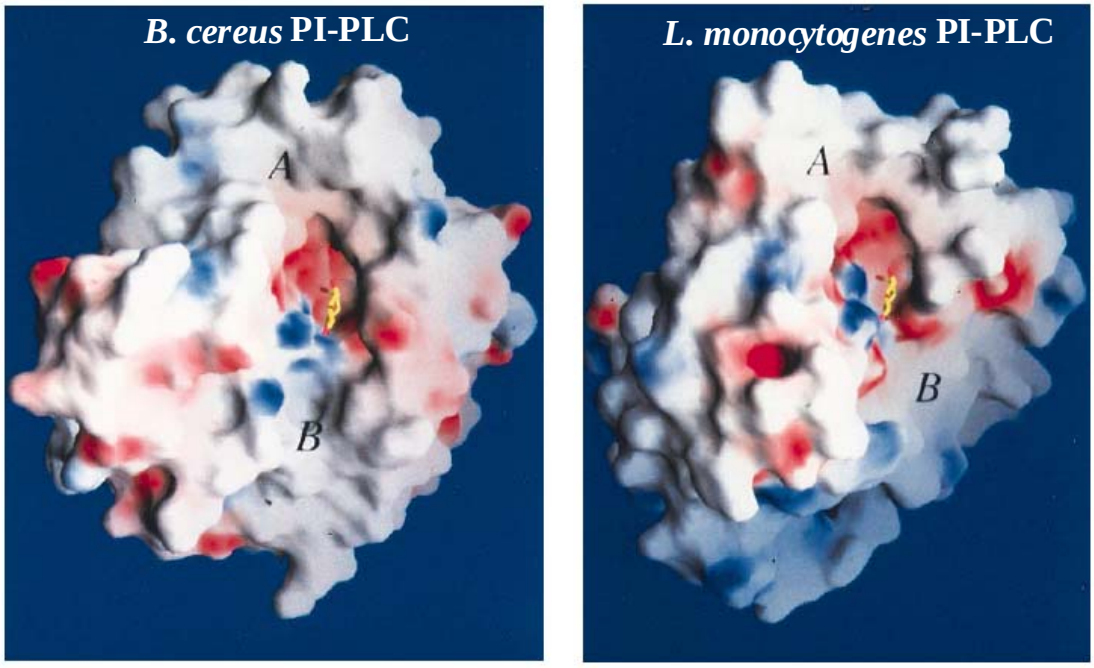

insertions and deletions are mostly in loops (Figure 1-12). Most residues of the active site pocket are conserved in both enzymes. These keep the inositol head group in an identical orientation and position (Figure 1-13). His-45 and His-93 of *L. monocytogenes* PI-PLC are found in the similar positions of His-32 and His-82, the critical catalytic residues, of the *B. cereus* enzyme. Mutagenesis studies confirmed the critical role of His-45 and His-93 for catalysis (Bannam and Goldfine, 1999). Thus, the same reaction mechanism should be used by *L. monocytogenes* PI-PLC. Other than the structure, the differences in the surface charge between these two enzymes (Figure 1-14) are important for the regulation of activity as will be shown in our results.

VII. Thesis directions

The aim of this dissertation is to understand the kinetic behavior of *L. monocytogenes* PI-PLC and its biological relevance. Our interest in this enzyme arose because (1) this enzyme was reported as a virulence factor in the escape of bacteria from phagolysosomes (Smith et al., 1995; Portnoy et al., 2002) and in modulation of host cell signaling pathways including Ca^{2+} signaling in macrophages (Goldfine and Wadsworth, 2002), and PI metabolism in endothelial cells and macrophages (Sibelius et al., 1996b; Goldfine and Wadsworth, 2002). (2) The preliminary studies revealed some distinct kinetic properties of this enzyme compared to the well studied *Bacillus* PI-PLC, named, salt activation and weak GPI activity (Goldfine and Knob, 1992). (3) The crystal structure of this enzyme has been solved and is very similar to that of the *Bacillus* PI-PLC. This structure provided us with a straightforward starting point.

The first part of my project was to obtain enough *L. monocytogenes* PI-PLC for diverse kinetic and biophysical studies. After replacing TGA (the normal stop codon at the position of Trp-35 of PI-PLC precursor) by TGG (the normal codon for Trp) and getting rid of the signal sequence, we have cloned the truncated *L. monocytogenes plc*A gene from strain 10403S into the pTYB11 vector. The recombinant *L. monocytogenes* PI-PLC without any extra N-terminal residues was overexpressed and purified using the IMPACT-CN system with a best yield of 6 mg/L.

The kinetic behaviors of this enzyme were then studied based on the assays used for *Bacillus* enzyme with slight modifications. In general, water-soluble synthetic short chain phosphatidylinositol and cIP along with PI/detergent mixed micelles were used as substrates to understand how salts and other phospholipids affect both steps of PI hydrolysis by the *L. monocytogenes* PI-PLC. Along with the salt activation and lack of surface dilution inhibition, *L. monocytogenes* PI-PLC exhibited an added complication that protein concentration also affected enzyme specific activity. The results indicate that *L. monocytogenes* PI-PLC binds tightly to anionic phospholipids (e.g., PI, PG) and tends to form aggregated complexes with those anionic lipids. The enzymatic activity is much lower for those complexes. The two types of activators previously shown for this enzyme work by different mechanisms: (i) neutral amphiphiles, which enhance both steps of catalysis regardless of the aggregation state of the substrate, bind directly, though weakly, to the protein and enhance its catalytic ability (at sufficiently high mole fractions the amphiphiles can prevent the enzyme from forming the aggregated complexes), while (ii) moderate ionic strength (e.g., salts) only affects the phosphotransferase reaction and then

only when an activating interface is present. The latter is likely to be the result of altering the surface electrostatics and reducing the formation of aggregated complexes, and possibly altering the residence time of the enzyme on interfaces. A model rationalizing the role of both types of activators in modulating the enzyme activity in situ is presented.

Based on the important interfacial regions (α-helix B and a particular loop) explored for the *B. thuringiensis* PI-PLC, we constructed several surface mutants (Trp-49, Thr-50, Leu-51, Leu-235, Thr-236, and Phe-237) in similar interfacial regions of *L. monocytogenes* PI-PLC to assess their contributions to surface binding and PI-PLC kinetics. The results suggest both α-helix B and the loop are kinetically important, particularly for the unusual kinetic traits of *L. monocytogenes* PI-PLC. Under our assay conditions, removal of just single hydrophobic residue (Leu-51, Leu-235, and Phe-237) at in these regions perturbed the unusual kinetic profile of *L. monocytogenes* PI-PLC in that none of the mutant enzymes showed the dramatically increased specific activity with decreasing enzyme concentration or with increasing TX-100 above X_{det}=0.8 as observed for wild type recombinant PI-PLC. Trp-49 appeared to be important for catalysis as W49A PI-PLC exhibited dramatically reduced phosphotransferase and cyclic phosphodiesterase activities. The fluorescence studies of Trp-49 and Phe-237 mutants together with the FRET assays of T50C and T236C with fluorophores covalently attached revealed the connection between the affinity of enzyme for the interface and its kinetic profile. However, lacking a way to quantify the interfacial binding affinities of mutants to various lipid surfaces prevents us from looking further into this issue at this time. The relevance of kinetic modes of activation to the role of PI-PLC in helping *L.*

monocytogenes escape from primary phagosomes is also discussed. One interesting mutant, F237W, although still having high activity, showed reduced plaque sizes in fibroblast infection, strongly suggesting that the high affinity of enzyme for the anionic phospholipids is linked to its role in infectivity.

Anther project addressed in this thesis is to explore the interactions of D-3-deoxy-diC_8PI molecules, designed to inhibit the PI3K/Akt pathway, with two different enzymes in the PI3K/Akt pathway. In vitro, these compounds were poor substrates and not inhibitors of the PLC. There was also little inhibition of PI3K observed except for 3-deoxy-diC_8PI enantiomers, suggesting that the 3-deoxy-diC_8PI molecules are unlikely to have a significant effect on PI3K in vivo.

Chapter 2:

Materials and methods

I. Materials

A. Molecular biology reagents

The pET-23a(+) vector, T4 DNA ligase, BL21(DE3), BL21(DE3)pLysS and NovaBlue *E. coli* strains were obtained from Novagen. Restriction enzymes and IMPACT-CN kit (including pTYB11 vector and ER2566 *E. coli* strains) were purchased from New England BioLabs. BL21-CondonPlus competent cells and Taq PCR Core Kit were from Stratagene. The oligonucleotide primers were ordered from Operon Biotechnologies. QIAprep Spin Miniprep Kit, QIAquick PCR Purification Kit, QIAquick Gel Extraction Kit, and QuikChange Site-Directed Mutagenesis Kit were from QIAGENE. 1 Kb Plus DNA Ladder and protein ladder for SDS-PAGE were from Molecular Probes, Inc. TEMED (N,N,N',N'-tetramethylethylenediamine) and basic proteins used as standards for the acidic native PAGE were ordered from Sigma. IPTG (isopropyl-β-D-thiogalactopyranoside) and antibiotics were from American Bioanalytical. The 30% acrylamide/bis solution, SDS (sodium dodecyl sulfate), ReadyStrip IPG gel strips, and 4-20% Criterion Tris-HCl gradient Precast Gels were from Bio-Rad. All other reagents for media, plates, and gel electrophoresis were obtained from Fisher Scientific. Recombinant p110α/p85α PI-3-kinase was purchased from Upstate Biotechnology, and a chimeric rat PLC, with the catalytic domain of phospholipase Cδ1 and the N-terminal PH domain of phospholipase Cβ1, was the gift of Dr. Suzanne Scarlata, University of New York at Stony Brook.

B. Resins

Resins purchased from Amersham Pharmacia Biotech include SP Sepharose fast flow, Sephadex G-100, and Sephadex G-10. AG 1-X8 (formate form, 100-200 mesh) was obtained from Bio-Rad and chitin bead resin was from New England BioLabs.

C. Phospholipids

Most of the lipids used in this work were purchased from Avanti Polar Lipids, Inc., and used without further purification. These included the long chain lipids 1-palmitoyl-2-oleoyl-phosphatidylcholine (POPC), 1-palmitoyl-2-oleoyl-phosphatidyl-serine (POPS), 1-palmitoyl-2-oleoyl-phosphatidylglycerol (POPG), 1-palmitoyl-2-oleoyl-phosphatidic acid (POPA), 1,2-dioleoyl-*sn*-glycero-3-phosphatidylmethanol (DOPMe), L-α-phosphatidylinositol (PI) from bovine liver, and the short chain phospholipids diheptanoylphosphatidylcholine (diC_7PC) and dihexanoylphosphatidylcholine (diC_6PC). Crude phosphatidylinositol (PI) was purchased from Sigma and short chain dibutyroyl-phosphatidylinositol (diC_4PI) was from Echelon Biochemicals. All the 3-deoxy-phosphatidylinositol derivatives used were gifts of Dr. Yingju Xu and Dr. Scott Miller, Boston College.

D. Fluorophore probes

Most of the fluorophore probes were purchased from Molecular Probes, Inc, including β-Pyr-C_{10}-PG (1-hexadecanoyl-2-(1-pyrenedecanoyl)-*sn*-glycero-3-phosphoglycerol, ammonium salt), β-BODIPY FL C_5-HPC (2-(4,4-difluoro-5,7-dimethyl-4-bora-3a,4a-diaza-s-indacene-3-pentanoyl)-1-hexadecanoyl-*sn*-glycero-3-

phosphocholine), and CPM (7-diethylamino-3-(4'-maleimidylphenyl)-4-methylcoumarin). Carboxyfluorescein (a mixture of 5- and 6-carboxyfluorescein) was ordered from Eastman Kodak Co.

E. Other chemicals

Isopropanol, DMSO, chloroform, ethanol, D_2O, Trizma base, HEPES, boric acid, glycerol, Triton X-100, *myo*-inositol, EDTA, sodium phosphate, NaOH, NaCl, and HCl were purchased from Sigma. Chemical cross-linking reagents, including EDC (1-ethyl-3-[3-dimethylaminopropyl]carbodiimide hydrochloride), DMS (dimethyl suberimidate·2HCl), APG (p-azidophenyl glyoxal monohydrate), and lysine blocking reagent citraconic anhydride (2-methylmaleic anhydride) were purchased from Pierce.

II. Methods

A. Molecular biology techniques

1. Cloning and overexpression systems

Two cloning and overexpression systems (pET and IMPACT-CN) were used in this thesis to clone the *plc*A gene for *L. monocytogenes* PI-PLC.

Both pET and IMPACT-CN systems are based on the T7 promoter-driven system originally developed by Studier and colleagues (Studier and Moffatt, 1986; Rosenberg et al., 1987; Studier et al., 1990). Figure 2-1 illustrates how the overexpression of the recombinant gene is regulated in the pET system. In pET vectors, the multiple cloning sites are placed downstream of a bacteriophage T7 transcription promoter, which is not

recognized by the *E. coli* RNA polymerase, and upstream of T7 terminator. For overexpression, T7 RNA polymerase (encoded by T7 gene 1) is provided by DE3 lysogen host strains. Because sequences of both T7 promoter and terminator are rare in *E. coli* and T7 RNA polymerase is about 5 times faster that *E. coli* RNA polymerase, the genes controlled by T7 promoter can be overexpressed in *E. coli*. The engineered DE3 phage fragment also contains *lac*UV5 promoter and *lac*I gene for *lac* repressor. A *lac*UV5 promoter-*lac* operator fragment precedes the T7 gene 1 as the transcriptional control switch for production of T7 RNA polymerase. The *lac* repressor protein binds tightly to the *lac* operator as a tetramer and specifically in the absence of IPTG, causing transcriptional repression by interfering with the binding of RNA polymerase to the *lac*UV5 promoter. In the presence of IPTG, this inducer binds to the *lac* repressor protein, dissociating it from *lac* operator and turning on the transcription of T7 RNA polymerase in the host cell. The translated T7 RNA polymerase then binds the T7 promoter in the vector and initiates the transcription of the cloned gene. Most pET vectors also contain *lac* operator immediately downstream of T7 promoter (named T7*lac* promoter) and *lac*I gene for stringent transcription control. With a high number of genetic backgrounds modified for various expression purposes, the pET system has been greatly expanded and proved to be a powerful system for the cloning and expression of recombinant proteins in *E. coli* (the desired product can comprise more than 50% of the total cell protein a few hours after induction).

Figure 2-1 Expression of the target gene is regulated with T7/*lac* promoter in pET expression system (adapted from Sørensen and Mortensen, 2005). Without IPTG, *Lac*I binds to *lac* operator as a tetramer to prevent the transcription of both T7 gene 1 and target gene. IPTG can bind to the *Lac*I tetramer to dissociate it from *lac* operator and turn on the transcriptions.

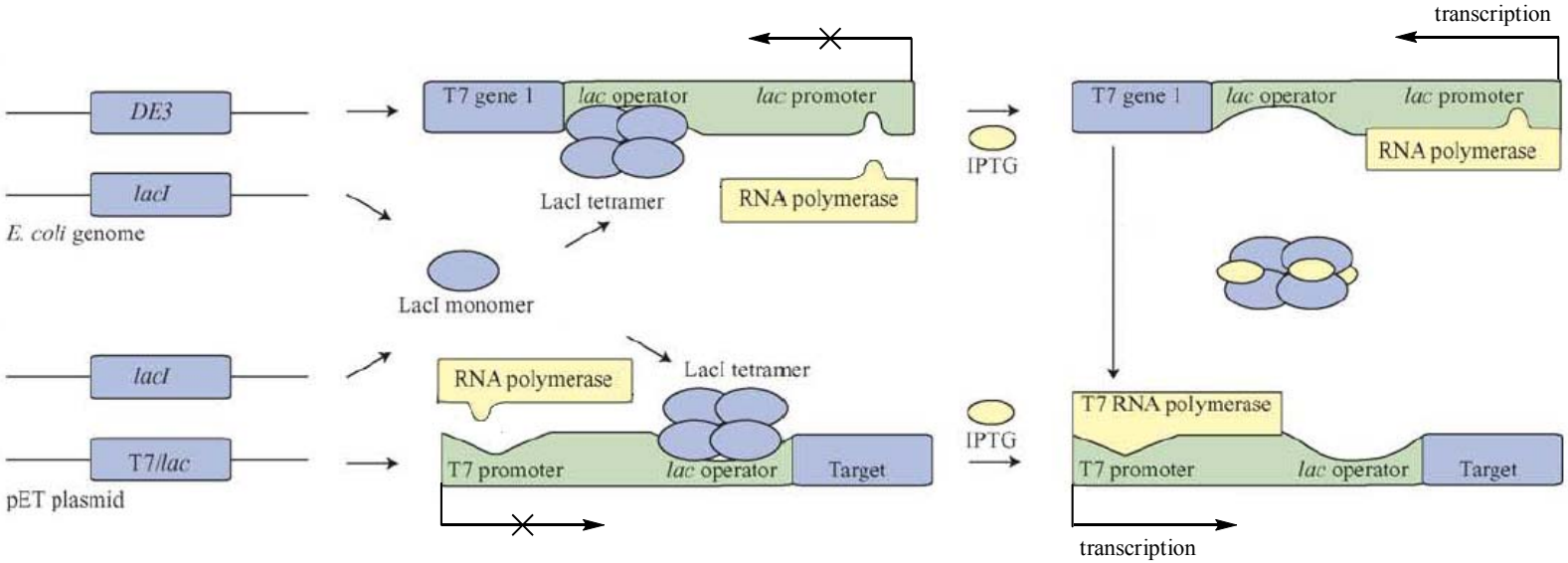

Novagen's pET system offers a wide selection of cloning and expression strategies. Target protein expressed in a pET system could be native or with fusion partner which may optionally be removed via protease cleavage. Using the inducible protein self splicing activity of an intein to remove a purification tag and give pure isolated protein in single chromatography step, the IMPACT-CN system provides a novel cloning and expression strategy for taking advantage of the power of the T7 promoter. Protein splicing is a post-translational processing event involving the excision of an internal protein segment, the intein, from a precursor protein and the concomitant ligation of the flanking N- and C-terminal regions (the exteins) (Perler et al., 1994). Studies revealed that the protein splicing of intein from the *Saccharomyces cerevisiae* VMA1 gene follows four chemical reaction steps (Xu et al., 1993; Chong et al., 1996; Xu and Perler, 1996; Chong et al., 1998): (1) formation of a linear thioester intermediate by an N-S acyl rearrangement at Cys-1 of intein; (2) formation of a branched intermediate by transesterification of the N-terminal extein from the Cys-1 to Cys-455 (the first residue of C-terminal extein); (3) release of the transitory extein ligation product (linked via thioester bond) through peptide cleavage coupled to succinimide formation at Asn-454 of intein; (4) formation of a stable spliced extein (linked by amide bond) by spontaneous S-N acyl rearrangement at Cys-455. Based on these studies, IMPACT-CN vectors have been developed to overexpress the target protein fused with N- or C-terminal of a modified VMA intein protein carrying a chitin binding domain (CBD) (Figure 2-2). In the C-terminal fusion vectors (pTYB1 and pTYB2), the Asn-454 of intein has been

Figure 2-2 The chemical mechanism of the thiol-inducible cleavage reactions catalyzed by the modified VMA intein (adapted from the IMPACT-CN manual). In the N-terminal fusion IMPACT-CN vectors, the CBD is inserted in a loop region of the intein without affecting its splicing and cleavage activity. N-extein contains partial maltose-binding protein to facilitate the translation start for the fusion precursor.

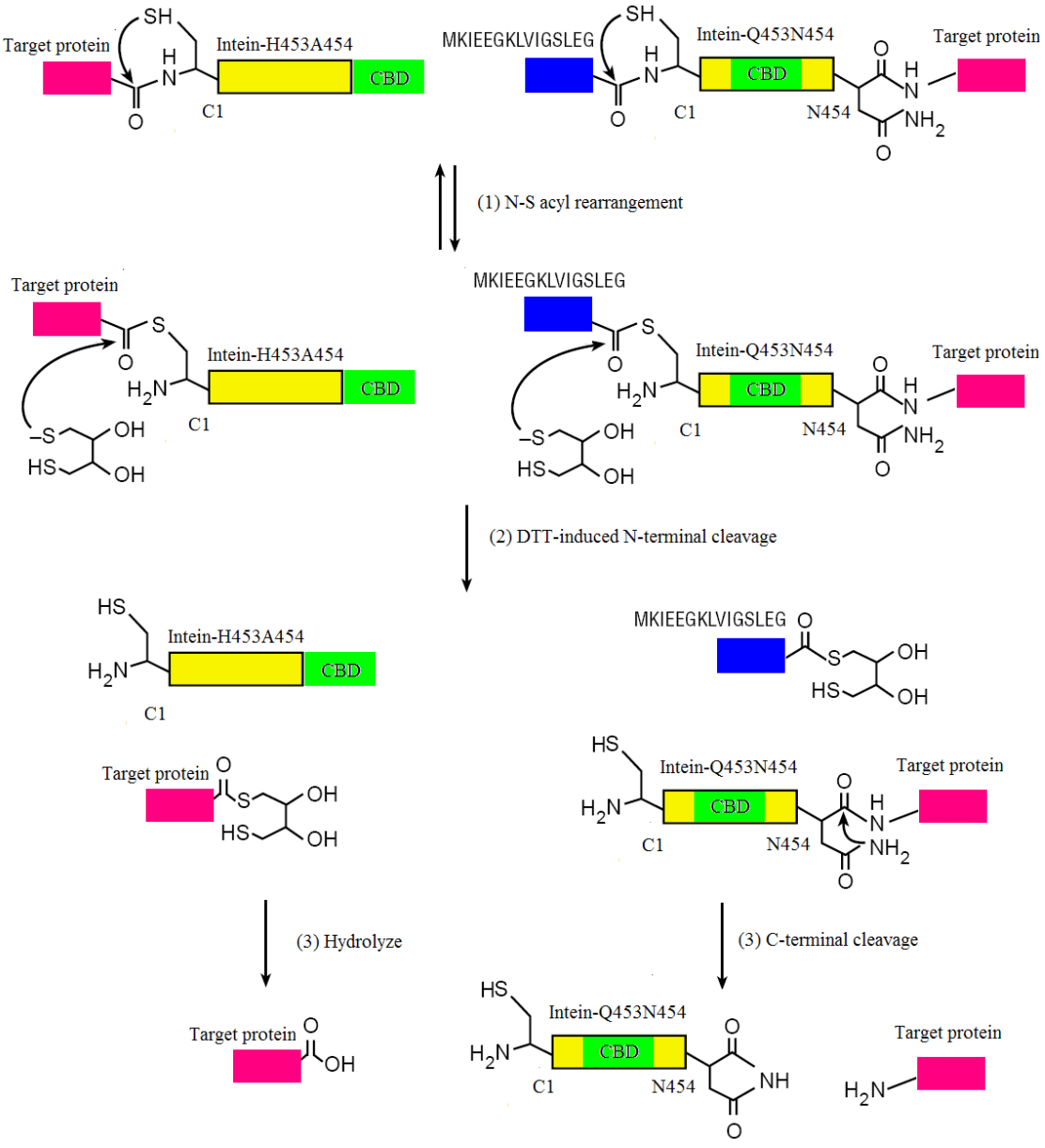

Figure 2-3 A schematic illustration of the IMPACT-CN system (adapted from the IMPACT-CN manual).

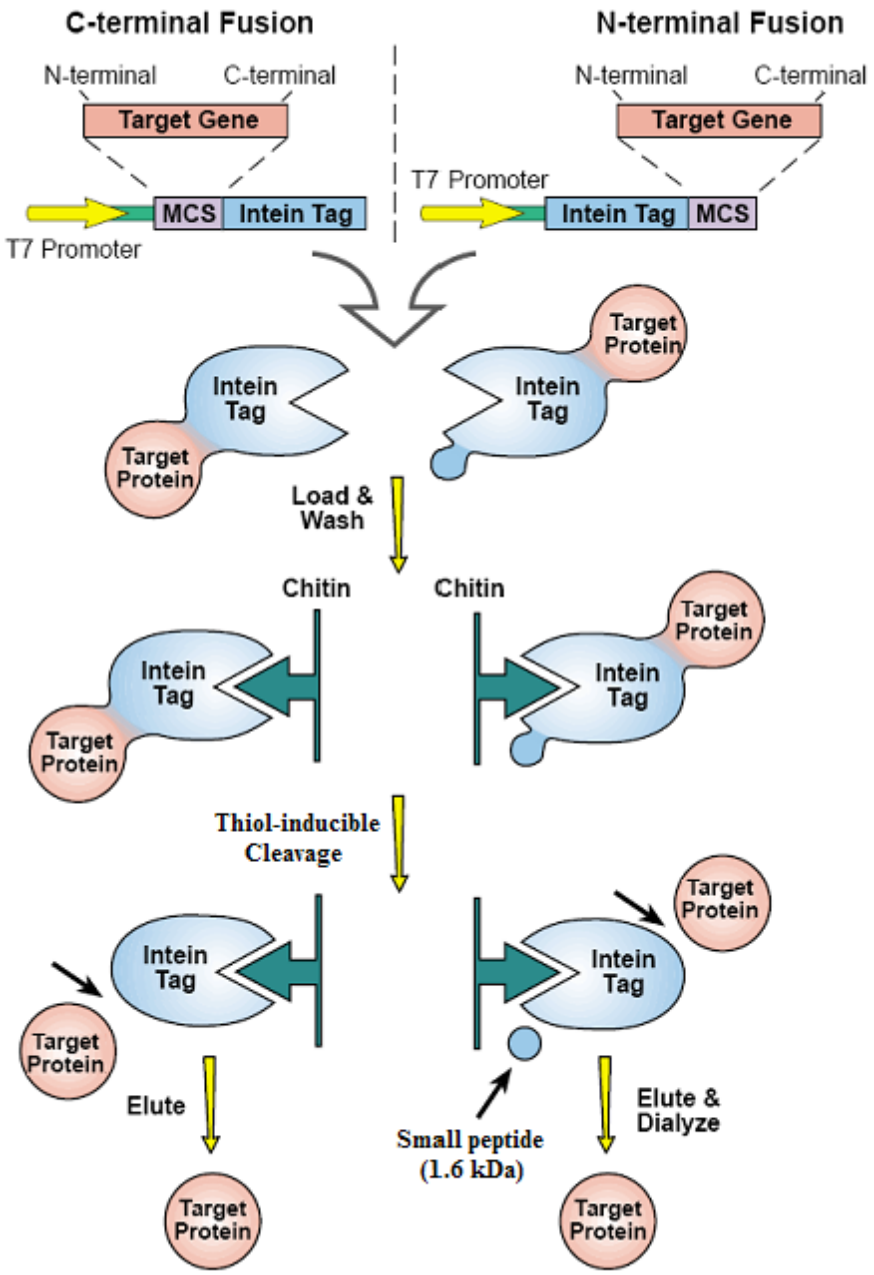

mutated to Ala to block the splicing reaction but still allowing the N-S acyl shift at Cys-1 of the intein. In the N-terminal fusion vectors (pTYB11 and pTYB12), the penultimate His-453 has been changed to Gln to attenuate the succinimide formation at Asn-454. With these modifications, the protein splicing activity of the intein has been converted into efficient, controllable peptide bond cleavage at both termini of the intein. As shown in Figure 2-3, the fusion precursor can specifically bind to the chitin beads while other *E. coli* host proteins are washed away. Soaking with cleavage buffet containing thiols such as DTT, β-mercaptoethanol or cysteine, the intein undergoes specific self-cleavage and releases the target protein. The purity of the recombinant protein from the affinity chromatography is usually very high and no further purification is required.

2. PCR cloning

The procedure for cloning PCR products is shown in Figure 2-4. To direct the insert orientation of target genes, different restriction endonuclease recognition sites allowing generation of sticky ends were incorporated into the PCR forward and reverse primers. The selected restriction sites should be uniquely located in the polycloning sites of the desired vector but not in the target genes. There should be at least 3 bases between the two chosen restriction sites in the desired vector to ensure the cleavage efficiency because many restriction enzymes cleave DNA much less efficiently towards the end of a fragment. Two restriction sites that have comparable digestion conditions (buffer and temperature) are preferred for performing the convenient double digestion of the PCR product. To clone the truncated *plc*A gene for mature PI-PLC into pET-23a(+), an *Nde*I

Figure 2-4 PCR cloning procedure.

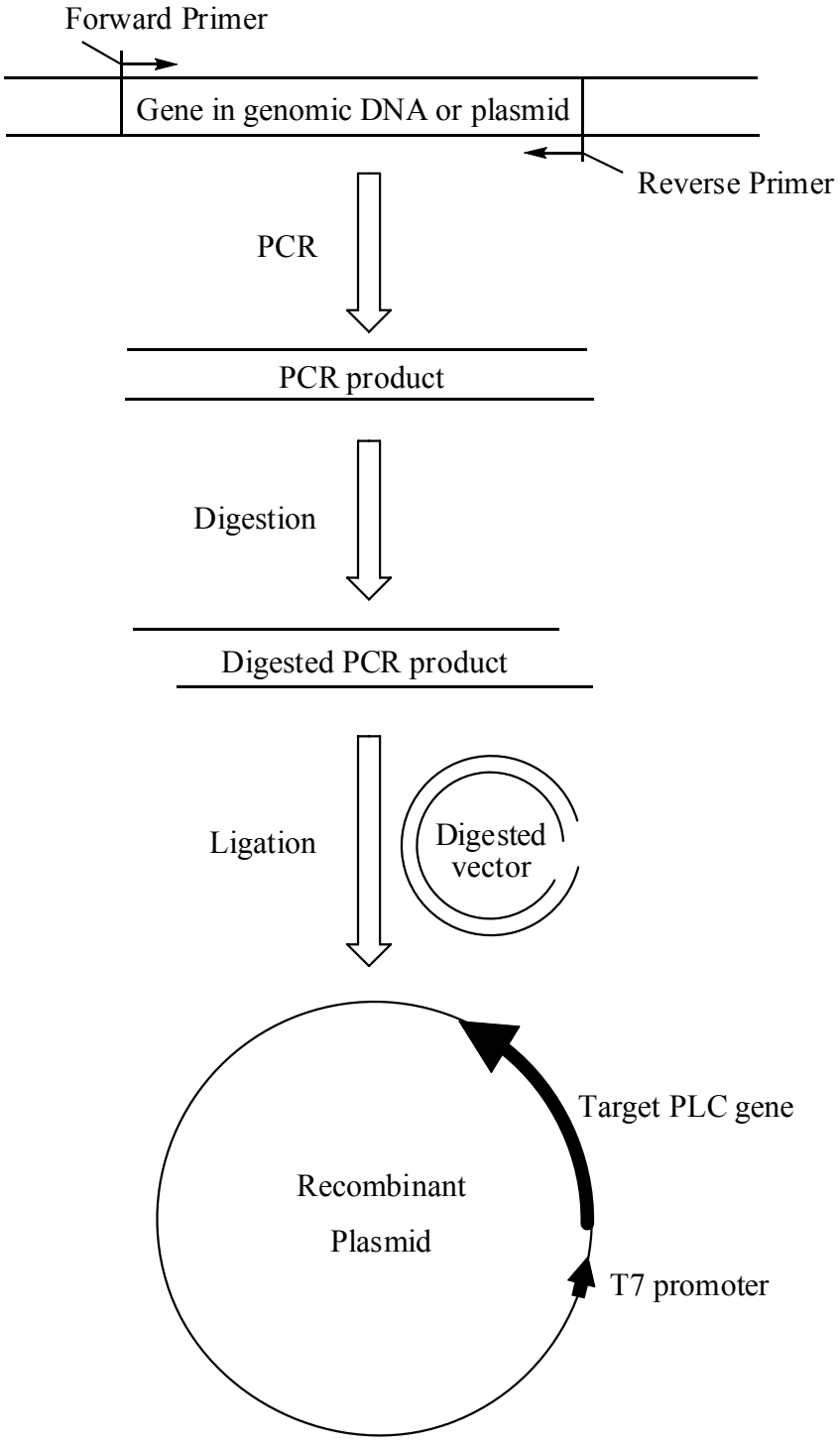

restriction site (catatg) was used in the forward primers as it conveniently contains the start codon (ATG). Primers were designed based on the following guidelines. (1) The 3'-end of primer overlaps with the 5'-end of target gene for forward primer or the antisense strand for reverse primer. The overlap should be long enough (more than 17 bases) to provide specificity of PCR. Although a primer ending in G or C is preferred to increase the efficiency of priming, it is recommended not to have more than three G or C bases at the 3'-end of primer which could stabilize the nonspecific annealing of the primer. A 3'-T should also be avoided as it is more prone to mispriming than other nucleotides. (2) Non-annealing overhang (like a restriction site) can be added to the 5'-end of primer since 5' terminal bases are less critical for primer annealing. A 5' extension of the restriction site with 2-10 bases greatly increases the cleavage efficiency of most enzymes. (3) The GC content of the primer is usually between 40 and 60%. (4) One should make sure the forward and reverse primers do not form a primer dimer (especially no complementary sequences at the 3'-end) or form significant secondary structure. (5) The primer pair should have similar melting temperatures (T_m). The primers used in all of the PCR cloning presented in this thesis are listed in Table 2-1.

Using the designed primers, the target genes were amplified from the pBS1462 by DNA polymerase chain reaction according to *Taq* PCR handbook (annealing temperature was set at 55°C). The PCR result was checked by electrophoresis of 10 µl of the product on a 1% agarose gel. The remaining PCR product was purified directly with a QIAquick PCR Purification Kit and doubly digested at 37°C for 4 hours with two restriction enzymes corresponding to the restriction sites incorporated in the primer pair. Because

the same selective marker (ampicillin resistance) is used in both parent vector (pBluescript II KS) and destination vector (pET-23a(+) or pTYB11), it is necessary to gel-purify the DNA fragment of interest to remove the original plasmid which will transform very efficiently. The desired vector was also doubly digested with the same set of endonucleases. Following vector digestion, it is usually worthwhile to gel-purify the digestion reaction mixture prior to ligation to remove residual nicked and supercoiled plasmid, which transform more efficiently compared to the desired ligation products. The digestion reaction mixtures of PCR product and vector were then electrophoresed on 1% agarose gel containing 1 μg/ml ethidium bromide. The bands with the expected size on the gel were cut and purified using the QIAquick Gel Extraction Kit. T4 DNA ligase was used to perform the ligation of digested-PCR product and digested-plasmid. After incubation at 16°C for 16 hours, the ligation mixture was transformed into NovaBlue *E. coli* competent cells for plasmid propagation and preparation. Positive colonies could be identified by restriction digestion and confirmed by double strand DNA sequencing. The constructed plasmids were then ready for being transformed into the expression competent cells for overexpression.

3. Site-directed mutagenesis

A series of PI-PLC mutants were constructed using Quik-Change™ Site-Directed Mutagenesis Kit. The QuikChange mutagenesis method (Braman et al., 1996) relies on linear amplification of both strands of plasmid template (isolated from dam^+ *E. coli* strains) by thermostable, nonstrand-displacing *PfuTurbo*® DNA polymerase. Extension of mutagenic oligonucleotide primers by the *PfuTurbo*® DNA polymerase generates

mutated plasmid containing staggered nicks. Thus, DNA synthesis always uses the parental plasmid as template, not the newly synthesized strands. The parental plasmid template is eliminated by incubation with *Dpn* I endonuclease which specifically digests DNA methylated at the sequence 5'-Gm^{6}ATC-3'. Because DNA isolated from dam$^+$ *E. coli* strains is dam (DNA-[N^6-adenine] methyltransferase) methylated, but DNA synthesized in vitro is not, *Dpn* I digestion enriches for the mutant plasmid (Nelson and McClelland, 1992). The resulting nicked mutagenic strands are transformed into XL1-Blue supercompetent cells where bacterial ligase repairs the nick and allows normal replication to occur. The four-step procedure of QuikChange mutagenesis method is displayed in Figure 2-5.

Mutagenic primers were designed according to the guidelines provided in QuikChange^{TM} Site-Directed Mutagenesis instructions. (1) Two primers containing the desired mutation (deletion or insertion) are located at the same sequence on opposite strands of the plasmid. (2) The desired mutation should be in the middle of the primer and flanked with more than 10 bases of unmodified nucleotide sequence. (3) The optimal primer should have 25-45 bases in length, at least 40% GC content, and terminal G or C bases. The T_m of primer, calculated with the formula below, is required to be no lower than 78°C. However, primers with lower melting temperature (70°C in our case) also worked. (4) The primer must be purified by polyacrylamide gel electrophoresis (PAGE) or liquid chromatography (e.g. HPLC or FPLC). The primers used in mutations are listed in Table 2-2.

$$T_m = 81.5 + 0.41\ (\%\ GC) - 675 / (\text{primer length in bases}) - (\%\ \text{mismatch})$$

Table 2-1 Primers used for cloning with restriction endonuclease recognition sites in capital letters and DNA fragments from the target gene underlined. Plasmid marked with * contains a stop codon (TGA) in the place of the codon for Trp-35 of PI-PLC precursor.

Template	Primers	Plasmid
pBS1462*	*Xba*I forward primer 5'-ggTCTAGAttctagtcctgctgtcc-3'	pET1339*
	*EcoR*I reverse primer 5'-ttgtaggaataaGAATTCttagttgaatttattgttttttatg-3'	
	*Xba*I forward primer 5'-ggTCTAGAttctagtcctgctgtcc-3'	pET1462*
	*Sal*I reverse primer 5'-ggaataatatGTCGACcagctcttcttggtgaag-3'	
	*Nde*I forward primer 5'- ttttatactttCATATGttcccattaggcggaaaagcatattc-3'	pET-F*
	*EcoR*I reverse primer 5'-ttgtaggaataaGAATTCttagttgaatttattgttttttatg-3'	
	*Nde*I forward primer 5'-ttttatactttCATATGtattcgcttaataactgaaataag-3'	pET-Y*
	*EcoR*I reverse primer 5'-ttgtaggaataaGAATTCttagttgaatttattgttttttatg-3'	
pBS1462-1w	*Nde*I forward primer 5'- ttttatactttCATATGttcccattaggcggaaaagcatattc-3'	pET-F-1w
	*EcoR*I reverse primer 5'-ttgtaggaataaGAATTCttagttgaatttattgttttttatg-3'	
	*Nde*I forward primer 5'-ttttatactttCATATGtattcgcttaataactggaataag-3'	pET-Y-1w
	*EcoR*I reverse primer 5'-ttgtaggaataaGAATTCttagttgaatttattgttttttatg-3'	
	*Sap*I forward primer 5'-ggtggttGCTCTTCcaacttcccattaggcggaaaag-3'	IMPACT-F
	*EcoR*I reverse primer 5'-ttgtaggaataaGAATTCttagttgaatttattgttttttatg-3'	
	*Sap*I forward primer 5'-ggtggttGCTCTTCcaactattcgcttaataactggaataag-3'	IMPACT-Y
	*EcoR*I reverse primer 5'-ttgtaggaataaGAATTCttagttgaatttattgttttttatg-3'	

Figure 2-5 QuikChange site-directed mutagenesis method (adapted from manufacturer's instructions). The annealing temperature was set as 68°C for *L. monocytogenes* PI-PLC.

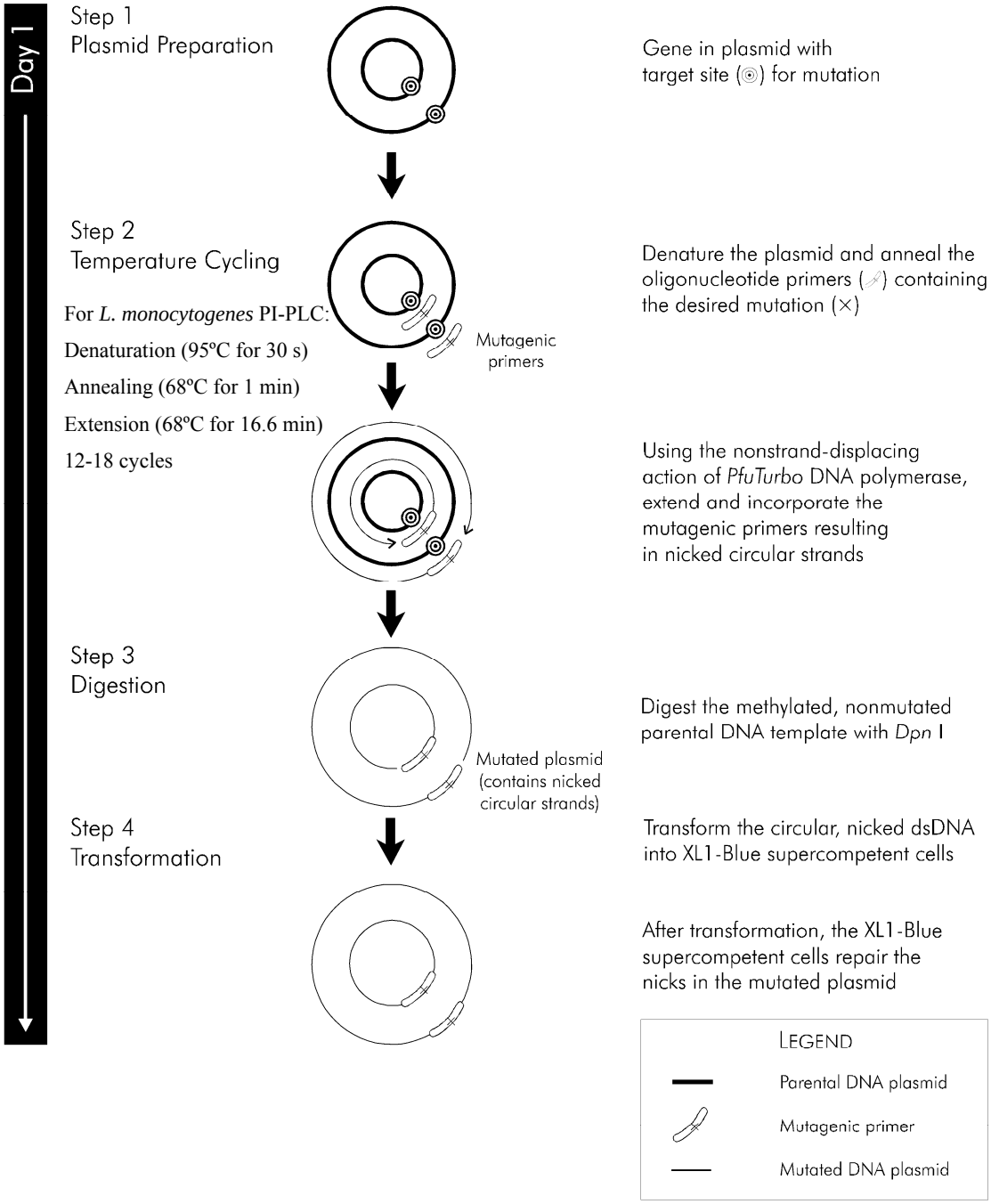

Table 2-2 Primers used for mutagenesis with the codon for desired mutations in capital letters and substitution bases underlined. Mutants are numbered from Tyr-30 of the PI-PLC precursor.

Template	Primers	Plasmid
pBS1462	5’-ggcggaaaagcatattcgcttaataac**TG<u>G</u>**aataagccaat-3’	pBS1462-1w *6W
	5’-attggcttatt**<u>C</u>CA**gttattaagcgaatatgcttttccgcc-3’	
IMPACT-Y	5’-cggagacatgacg**<u>GC</u>G**acattaaccaaaccactgg-3’	IMPACT-Y W49A
	5’-ccagtggtttggttaatgt**C<u>GC</u>**cgtcatgtctccg-3’	
IMPACT-Y	5’-ggagacatgacgtgg**<u>GG</u>A**ttaaccaaaccactgg-3’	IMPACT-Y T50G
	5’-ccagtggtttggttaa**T<u>CC</u>**ccacgtcatgtctccg-3’	
IMPACT-Y T50G	5’-ggagacatgacgtgg**<u>T</u>G<u>C</u>**ttaaccaaaccactgg-3’	IMPACT-Y T50C
	5’-ccagtggtttggttaa**G<u>C</u>A**ccacgtcatgtctccg-3’	
IMPACT-Y	5’-ggagacatgacgtggaca**<u>GC</u>A**accaaaccactgg-3’	IMPACT-Y L51A
	5’-ccagtggtttggt**T<u>GC</u>**tgtccacgtcatgtctcc-3’	
IMPACT-Y	5’-gcgccacttca**<u>GC</u>A**acattcacacctcgtcag-3’	IMPACT-Y L235A
	5’-ctgacgaggtgtgaatgt**T<u>GC</u>**tgaagtggcgc-3’	
IMPACT-Y	5’-gcgccacttcatta**<u>GG</u>A**ttcacacctcgtcag-3’	IMPACT-Y T236G
	5’-ctgacgaggtgtgaa**T<u>CC</u>**taatgaagtggcgc-3’	
IMPACT-Y T236G	5’-gcgccacttcatta**<u>T</u>G<u>C</u>**ttcacacctcgtcag-3’	IMPACT-Y T236C
	5’-ctgacgaggtgtgaa**G<u>C</u>A**taatgaagtggcgc-3’	
IMPACT-Y	5’-gcgccacttcattaaca**T<u>GG</u>**acacctcgtcag-3’	IMPACT-Y F237W
	5’-ctgacgaggtgt**<u>CC</u>A**tgttaatgaagtggcgc-3’	
IMPACT-Y	5’-gcgccacttcattaaca**<u>GC</u>C**acacctcgtcag-3’	IMPACT-Y F237A
	5’-ctgacgaggtgt**<u>GG</u>C**tgttaatgaagtggcgc-3’	
IMPACT-Y W49A	5’-gcgccacttcattaaca**<u>GC</u>C**acacctcgtcag-3’	IMPACT-Y W49A/F237A
	5’-ctgacgaggtgt**<u>GG</u>C**tgttaatgaagtggcgc-3’	

The mutagenesis was performed following the protocol in the manual with modifications. Briefly, 5-50 ng of the double-stranded, supercoiled plasmid template and 125 ng of mutagenic sense and antisense primers (an excess concentration of primers should be used during the temperature cycling) were added in a 50 µl reaction mixture containing deoxyribonucleotides, reaction buffer, and *PfuTurbo*® DNA polymerase. The cycling parameters were set according to the manufacturer's recommendations except the suggested annealing temperature (55°C) was increased to that used in extension (68°C) to avoid the effect of primer dimer formation. The cycling condition used was denaturation at 95°C for 30 s, annealing at 68°C for 1 min and extension at 68°C for 16.6 min, with 12-18 cycles. The linear amplification product was treated with *Dpn* I for 1 h at 37°C and transformed into XL1-Blue supercompetent cells for plasmid propagation and preparation. The QuikChange™ Site-Directed Mutagenesis Kit works for simultaneously changing at most two bases of IMPACT-Y may be due to the large size of IMPACT-Y (8243 bp). Stepwise mutagenesis was applied if all three bases of a codon had to be changed (the revised manual suggests QuikChange® XL Site-Directed Mutagenesis Kit for large targets ~8 kb). By using high fidelity *PfuTurbo*® DNA polymerase, low cycle number (12-18), and primers designed only to copy the parental strands in a linear fashion, unwanted mutations were minimized. All mutants were confirmed with double strand DNA sequencing (done by Sequegen Company).

4. Transformation

The $CaCl_2$ method was used for transformation of *E. coli* cells. 1 µl plasmid (isolated with QIAprep Spin Miniprep kit) or 1 µl *Dpn* I-treated mutagenesis reaction mixture or 10 µl ligation reaction mixture was mixed gently with 50-100 µl competent cells and incubated on ice for 30 min. The transformation mixture was then heat shocked at 42°C for 30-45 sec according to the competent cell used and the incubated on ice for 2 min. 500 µl fresh LB or NZY^+ media without antibiotics was added and the cells were grown at 37°C in a Rollerdrum for 1 hour. After incubation, 200 µl of the mixture was spread on LB agar plate containing appropriate antibiotics and incubated overnight at 37°C.

5. Plasmid DNA isolation

Plasmid preparations were performed with QIAprep Spin Miniprep Kit following the protocol using a microcentrifuge. DNA was eluted with water at the final step, quantified via spectrophotometric measurement of UV absorption at 260 nm, and stored at -20°C.

B. Overexpression and purification of recombinant *L. monocytogenes* PI-PLC

1. Expression of recombinant PI-PLC cloned in pET-23a(+)

The recombinant plasmid pET1339 (or pET1462, pET-F-1w, and pET-Y-1w) was transformed into several BL21 *E. coli* host strains (BL21(DE3), BL21(DE3)pLYsS, BL21-CondonPlus(DE3)-RIL, or BL21-CodonPlus(DE3)-RP) for expression. A single colony of transformed BL21 *E. coli* cell was grown in 5 ml of LB medium in the

presence of 100 μg/ml ampicillin and 34 μg/ml chloroamphenicol (not added for transformed BL21(DE3) cells) overnight at 37°C. An aliquot (2 ml) of the overnight culture was used to inoculate 2 L fresh LB medium with the antibiotics in a rotary shaker (200 rpm) at 37°C. Expression of recombinant PI-PLC was induced by adding IPTG at a final concentration of 0.4 mM when the growing culture reached an optical density between 0.6 and 0.8 at 600 nm. The culture was incubated at 37°C for 3 h or 30°C for 8 h after induction.

To check the expression of recombinant PI-PLC in BL21 *E. coli* strains, cells were harvested by centrifugation at 5,000 rpm for 10 min, resuspended in 20 ml ice-cold buffer containing 20 mM Tris-HCl, pH 7.0, and lysed by sonication on ice for 10 × 30 s. Cell debris was separated from the supernatant by centrifugation at 15,000 rpm for 30 min and dissolved in 10 ml ice-cold Tris-HCl buffer containing 1% SDS (pH 7.0). 200 ml of cell culture medium (with the cells removed) was concentrated to ~1 ml using a Millipore Centriprep YM-10. No PI hydrolysis activity was detected in the cell extract supernatant, solubilized cell debris, or concentrated culture medium. SDS-PAGE analysis of them did not show obvious overexpression of a protein band with 33 kDa molecular mass. So we abandoned further attempts on purification.

2. Overexpression and purification of recombinant PI-PLC cloned in pTYB11

The recombinant plasmid IMPACT-F or IMPACT-Y was transformed into ER2566 competent cells for expression. A single colony of ER2566 containing the recombinant plasmid was grown in 5 ml of LB medium in the presence of 100 μg/ml ampicillin overnight at 37°C. An aliquot (5 ml) of the overnight culture was used to

inoculate 2 L fresh LB medium with the antibiotic in a rotary shaker (200 rpm) at 37°C. Expression of recombinant PI-PLC was induced by adding IPTG at a final concentration of 0.8 mM when OD_{600} of growing culture was between 0.7 and 0.8. After induction, the culture was incubated at 16°C for 20 h. The expression of recombinant PI-PLC in ER2566 was checked in the same way used to test that in BL21 *E. coli* strains. The cell extract supernatant of ER2566 harboring IMPACT-Y had high PI-PLC activity, albeit no obvious band of 88 kDa on SDS-PAGE gel. To obtain the homogeneous PI-PLC, the ER2566 cells containing IMPACT-Y were harvested by centrifugation (5,000 rpm for 10 min) and stored at -80°C until needed.

The frozen cell pellets from 2 L culture were thawed at room temperature, resuspended in 50 ml ice-cold column buffer (20 mM Tris-HCl, 0.5 M NaCl, pH 8.4), sonicated for 10 × 30 s on ice, and centrifuged at 15,000 rpm for 30 min to remove the cell debris. The cell extract supernatant was loaded slowly (0.4 ml/min) onto an affinity column of chitin beads (~20 ml) equilibrated with 200 ml column buffer. After loading, the chitin column (2.5 cm × 20 cm) was washed sequentially with 20 ml column buffer at 1 ml/min, at least 200 ml washing buffer (20 mM Tris-HCl, 1 M NaCl, pH 8.0) at 2 ml/min to thoroughly remove the unbound contaminants, and 60 ml cleavage buffer (20 mM Tris-HCl, 0.5 M NaCl, 50 mM DTT, pH 8.4) at 2 ml/min. The on-column cleavage of fusion protein was allowed to proceed at room temperature for 20 h. Cleaved PI-PLC protein was eluted from the column with 200 ml dialysis buffer (20 mM Tris-HCl, pH 7.0). Fractions containing PI-PLC activity (usually the first 50 ml) were pooled, dialyzed twice at 4°C to remove co-eluted DTT, salts and a small peptide (1.6 kDa), passed

through a 0.22 μm filter, and concentrated using Millipore Centriprep YM-10 to 1-10 mg/ml. All protein concentrations were determined by Lowry assay (Lowry et al., 1951). The best yield for recombinant *L. monocytogenes* PI-PLC was about 6 mg/L. The stock solution can be stored at 4°C without activity loss for ~1 month.

The SDS-PAGE analysis (Figure 3-11) showed that the purity of PI-PLC after the chitin column was more than 85% and that PI-PLC was contaminated with a band around 50 kDa, which should be the intein tag judging from the SDS-PAGE gel of chitin beads after elution of PI-PLC. If needed, a SP Sepharose Fast Flow column (1.5 cm × 15 cm) was used to further purify PI-PLC right after dialysis. The dialyzed eluate from the chitin column was applied at 2 ml/min onto the strong cation exchange column (~25 ml) equilibrated with 100 ml starting buffer (50 mM sodium phosphate buffer, pH 7.0). The protein was eluted using a NaCl gradient ranging from 0 to 0.5 M in 50 mM sodium phosphate (pH 7.0) at rate of 2 ml/min, dialyzed to remove the high salts, filtered and concentrated. Only the PI-PLC band was observed on the SDS-PAGE gel after these two columns.

C. Chemical modification of lysine residues of *L. monocytogenes* PI-PLC

1. Citraconic Anhydride modification

Modification was carried out using citraconic anhydride as a specific blocking agent for lysine residues. As depicted in Figure 2-6, chemical modification of PI-PLC with citraconic anhydride changes the positive charges of lysine residues on the protein

Figure 2-6 The reaction of citraconic anhydride with an amine-containing molecule at pH 8 and followed by deblocking of the amine at pH 3-4 (adapted from manufacturer's instructions).

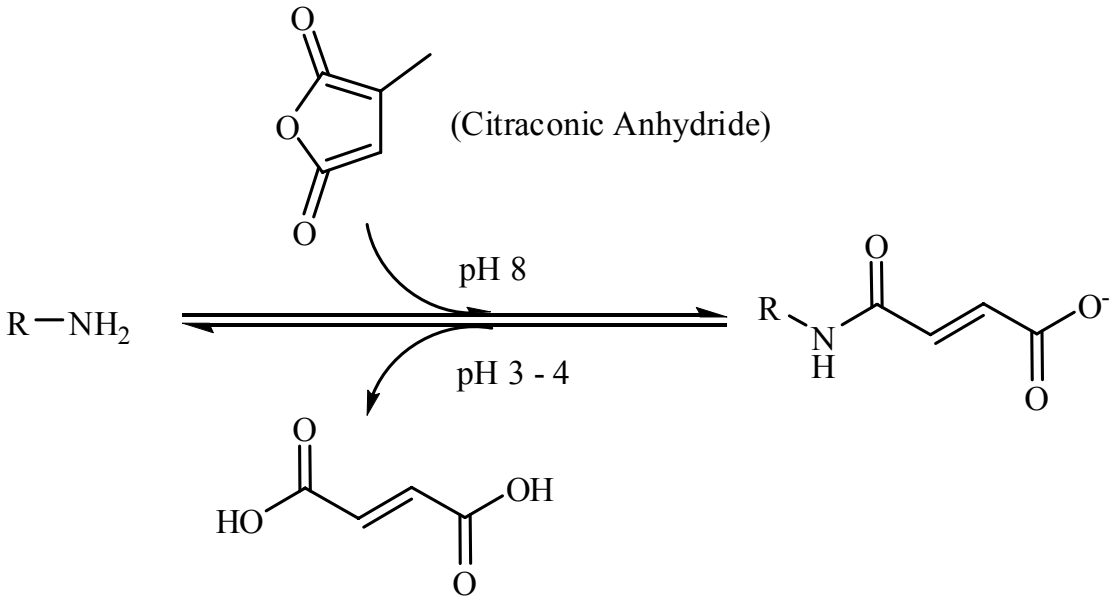

surface to negative ones. Sodium phosphate, 0.5 M at pH 8.5, was used to provide adequate buffer capacity. The PI-PLC to be modified was purified with two columns (chitin column and SP Sepharose Fast Flow column), dialyzed against reaction buffer, and concentrated. 200 µl PI-PLC (6.5 mg/ml) was incubated with 1 µl to 50 µl citraconic anhydride (113 mM, diluted with reaction buffer) in 1 ml of reaction buffer at room temperature for 3 h. The pH of the reaction mixture was monitored and remained stable at 8.5 during the reaction. The reaction mixture was then dialyzed extensively against 20 mM Tris-HCl (pH 7.0) to quench the reaction. The Tris containing a primary amino group, reacts with the excess citraconic anhydride, and changes the stock buffer for PI-PLC.

2. Two-dimensional gel electrophoresis

The charge heterogeneity of citraconic anhydride modified PI-PLC was checked using two-dimensional polyacrylamide gel electrophoresis with immobilized pH gradients (IPG-Dalt) (Görg et al., 1988; Görg, 1998). The first dimension, isoelectric focusing (IEF), was performed in ReadyStrip IPG gel strips (pH gradient 3-10, 11 cm) using sample in-gel rehydration. Protein, 200 µl in rehydration buffer (9M urea, 4% CHAPS, 15 mM DTT, 0.2% Bio-Lyte, and traces of bromophenol blue crystals) was loaded onto the middle of an IPG strip which was then covered with mineral oil and rehydrated on a Bio-Rad Protean IEF cell under active condition at 20°C for 12 h. The strips were run with the following 4-step program (all steps with a current limit of 50 µA per gel): 250 V, linear ramp for 15 min; 8,000 V, linear ramp for 2.5 h; 8,000 V, for a total of 35,000 V-hr; and 500 V, for hold. To prepare for the second dimension, the strips

were removed from the focusing tray, equilibrated with buffer containing 6 M urea, 2% SDS, 0.375 Tris-HCl, pH 8.8, 20% glycerol, and DTT or β-mercaptoethanol, washed with electrophoresis running buffer (25 mM Tris-base, 200 mM glycine, 0.1% SDS), layered on 4-20% Criterion Tris-HCl gradient Precast Gels, and embedded in place with 0.5% agarose melted in the electrophoresis running buffer. Electrophoresis was performed at 90 V for ~2.5 h until the dye front ran off the gel. Gels were then stained overnight with Coomassie Brilliant Blue.

D. Determination of *L. monocytogenes* PI-PLC native molecular weight

1. Gel filtration

Gel filtration was carried out at room temperature on a Sephadex G-100 column (1.5 cm × 75 cm). Sephadex G-100 resin (~ 8 g of 40-120 μm particle size, 15-20 ml/g bed volume, 4-150 kDa fractionation range) was hydrated with boiling deionized water (passed through a 0.2 μm filter) for 3 h, degassed gently after decanting the very fine particles, and packed at 1 ml/min. The column was equilibrated with 50 mM Tris-HCl, pH 7.0 and 0 or 500 mM NaCl buffer. The void volume was measured with Blue Dextran (2,000 kDa), and the column was calibrated with sweet potato β-amylase (200 kDa), yeast alcohol dehydrogenase (150 kDa), bovine serum albumin (66 kDa), bovine erythrocyte carbonic anhydrase (29 kDa), and horse heart cytochrome c (12.4 kDa). The protein sample (0.5 ml) was loaded onto the column and eluted with the same buffer used for equilibration at a flow rate of 0.3 ml/min. The eluate was monitored with an on-column UV detector at 280 nm and collected in 1 ml fractions. A plot of log molecular

mass vs. elution volume should be linear over the useful fractionation range of gel for roughly spherical proteins.

2. Acidic nondenaturing acrylamide gel electrophoresis

Standards and *L. monocytogenes* PI-PLC (~5μg of each) mixed with 64 mM acetate-KOH buffer (pH 6.8) containing 37% glycerol and traces of methyl green were electrophoresed on polyacrylamide mini slab gels based on an acidic-native gel protocol for basic proteins (http://wolfson.huji.ac.il/purification/Protocols/PAGE_Acidic.html) in which the acetate-KOH buffer was used to prepare the gels. The pH of the separating gel was 4.3 while that of stacking gel was 6.8. The electrophoresis running buffer (pH 4.3) consisted of 0.35 M β-alanine and 0.14 M acetate. Three commercially available basic proteins, lentil lectin (98 kDa), chicken egg white lysozyme (14.3 kDa), and bovine pancreas α-chymotrypsinogen (25.6 kDa), were used as standards. With the power polarity reversed, the electrophoresis was conducted at a constant voltage of 120 V in the cold room (4°C) until the dye front approached the bottom of the gel (~1 h). The positions of methyl green were marked and the gels were stained with Coomassie Brilliant Blue overnight. Plots of protein relative mobility versus acrylamide concentration (7, 10, 12 and 15%), provided a negative slope that varied linearly with the molecular weight. The standard curve from this slope was used to extract a native mass for *L. monocytogenes* PI-PLC.

3. Laser light scattering

L. monocytogenes PI-PLC after the two-column purification was sent to HHMI Biopolymer Facility and W. M. Keck Foundation Biotechnology Resource Laboratory to determine native protein molecular weights by laser light scattering (LS) (Folta-Stogniew and Williams, 1999). The chromatography mode in which coupled size exclusion chromatography (SEC) serves solely as a fractionation step was first applied. Three detectors (LS, UV, and refractive index (RI)) are connected in series after the SEC column. The UV profile of the eluate (Figure 2-7) indicated that protein interacted with the column matrix dramatically and only a very small portion (~2%) protein was eluted at a retarded time (~20 ml, the region where small species, e.g. DTT, are normally eluted). The remaining protein sample was thus analyzed by micro-batch approach in which the sample from an injector loop was flown through the system to collect UV/LS/RI signals while the buffer was continuously delivered from the HPLC system. Conditions (1.1 ml protein sample, 500 μl sample loop, and 0.3 ml/min for 1 min 20 sec) were established to provide a reading "plateau" (~0.2 ml, free of air and particle) in all three detectors (Figure 2-7). Transferrin with a comparable extinction coefficient to *L. monocytogenes* PI-PLC was used as a standard and the same calibration constant was applied to analyze the PI-PLC sample. The concentrations of PI-PLC during the reading plateau were measured with the UV absorbance at 280 nm (extinction coefficient=33710 $M^{-1} \cdot cm^{-1}$, 1 cm length). The molecular weight was determined by solving the equation (Wyatt, 1993) that relates the excess scattered light to the concentration of solute and the weight-

Figure 2-7 Light scattering analysis of *L. monocytogenes* PI-PLC. (A) UV trace (absorbance at 280 nm) of eluent from LS-SEC/UV/RI analysis; (B) UV traces of PI-PLC and transferrin from LS micro-bath analysis; (C) LS traces of PI-PLC and transferrin, detected at 90° angle, from LS micro-bath analysis.

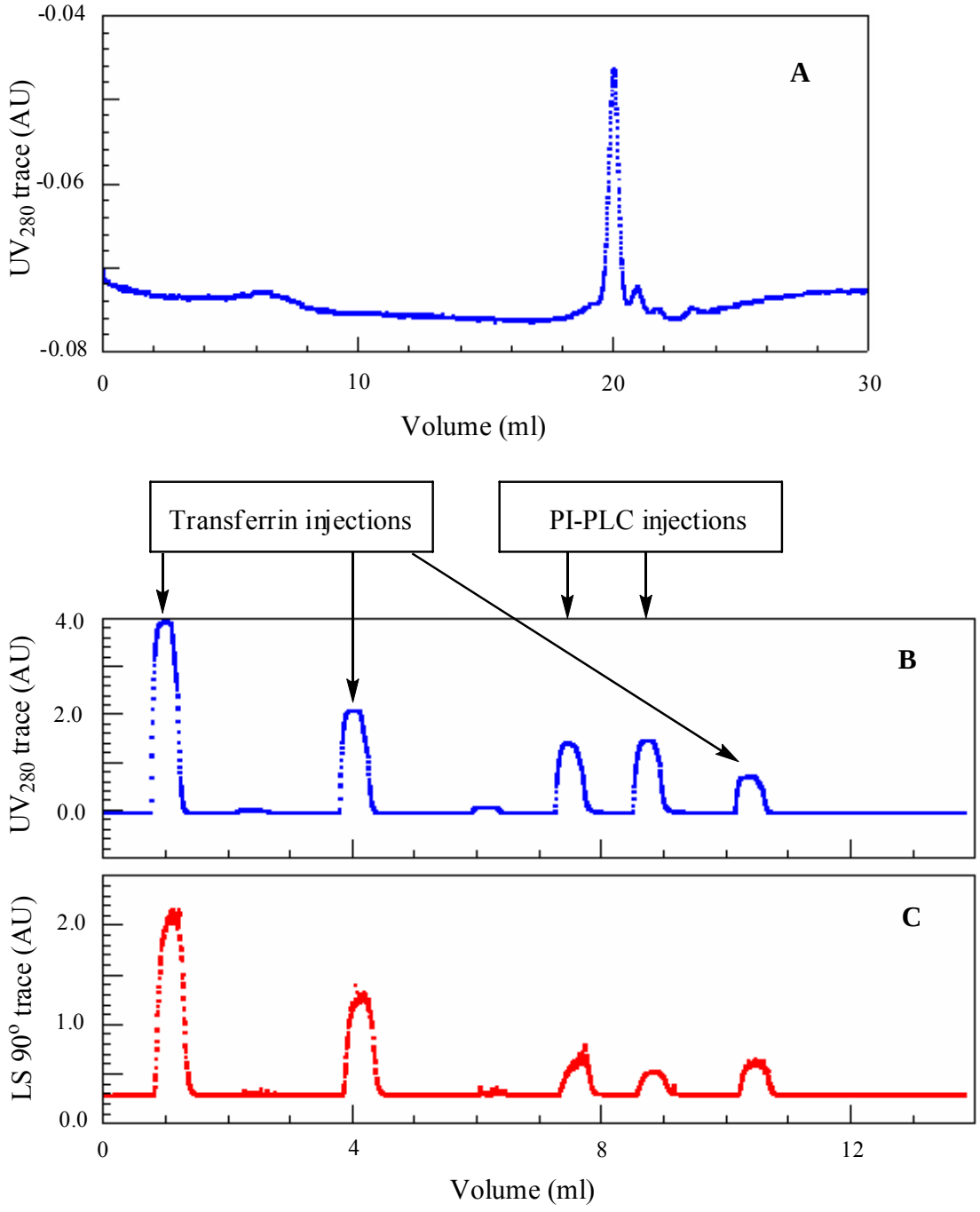

average molecular weight by ASTRA calculations (http://info.med.yale.edu/wmkeck/6_16_98/Astra2a.htm#Calculation of MW by).

E. Enzymatic synthesis and purification of cIP

Crude soybean PI (50%) was used for the enzymatic generation of cIP as described previously (Zhou et al., 1997a) by taking the advantage of the fact that the phosphotransferase (PI cleavage) activity is much higher than the phosphodiesterase (cIP hydrolysis) activity for bacterial PI-PLC. The reaction condition was modified for *L. monocytogenes* PI-PLC. One gram of crude PI was dissolved overnight in 15 ml of 50 mM Tris-HCl, pH 7.0, containing 220 mM Triton X-100 and 150 mM NH_4Cl (this salt was added to activate the PI cleavage but inhibit the cIP hydrolysis by *L. monocytogenes* PI-PLC). Enzyme (20 μg) was added and the reaction progress (at 25 °C) was monitored using ^{31}P NMR spectroscopy. After the PI was mostly hydrolyzed to cIP (when the height of the cIP peak no longer increased), further reaction (e.g., hydrolysis of cIP to I-1-P) was quenched by the addition of chloroform. The lipids (DAG and unhydrolyzed PI) in the reaction mixture were then extracted from the aqueous phase with a chloroform-methanol (about 4:1) solution. Typically, a clear aqueous phase could be achieved after 4 to 6 extractions. cIP stayed in the aqueous phase and was purified using an AG 1-X8 (formate form, 100-200 mesh) anion exchange column (1.5 cm × 20 cm). AG 1-X8 resin, 10 g, was suspended in deionized water and packed in the column at 2 ml/min. The aqueous phase from the extraction was then applied, the column was eluted with 60 mM ammonium formate buffer (~pH 7.4) at a flow rate of 1 ml/min, and 5-ml fractions were collected. The fractions containing cIP (detected by ^{31}P NMR) were lyophilized to

remove ammonium formate. Typically, 100 mg of pure cIP could be obtained from 1 g crude PI.

F. Vesicle preparation

Lipid stock solution supplied in chloroform was placed in a 20 ml glass scintillation vial, and the chloroform was removed with a rotary evaporator. The resulting lipid film was dissolved in 5 ml water, frozen on dry ice, lyophilized overnight, and rehydrated with appropriate buffer. Lipids supplied as powder were dissolved in the buffer directly. To prepare small unilamellar vesicles, the chilled phospholipids suspensions were sonicated on ice using a Branson sonifier W-150 ultrasonic cell disruptor with a 1-cm-diameter probe until maximum clarity was achieved (with 1-min on, 1-min off cycle). Vesicles were centrifuged in a bench-top centrifuge (14,000 rpm for 3 min) to remove residual titanium particles.

G. PI-PLC activity assay

The specific activity of PI-PLC was measured using ^{31}P NMR spectroscopy (at 202.3 MHz on a Varian Inova 500 spectrometer). NMR parameters were based on those previously reported (Volwerk et al., 1990; Zhou et al., 1997a) with some modifications. A 8.5 μs pulse width (90°), 14998 Hz sweep width, and variable number of transients were used. Two types of assays (end-point and continuous time point) were used for phosphotransferase activity (PI as substrate) and phosphodiesterase activity (cIP as substrate) respectively. Except for diC_4PI, experiments were run in duplicate, the average specific activities were reported (typical errors <15%).

For long chain PI from bovine liver (8 mM) dispersed in diC_7PC or Triton X-100 micelles, or in SUVs in the absence and presence of POPC in 50 mM HEPES, pH 7.0, containing 0.5 mg/ml BSA, enzyme (between 0.01 and 7.2 μg/ml) was added to the 200 μl assay mixture and incubated at 25°C. The reaction was quenched by the addition of 400 μl chloroform at appropriate incubation times (from 1 min to a few hours) which were chosen so that less than 20% PI cleavage occurred. The protein concentrations were kept constant within the same series of assays as protein concentration also affects the activity of *L. monocytogenes* PI-PLC. The cIP content in the aqueous phase (separated from the organic layer using centrifugation at 14,000 rpm for 6 min) was quantified in the ^{31}P NMR spectrum using added glucose-6-phosphate (1 mM) as an internal standard (Figure 2-8A). Triton X-100 and salt effects were also measured using the water-soluble substrate diC_4PI. In this assay, 100 μl assay mixture containing 2 mM diC_4PI and 1.6 μg/ml enzyme were used. PI-PLC activities toward diC_8PI and the 3-deoxy-diC_8PI derivatives were also measured with the end-point assay. The assay buffer for the recombinant *L. monocytogenes* PLC was 50 mM Tris-HCl, 0.5 mg/ml BSA, pH 7.0, and incubation was at 28˚C. For the recombinant PLCδ1, the assay buffer was 50 mM Tris-HCl, 0.5 mM $CaCl_2$, pH 7.5, and incubation was at 34˚C.

In the continuous time point assay for cIP hydrolysis, the release of I-1-P product was monitored as a function of time until 20% of the cIP was converted to I-1-P using a ^{31}P NMR experiment where the pre-acquisition delay (pad) was arrayed (Figure 2-8B). A control spectrum was acquired prior to the addition of enzyme (t=0 min). The reaction was initiated by adding 3.6 or 7.2 μg/ml PI-PLC to 400 μl assay mixture in a NMR tube

typically containing 10 mM cIP in the absence and presence of different additives (diC_7PC, POPC, DOPMe, POPS, salts) in 50 mM imidazole buffer (pH 7.0), incubated at 25°C, and monitored for a period of time, typically from at least 30 minutes to a few hours. The rate of cIP hydrolysis was calculated from the slope of I-1-P production as a function of incubation time. The I-1-P concentration at various time points was calculated from the ratio of I-1-P to cIP since the total amount of I-1-P and cIP equals to that of starting cIP.

H. PI3K activity assay

PI3K (2 μg) was added to a reaction mixture containing 50 mM Tris-HCl, pH 7.5, 0.1 mg/ml BSA, 50 mM NaCl, 5 mM $MgCl_2$, 2 mM ATP, 1 mM diC_8PI and 0 to 3 mM of the 3-deoxy-diC_8PI analogues. The reaction was incubated at 22˚C for 3 h and stopped by the addition of 10 mM EDTA. The phosphorylation on O-3 of PI and PI analogues was monitored by ^{31}P NMR spectroscopy using the NMR resonance of the phosphate attached to the glycerol backbone as an internal standard. If PI(5)P was included in the reaction mixture, the contribution of the phosphate at O-5 (calculated from the ratio of it to the phosphate attached to glycerol) was considered to calibrate the activity as the phosphate peaks at O-3 and O-5 were not separated well under the assay condition (Figure 2-8C).

Figure 2-8 NMR spectra for the activity assays of (A) the PI-PLC phosphotransferase reaction, (B) the PI-PLC cyclic phosphodiesterase reaction, and (C) the PI3K reaction.

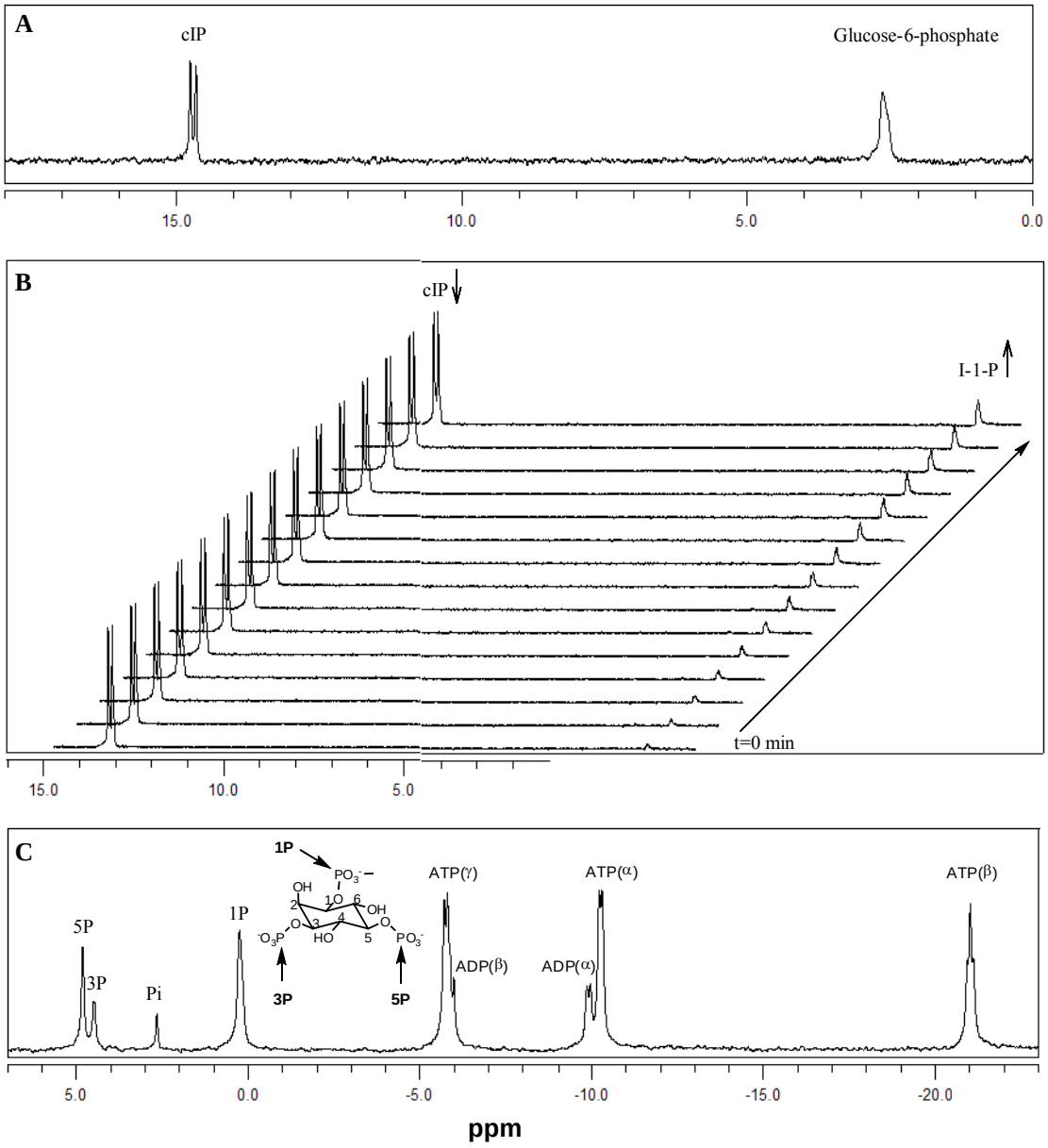

I. Interaction of PI-PLC with lipid surfaces

1. Filtration/centrifugation/SDS-PAGE assay

A simple binding assay (Stieglitz et al., 1999; Wehbi et al., 2003a) based on filtration and centrifugation was tried to characterize the binding of *L. monocytogenes* PI-PLC to vesicle interfaces. Typically, 25 μg of PI-PLC was incubated at room temperature for 15 min with an aliquot of phospholipid vesicles solution (2 ml) in 10 mM Tris-HCl buffer, pH 7.0. The vesicle bound protein was separated from free protein using an Amicon centricon-100 filter with 100 kDa molecular mass cutoff. A control containing the same amount of PI-PLC in Tris-HCl buffer, pH 7.0, with no phospholipids present was used to measure the recovery efficiency of free enzyme from the filtration/centrifugation step. Filtrates, which contained only the free protein, were lyophilized, dissolved with 40 μl SDS sample loading buffer, and analyzed by SDS-PAGE. Band intensities were quantified by NIH Image 1.61 software and used to calculate the amount of free protein from phospholipid containing samples by comparing their intensities to that of the control. The amount of vesicle bond protein was then evaluated as the amount difference between the total added protein and the quantified free protein. Binding could then be analyzed using Langmuir adsorption isotherm (Cho et al., 2001a) to yield the dissociate constant and number of lipid binding sites per PI-PLC molecule.

2. Monolayer penetration by PI-PLC

Lipid monolayers have been used to characterize the ability of proteins to penetrate into the membrane (Verger and Pattus, 1982; Wehbi et al., 2003b). Lipid monolayers were formed by spreading 5 to 10 μl of the appropriate lipids (POPC, or DOPMe, or a mixture of 70% POPC and 30% DOPMe) dissolved in ethanol/hexane (1:9, v/v) onto 10 ml of 50 mM HEPES, pH 7.0, with KCl at three different concentrations (0, 0.16, or 0.5 M) contained in a circular Teflon trough (4 cm diameter × 1 cm deep). The surface pressure (π) of subphase (the solution in the trough) was measured using a Wilhelmy plate attached to a computer-controlled tensiometer as described for the *B. thuringiensis* PI-PLC (Wehbi et al., 2003b). The subphase was gently mixed with a magnetic stir bar and the monolayer was allowed to equilibrate until a stable surface pressure (defined as the initial surface pressure, π_0) was obtained. Then a protein solution was injected into the subphase through a small hole in the side of the trough without disruption of the monolayer. The change in surface pressure ($\Delta\pi$) was measured as a function of time. Since the value of $\Delta\pi$ depends on the protein concentration in the low concentration range, protein concentration in the subphase was maintained high enough (above 3 μg/ml for PI-PLC) to ensure the observed $\Delta\pi$ represented a maximal value (Medkova and Cho, 1998). In general, $\Delta\pi$ is inversely proportional to the π_0 of the lipid monolayer and extrapolations of the $\Delta\pi$ versus π_0 plot to $\pi_0=0$ and $\Delta\pi=0$ yield the maximum $\Delta\pi$ obtainable and the critical surface pressure (π_c) that specifies an upper limit of π_0 into which a protein can penetrate respectively.

3. Carboxyfluorescein leakage assay of vesicle integrity

To monitor vesicle leakage promoted by the bound *L. monocytogenes* PI-PLC, assays were performed according to literature procedure (Ravoo et al., 1999) with modifications. Carboxyfluorescein (Figure 2-11A), which is self-quenched at high concentration, was entrapped in the vesicle as a release marker. Briefly, vesicles were prepared by sonication of 20 mM of the appropriate lipids (POPC or DOPMe) with a solution of 100 mM carboxyfluorescein in 10 mM HEPES, pH 7.1, with 0 or 100 mM $(NH_4)_2SO_4$. The nonencapsulated carboxyfluorescein was removed by rapid filtration of the vesicle solution through a Sephadex G-10 (fractionation range <700 Da) column (1.0 cm × 20 cm) at room temperature using the corresponding HEPES buffer as the eluent. The carboxyfluorescein entrapped vesicles were used right after gel filtration. Vesicle integrity in the absence or presence of PI-PLC protein was monitored by the carboxyfluorescein fluorescence using an excitation wavelength of 490 nm and an emission wavelength of 520 nm. Leakage at time t was expressed in percentage relative to the initial fluorescence F_0 and the maximum fluorescence F_{TX} obtained after complete lysis of the vesicles by the addition of 25 mM Triton X-100 according to $(F_t - F_0) / (F_{TX} - F_0) \times 100\%$. All the carboxyfluorescein assays were carried out in the dark and a narrow excitation slit width (1 nm) was used to minimize photobleaching of the carboxyfluorescein.

4. Turbidity assay of macroscopic aggregation

Aggregation and fusion of vesicles (POPC, POPG, DOPMe) promoted by PI-PLC were monitored by the increase in turbidity of the solution (Stieglitz et al., 2001) after the

addition of protein. The vesicle stock solutions were prepared by sonication of phospholipids in 50 mM HEPES, pH 7.0, and centrifuged at 15,000 rpm for 30 min with a bench-top centrifuge to get rid of bigger vesicles prior to the assay. The optical density of the vesicle solution (0.172 mM POPG / 0.62 mM POPC or 0.86 mM DOPMe / 3.1 mM POPC or 3.1 mM POPC) was then measured at 350 nm as function as time after the addition of PI-PLC (protein, 4 μg to 1.5 mg, was added at t=10 min) and the baseline turbidity was provided by monitoring the OD_{350} of corresponding vesicles without protein. After a stable OD_{350} was reached, the solution was centrifuged at 15,000 rpm for 10 min and both the precipitate (washed by buffer, dissolved with guanidine/salts, or dissolved with Triton X-100, or extracted with chloroform/methanol) and supernatant were subjected to analysis by SDS-PAGE and NMR spectroscopy.

5. ^{31}P NMR linewidth to monitor protein binding

Changes in phospholipid ^{31}P linewidths were used to monitor the binding of diC_6PC and diC_7PC to *L. monocytogenes* PI-PLC (2 mg/ml). The linewidth of the PC resonance was measured at various concentrations (0.1-20 mM) in the absence and presence of enzyme. Linewidth changes upon micellization of both of these short-chain lipids were small, so that the difference in linewidth caused by the presence of enzyme was initially assumed to reflect the amount of ligand bound to the enzyme in fast exchange with free ligand. As discussed previously (Zhou et al., 1997b), the difference in linewidth in the presence and absence of ligand at a given ligand concentration, ($\Delta\upsilon_{obs}$-$\Delta\upsilon_o$), is a function of total concentration of enzyme (E_T) and ligand ($[PC]_T$), the bound

linewidth for the E·PC complex ($\Delta\upsilon_b$), the dissociation constant (K_d), and n, the number of ligands bound per enzyme molecule. If there are multiple, independent binding sites for the PC (to form $E{\cdot}PC_n$) leading to the change in linewidth, and if the free [PC]>>[E·PC] complex, then the following equation holds:

$$\left(\Delta\upsilon_{obs} - \Delta\upsilon_o\right) = \frac{n \times E_T \times [PC]_T^{n-1} \times \left(\Delta\upsilon_b - \Delta\upsilon_o\right)}{K_d + [PC]_T^n}$$

6. Chemical cross-linking of PI-PLC

To check if *L. monocytogenes* PI-PLC aggregates on phospholipid interfaces, chemical cross-linking assays in the absence and presence of various phospholipid interfaces were performed. Three reagents, EDC, DMS, and APG were tried to trap any protein aggregates formed (Figure 2-9 and Figure 2-10). PI-PLC for cross-linking assays was purified by elution through two columns and dialyzed against the appropriate reaction buffer. The lipid surface was provided by micellar diC_7PC (0.5-15 mM) or vesicle POPC (2 mM). Crosslinking by EDC, a carboxyl and amine-reactive zero length cross-linker, were carried out by incubating 300 μg/ml of PI-PLC with 50 mM of EDC in 100 mM MES, pH at 5.0 or 7.0, at room temperature for 4 h. Reaction mixtures were then dialyzed against 10 mM Tris-HCl, buffer of pH 7.0 at 4°C to remove excess EDC, lyophilized, dissolved with SDS loading buffer, and analyzed by SDS-PAGE. Crosslinking by DMS, an imidoester cross-linker with an 11 Å spacer arm, were carried out by incubating 250 μg/ml of PI-PLC with 10 mM of DMS in 200 mM HEPES, pH 8.0,

Figure 2-9 Structure of (A) EDC (1-ethyl-3-[3-dimethylaminopropyl]carbodiimide hydrochloride) and (B) DMS (dimethyl suberimidate·2HCl) with 11.0 Å spacer arm. (C) EDC cross-linking reaction scheme; (D) DMS cross-linking reaction scheme.

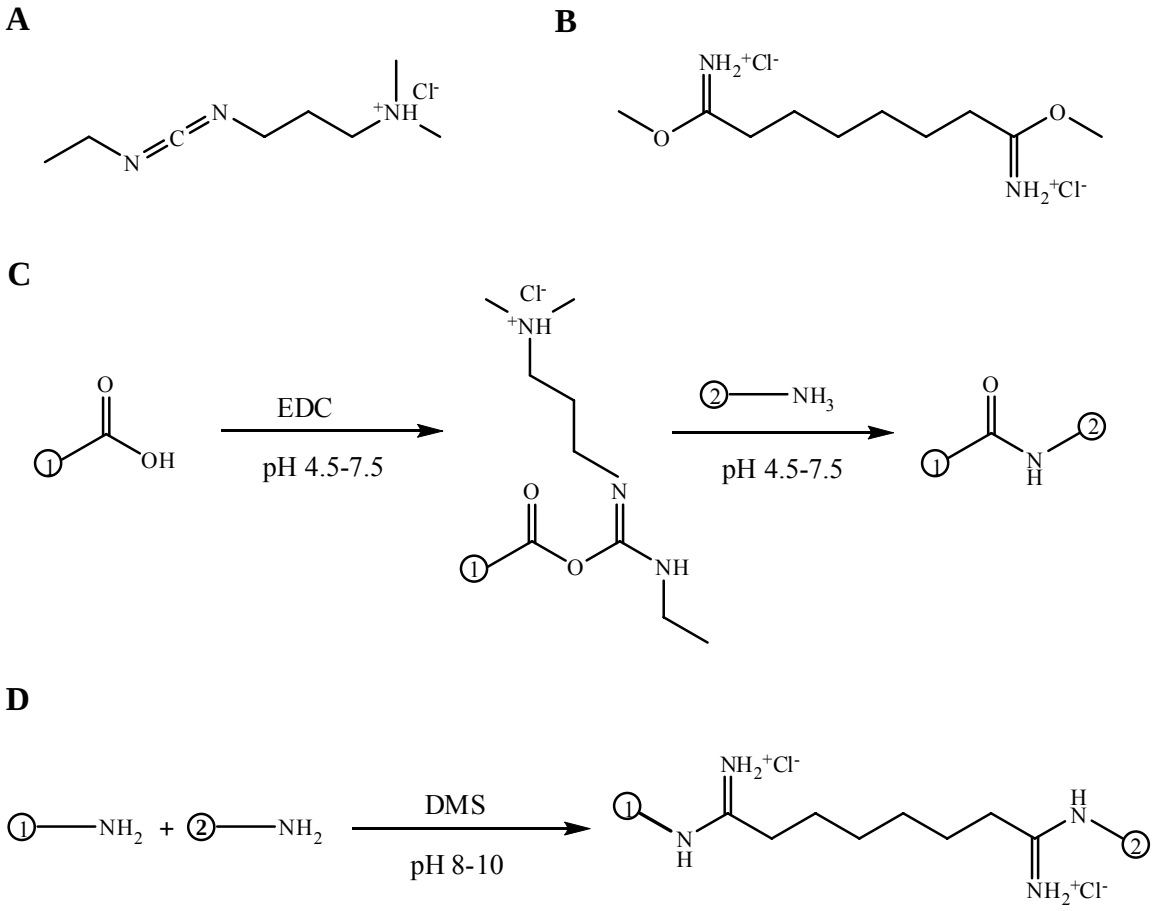

Figure 2-10 (A) Structure of APG (p-azidophenyl glyoxal monohydrate) with 9.3 Å spacer arm; (B) APG cross-linking reaction scheme.

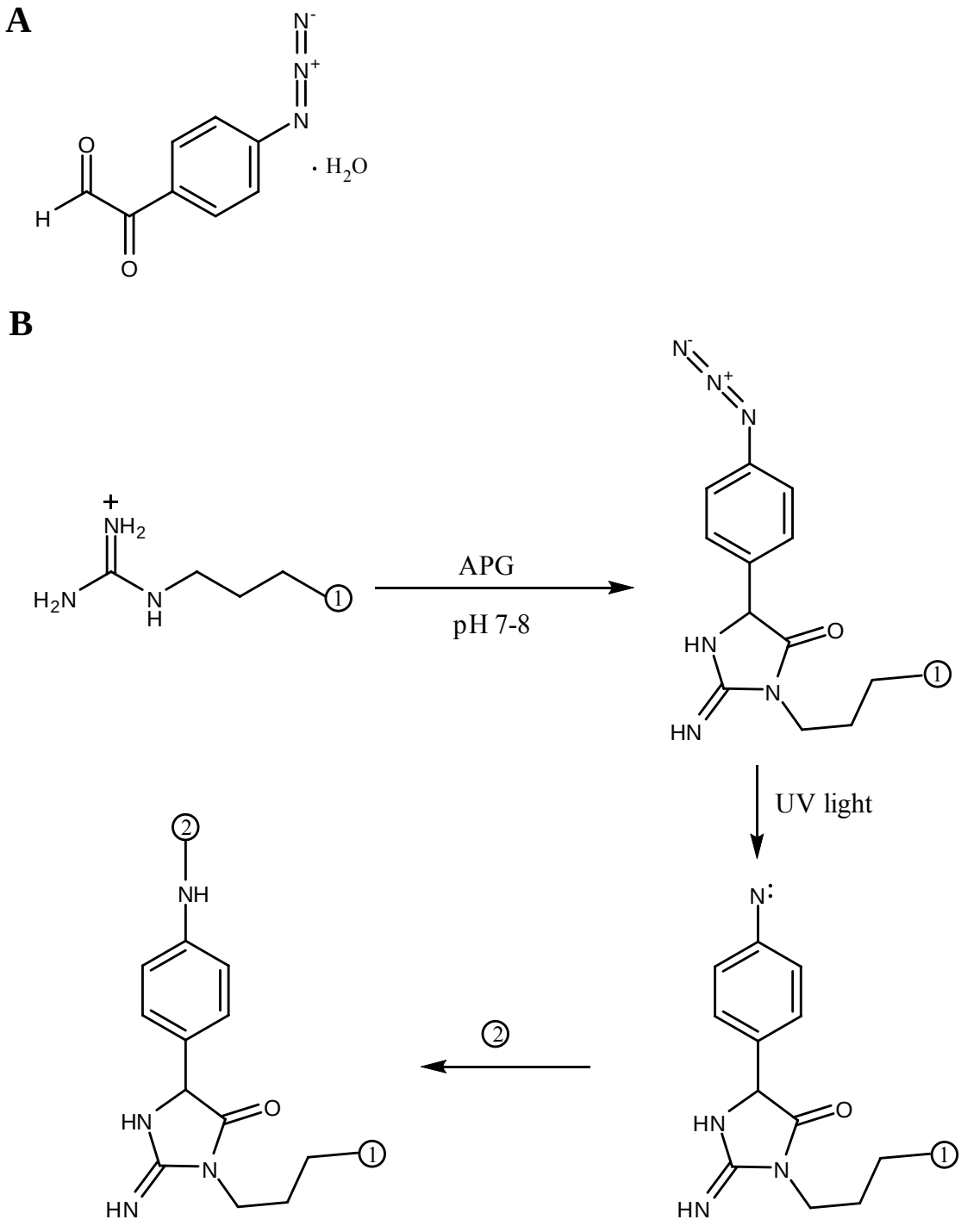

Figure 2-11 Structures of fluorescent labels: (A) (5 or 6)-carboxyfluorescein, (B) pyrene, (C) CPM, (D) BODIPY, and (E) CPM-PI-PLC.

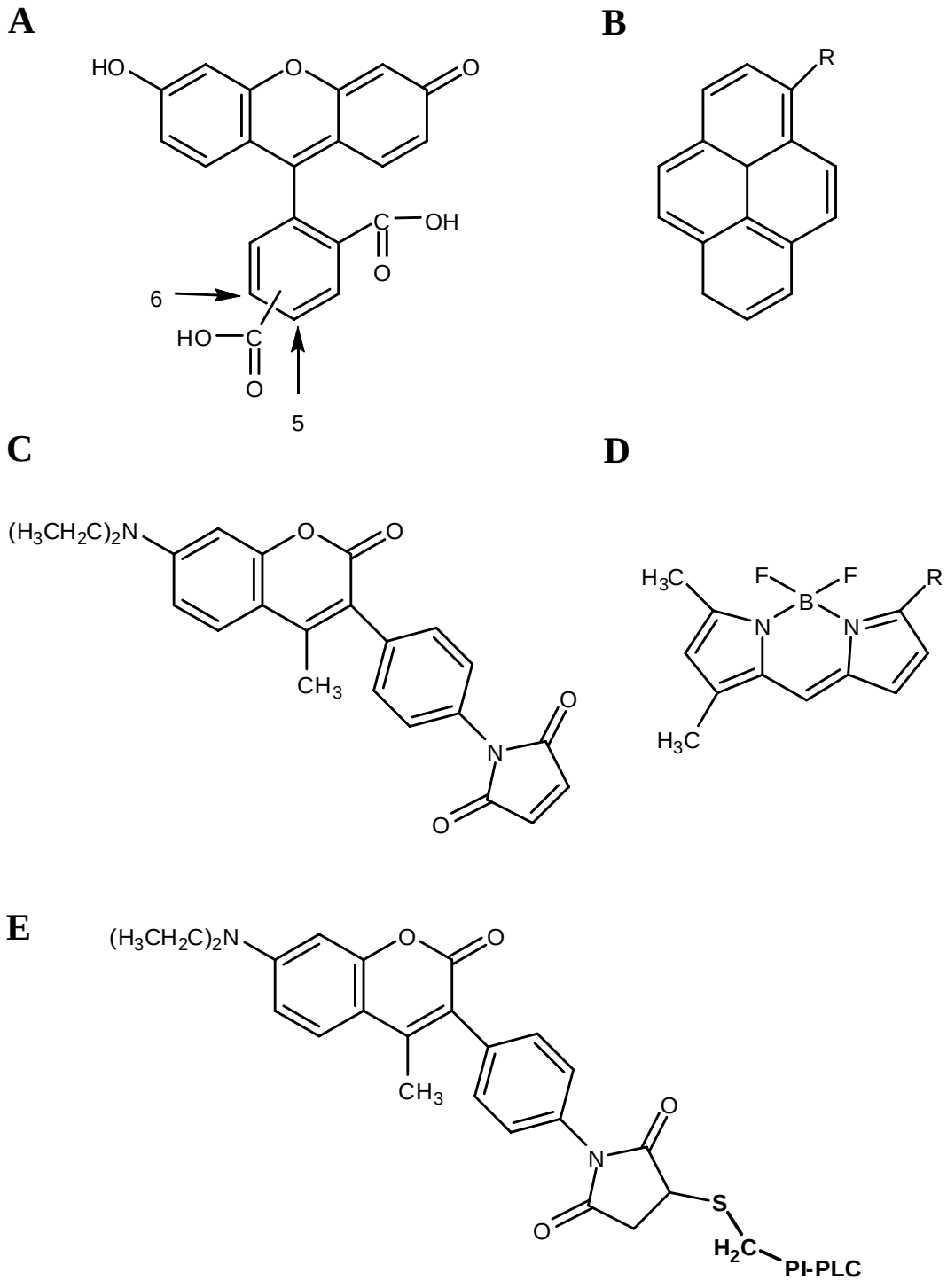

at room temperature for 2 h. The reaction was quenched with dialysis against Tris-HCl buffer (pH 8.0) and checked with SDS-PAGE. Crosslinking with APG, a heterobifunctional cross-linker (spacer arm length 9.3 Å) with a phenylglyoxal group targeting the guanidium side chain of Arg residues and a nonspecific photoactivatable phenyl azide group, were performed in two steps: 2 mg/ml PI-PLC was incubated in the dark with 2.4 mM of APG in 20 mM of sodium phosphate, pH 7.5, for 6 h at room temperature; the subsequent photoactivation was performed with a 254 nm UV light source for 15 min at room temperature. Upon completion, the reaction mixture was dialyzed in the dark to get rid of the excess APG and checked with SDS-PAGE.

7. Fluorescence spectroscopy

Fluorescence spectroscopy has been widely used to monitor environmental and conformational changes of macromolecules. Except for self-quenching carboxyfluorescein, several other types of fluorophores (Figure 2-11), including the intrinsic tryptophanyl residues of PI-PLC, pyrene, and BODIPY-CPM fluorescence resonance energy transfer (FRET) pair, were tried to study the effect of interfaces on the PI-PLC with steady-state fluorescence. All the fluorescence studies were done at 25°C using a SPEX FluoroLog®-3 spectrofluorometer, typically with 1 nm excitation slit width and 5 nm emission slit width. Different conditions were used based on the fluorophores monitored. The intrinsic fluorescence (from the tryptophanyl residues) of 100 μg/ml PI-PLC in the absence or presence of various phospholipids (diC_6PC, diC_7PC, POPC, POPA, POPS, DOPMe) in 50 mM HEPES, pH 7.0, with 2 mM EDTA, was monitored between 300 and 380 nm using an excitation wavelength of 290 nm. (2) The fluorescence spectra

of β-Pyr-C_{10}-PG in 50 mM HEPES, pH 7.0, dissolved in diC_7PC micelles or co-sonicated with POPC / POPG, were acquired with an excitation wavelength of 350 nm and the emission measured between 360 and 600 nm. For clustering in micelles, 20 μM β-Pyr-C_{10}-PG was added to 3 mM diC_7PC (ratio of micellar PC to the β-Pyr-C_{10}-PG ~ 150/1); for clustering of PG in SUVs, 100 μM β-Pyr-C_{10}-PG was added to SUVs containing 2 mM POPC and 0.1 mM unlabeled PG (ratio of PC to total PG = 10/1). By monitoring the ratio of the pyrene excimer (excited-state dimer) to monomer fluorescence intensity versus the PI-PLC concentration, the changes in distribution of pyrene-containing acryl chains in the mixed micelle or vesicle induced by PI-PLC, if any, could be detected. (3) FRET experiments involving CPM, attached via a maleimide to a cysteine residue of protein, as the donor used excitation at 387 nm and with emission monitored at 472 nm for CPM quenching due to energy transfer to the BODIPY dye labeled on the acyl chain of phospholipids (β-BODIPY FL C_5-HPC). The acceptor sensitization was simultaneously monitored at 516 nm. In these fluorescence experiments, 10 μg/ml labeled protein and 100 μM phospholipids (containing 2.5% BODIPY labeled lipids) were used. To label cysteine mutants of PI-PLC, 100 μg/ml protein was incubated with 24 μM CPM in 3 ml 20 mM Tris-HCl, pH 7.0, at room temperature for 2 h. The reaction was monitored by the fluorescence intensity at 472 nm (excitation at 387 nm) as there is a great fluorescence increase when CPM dyes couple with thiol groups. Upon completion, the reaction mixture was dialyzed to remove free CPM.

J. Circular dichroism spectroscopy

CD spectroscopy was used to monitor secondary structure and thermal denaturation of proteins. All samples used for CD experiments had protein in 10 mM borate buffer, pH 7.0. In wavelength scan experiments, 0.2-0.3 mg/ml PI-PLC was used in 1 mm cells to collect CD spectrum between 300 and 190 nm using an AVIV Circular Dichroism model 202 spectrometer. Secondary structure content was estimated with CDNN using molar ellipticity in the 200 to 260 nm range (Böhm et al., 1992; Andrade et al., 1993). Thermal stability of protein (0.02 mg/ml in 1 cm cells) was assessed using CD by following ellipticity changes at 222 nm (primarily α-helix) as temperature increased from 20 to 90°C with 1°C increase interval (within ±0.2°C of the set value and with 1 min equilibration time). T_m was the temperature point at which maximum derivative of θ_{222} reached.

K. Plaque formation assay of fibroblast infection

The size of plaques generated as *L. monocytogenes* infects target mammalian cells was used as a measure of infectivity of the F237W mutant compared to WT PI-PLC. This assay, performed as described previously (Sun et al., 1990), quantifies the infection of mouse fibroblast L2 cells by measuring the plaque size. The wild type PI-PLC gene (*plcA*) or F237W PI-PLC gene was inserted into the *p*AM401, which contains the *plc*A gene promoter with the *L. monocytogenes* PI-PLC original signal peptide sequence. These *p*AM401 plasmids were then electroporated into strain DP-L1552 (*Δplc*A, no *L. monocytogenes* PI-PLC expression). The modified *L. monocytogenes* strains were then

used to infect monolayer cultures of mouse fibroblast L2 cells. The cell monolayer was then washed with PBS three times, covered with 1% DMEM-containing agarose with 10 μg/ml gentamicin, and incubated at 37°C for 3 days. Plaques formed were then visualized by staining the cells with neutral red. The mean plaque diameter formed by each strain was compared with the mean plaque diameter of strain 10403S, the *L. monocytogenes* WT strain where the PI-PLC gene is chromosomal (Bishop and Hinrichs, 1987). The relative plaque size is reported as a percentage of 10403S plaque size.

Chapter 3:

Cloning and expression of *L. monocytogenes* PI-PLC

I. Introduction

Since Kemp et al. (1959) showed the presence of PI-PLC enzymatic activity in rat liver, the observations that mammalian PI-PLC enzymes may play important roles in agonist-stimulated phosphoinositide metabolism and signaling (Michell, 1975; Berridge and Irvine, 1987; Nishizuka, 1992) greatly propelled the studies of their molecular characterization. Numerous eukaryotic PI-PLC isozymes from a diverse range of sources, including different animals tissues, filamentous fungi, yeasts, protozoan parasite, and plants, have been isolated and their corresponding cDNA sequences determined since the late 1980s (Nozaki et al., 1999; Rebecchi and Pentyala, 2000; Pan et al., 2005). The early studies aimed at isolating of PI-PLC from eukaryotic sources were complicated by the enzyme heterogeneity (the existence of more than one isozyme in the same source) in addition to the complex purification schemes and low yields (often in the microgram range). In contrast, bacterial PI-PLCs are secreted in relatively large quantities across the cell membrane into the culture medium. Milligram quantities of PI-PLCs were purified to homogeneity from cultures of *Staphylococcus aureus* (Low and Finean, 1977; Low, 1981), *Bacillus cereus* (Ikezawa et al., 1976; Ohyabu et al., 1978; Kominami et al., 1985), and *Bacillus thuringiensis* (Taguehi et al., 1980), although the yields of these purification schemes still were lower than one milligram per liter of culture. By the use of recombinant DNA technology, PI-PLCs can be obtained with much higher yields via more rapid procedures (Koke et al., 1991).

The initial plasmids pDP1462 and pBS1462 for the PI-PLC from *Listeria monocytogenes* were kindly provided by Dr. Howard Goldfine, University of

Pennsylvania. The construction of plasmid pDP1462 has been described (Camilli et al., 1993). *L. monocytogenes* genes *prf*A for a positive regulatory protein and *plc*A for PI-PLC, gene bases -810 to 1349 (Mengaud et al., 1989), were amplified from wild-type 10403S strain (Portnoy et al., 1988) chromosomal DNA and ligated into *E. coli-S. faecalis* shutter vector pAM401 (Wirth et al., 1986) with *Xba*I and *Sal*I sites. The pBS1462 plasmid was made by inserting the same genes of interest into the smaller pBluescript II KS phagemid vector using the same restriction sites to facilitate creating mutants. Goldfine and Knob transformed a similar plasmid (pAM401:: *plcA prfA*) into the 10403S strain, and purified about 1 mg homogeneous PI-PLC from the culture of *L. monocytogenes* without specifying the culture volume used (Goldfine and Knob, 1992). Expressing the *plcA* gene in *L. monocytogenes* strains can avoid the potential problems associated with heterologous gene expression, such as protein misfolding, toxicity of recombinant protein to the host, recognizing and cleaving the signal peptide of interest protein correctly, as well as different codon usage in the host system. However, expressing *L. monocytogenes* PI-PLC in an *E. coli* background is worth a try considering the relative simplicity of the protein (small protein size with 33 kDa molecular mass, and lack of cysteine residues) in addition to the ability of *E. coli* to grow rapidly and at high density on inexpensive medium. *E. coli* also lacks a PI-PLC activity. Moser et al. (1997) expressed and purified crystallographic qualities of *L. monocytogenes* PI-PLC. They obtained 1.2 to 1.5 mg per liter from *E. coli* BL21 transformed with the expression plasmid plcA-1, constructed by inserting the gene for predicted mature PI-PLC (Leimeister-Wächter et al., 1991) into *Nhe*I-*Xho*I digested pIT vector (Moser et al., 1997).

As the pIT vector (Koke et al., 1991) is not commercially available, we cloned and expressed *L. monocytogenes* PI-PLC in two cloning/expression systems (pET and IMPACT) using pBS1462 plasmid as template since we did not have the DNA sequence of the pAM401 vector. This procedure was used to generate PI-PLC for diverse kinetic and biophysical studies.

II. Experiments and Results

A. Cloning of *L. monocytogenes plcA* gene with or without *prf*A gene into pET-23a(+)

The *plc*A gene in plasmids pDP1462 and pBS1462 encodes the PI-PLC precursor of 317 residues with an N-terminal signal sequence. If PI-PLC is secreted through the general secretary pathway (Sec machinery), the signal peptide targets the precursor protein to the cytoplasmic membrane and initiates its translocation across the membrane. Once translocated, the signal peptide is cleaved by signal peptidase (SPases) (Raynaud and Charbit, 2005). At the time we constructed plasmids for expressing *L. monocytogenes* PI-PLC, two different cleavage sites of signal sequence were reported (Leimeister-Wächter et al., 1991; Goldfine and Knob, 1992; Moser et al., 1997). Since the signal peptide may be recognized by *E. coli* secretion machinery, we amplified the entire *plc*A gene of *L. monocytogenes* containing signal sequence, bases 294 to 1349 Mengaud et al., 1989), from pBS1462 with the forward primer used to construct pDP1339 (Camilli et al., 1993). The reverse primer was designed simply by taking a fragment of the *plc*A gene antisense strand (base 276 to 318) (Mengaud et al., 1989) in which 6 bases (288 to 293) were replaced by the *Eco*RI restriction site (gaattc).

The PCR products were purified directly by QIAquick PCR Purification Kit, doubly digested with *Xba*I and *EcoR*I to generate sticky ends, and purified again by QIAquick PCR Purification Kit. When needed, agarose gel electrophoresis combined with QIAquick Gel Extraction Kit was used to isolate a DNA fragment of specific molecular weight but with lower DNA recovery. pET-23a(+) was digested with the same set of endonucleases, purified and then ligated to the digested PCR products. The loss of ribosome binding site in *Xba*I-*EcoR*I-digested pET-23a(+) is compensated by the ribosome binding site of the *plc*A gene (aaggag, same as that of pET-23a(+) vector). NovaBlue *E. coli* competent cells were transformed with the ligation products and grown at 37°C on the LB-agar-plate with 100 μg/ml ampicillin. To screen the positive clones, four colonies were picked and inoculated into 5 ml LB medium containing 100 μg/ml ampicillin and grown overnight at 37°C. Plasmids were purified from these cultures with QIAprep Miniprep and doubly digested with *Xba*I and *EcoR*I to identify the positive clones. The positive clones showed a 1062-bp DNA band on the agarose gel after digestion and were further confirmed by double strand DNA sequencing with T7 promoter primer and T7 terminator primer. The graphic map of constructed plasmid of pET1339 showing the unique restriction sites from common restriction enzyme database of PlasMapper (http://wishart.biology.ualberta.ca/PlasMapper) is displayed in Figure 3-1.

BL21 *E. coli* host strains (BL21(DE3) and its pLysS derivative for stringent transcription control) were transformed with plasmid pET1339 for overexpression of recombinant protein. Aliquots of cell extract supernatants, solubilized cell debris

Figure 3-1 Graphic map of recombinant pET1339 created with PlasMapper. Using plasmid pBS1462 as template, *L. monocytogenes plc*A gene was amplified by PCR using primers 5'-ggTCTAGAttctagtcctgctgtcc-3' and 5'-ttgtaggaataaGAATTCttagttgaatttattgttttttatg-3'. The 30 cycle PCR product was doubly digested with *Xba*I and *EcoR*I and ligated to *Xba*I-*EcoR*I digested pET-23a(+). The insertion of the target gene was checked by DNA sequencing with T7 promoter primer and T7 terminator primer.

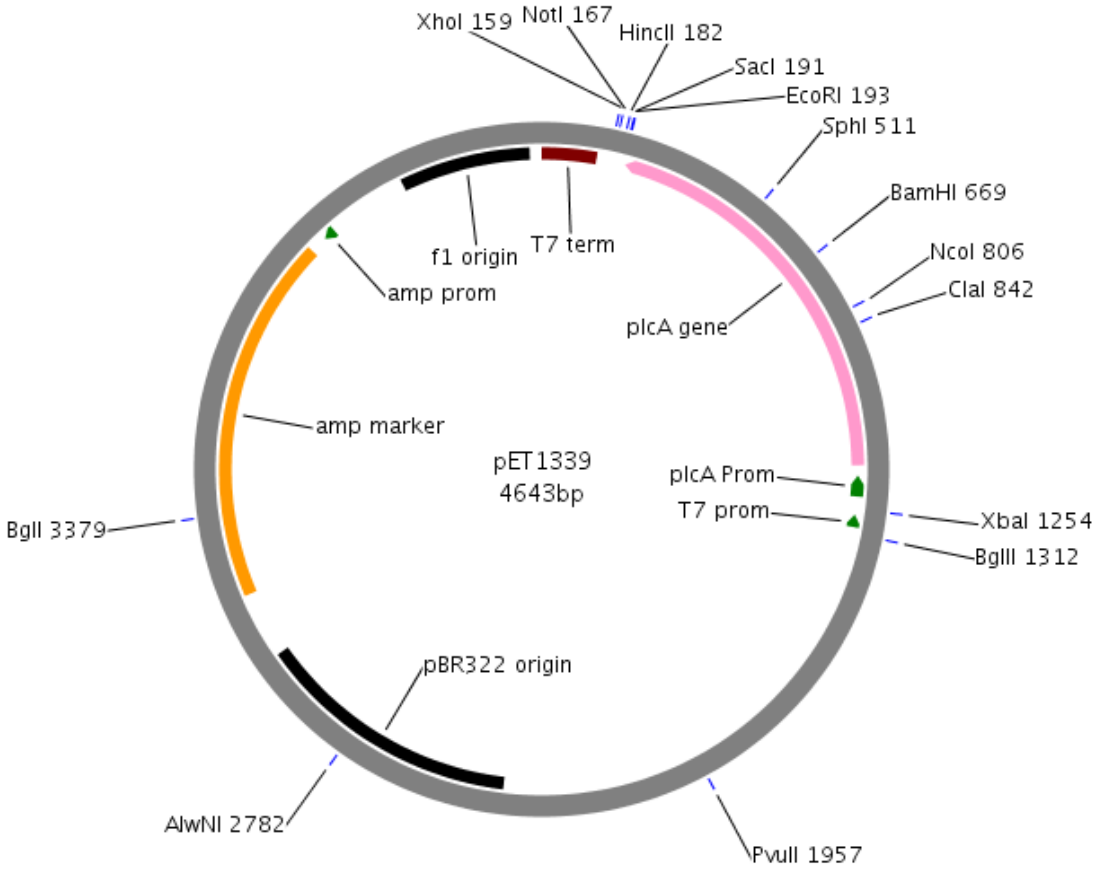

(resuspended in half the supernatant volume with 1% SDS), and concentrated *E. coli* culture media were incubated respectively with an optically clear mixture of 2 mM PI and 8 mM Triton X-100 in 25 mM HEPES buffer (pH 7.5) overnight at room temperature and then checked for PI-PLC activity with ^{31}P NMR spectroscopy by monitoring the generation of cIP and I-1-P. No PI hydrolysis activity was detected in any of them even after extended incubation of up to 1 week. SDS-PAGE analysis of the concentrated culture media, cell extract supernatants and solubilized cell debris did not show obvious overexpression of a protein band with 33 kDa molecular mass.

The entire *plc*A gene, inserted after the T7 promoter in pET1339, carries its own promoter with -10 region (tagaat) related to the *E. coli* consensus sequence (tataat) and a palindromic sequence of 14 bp (ttaacaaatgttaa) in the -40 region (Mengaud et al., 1989). The *plc*A gene promoter lacks the -35 region. PrfA protein can recognize this 14-bp palindrome and activate the transcription of *plc*A (Mengaud et al., 1991; Leimeister-Wächter et al., 1992). Co-expression of *plcA* and *prfA* genes could enhance the expression of recombinant PI-PLC in *E. coli*. Therefore, we constructed a pET1462 plasmid containing the *plc*A and *prf*A genes. The DNA fragment of interest, base -810 to 1349 (Mengaud et al., 1989), was amplified from pBS1462 with the same primer pair used in making pDP1462 (Camilli et al., 1993). However, no colonies grew on the plate spread with NovaBlue cells transformed with the ligation product. The failure to subclone the *plc*A and *prf*A genes into the pET-23a(+) is because of the low digestion efficiency of PCR products by *Sal*I. In the reverse primer, the *Sal*I restriction site has only 2 bases (gg) at the 5' end. For oligo sequences with 2 (gc) or 4 nucleotides (acgc) at the 5' end of *Sal*I

site incubated at 20°C with 20 units *Sal*I, only 10% was reported to be cleaved after 2 hours and 50% to 75% was cleaved after 20 hours (http://www.neb.com/nebecomm/tech_reference/restriction_enzymes/cleavage_olignucleotides.asp). Therefore, we modified the reverse primer by inserting an extra non-complementary sequence of aataatat between the *Sal*I site and 5'-terminal gg to ensure the efficient cleavage of PCR products. By using the modified reverse primer, we obtained the plasmid pET1462 (Figure 3-2). The *Xba*I-*Sal*I digested pET1462 showed a 2166-bp DNA band on the agarose gel. Again, the attempts to express the *L. monocytogenes* PI-PLC with various BL21 strains harboring pET1462 were not successful.

The failures were unexpected since the successful expressions of recombinant *L. monocytogenes* PI-PLC in *E. coli* have been reported (Leimeister-Wächter et al., 1991; Moser et al., 1997). Leimeister-Wächter et al. constructed several plasmids containing different combinations of *plc*A with neighboring genes from *L. monocytogenes* EGD strain, pLM48 (pUC18::*plc*A*lis*A), pLM48-202 (pUC18::*plc*A) and pLM50 (pUC18::*plc*A*prf*A). The expression level of PI-PLC from these plasmids, checked by radioactive labeling with [^{35}S]-methionine, was consistent with the level of detectable PI-PLC activity, increasing in the order pLM48<pLM48-202<pLM50. In this communication, no attempt to purify the recombinant PI-PLC was mentioned. Although Leimeister-Wächter et al did not clarify in which cell compartment the recombinant protein was located, the way they detected PI-PLC activity was from the generation of a

Figure 3-2 Graphic map of recombinant pET1462 created with PlasMapper. Using plasmid pBS1462 as template, *L. monocytogenes plc*A gene and *prf*A gene were amplified by PCR using primers of 5'-ggTCTAGAttctagtcctgctgtcc-3' and 5'-ggaataatatGTCGACcagctcttcttggtgaag-3'. The 30 cycle PCR product was doubly digested with *Xba*I and *Sal*I and ligated to *Xba*I-*Sal*I digested pET-23a(+). The insertion of target genes was checked by DNA sequencing with T7 promoter primer and T7 terminator primer.

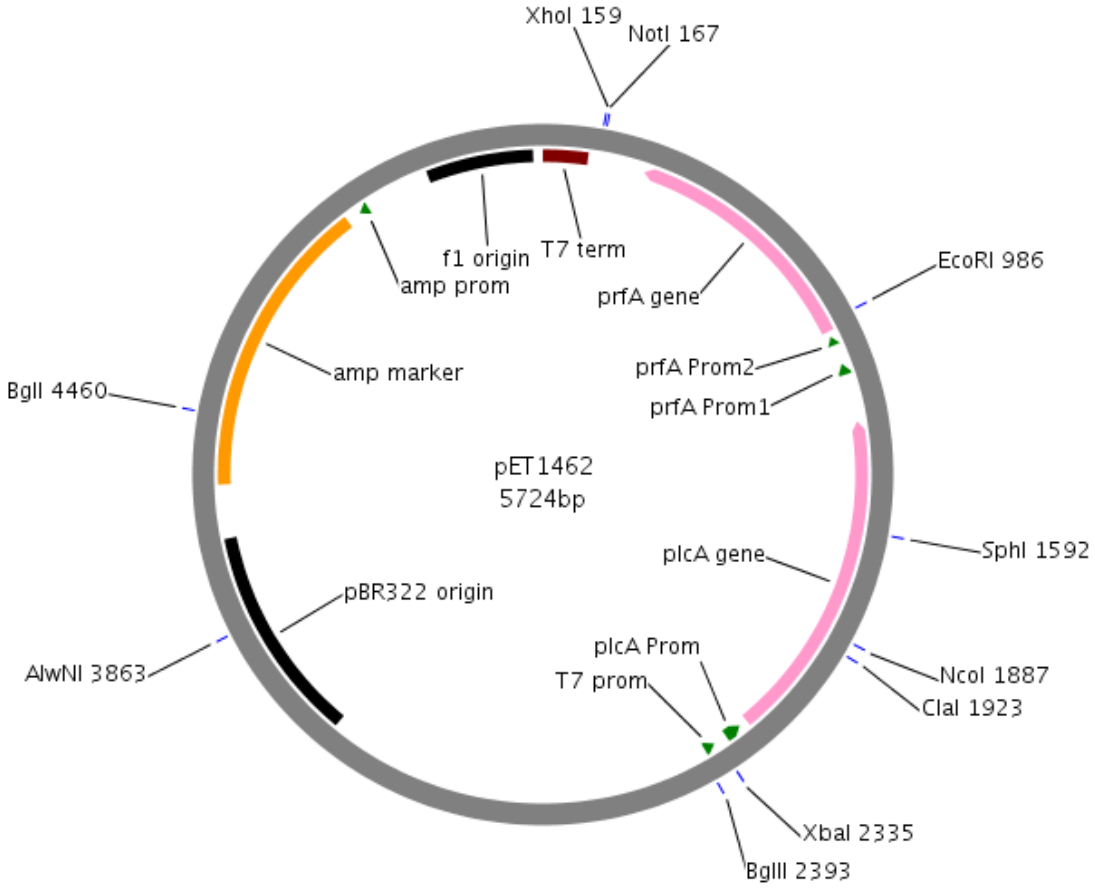

turbid halo around the colony on PI-containing-plates, the same assay used to check PI-PLC activity of *L. monocytogenes* strains and may indicate that recombinant PI-PLC was secreted as well. These results indicate that *E. coli* secretion machinery can recognize the signal peptide of *L. monocytogenes plc*A gene and direct the secretion of PI-PLC precursor across the cytoplasmic membrane where the protein may diffuse or leak into the extracellular medium due to the lack of efficient pathways for translocation through the outer membrane in *E. coli*. The expression of recombinant *plc*A in *E. coli* is also regulated by PrfA in the presence of *plc*A promoter.

As we were not sure of the reasons for the failures, we wanted to simplify the transcriptional regulation of the recombinant gene by taking off the promoter of the *plc*A gene, thus eliminating the potential effect of the 14-bp palindrome on the transcription. Except for extracellular medium, recombinantly expressed proteins can be directed to cytoplasm or the periplasm with various advantages and disadvantages. Expression in the cytoplasm is normally preferable since production yields are high. Although PI-PLC is involved in lysis of host vacuoles, the fact that PI is only a minor component of *E. coli* (Ames, 1968; Cronan and Vagelos, 1972; Lechevalier, 1977; Kozloff et al., 1991) made us keep the expressed recombinant PI-PLC in cytoplasm of *E. coli* by removal of its signal sequence.

B. Cloning of mature *L. monocytogenes plc*A gene into pET-23a(+)

Our next attempt was to clone the gene for mature PI-PLC, i.e., protein without the signal peptide. The same reverse primer designed for the plasmid pET1339 was used to introduce an *EcoR*I restriction site immediately after the gene stop codon, TAA, which

is preferred among the three possible stop codons because it is less prone to read-through than TAG and TGA (Sharp and Bulmer, 1988). If needed, 2 or 3 stop codons can be added in series to increase the translation termination efficiency.

To design the forward primer, we needed to know where mature *L. monocytogenes* PI-PLC starts. The signal sequence was first predicted to be 22 amino acids (Leimeister-Wächter et al., 1991). However, N-terminal amino acid sequence analysis of the homogeneous PI-PLC purified from the culture fluid of *L. monocytogenes* revealed that the signal peptide cleavage site was between Ala-29 and Tyr-30 (Goldfine and Knob, 1992), in agreement with the prediction results of program SignalP (Figure 3-3). The graphic output from SignalP-NN prediction (using neural network) comprises three scores. The C-score is only significantly high at the first residue in the mature protein. S-score is high at all residues of signal peptides. And the Y-score is the combination of C- and S-scores, also high for the first residue of mature protein. The SignalP-HMM prediction is based on the hidden Markov model to tell if the submitted sequence contains a signal peptide and assigns scores for n-, h-, and c-regions of the peptide, if one is found. Both predictions are consistent with the cleavage site between Ala-29 and Tyr-30. The classical signal peptides contain three recognizable domains, a positively charged n-region, a central hydrophobic h-region, and a neutral but polar c-region. The average signal peptides from Gram-positive bacteria are 32 amino acids, much longer than those from other organisms (Nielsen et al., 1997a; Nielsen et al., 1997b). In general they have a longer h-region (von Heijine and Abrahmsen, 1989). The

Figure 3-3 Prediction of *L. monocytogenes* PI-PLC precursor signal peptide cleavage site with program SignalP (http://www.cbs.dtu.dk/services/SignalP/). Only the N-terminal 70 amino acid residues of precursor are shown. Refer to text for details.

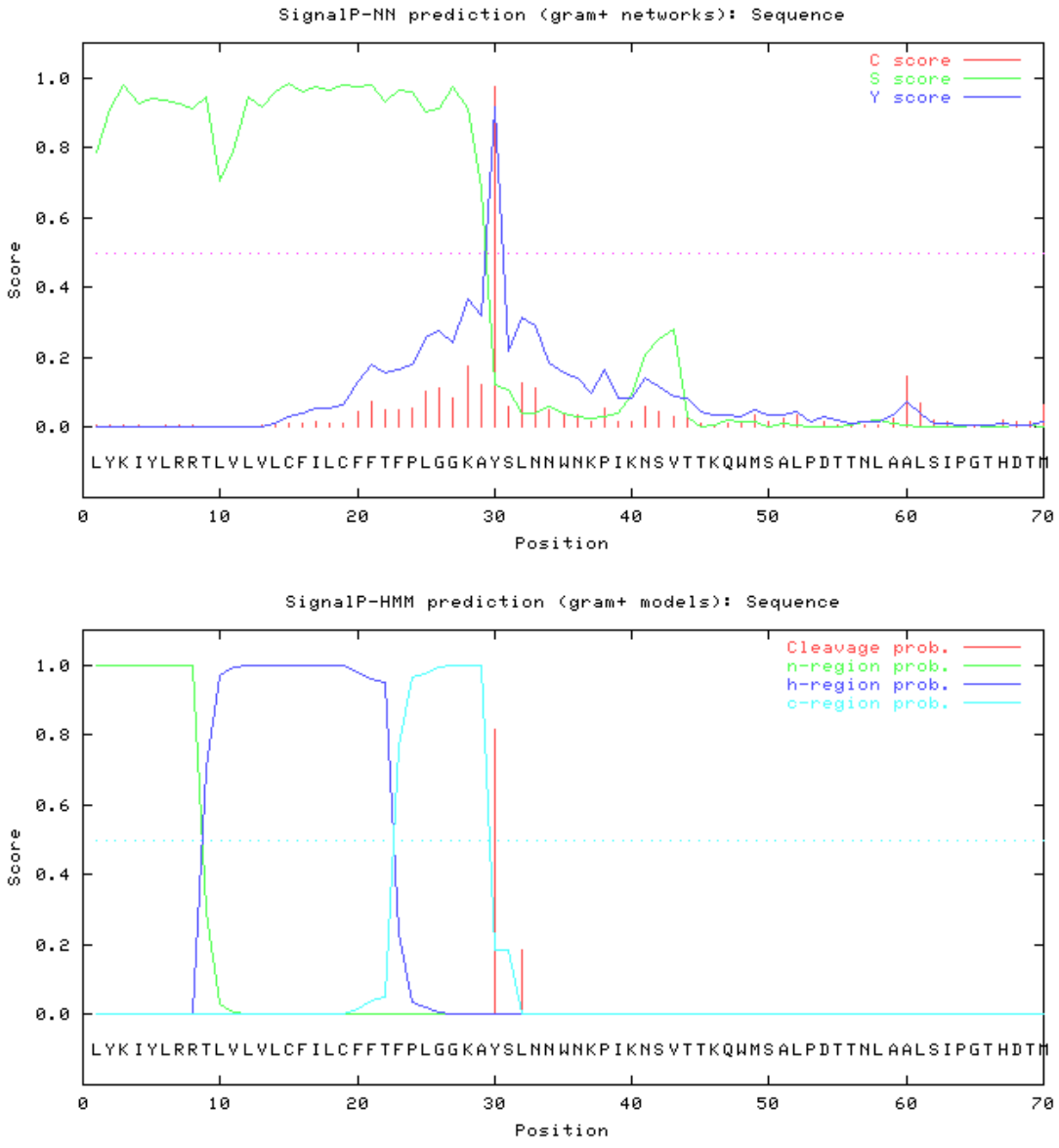

29-amino acid-signal peptide (LYKNYLQRTLVLLLCFILYFFTFPLGGKA) exhibits the signal peptide cleavage-site specificity (Perlman and Halvorson, 1983; von Heijine, 1983; von Heijine, 1985) including a helix-breaking residue (Pro) at the -6 position relative to the cleavage site, and small residues at the -3 (Gly) and -1 (Ala) positions which are all absent in another predicted signal peptide (LYKNYLQRTLVLLLCFILYFFT). Surprisingly, the later work of Moser et al. still took Phe-23(numbered from the N-terminus of the signal peptide) as the first residue of mature PI-PLC (Moser et al., 1997). We thus designed two forward primers to insert into pET-23a(+) *plc*A genes starting from the codons for Phe-23 and Tyr-30 of the precursor respectively. Adding an *Nde*I site (catatg) prior to the truncated *plc*A gene could initiate the translation of the target gene with only one extra amino acid (Met) ahead of the recombinant PI-PLC. Eleven bases (ttttatacttt) from the *plc*A gene, base 50 to 60 relative to the start codon of PI-PLC precursor gene, were taken as the 5' terminus for both primers before the *Nde*I site to ensure the efficient cleavage of PCR products. The graphic maps of constructed plasmids pET-F and pET-Y are shown in Figure 3-4 and Figure 3-5. The *Nde*I-*Eco*RI digested pET-F and pET-Y showed 893-bp and 872-bp DNA bands, respectively, on the agarose gel.

The DNA sequencing results of pET-F and pET-Y using the T7 promoter primer revealed both plasmids had an unexpected stop codon, TGA, in the place of the codon for Trp-35 of PI-PLC precursor from EGD strain (accession number: CAA38438). Using the forward primer designed to clone the pET1462, we then checked this gene region of

Figure 3-4 Graphic map of recombinant pET-F created with PlasMapper. Using plasmid pBS1462 as template, *L. monocytogenes* partial *plc*A gene for PI-PLC from Phe-23 was amplified by PCR using primers of 5'- ttttatactttCATATGttcccattaggcggaaaagcatattc-3' and 5'-ttgtaggaataaGAATTCttagttgaatttattgttttttatg-3'. The 30 cycle PCR product was doubly digested with *Nde*I and *EcoR*I and ligated to *Nde*I-*EcoR*I digested pET-23a(+). The insertion of target gene was checked by DNA sequencing with T7 promoter primer and T7 terminator primer.

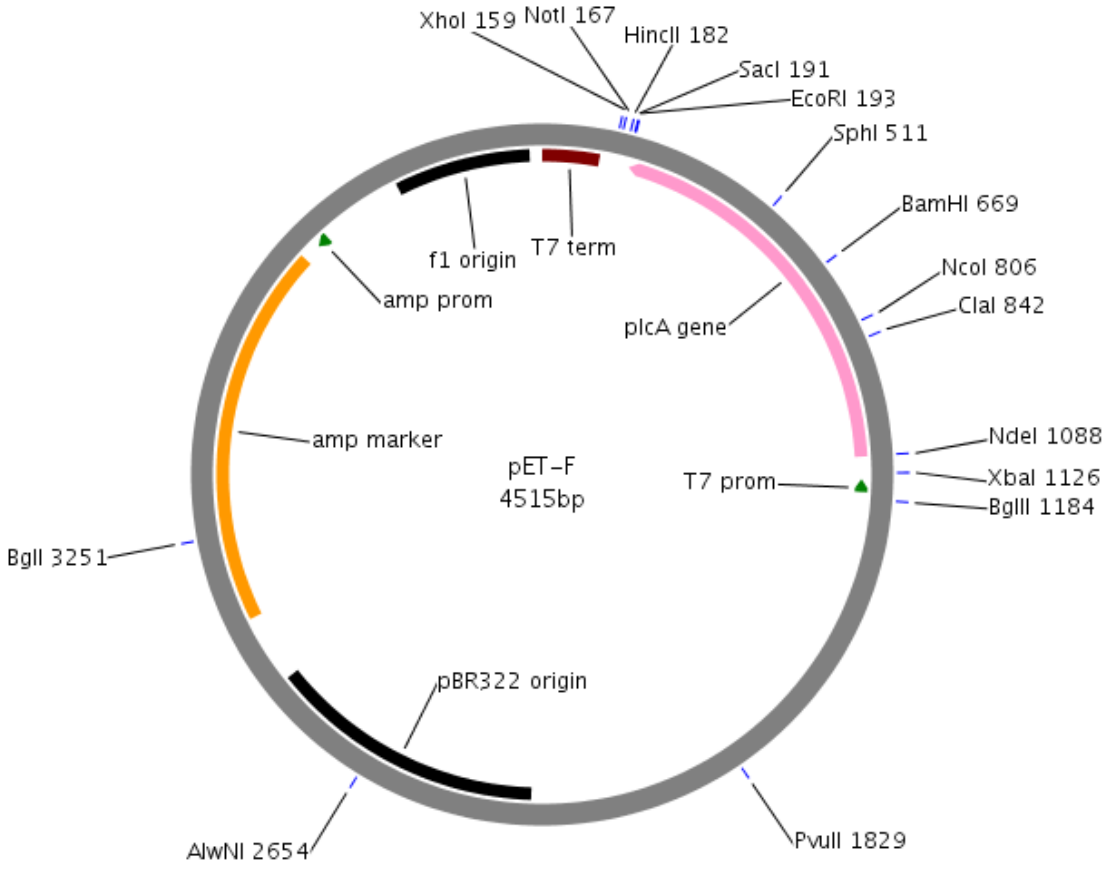

Figure 3-5 Graphic map of recombinant pET-Y created with PlasMapper. Using plasmid pBS1462 as template, *L. monocytogenes* partial *plc*A gene for PI-PLC from Tyr-30 was amplified by PCR using primers of 5'-ttttatactttCATATGtattcgcttaataactgaaataag-3' and 5'-ttgtaggaataaGAATTCttagttgaatttattgttttttatg-3'. The 30 cycle PCR product was doubly digested with *Nde*I and *EcoR*I and ligated to *Nde*I-*EcoR*I digested pET-23a(+). The insertion of target gene was checked by DNA sequencing with T7 promoter primer and T7 terminator primer.

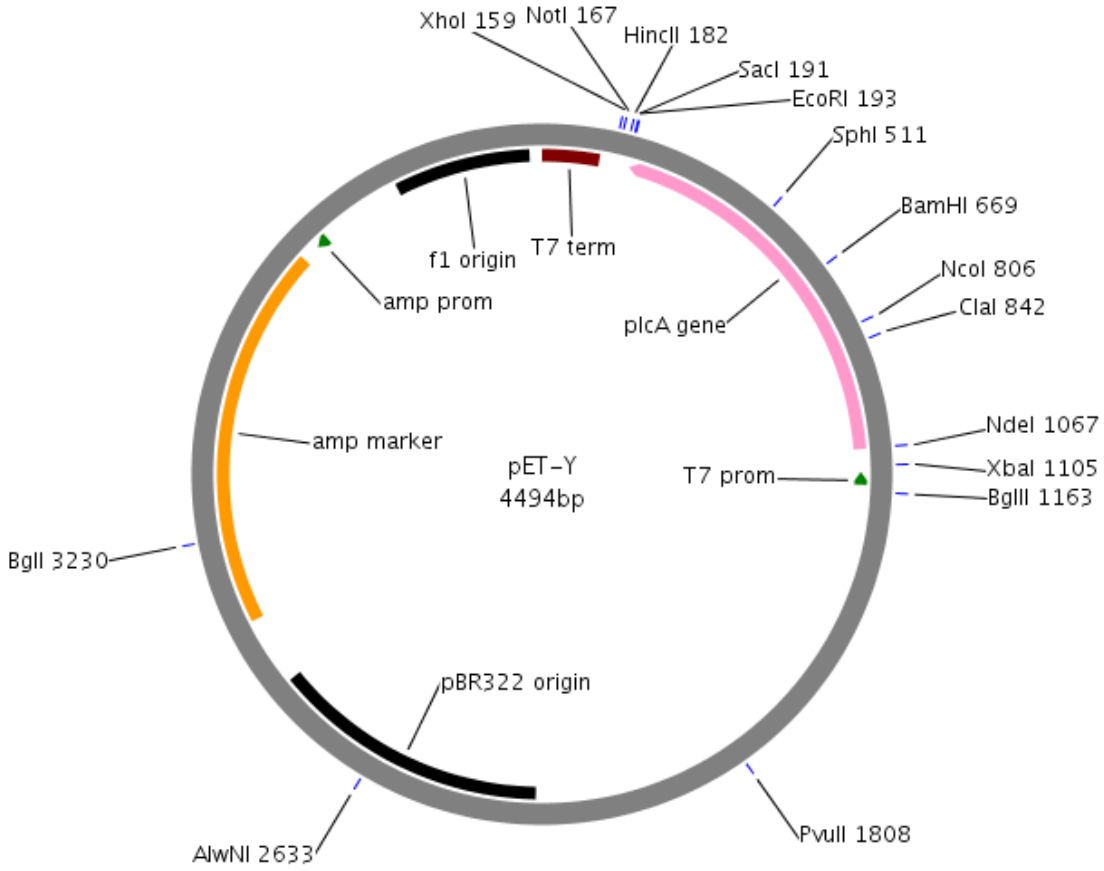

pDP1462 and pBS1462 by DNA sequencing, the TGA codon did exist in both original plasmids. It is reasonable to believe that pET1339 and pET1462 also carry this stop codon, which may account for the failures to express recombinant PI-PLCs from *E. coli*. After rechecking the sequencing results of pET1339 and pET1462, we found this TGA codon in both plasmids. This stop codon, however, is unlikely an error induced by PCR because pDP1462 has been transformed into the *L. monocytogenes* 10403S strain to obtain PI-PLC (Goldfine and Knob, 1992). It has been reported that TGA codes at low efficiency for Trp in *B. subtilis* and, presumably in *E. coli* (Hatfield and Diamond, 1993).

To optimize overexpression of the recombinant protein, we used the QuikChange™ Site-Directed Mutagenesis Kit to change the TGA codon in pBS1462 to TGG, the codon for Trp-35 in the published *plc*A gene sequence from *L. monocytogenes* EGD strain (nucleotide accession number: X54618). The 41-base mutagenic primers containing the mutated base were designed according to the manual. The mutagenesis was first performed using the suggested thermal-cycle parameters (denaturation at 95°C, annealing at 55°C and extension at 68°C), and various false positives were obtained. Partial or multiple copies of mutagenic primers were incorporated into the desired mutant region of these false positives. These false mutants may be caused by the primer self-annealing. The oligo plots of the mutagenic primers showed 10 short primer-dimer complements in the length of 4-5 bps. Either increasing the annealing temperature or decreasing the primer concentration can help to reduce those non-specific primer-primer bindings. Since excess primers concentrations are need for the mutagenesis, we thus modified the thermal-cycle parameters by simply increasing the annealing temperature to

68°C. Using this new thermal cycle (denaturation at 95°C, annealing at 68°C and extension at 68°C), we obtained the modified pBS1462, named pBS1462-1w, which was used as template for the following cloning. The gene for the PI-PLC precursor from 10403S strain in pBS1462-1w was then screened using the primers listed in Table 3-1. The DNA sequence determined was translated into the amino acid sequence which was then aligned with that of the published EGD strain *L. monocytogenes* PI-PLC using the Blast program. As shown in Figure 3-6, the 10403S strain PI-PLC differs from the published one at amino acids 76 (Ile→Met), 112 (Asn→Lys), and 119 (Phe→Tyr) in the mature protein and 4 (Asn→Ile), 7 (Gln→Arg), 13 (Leu→Val), 19 (Tyr→Cys) in signal peptide. These amino acids mutants were conserved in the pDP1462 checked by DNA sequencing using the T7 promoter primer. The plasmids pET-Y-1w and pET-F-1w were cloned from pBS1462-1w with the same primers for pET-F and pET-Y except the stop codon in the forward primer for pET-Y was changed to TGG also. Changing of TGA to TGG in the *plc*A gene generated a new *Bsr*I restriction site (Figure 3-7, Figure 3-8). The entire DNA sequence of inserted target gene was sequenced with the T7 promoter primers, G74 and G192, and compared with pBS1462 to prevent introduction of PCR-induced errors.

The pET-Y-1w and pET-F-1w plasmids should have some advantages over plasmids pET1339 and pET1462 in transcription and translation of the recombinant PI-PLC. First, the target gene is only under the control of strong bacteriophage T7 transcription as the promoter regions of the *plc*A gene are deleted. Second, the initiation

Table 3-1 Primers for sequencing *plc*A gene of *L. monocytogenes* PI-PLC in the constructed plasmids.

T7 promoter	5'-TAATACGACTCACTATAGGG-3'
G74	5’-GGAGACATGACGTGGACATTAACCAAACC-3’
G192	5’-GGAAAAATATTATTACTTTCAGAGAACC-3’
T7 terminator primer	5’-GCTAGTTATTGCTCAGCG-3’
Intein forward primer	5’-CCCGCCGCTGCTTTTGCACGTGAG-3’
T7 terminator reverse primer	5’-TATGCTAGTTATTGCTCAG-3’

Figure 3-6 Translation of *plc*A gene for 10403S *L. monocytogenes* PI-PLC precursor with rare codons (in *E. coli*) underlined. The differences from published EGD amino acid sequence (UniProtKB entry: P34024) are indicated.

```
ttgtataagatttatttacgacgcacattagttttagtactctgttttattttatgcttt
 L  Y  K  I  Y  L  R  R  T  L  V  L  V  L  C  F  I  L  C  F
          N        Q                    L                 Y
tttactttcccattaggcggaaaagcatattcgcttaataactgaaataagccaataaag
 F  T  F  P  L  G  G  K  A  Y  S  L  N  N  W  N  K  P  I  K

aactctgtaactacaaaacaatggatgtccgctctacctgacacaacaaacctagcagcg
 N  S  V  T  T  K  Q  W  M  S  A  L  P  D  T  T  N  L  A  A

ctctctataccaggtacacacgatacgatgagctataacggagacatgacgtggacatta
 L  S  I  P  G  T  H  D  T  M  S  Y  N  G  D  M  T  W  T  L
                                             I

accaaaccactggctcaaacgcaaacgatgtcattgtatcaacaattagaagcaggaata
 T  K  P  L  A  Q  T  Q  T  M  S  L  Y  Q  Q  L  E  A  G  I

cggtacatcgatattagagcaaaggacaatctcaaaatttaccatgggccaatttattta
 R  Y  I  D  I  R  A  K  D  N  L  K  I  Y  H  G  P  I  Y  L
                                 N                    F
aatgcatcactttcaggtgtattagaaacgattactcaatttttaaagaaaaatccaaaa
 N  A  S  L  S  G  V  L  E  T  I  T  Q  F  L  K  K  N  P  K

gaaaccattattatgcgtttaaaagacgagcaaaacagcaacgatagttttgattatcgg
 E  T  I  I  M  R  L  K  D  E  Q  N  S  N  D  S  F  D  Y  R

atccaaccactaatcaacatttataaagattatttttacactactcccagaactgacacg
 I  Q  P  L  I  N  I  Y  K  D  Y  F  Y  T  T  P  R  T  D  T

agcaataaaatccctacattaaaagatgtccgcggaaaaatattattactttcagagaac
 S  N  K  I  P  T  L  K  D  V  R  G  K  I  L  L  L  S  E  N

cacacaaaaaagccattagtcattaactcacgcaaattcggcatgcagttcggcgcacct
 H  T  K  K  P  L  V  I  N  S  R  K  F  G  M  Q  F  G  A  P

aaccaagtaattcaagatgactacaatggtccgagtgtgaaaacaaaattcaaagagatt
 N  Q  V  I  Q  D  D  Y  N  G  P  S  V  K  T  K  F  K  E  I

gtccagactgcttatcaagcttccaaagcggacaataaacttttttcttaaccatattagc
 V  Q  T  A  Y  Q  A  S  K  A  D  N  K  L  F  L  N  H  I  S

gccacttcattaacattcacacctcgtcagtatgctgcagcattaaacaacaaagtagag
 A  T  S  L  T  F  T  P  R  Q  Y  A  A  A  L  N  N  K  V  E

caattcgtactcaacttaacatcggaaaaagttcgaggattaggcatactaatcatggac
 Q  F  V  L  N  L  T  S  E  K  V  R  G  L  G  I  L  I  M  D

ttccccgaaaaacaaacaattaaaaacatcataaaaaacaataaattcaactaa
 F  P  E  K  Q  T  I  K  N  I  I  K  N  N  K  F  N  -
```

Figure 3-7 Graphic map of recombinant pET-F-1w created with PlasMapper. Using plasmid pBS1462-1w as template, *L. monocytogenes* partial *plc*A gene for PI-PLC from Phe-23 was amplified by PCR using primers 5'-ttttatactttCATATGttcccattaggcggaaaagcatattc-3' and 5'-ttgtaggaataaGAATTCttagttgaatttattgtttttatg-3'. The 30 cycle PCR product was doubly digested with *Nde*I and *EcoR*I and ligated to *Nde*I-*EcoR*I digested pET-23a(+). The entire DNA sequence of inserted target gene was sequenced with T7 promoter primer, G74 and G192 and compared with pBS1462 to prevent introduction of PCR-induced errors.

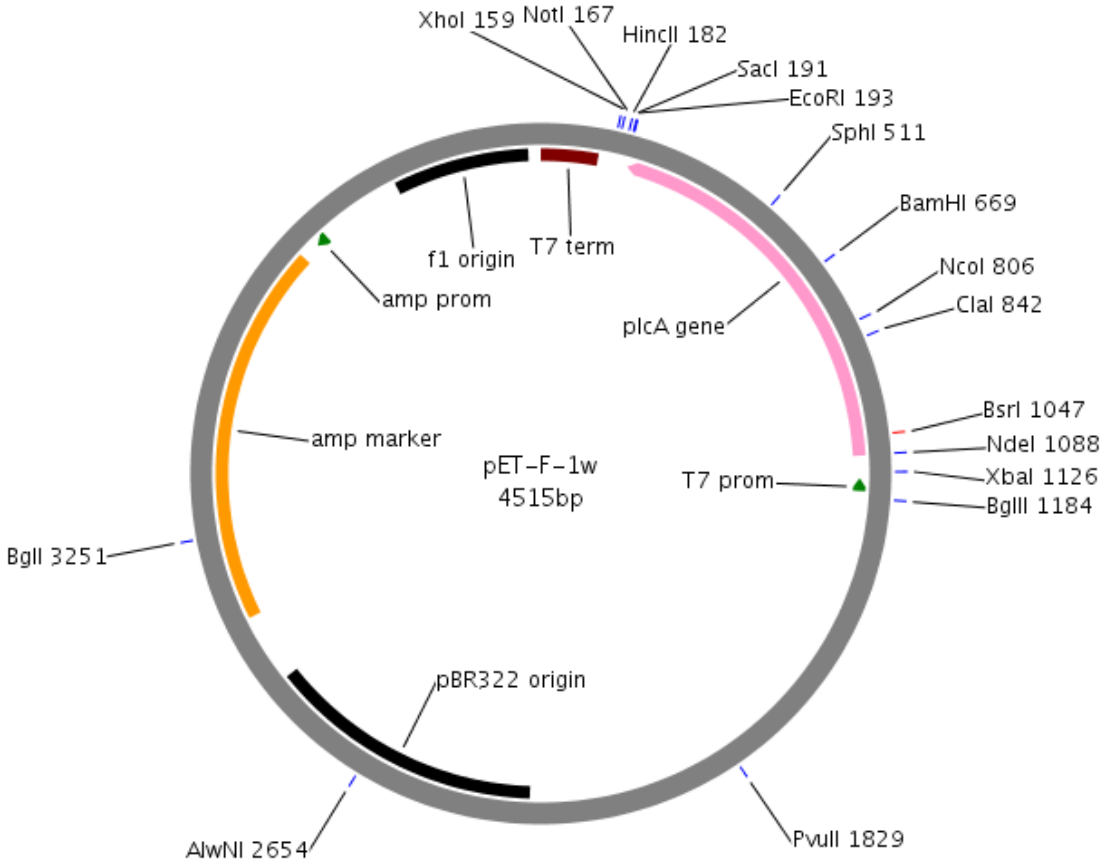

Figure 3-8 Graphic map of recombinant pET-Y-1w created with PlasMapper. Using plasmid pBS1462-1w as template, *L. monocytogenes* partial *plc*A gene for PI-PLC from Tyr-30 was amplified by PCR using primers of 5'-ttttatactttCATATGtattcgcttaataactggaataag-3'(TGA was replaced with TGG) and 5'-ttgtaggaataGAATTCttagttgaatttattgtttttatg-3'. The 30 cycle PCR product was doubly digested with *Nde*I and *Eco*RI and ligated to *Nde*I-*Eco*RI digested pET-23a(+). The entire DNA sequence of inserted target gene was sequenced with T7 promoter primer, G74 and G192 and compared with pBS1462 to prevent introduction of PCR-induced errors.

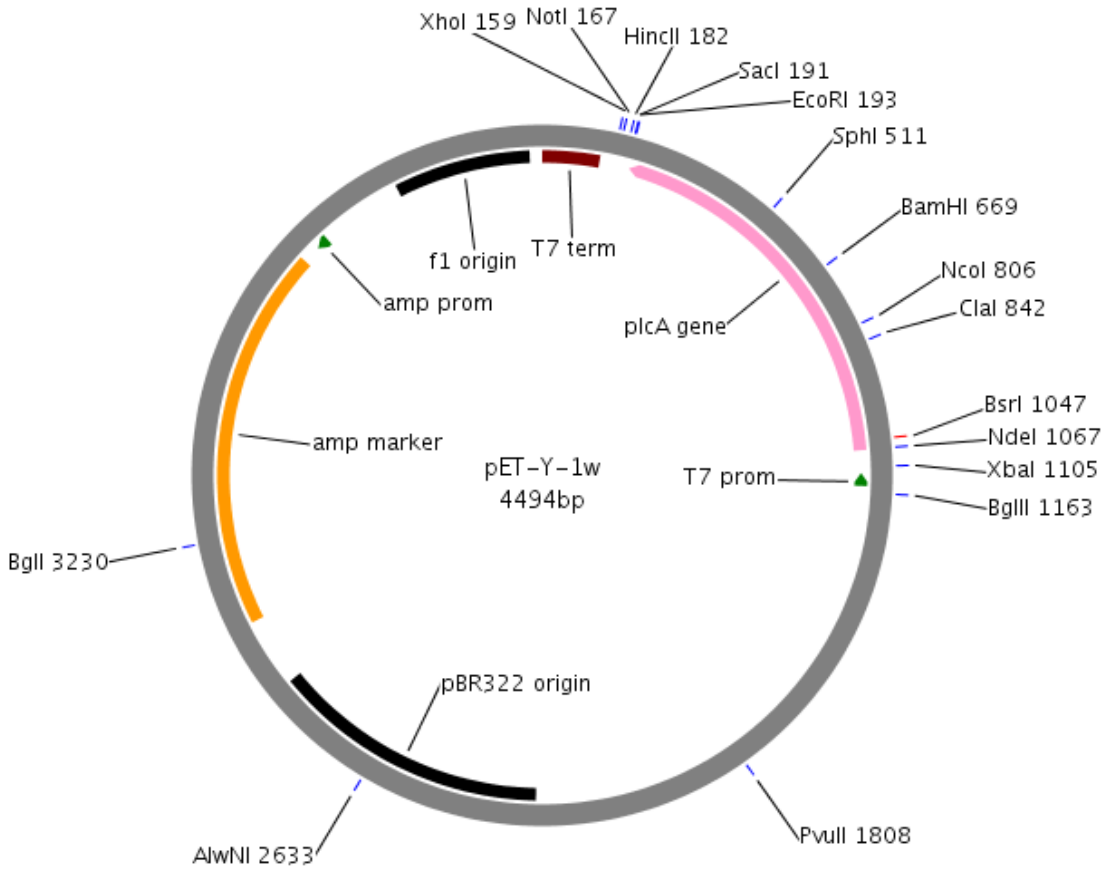

codon TTG used in the *plc*A gene is replaced with the more popular start codon ATG. The start codons used in *E. coli* were reported as 91% ATG, 8% GTG, and 1% TTG (Hannig and Makrides, 1998). Also, the codon for Trp-35 was changed from TGA to TGG, the normal codon for Trp.

pET-Y-1w and pET-F-1w were first transformed into BL21(DE3) and BL21(DE3)pLysS for overexpression. Analysis of the PI-PLC activity in cell extracts supernatants, solubilized cell debris and concentrated culture media detected no PI-PLC activity. Also no overexpressed protein band corresponding to a MW of 33 kDa could be detected by SDS-PAGE.

We also tried BL21-CondonPlus(DE3)-RIL and BL21-CodonPlus(DE3)-RP strains to provide rare codon tRNAs pool for expression because a number of rare codons are used in the *plc*A gene from *L. monocytogenes* 10403S strain (Figure 3-6). Several adjustments were tested including decreasing the incubation temperature (30°C) after IPTG induction and using the less degradation susceptible carbenicillin. However, none of theses modifications helped.

It was also possible that *L. monocytogenes* mature PI-PLC was expressed in the cytoplasm but misfolded. It could then be segregated into inclusion bodies and then degraded by proteases. In either case its expression level was too low to be detected by SDS-PAGE. Inclusion bodies can be separated easily and solubilized using urea or guadinium hydrochloride, from which, native target protein may be refolded in vitro either by dilution, dialysis or on-column refolding methods (Middelberg, 2002). However, refolding requires time consuming efforts with reduction in protein yield and the resultant

protein does not always regain biological activity. Refolding may not be a good general way to obtain interesting mutants as well since refolding is never guaranteed. Several approaches may be taken to address such protein expression problems. One strategy, for example, is to generate a fusion protein of the target protein and a fusion partner. Alternatively, the target protein can be co-expressed with molecular chaperones to help protein folding. Although there have some successful reports for the latter strategy, unfortunately, it is a trial and error process to specify the match between target protein and working chaperones (Georgiou and Valax, 1996; Hannig and Makrides, 1998). A third way in which target protein may be expressed is through the use of a periplasmic leader sequence.

C. Cloning and overexpression of mature *L. monocytogenes plc*A gene into pTYB11

Fusion proteins were originally exploited to facilitate protein purification and immobilization by using different kinds of molecular tags that can be used for affinity purification (Stevens, 2000). It soon became apparent that fusion partners might protect passenger proteins from intracellular proteolysis (Martinez et al., 1995; Jacquet et al., 1999), improve the solubility of passenger proteins (Davis et al., 1999; Kapust and Waugh, 1999), or be used as specific expression reporters (Waldo et al., 1999). High expression levels can often be transferred from an N-terminal fusion partner to a poorly expressing passenger probably as a result of mRNA stabilization (Arechaga et al., 2003). The IMPACT-CN appears to be an attractive protein purification system (Szweda et al., 2001; Byun et al., 2002; Massimelli et al., 2005). It provides two interesting vectors (pTYB1 and pTYB11) that enable the target gene to be cloned immediately adjacent to

the intein cleavage site, generating a fusion protein that could be purified in a single chromatographic step. The native recombinant protein without modifications could then be released from the fusion precursor by taking advantage of thiol induced self-cleavage activity of inteins. The N-terminal fusion vector, pTYB11, was used since the *L. monocytogenes* PI-PLC precursor normally contains an N-terminal signal peptide. To obtain the "native" mature PI-PLC, a *Sap*I restriction site must be used for cloning the 5' end of target gene. Two forward primers were thus designed for cloning into pTYB11. 5'-ggtggttGCTCTTCcaacNx-3' (*Sap*I site underlined) was generated by replacing the Nx with 5' end of the target genes (19 or 24 bases in order to terminate the primers in base of G or C). The same reverse primer containing an *EcoR*1 restriction site was used. Target genes flanked with *Sap*I and *EcoR*I sites were amplified by PCR. Because the *Sap*I site was lost after the cloning, we screened the positive colonies by *Xba*I-*EcoR*I double digestion. The results showed a DNA band of 2504-bp for IMPACT-F (Figure 3-9) and 2483-bp for IMPACT-Y (Figure 3-10) on the agarose gel. The entire DNA sequence of the inserted target gene was sequenced with Intein forward primer G74 and T7 terminator reverse primer and compared with that of pBS1462 to prevent introduction of PCR-induced errors.

The plasmids IMPACT-F and IMPACT-Y were transformed into ER2566 *E. coli* host cells for overexpression. LB media containing 100 μg/ml ampicillin was inoculated at 37°C with 5 ml freshly grown cultures and inoculated until the OD_{600} reached 0.7. IPTG was added to the final concentration of 0.4 mM for induction of PI-PLC expression.

Figure 3-9 Graphic map of recombinant IMPACT-F created with PlasMapper**.** Using plasmid pBS1462-1w as template, *L. monocytogenes* partial *plc*A gene for PI-PLC from Phe-23 was amplified by PCR using primers 5'-ggtggttGCTCTTCcaacttcccattaggcggaaaag-3' and 5'-ttgtaggaataaGAATTCttagttgaatttattgtttttatg-3'. The 30 cycle PCR product was doubly digested with *Sap*I and *EcoR*I and ligated to *Sap*I-*EcoR*I digested pTYB11. The entire DNA sequence of inserted target gene was sequenced with Intein forward primer, G74 and T7 terminator reverse primer and compared with pBS1462 to prevent using a gene with the PCR-induced errors.

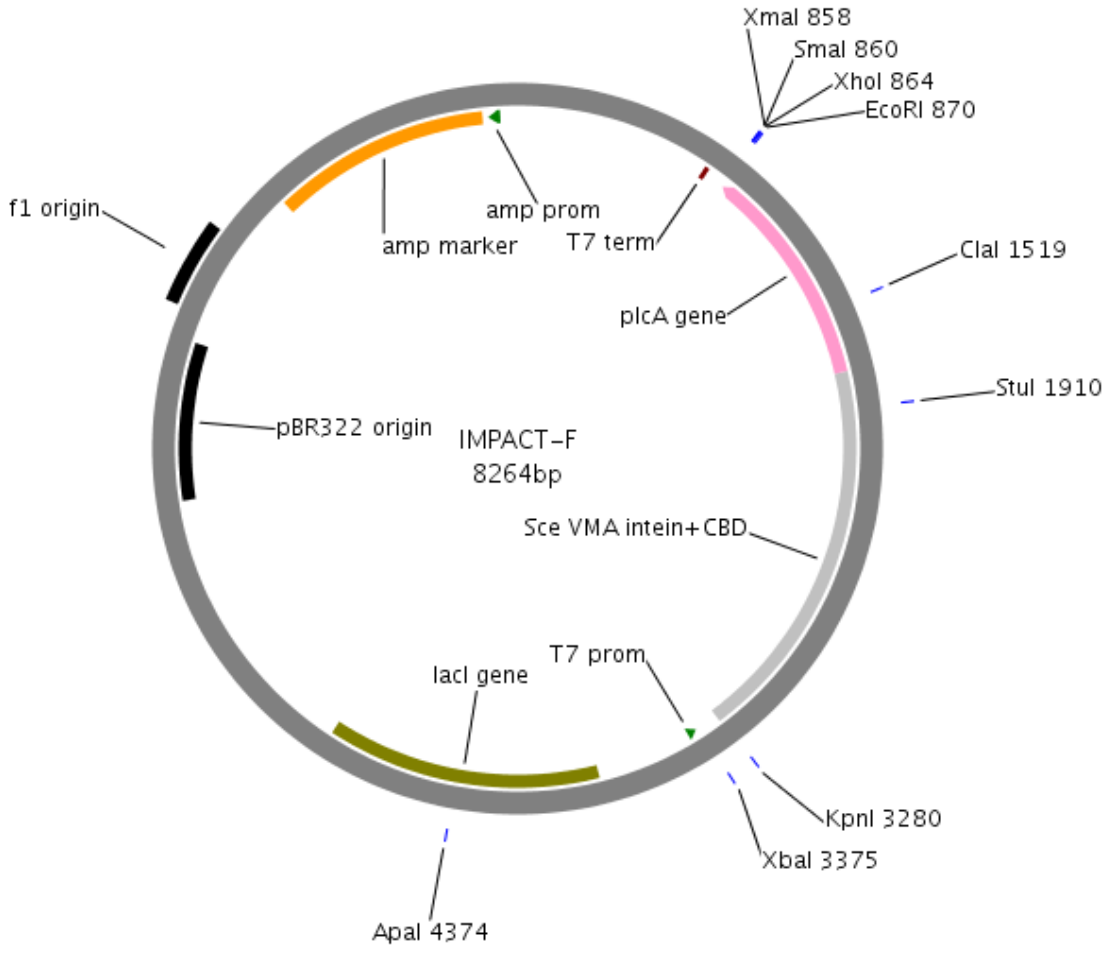

Figure 3-10 Graphic map of recombinant IMPACT-Y created with PlasMapper. Using plasmid pBS1462-1w as template, *L. monocytogenes* partial *plc*A gene for PI-PLC from Tyr-30 was amplified by PCR using primers 5'-ggtggttGCTCTTCcaactattcgcttaataactggaataag-3' and 5'-ttgtaggaataaGAATTCttagttgaatttattgtttttatg-3'. The 30 cycle PCR product was doubly digested with *Sap*I and *EcoR*I and ligated to *Sap*I-*EcoR*I digested pTYB11. The entire DNA sequence of inserted target gene was sequenced with Intein forward primer, G74 and T7 terminator reverse primer and compared with pBS1462 (to check for PCR-induced errors).

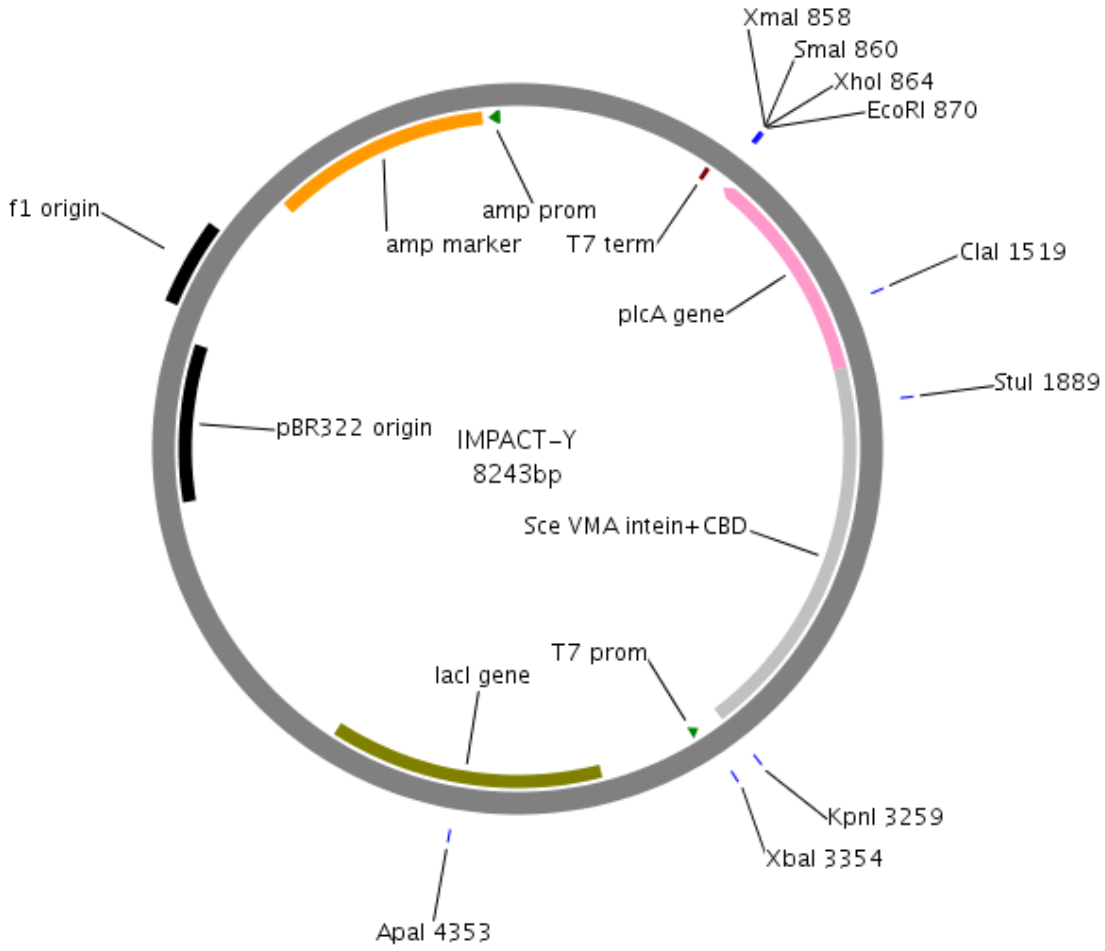

The cells continued to grow at 15°C overnight. Cell extract supernatants, solubilized cell debris, and concentrated culture media were then analyzed for PI-PLC activity. This time, the reaction mixture did become turbid immediately after adding the cell extract supernatants of ER2566 transformed with IMPACT-Y. It took much longer time (several hours) for the turbidity to show up when adding the same volume of cell extract supernatants of ER2566 harboring IMPACT-F. This turbidity is caused by the insoluble DAG released from PI by PI-PLC. PI-PLC hydrolysis activities were detected by NMR in the supernatants of both kinds of ER2566 cells, but not in their culture media and the solubilized cell debris. However, there was still no obvious overexpressed protein band corresponding to a MW of 88 kDa on SDS-PAGE gel of lysed cell supernatants and solubilized cell debris. Purification of the protein was achieved by elution of the supernatant on a chitin column. After loading supernatant (0.5 ml/min), the chitin column was washed with high salt column buffer and then DTT containing cleavage buffer at flow rate of 1 ml/min. The on-column cleavage of the fusion protein was carried at room temperature for 20 hours to ensure a sufficient yield of *L. monocytogenes* PI-PLC (this protein was reported to be stable at room temperature for several days (Goldfine and Knob, 1992)). The target protein, released from the precursor, was eluted from the column with dialysis buffer the next day. DTT and the co-eluted small peptide (1.6 kDa) were removed by dialysis at 4°C. Protein was then concentrated and analyzed by SDS-PAGE. For ER2566 harboring IMPACT-F, very little PI-PLC was purified; it could be detected with NMR by its activity but was not detected by SDS-PAGE. Recombinant PI-PLC in milligram amounts was obtained from the ER2566 with IMPACT-Y (Figure

3-11). It is unlikely that the much higher protein yield of PI-PLC (starting from Tyr-30) is caused only by a higher level of expression, since even the expression of PI-PLC (starting from Tyr-30) is very poor. It is more reasonable to assume that fusion precursor with the extra 7 amino acids at the N-terminus of PI-PLC was folded improperly since very little activity was observed in cell extract supernatants. Misfolded protein precursor may aggregate into inclusion bodies leading to the low yield. These results strongly indicate that Tyr-30, not Phe-23, is the first amino acid for mature PI-PLC (Goldfine and Knob, 1992; Ryan et al., 2002). We thus abandoned the further attempts on generating PI-PLC starting from Phe-23.

Conditions for optimizing recombinant PI-PLC yield were explored in some depth and the following observations were made. (1) The OD_{600} range for optimum induction of the cell cultures is 0.7-0.8. (2) A higher IPTG concentration (0.8 mM) is preferred as the T7/lac promoter is used in the IMPACT system to control the expression of the fusion gene. (3) Several induction conditions including 30°C for 6 hours or 15-25°C overnight were tested. After induction, incubation at a lower temperature (16°C) for longer time (20 hours) should be used to help folding of the fusion precursor. (4) A slower flow rate (0.4 ml/min) is best for loading the cell extract supernatant on the chitin column. (5) Faster washing and elution rates (2 ml/min) can be used without impairing the column binding of fusion protein. With these modified conditions, the best yield for recombinant *L. monocytogenes* PI-PLC was about 6 mg/L.

Figure 3-11 SDS-PAGE showing overexpression and purification of recombinant *L. monocytogenes* PI-PLC cloned in the IMPACT purification system (IMPACT-Y). The lanes represent protein content of (1) lysed cell extract, (2) flow through from the chitin column when loading, (3) wash from the column after loading, (4) wash from the column right before adding DTT, (5) protein eluted after incubation of column with DTT. Molecular masses for the standard proteins are 176.5, 113.7, 80.9, 63.8, 49.5, 37.4, and 26.0 kDa.

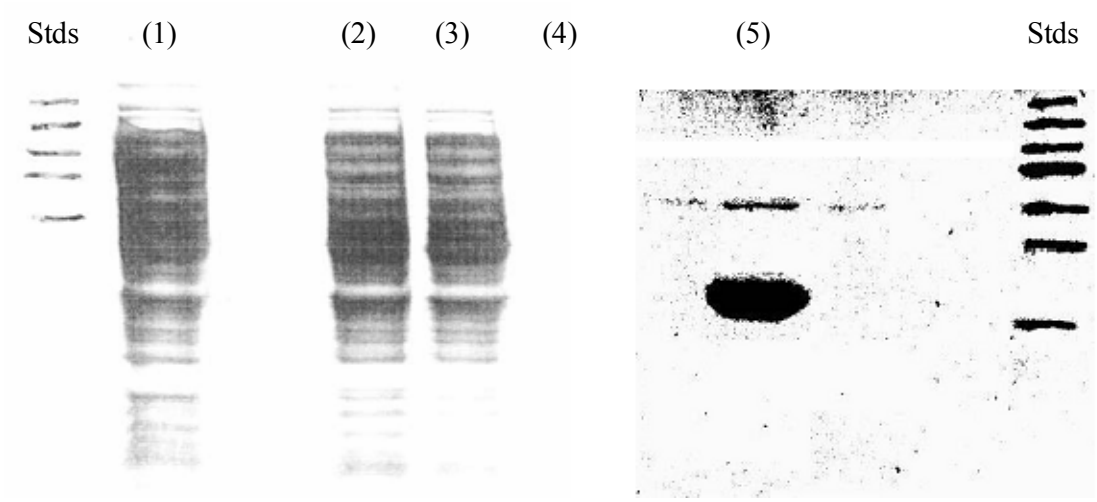

III. Summary and Discussion

We have cloned the *L. monocytogenes plc*A gene from strain 10403S, in whole or truncated forms, into both the pET-23a(+) vector and pTYB11 vector. The attempts to overexpress the cloned *plc*A gene in pET-23a(+) were not successful. The presence of a TGA codon for Trp-35, which is a normal terminator codon in *E. coli*, may account for no observed overexpression of the whole *plc*A gene cloned into pET-23a(+). The failure in obtaining PI-PLC with the truncated *plc*A gene for the mature protein in pET-23a(+), however, has another cause since TGA was replaced by TGG, the normal Trp codon in *E. coli*. According to http://www.biotech.ou.edu/, a web server for evaluation of protein solubility when it is overexpressed in *E. coli*, mature *L. monocytogenes* PI-PLC possesses an insolubility probability of 82.5%. The prediction is based on the revised Wilkinson-Harrison solubility model with two critical parameters, the approximate average charge and the turn-forming residue content (Wilkinson and Harrison, 1991; Davis et al., 1999; Harrison, 2000). If this is correct, it explains why we could not get recombinant PI-PLC. However, the intein tag, the carrier protein used in the IMPACT-CN system, was also predicted to be insoluble in *E. coli*, suggesting the prediction may not be consistent with the experimental result. The fact that no PI-PLC activity was found in the crude cell extracts is also inconsistent with the insolubility explanation because some proportion of the target protein is usually soluble within the cell even when inclusion bodies are formed. Except for solubility, the causes reported to prevent efficient heterologous protein production in *E. coli* are biased codon usage, gene product toxicity, mRNA secondary structure, and mRNA stability (Kane, 1995). Cloning of the partial *L. monocytogenes*

*plc*A gene for mature PI-PLC into pTYB11 (IMPACT-Y) enables us to get native target protein without any extra N-terminal residues. Although the expression is poor (no obvious overexpression band in SDS-PAGE), the yield was still up to 6 mg/L. Apparently, the carrier protein does benefit the overexpression of target protein, possibly by the use of fusion mRNA or keeping the fusion protein soluble. The extremely low yield of PI-PLC produced from the ER2566 carrying IMPACT-F, which differs from IMPACT-Y by the extra nucleotide sequence coding for a short peptide from Phe-23 to Ala-29, could be caused by a folding problem. Increasing the incubation temperature to 30°C after induction impaired the PI-PLC activity of supernatant further (longer time needed for assay mixture to become turbid).

An alternative strategy to obtain recombinant *L. monocytogenes* PI-PLC was to use vectors that enable export into the periplasm, which is a more favorable environment for folding. In the pET system, several vectors carrying signal peptides can be tried for this purpose. Since the amount of PI-PLC produced by IMPACT-Y is enough for the following studies, we did not explore this further. Moser et al. (1997) and later Ryan et al. (2002) did purify recombinant *L. monocytogenes* PI-PLC from *E. coli* periplasmic spaces by using the pHS1403 based vectors containing STII signal sequence (Koke et al., 1991).

The IMPACT^{TM} system (IMPACT-CN and IMPACT-TWIN) regulates the expression of target proteins the same way as the pET expression system. The tight regulation is obtained by incorporating the T7 promoter into the vector to control the transcription of the target gene and introducing the gene for T7 RNA polymerase into the host chromosome under the control of IPTG inducible *lac* operator. The IMPACT^{TM}

system contains seven expression vectors for flexible construction of fusion protein containing an intein tag. With more than 40 different plasmids, the pET system provides various cloning and expression strategies with many more choices than IMPACT^{TM} in the fusion partners for purification, detection, solubility, and translocation. However, the use of the intein tag of the IMPACT^{TM} system does provide an advantage on releasing the target protein without protease, which can be costly and non-specific. In addition to a thio-inducible intein tag, IMPACT-TWIN also provides pH and temperature inducible intein-tag for proteins sensitive to reducing agents. Also, the ability of IMPACT^{TM} to yield purified protein in a single column step enables purification of those poorly expressed recombinant proteins, like *L. monocytogenes* PI-PLC.

Chapter 4:

Activation of *L. monocytogenes* PI-PLC by interfaces and salts

I. Introduction

Bacterial PI-PLC catalyzes the calcium-independent hydrolysis of PI in two steps: (i) an intramolecular phosphotransferase reaction at a phospholipid aggregate surface to produce DAG and water-soluble cIP, followed by (ii) a cyclic phosphodiesterase reaction where cIP is hydrolyzed to I-1-P. The second reaction occurs with a soluble monomeric substrate and is much slower (with both lower V_{max} and significant higher K_m) than the first one (Volwerk et al., 1990; Zhou et al., 1997a). Previous studies of the PI-PLC from *Bacillus* sp. highlight several kinetic properties common to a wide range of phospholipase enzymes. That bacterial PI-PLC exhibits (i) "interfacial activation", an enhanced V_{max}/K_m, toward aggregated PI compared to monomeric PI (Hendrickson et al., 1992; Lewis et al., 1993; Volwerk et al., 1994), (ii) "surface dilution inhibition", a decrease in specific activity as the surface concentration of the substrate is diluted with detergents or other phospholipids while keeping the total substrate concentration constant (Zhou et al., 1997a), and (iii) "scooting mode catalysis", where enzyme completes several rounds of substrate turnover at the substrate interface before dissociating from the particle (Volwerk et al., 1994). The *Bacillus* sp. PI-PLC is also active towards GPI linkages (Low et al., 1988).

PI-PLC from *Listeria monocytogenes*, a ubiquitous foodborne intracellular pathogen of humans and animals, plays a role as virulence factor for the organism by aiding escape of the bacterium from the primary vacuole in macrophages (Camilli et al., 1993). This phospholipase has been proposed to disrupt the inner membrane of the spreading vacuole (Alberti-Segui et al., 2007). *L. monocytogenes* PI-PLC appears to

share the same general base and acid catalysis mechanism as *Bacillus* sp. PI-PLC (Bannam and Goldfine, 1999), and the enzyme has been shown to be activated by short-chain phosphatidylcholine (PC) molecules as well (Ryan et al., 2002). There are, however, several major differences of the *L. monocytogenes* PI-PLC from *Bacillus* homologues, namely a high pI (above 9), kinetic activation by salts, and relatively weak activity toward GPI anchors (Goldfine and Knob, 1992; Hatfield and Diamond, 1993).

In my work, water-soluble synthetic short chain phosphatidylinositol and cIP along with PI/detergent mixed micelles and PI/PC vesicles were used as substrates to understand how salts and other phospholipids affect both steps of PI hydrolysis by the *L. monocytogenes* PI-PLC. The results indicate that *L. monocytogenes* PI-PLC binds tightly to anionic phospholipids (e.g., PI, PG) and tends to form aggregated complexes with those anionic lipids. The enzymatic activity is much lower for those complexes. The two types of activators previously shown for this enzyme work by different mechanisms: (i) neutral amphiphiles, which enhance both steps of catalysis regardless of the aggregation state of the substrate, bind directly, though weakly, to the protein and enhance its catalytic ability (at sufficiently high mole fractions the amphiphiles can prevent the enzyme from forming the aggregated complexes), while (ii) moderate ionic strength (e.g., salts) only affects the phosphotransferase reaction and then only when an activating interface is present. The latter is likely to be the result of altering the surface electrostatics and reducing the formation of aggregated complexes, and possibly altering the residence time of the enzyme on interfaces. A model rationalizing the role of both types of activators in modulating the enzyme activity in situ is presented.

II. Specific activity behavior of *L. monocytogenes* PI-PLC

A. Dependence of *L. monocytogenes* PI-PLC specific activity on protein concentration

Previously, the pH behavior for the *L. monocytogenes* PI-PLC phosphotransferase reaction was shown to vary slightly with the detergent matrix for the PI. A sharp optimum pH of 7.0 was observed toward PI solubilized in deoxycholate micelles with less than 30% activity at pH 6.5 and pH 7.5 (the suspension of PI in deoxycholate was no longer clear below pH 6.5), while a broad optimum pH range, from 5.5 to 6.5, was observed for enzyme acting on PI in TX-100 micelles (Goldfine and Knob, 1992). For comparison we tested the effect of pH on the phosphodiesterase reaction in the absence of detergent. The enzyme was optimally active towards cIP at pH 7.0, with 67% and 57% maximum activity at pH 6.5 and 7.5 respectively (Figure 4-1). Thus, pH 7.0 was used for both phosphotransferase and cyclic phosphodiesterase kinetic assays.

PI can be presented to PI-PLC in a range of different matrices – micelles, unilamellar vesicles or water/organic solvent co-mixtures (Volwerk et al., 1990; Lewis et al., 1993; Zhou et al., 1997a; Zhou and Roberts, 1998; Wehbi et al., 2003a). Differences in PI-PLC activity toward the different types of interfaces can often provide insights into what factors control the activity of this enzyme. However, *L. monocytogenes* PI-PLC exhibited an added complication that protein concentration also affected enzyme activity. Since the assay for phosphotransferase activity is not continuous, we monitored the generation of cIP (using 0.02, 0.41, or 1.7 μg/ml PI-PLC) toward PI/TX-100 micelles at

Figure 4-1 Dependence of cIP hydrolysis by *L. monocytogenes* PI-PLC on the pH of the solution. Assay conditions included 50 mM imidazole, 10 mM cIP, 3.6 μg/ml enzyme.

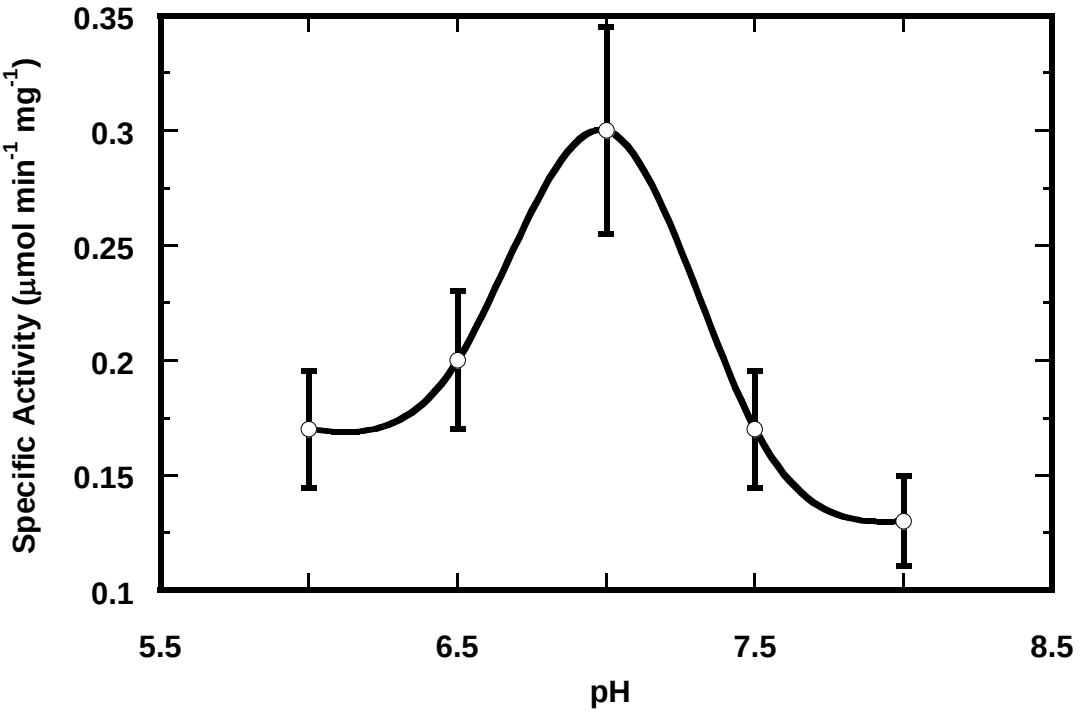

various time points to avoid the influence of a lag or burst in product formation. The specific activities determined for a given sample were all consistent (within 15% errors) in the range of 8-20% PI hydrolysis. This suggested that the time scale for PI-PLC binding to the substrate PI micelles was relatively short, and that products had little effect on enzyme activity. As shown in Figure 4-2, the phosphotransferase activity of *L. monocytogenes* PI-PLC toward PI (8 mM) in TX-100 (32 mM) mixed micelles increased dramatically from 147 to 1190 $\mu mol \cdot min^{-1} \cdot mg^{-1}$ as protein was diluted from 0.41 to 0.01 μg/ml. Further dilution of the protein had only a small effect on specific activity. A similar dependence of specific activity on protein concentration was also observed with PI/diC_7PC mixed micelles (Figure 4-2). To rule out any possible inhibitors from the expression/purification system, purified recombinant *L. monocytogenes* PI-PLC was further purified with cation exchange or gel filtration (with high salt concentration) chromatography, and the concentration dependence of specific activity on enzyme concentration still persisted.

The loss of activity with high enzyme concentration has been discussed by Wang (1999) for an association-dissociation enzyme system. PI-PLC could be aggregating in solution with the monomer more active than oligomer. Therefore, we tried several ways to check the aggregation state of *L. monocytogenes* PI-PLC in solution. Gel filtration was first applied. However the enzyme interacted anomalously with gel filtration resins even in the presence of 0.5 M NaCl, so that another method was needed. Native gel electrophoresis can often be used to measure the native molecular mass of the

Figure 4-2 Dependence of *L. monocytogenes* PI-PLC phosphotransferase activity on enzyme concentration (μg/ml). Assay conditions included 50 mM HEPES, pH 7.0, 8 mM PI solubilized in either 32 mM TX-100 (o) or 32 mM diC_7PC (•).

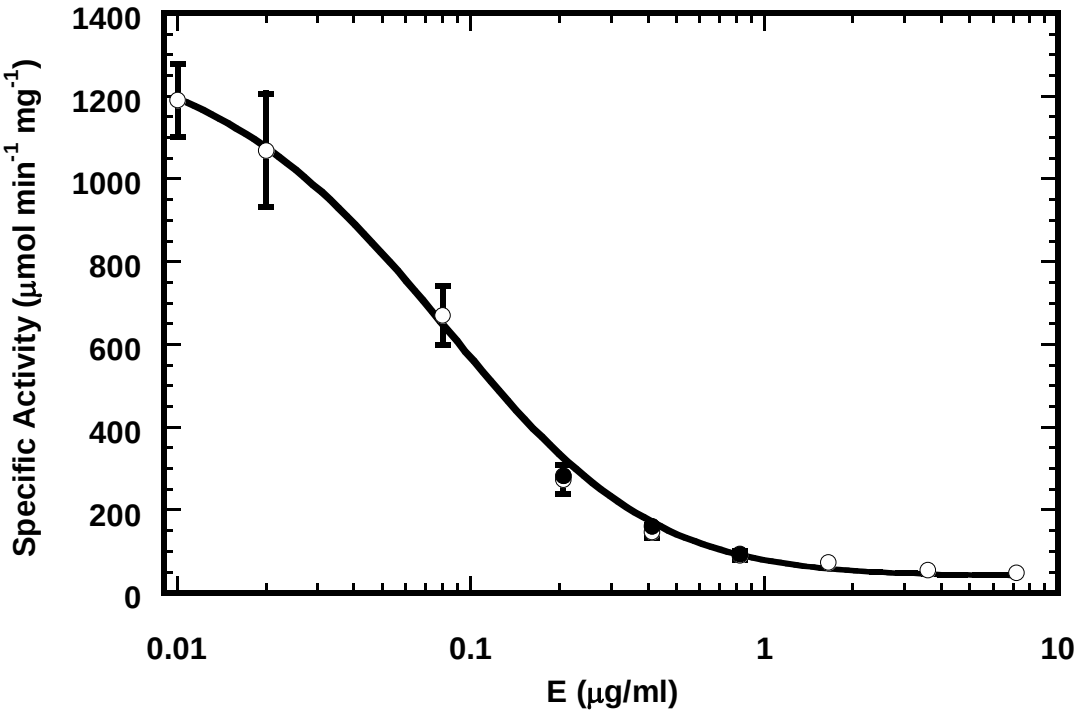

protein. For an enzyme with a high pI, an acidic buffer system and standard proteins carrying positive charges are required. Within the range of acrylamide concentrations used (7-15%), only one band was observed for up to 50 μg *L. monocytogenes* PI-PLC on the gel. But with only three commercially available basic proteins as standards, the errors in estimating the native molecular weight were too high for a definitive answer. Laser light scattering is another method for characterizing the native molecular mass of proteins. This measurement on *L. monocytogenes* PI-PLC was provided by the HHMI Biopolymer Facility and W. M. Keck Foundation Biotechnology Resource Laboratory (Yale University). The average molecular mass for *L. monocytogenes* PI-PLC was determined as 28.2 kDa at a concentration of 0.14 mg/ml - well above that used in the kinetic assays. This is quite close to the predicted molecular weight of 33 kDa determined from the sequence. Thus, this PI-PLC exists as a monomer in solution in the absence of detergent. If the protein aggregation does account for the dependence of specific activity on protein concentration, the oligomerization of PI-PLC must only occur in presence of an interface or the anionic substrates. Cross-linking of the protein with EDC, DMS, and APG was tried to assess this possibility. However, with EDC and DMS no aggregate states were trapped. With APG, enzyme (2 mg/ml) aggregates were detected (Figure 4-3). At protein concentrations used in assays such oligomerization is unlikely to occur unless it is catalyzed by interfaces.

The phosphodiesterase activity of *L. monocytogenes* PI-PLC toward 5 to 40 mM cIP without detergent was investigated at two different protein concentrations. Because

Figure 4-3 SDS-PAGE of APG cross-linking assays: lane 1, MW markers; lane 2, pure PI-PLC; lane 3, APG crosslinked PI-PLC. For assay, 2 mg/ml PI-PLC was incubated in the dark with 2.4 mM of APG in 20 mM sodium phosphate, pH 7.5, for 6 h at room temperature; the subsequent photoactivation was performed with a 254 nm UV light source for 15 min at room temperature. Upon completion, the reaction mixture was dialyzed in the dark to get rid of the excess APG and checked with SDS-PAGE.

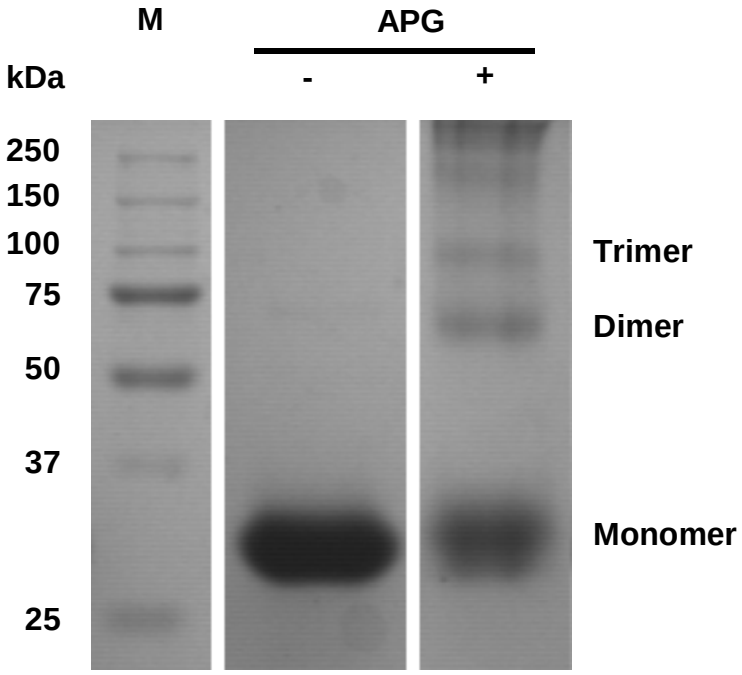

cIP is a poorer substrate than PI, considerably higher enzyme concentrations (3.6 or 7.2 μg/ml) were needed. In this high range of enzyme concentration, the activity is low and varies little between these two protein concentrations. However, there is a very significant difference in kinetic parameters extracted for the two different enzyme concentrations (Figure 4-4). In both cases, the data could be fit to the Michaelis-Menten equation: V_{max}=0.7±0.1 μmol·min^{-1}·mg^{-1} and K_m=12.5±5.0 mM at the lower PI-PLC concentration (3.6 μg/ml), and V_{max}=2.0±1.0 μmol·min^{-1}·mg^{-1} with K_m=100±62 mM at double the enzyme concentration. Although the errors in V_{max} and K_m are large, the major effect of the higher enzyme concentration appears to be an increase in 'K_m' for water-soluble substrate cIP. Although *L. monocytogenes* PI-PLC exists as monomer in solution as shown by the laser light scattering measurement, variations in enzyme concentration show different extents of activation for cIP cleavage, indicating that the enzyme may aggregate with the substrate present (in this case soluble cIP).

B. Effect of detergent or vesicle interface on PLC activities

The *Bacillus* sp. PI-PLC enzymes exhibits a specific activation of both phosphotransferase and phosphodiesterase steps by interfaces containing phosphatidylcholine (or phosphatidylethanolamine) (Zhou et al., 1997a). It has been suggested that such an activation also occurs for the *L. monocytogenes* PI-PLC (Goldfine and Knob, 1992). Therefore, we examined the effect of micelle matrix on the phosphotransferase activity of recombinant *L. monocytogenes* PI-PLC toward PI dispersed in TX-100. The enzyme concentration, as well as detergent, was varied (0.02,

Figure 4-4 Effect of cIP concentration on *L. monocytogenes* PI-PLC phosphodiesterase activity: (o) 3.6 µg/ml, and (•) 7.2 µg/ml PI-PLC. Assay conditions included 50 mM imidazole, pH 7.0, and variable cIP concentration.

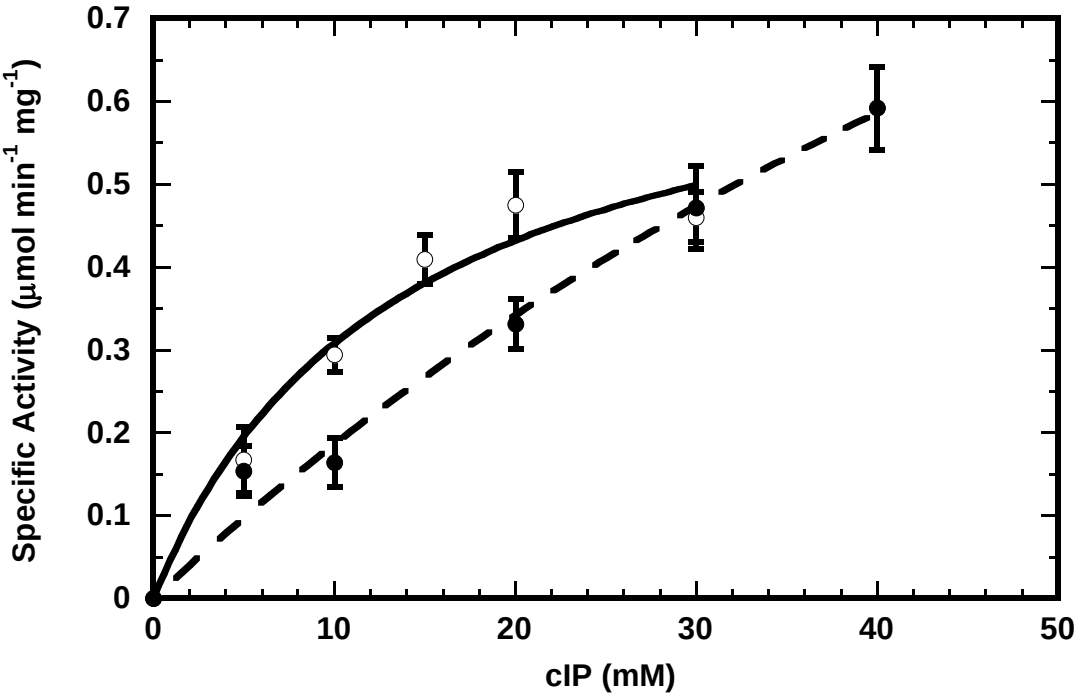

0.2, or 0.4 μg/ml protein). TX-100 is a nonionic detergent that clarifies PI bilayers at >2:1 TX-100/PI (Zhou et al., 1997a). If the surface concentration of PI is important for *L. monocytogenes* PI-PLC activity, then increasing TX-100 at fixed PI (8 mM) will eventually "inhibit" the enzyme leading to lower specific activity. Such surface dilution inhibition has been documented for the *B. thuringiensis* PI-PLC (Zhou et al., 1997a). However, in our hands, *L. monocytogenes* PI-PLC presented different kinetic patterns depending on the protein concentration (Figure 4-5A). For 0.4 μg/ml enzyme, the enzyme exhibited no decrease in activity up to X_{det} = 0.94 (16:1 TX-100/PI). In fact, the enzyme phosphotransferase activity *increased* dramatically as the surface concentration of the detergent increased above 0.90. The same amount of PI-PLC exhibited the same specific activities towards PI presented in diC_7PC micelles. A similar trend, but with higher specific activities, was observed when the protein concentration in the assay was decreased two-fold.

At a much more dilute concentration, 0.02 μg/ml, a more typical 'surface dilution curve' was observed with the maximum phosphotransferase activity around 3.5:1 TX-100/PI. This detergent/substrate ratio for optimal activity is higher than what is needed to minimally solubilize PI (2:1 TX-100/PI). It has been reported that PI in predominantly PC bilayers is partially demixed (Redfern and Gericke, 2004). A similar demixing in mixed micelles could occur unless an excess of detergent is used. Alternatively, this could reflect a distinct activation by the detergent. At the very low concentration of this PI-PLC, the specific activity of *L. monocytogenes* PI-PLC decreased above X_{det}= 0.80 as might be expected for a regime where the surface concentration of

substrate influences the enzyme action. Comparing the activity curves of three protein concentrations in Figure 4-5A shows that significantly increased TX-100 could compensate for the lower specific activity at high enzyme concentration, since comparable high activities (1155 and 1260 μmol $min^{-1}mg^{-1}$) were achieved for all the protein concentrations examined. If the protein concentration decreased further, a lower optimum TX-100/PI ratio would be expected. However, 0.02 μg/ml is the limit of our assay system. Using [^{3}H]PI as substrate, the phosphotransferase activity of PI-PLC was previously measured at 0.003 μg/ml enzyme. The optimal *L. monocytogenes* PI-PLC specific activity (~2900 $\mu mol \cdot min^{-1} \cdot mg^{-1}$) toward 0.08 mM PI micelles dispersed in TX-100 or deoxycholate was reported at a ratio of 10:1 TX-100/PI or 30:1 deoxycholate/PI (Goldfine and Knob, 1992). The higher specific activity than what we observe with low PI-PLC or moderate PI-PLC with high mole fractions of detergent (X_{det}) is likely due to the addition of moderate salt, ammonium sulfate, in the previous report

We checked the effect of diC_7PC (a zwitterionic synthetic short-chain phosphatidylcholine that forms micelles) on PI cleavage by *L. monocytogenes* PI-PLC. As shown in Figure 4-5A, the data for PI dispersed in diC_7PC agrees well with that for PI/TX-100 mixed micelles at the same enzyme concentration (0.4 μg/ml), although there was a slightly lower specific activity at relatively high mole fraction of detergent. The similarity in the effects of various detergents on the phosphotransferase activity of PI-PLC is not observed for *Bacillus* sp. homologs. For *B. thuringiensis* PI-PLC, a higher ratio of detergent to PI was required for the maximal activity using diC_7PC compared to

TX-100 (6:1 for diC_7PC/PI versus 2:1 for TX-100/PI). The specific activity with the short-chain PC micelles was also increased 3.5-fold (Zhou et al., 1997a).

The activity of *L. monocytogenes* PI-PLC toward a fixed bulk concentration of PI (8 mM) diluted in a POPC vesicle matrix was also studied. Compared with PI/TX-100 micelles, unilamellar vesicles of long-chain PI are poor substrates for PI-PLC from *L. monocytogenes*, necessitating high protein concentrations for these assays. At a protein concentration of 1.6 μg/ml, the enzyme phosphotransferase activity increased about 2-fold as the mole fraction of POPC increased from 0 to 0.2. A slightly larger activation (2.5-3-fold) at 0.2 mole fraction POPC was reported for *B. thuringiensis* PI-PLC (Pu et al., 2008a). Once the POPC mole fraction was greater than 0.2 (at fixed PI), the *L. monocytogenes* PI-PLC specific activity stayed constant until a POPC mole fraction of 0.5 and then decreased as the mole fraction increased further to 0.8 (Figure 4-5B). This behavior is consistent with the weak surface dilution inhibition observed in the PI micelle system. Similar to PI/TX-100 micelles, higher activities toward PI/POPC SUVs were also observed at a lower enzyme concentration (0.4 μg/ml) except for PI pure SUVs where the specific activities were 1.3 and 3.7 $\mu mol \cdot min^{-1} \cdot mg^{-1}$ for 0.4 and 1.6 μg/ml enzyme, respectively. The effect of 0.2 mole fraction POPC is unlikely to be the result of a specific interaction of the enzyme with that zwitterionic phospholipid since the presence of POPC could not compensate for the activity loss at higher protein concentration (Figure 4-5B).

Examining amphiphile effects with monomeric substrate, in this case cIP, is one

Figure 4-5 (A) Dependence of *L. monocytogenes* PI-PLC phosphotransferase activity on mole fraction of detergent: 0.4 μg/ml PI-PLC with 8 mM PI solubilized in TX-100 (Δ) or diC$_7$PC (X); 0.02 μg/ml (o) or 0.2 μg/ml (•) PI-PLC with PI solubilized in TX-100. (B) Dependence of phosphotransferase activity on mole fraction of POPC in PI (8 mM)/POPC SUVs with 0.4 μg/ml (o) or 1.6 μg/ml (•) enzyme. Reactions were carried out with 8 mM PI and the indicated amphiphile dispersed in 50 mM HEPES, pH 7.0.

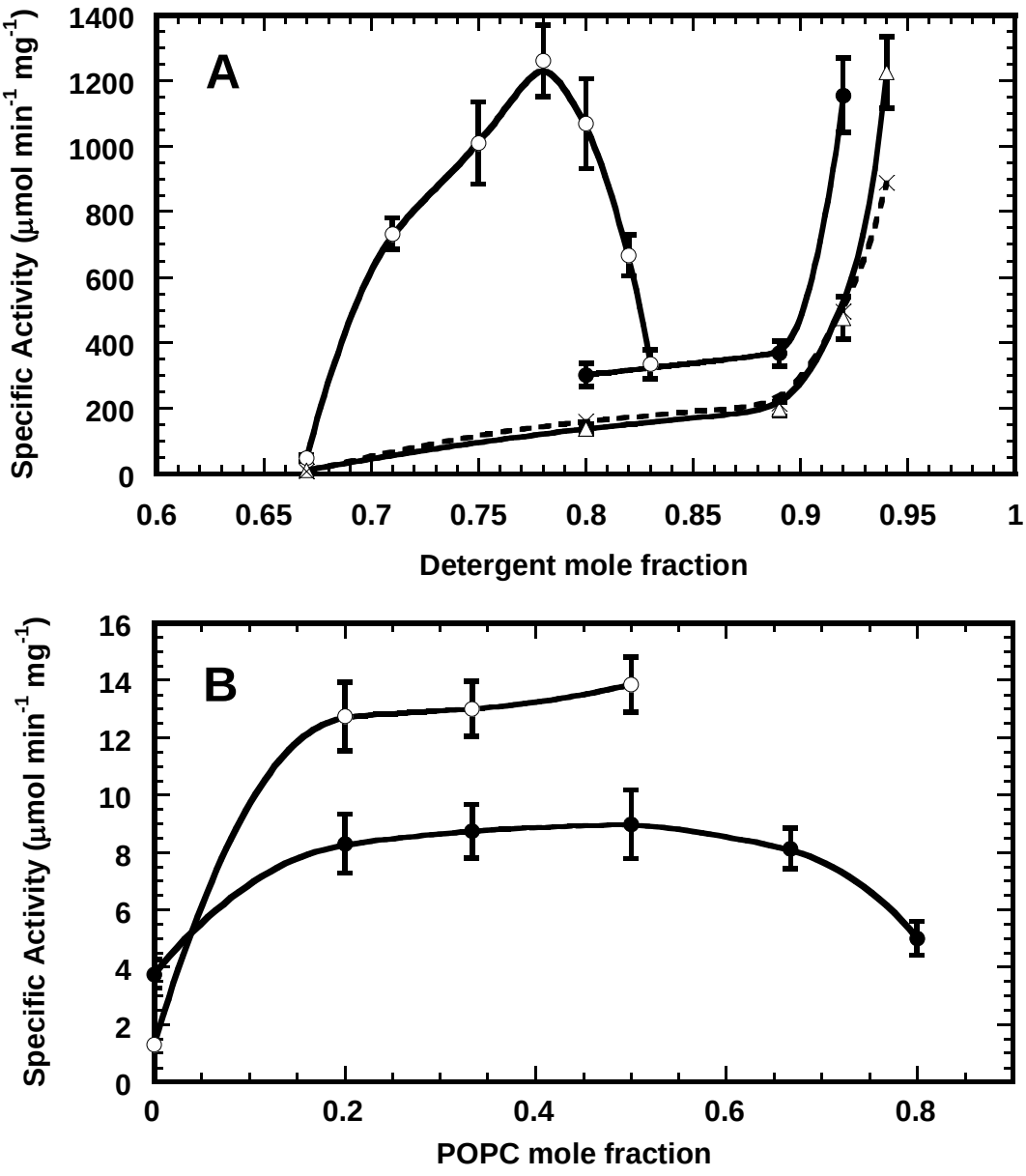

way of separating activator effects that alter the substrate versus those that alter the enzyme. With cIP at a fixed concentration, we can screen different additives for their effect on *L. monocytogenes* PI-PLC activity towards this monomeric substrate. Ryan and coworkers (2002) have shown that diC_6PC at concentrations below its CMC activate this enzyme with respect to non-natural water-soluble PI substrates. In our system, the plot of phosphodiesterase specific activity of *L. monocytogenes* PI-PLC versus diC_6PC concentration was biphasic (Figure 4-6A). Below the CMC of diC_6PC (14 mM), there was a 12-fold increase in activity upon the addition of 5 mM diC_6PC followed by a small rate drop. A second increase in specific activity was observed around the CMC of diC_6PC, with PI-PLC activity 20-fold activity higher than for cIP alone. A slightly more hydrophobic amphiphile, diC_7PC, also enhanced the activity of the enzyme toward the natural soluble substrate cIP (Figure 4-6A). With 10 mM cIP (below its K_m), there was a 4-fold increase in *L. monocytogenes* PI-PLC specific activity upon the addition of 1.5 mM diC_7PC (the CMC of the lipid alone). The *L. monocytogenes* PI-PLC specific activity toward cIP kept increasing as the PC micelle concentration was increased to 32 mM. The sigmoidal dependence of specific activity on diC_7PC concentration is consistent with PC surfaces acting as more potent activators than PC monomers. The effective 'K_d' or $S_{0.5}$ for this activation occurred at 3.8 mM diC_7PC. The requirement for the higher amount of diC_7PC micelles to activate *L. monocytogenes* PI-PLC compared to *B. thuringiensis* PI-PLC (Zhou et al., 1997a) suggests a weaker binding of the Listeria enzyme to this surface.

Figure 4-6 (A) Effect of diC_6PC (o) or diC_7PC (•) on cIP (10 mM) hydrolysis by 3.6 μg/ml PI-PLC in 50 mM imidazole, pH 7.0. (B) Effect of POPC SUVs (Δ) on cIP (10 mM) hydrolysis by 3.6 μg/ml PI-PLC. The X indicates the effect of 2 mM POPC/0.1 mM POPS vesicles on cIP hydrolysis.

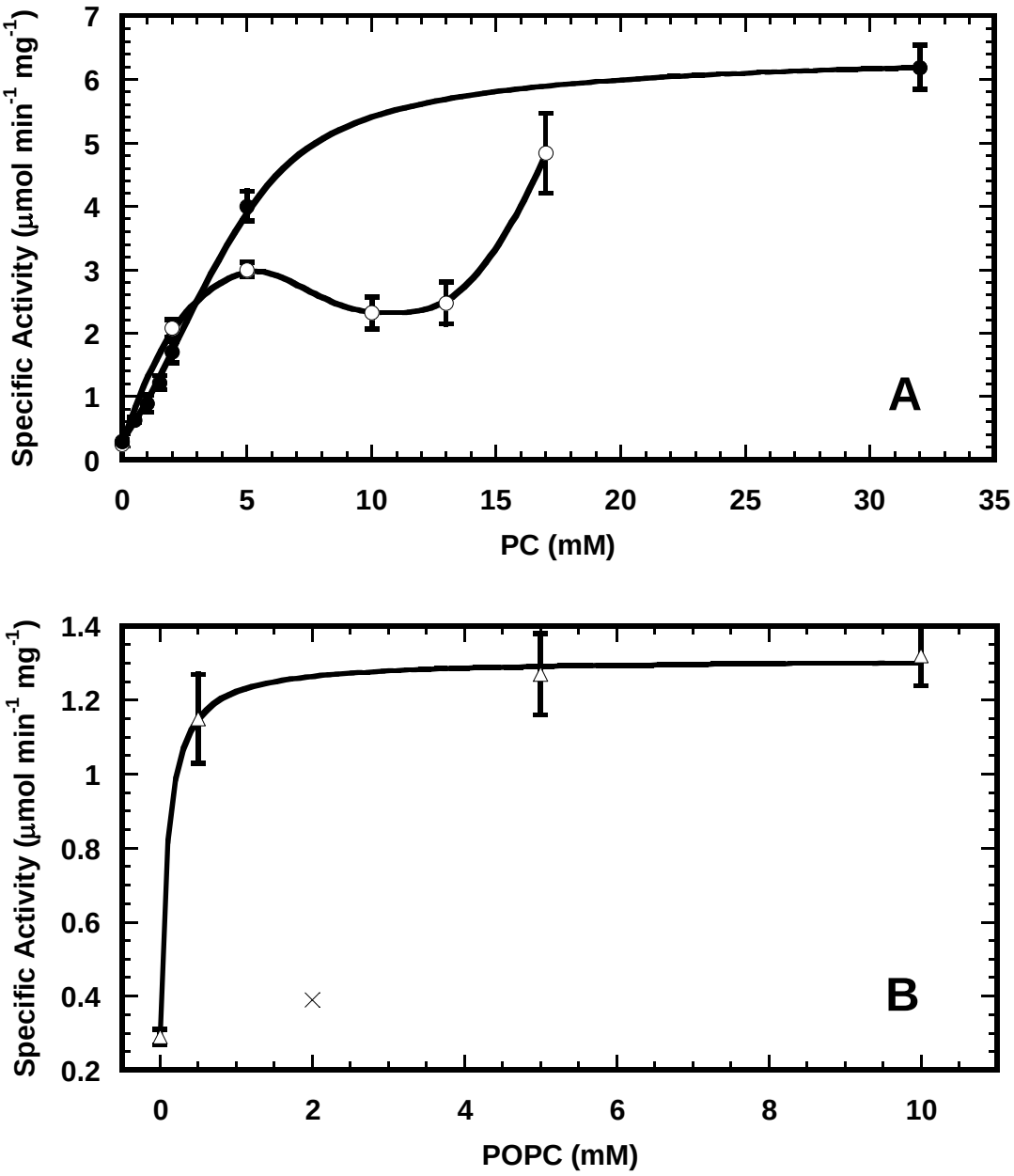

Table 4-1 Effect of different additives on cIP (10 mM) hydrolysis by *L. monocytogenes* PI-PLC[a].

Assay system	PI-PLC (μg/ml)	Additive	(mM)	Relative activity [a]
cIP	7.2	TX-100	3	14.8
cIP	7.2	diC_7PC	5	15.1
cIP	7.2	POPC	2	4.38
cIP	7.2	DOPMe	1	<0.1
cIP	7.2	POPS	1	0.43
cIP	3.6	POPC	2	7.94
cIP + 2 mM POPC	3.6	POPS	0.1	0.31
cIP	7.2	$(NH_4)_2SO_4$	150	0.65
cIP + 5 mM diC_7PC	7.2	$(NH_4)_2SO_4$	100	0.83

[a]Assays measured in 50 mM HEPES, pH 7.0, 25°C. Relative activity is the ratio of the specific activity measured with the additive present compared to the activity in the absence of that additive (salts or lipids). For 10 mM cIP in the absence of additives, the enzyme specific activity was 0.29 $\mu mol \cdot min^{-1} \cdot mg^{-1}$ for 3.6 μg/ml protein or 0.16 $\mu mol \cdot min^{-1} \cdot mg^{-1}$ for 7.2 μg/ml protein.

POPC SUVs also enhanced cIP hydrolysis (Figure 4-6B and Table 4-1) with an $S_{0.5}$<0.05 mM, although the maximum activity was considerably less than for diC_7PC or TX-100 activation. SUVs composed of anionic non-substrate phospholipids (POPS and DOPMe) strongly inhibited the cIP hydrolysis reaction (Table 4-1). Vesicles with 0.2 mole fraction POPS disproportionately reduced *L. monocytogenes* PI-PLC activity toward cIP. Therefore, the enzyme must bind to those anionic phospholipids more tightly than it binds to POPC.

Unlike what is observed for *B. thuringiensis* PI-PLC, TX-100 was also an effective activator of cIP hydrolysis by *L. monocytogenes* PI-PLC. Comparable activities were obtained with 3 mM TX-100 or 5 mM diC_7PC (Table 4-1). Since the substrate cIP is monomeric, the amphiphile must activate *L. monocytogenes* by a direct interaction. However, whether in doing so it disfavors substrate-induced protein aggregation or promotes a more active form of the enzyme is not known.

C. Effect of salts

Salt activation of PI cleavage by *L. monocytogenes* PI-PLC has been documented previously (Goldfine and Knob, 1992). Although no explanation was proposed, it was noted that in the absence of high salt, *L. monocytogenes* PI-PLC in solution behaved as a large aggregate on gel filtration columns, but that 1 M $(NH_4)_2SO_4$ attenuated this behavior (Goldfine and Knob, 1992). Salts can enhance hydrophobic interactions (e.g., promote insertion of protein hydrophobic side chains into bilayers) as well as weaken electrostatic interactions that hold complexes together. With this in mind, we examined the effect of several different salts ($(NH_4)_2SO_4$, NH_4Cl, K_2SO_4, and KCl) on

L. monocytogenes PI-PLC cleavage of PI in TX-100 or diC_7PC mixed micelles and hydrolysis of cIP. As shown in Table 4-2, the ionic strength, and not the salt identity, was important for *L. monocytogenes* PI-PLC activation towards PI in micelles. Two enzyme concentrations were examined for PI cleavage. At fixed enzyme concentration and 8 mM PI (solubilized in 32 mM TX-100), *L. monocytogenes* PI-PLC activity displayed a hyperbolic dependence on concentration of $(NH_4)_2SO_4$ (Figure 4-7). For 0.2 μg/ml *L. monocytogenes* PI-PLC, the apparent V_{max} was 2022±202 μmol·min^{-1}·mg^{-1} with an apparent K_d for the salt of 38±16 mM; for 1.6 μg/ml *L. monocytogenes* PI-PLC, the apparent V_{max} decreased somewhat to 1355±256 μmol·min^{-1}·mg^{-1} with a comparable K_d 42±20 mM. The lower V_{max} extrapolated from the salt dependence of activity at an 8-fold higher *L. monocytogenes* PI-PLC concentration indicates that the presence of salt does not completely eliminate the unfavorable factors associated with high enzyme concentration. However, the ratio of specific activity for 0.21 μg/ml PI-PLC compared to 1.6 μg/ml at 0, 20, and 100 mM $(NH_4)_2SO_4$, (3.7, 1.6, and 1.5, respectively) decreases suggesting that $(NH_4)_2SO_4$ does partially compensate for the high enzyme concentration.

The salt effect was also studied with PI presented in vesicles. With 1.6 μg/ml enzyme and $(NH_4)_2SO_4$ (100 mM) added to PI (8 mM) SUVs, the enzyme specific activity increased only 1.3-fold (Table 4-3). For comparison, when the PI was co-sonicated with 8 mM POPC (0.5 mole fraction PI vesicles), enzyme activity increased about 2.4 fold compared to pure PI SUVs. If salt was added to the cosonicated PI/POPC (1:1) SUVs, the increase in PI-PLC specific activity was much more dramatic – about a

Table 4-2 Effect of 0.30 OsM salts on the specific activity of *L. monocytogenes* PI-PLC toward PI solubilized in 32 mM TX-100. Assays used 0.2 µg/ml PI-PLC in 50 mM HEPES, pH 7.0.

Salt	(M)	Specific Activity ($\mu mol \cdot min^{-1} \cdot mg^{-1}$)
-	0.00	274
$(NH4)_2SO_4$	0.10	1431
NH_4Cl	0.15	936
K_2SO_4	0.10	1120
KCl	0.15	1034

Figure 4-7 Effect of $(NH_4)_2SO_4$ on the rate of cleavage of PI (8 mM) solubilized in 32 mM TX-100: (•) 0.2 μg/ml and (o) 1.6 μg/ml PI-PLC.

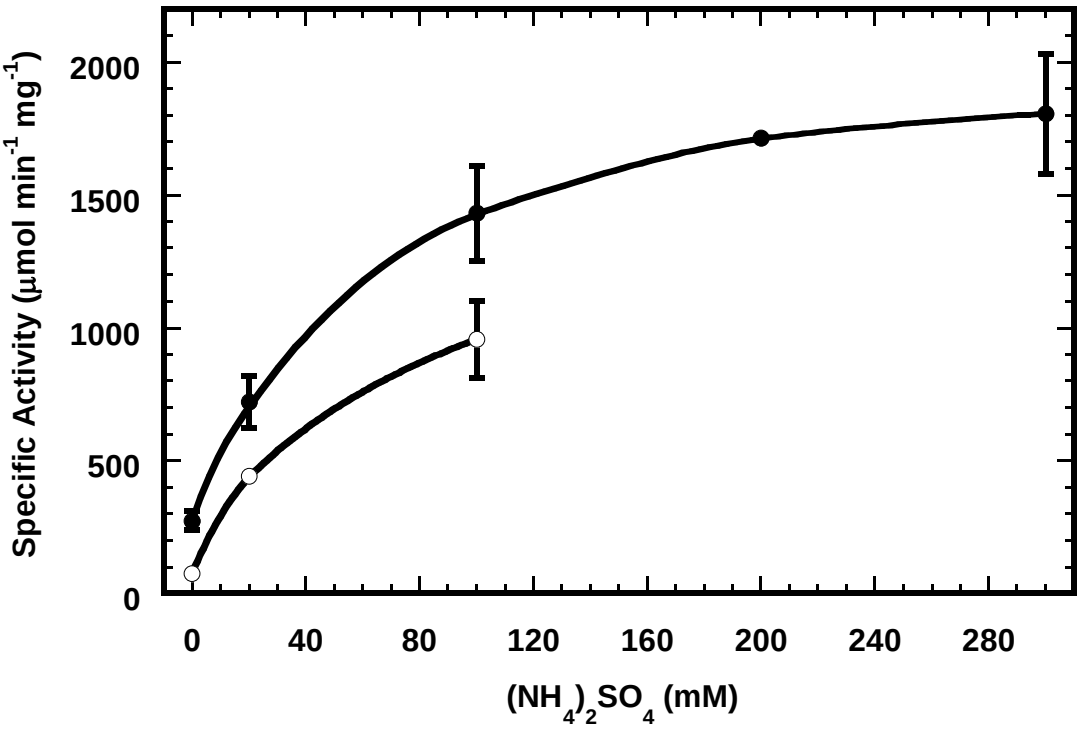

Table 4-3 Effect of $(NH_4)_2SO_4$ on *L. monocytogenes* PI-PLC (1.6 µg/ml) cleavage of PI (8 mM) vesicles and PI/PC (1:1) cosonicated vesicles.

POPC (8 Mm)	$(NH_4)_2SO_4$ (100 mM)	Specific Activity ($\mu mol \cdot min^{-1} \cdot mg^{-1}$)
-	-	3.8
-	+	4.8
+	-	9.0
+	+	127

34-fold increase. To see if a zwitterionic / neutral amphiphile is critical for the large salt activation shown in PI/detergent assays, we checked the effect of salt on the activity of *L. monocytogenes* PI-PLC toward pure PI SUVs. Surprisingly, the activity increased in a sigmoidal fashion from 6 $\mu mol \cdot min^{-1} \cdot mg^{-1}$ with 100 mM KCl to 330 $\mu mol \cdot min^{-1} \cdot mg^{-1}$ with 200 mM KCl in the absence of other amphiphiles (Figure 4-8). With 300 to 1500 mM KCl, the activity remained around 500 $\mu mol \cdot min^{-1} \cdot mg^{-1}$, comparable to that toward 0.08 mole fraction PI dispersed in TX-100 (or diC_7PC) micelles for the same enzyme concentration.

In contrast to its activation of PI cleavage by *L. monocytogenes* PI-PLC, $(NH_4)_2SO_4$ (as well as other salts) inhibited cIP hydrolysis whether diC_7PC was present or not (Table 4-1). These results make it unlikely that salts biases the enzyme toward a more active conformation, otherwise, it should have enhanced cIP hydrolysis as well as PI cleavage. The added salt could alter the properties of substrate interfaces making them more susceptible to *L. monocytogenes* PI-PLC or it could alter the interaction of the enzyme with the interface. One way of testing these explanations is to examine the effect of salts and amphiphiles on cleavage of diC_4PI, a soluble phosphodiesterase substrate with no tendency to partition into aggregates as long as the substrate concentration is low (the CMC for this lipid is likely to be >150 mM since diC_4PC has a CMC of 250 mM (Bian and Roberts, 1992) and other short-chain PI species exhibit CMC values comparable to the same chain length PC compound (Garigapati and Roberts, 1993)). As a way of ruling out any aggregation of the diC_4PI induced by the amphiphile or salt, the ^{31}P

Figure 4-8 Effect of KCl on *L. monocytogenes* PI-PLC (0.4 μg/ml) cleavage of PI (8 mM) vesicles.

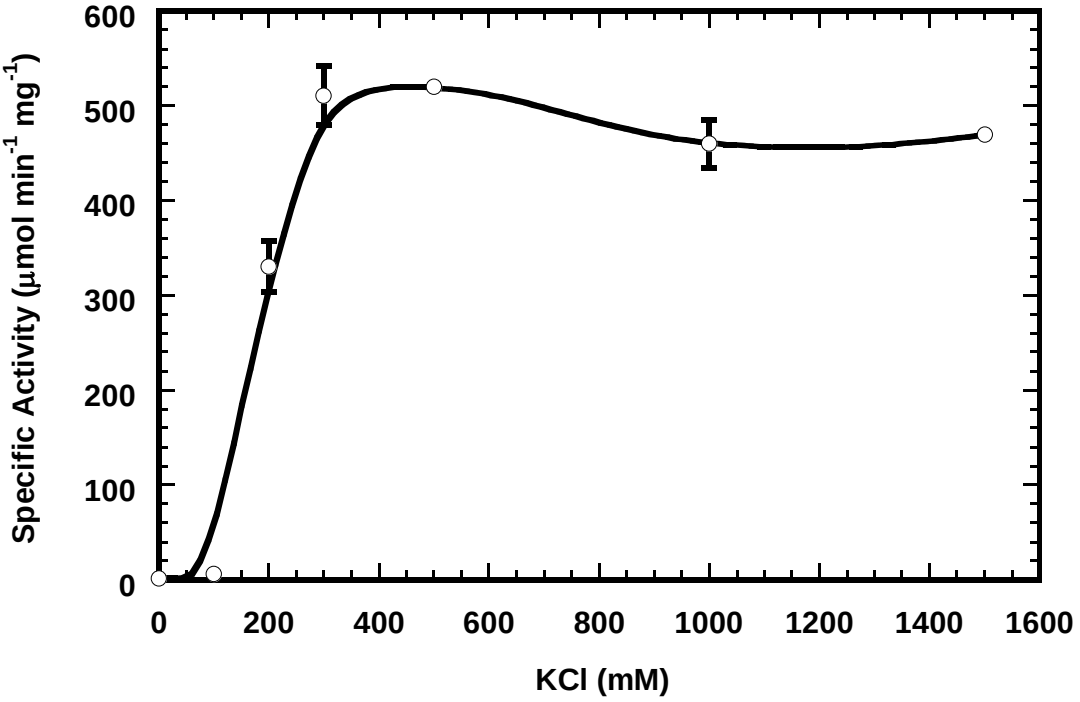

linewidth of 2 mM diC_4PI was measured in buffer in the absence and presence of 100 mM KCl, 100 mM TX-100, and then both components. The linewidth, 1.6±0.1 Hz, was unchanged with the additives.

Keeping the diC_4PI concentration at 2 mM, we measured the effect of KCl and TX-100 on *L. monocytogenes* PI-PLC activity towards the soluble substrate (Figure 4-9). With either 75 mM KCl or 32 mM TX-100 only, the specific activity of *L. monocytogenes* PI-PLC toward diC_4PI increased slightly (about 1.6-fold). However, if both salt and TX-100 were present, there was ~14-fold increase in *L. monocytogenes* PI-PLC toward diC_4PI. A similar synergistic effect was observed with monomeric diC_6PC added – a much larger activation was seen with both KCl and amphiphile present. This synergistic effect cannot reflect altering the substrate interface because the substrate is monomeric. This suggests that for the phosphotransferase reaction, the presence of an amphiphile, regardless of its aggregation state, is important for the kinetic activation observed with moderate ion strength. KCl (0.1 M) could lower the CMC of diC_6PC slightly, but the effect in the absence of enzyme is not significant (Lin et al., 1986). However, the decrease in activity toward cIP with monomeric diC_6PC for *L. monocytogenes* PI-PLC (Figure 4-6A and Ryan et al., 2002) may suggest that the enzyme itself could nucleate 'mini'-micelle formation when it binds a diC_6PC molecule. Studies of *B. thuringiensis* PI-PLC showed that monomeric diC_6PC can bind to the protein, at a site distinct from the catalytic site, and activate the enzyme (Zhou et al., 1997b). DiC_4PI is a poor substrate for *L. monocytogenes* PI-PLC, necessitating long incubation time (2 to

Figure 4-9 Synergistic effect of salts and amphiphiles on the phosphotransferase activity of *L. monocytogenes* PI-PLC toward: (▨) PI/POPC cosonicated SUVs; (□) diC_4PI/TX-100; (⊠) diC_4PI/diC_6PC.

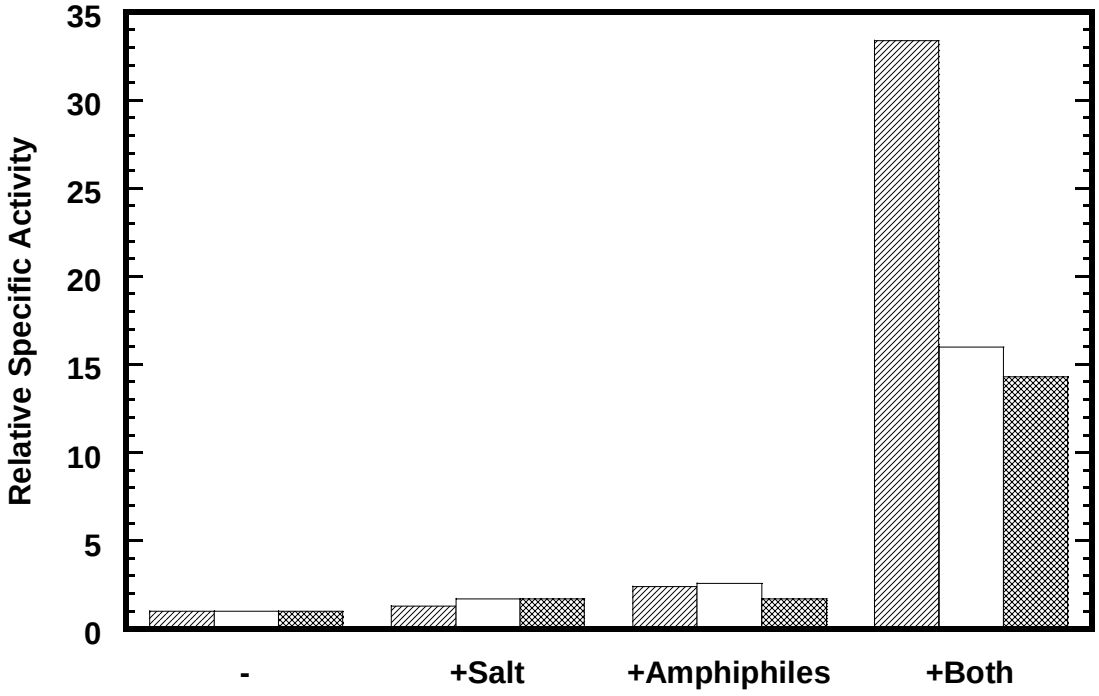

[a]Assays measured in 50 mM HEPES, pH 7.0 with 1.6 μg/ml enzyme. Relative activity is the ratio of the specific activity measured with the additive present compared to that in the absence of that additive (salts or amphiphiles).

[b]The control enzyme activity is 3.8, 0.7, and 1.2 $\mu mol \cdot min^{-1} \cdot mg^{-1}$ for PI/POPC (8 mM: 8 mM) cosonicated vesicle, diC_4PI/TX-100 (2 mM: 32 mM), and diC_4PC/diC_6PC (2 mM:5 mM).

5 h) if the same enzyme concentration is to be used in the absence and presence of salts and amphiphiles. With TX-100 present, final products included both cIP and I-1-P for incubation times longer than 1 h. However, if diC_6PC was used as the amphiphile, cIP was the only product even after 2 h. There is a difference when the *L. monocytogenes* PI-PLC interacts with TX-100 versus a short-chain PC molecule such that binding of diC_6PC to the protein promoted cIP release from active site.

III. Binding PI-PLC to interfaces

Short-chain PC molecules activate the *L. monocytogenes* PI-PLC toward cIP in the absence of salt, so there must be a direct interaction of the enzyme with the PC molecules. This was probed by ^{31}P NMR linewidth studies as has been done previously for the *B. thuringiensis* PI-PLC (Zhou et al., 1997b). As shown in Figure 4-10A, a threshold of PC (≥1 mM) was needed before significant broadening (0.8 Hz maximum under the conditions used) was detected. As more PC was added, the linewidth difference in the presence and absence of *L. monocytogenes* PI-PLC decreased. This type of profile is typical for multiple PC molecules interacting with the enzyme (and occupation of all these sites needed before the measured spectral change occurs). As shown in Figure 4-10B, the linewidth difference for diC_7PC caused by the presence of *L. monocytogenes* PI-PLC (2 mg/ml) was consistent with a n value of 3-4, $(\Delta\upsilon_b-\Delta\upsilon_0) = 5.5\pm0.6$ Hz, and $K_D = 1.5\pm0.6$ mM. The analysis with diC_6PC binding to *L. monocytogenes* PI-PLC yielded the same n, $(\Delta\upsilon_b-\Delta\upsilon_0) = 3.3\pm0.8$ Hz, and $K_D = 17\pm10$ mM (data not shown). In both cases,

Figure 4-10 (A) ^{31}P linewidth (Hz) of diC_7PC in the absence (♦) and presence (■) of *L. monocytogenes* PI-PLC. The dotted line indicates the CMC of pure diC_7PC. (B) Increase in linewidth (Hz) for diC_7PC induced by the inclusion of 2 mg/ml PI-PLC (differences in linewidth in (A)). The line represents the optimized fit to $(\Delta\upsilon_{obs}-\Delta\upsilon_0)=nE_T[PC]_T^{n-1}((\Delta\upsilon_b-\Delta\upsilon_0)/\{K_D + [PC]_T^n\}$ as described in the methods section.

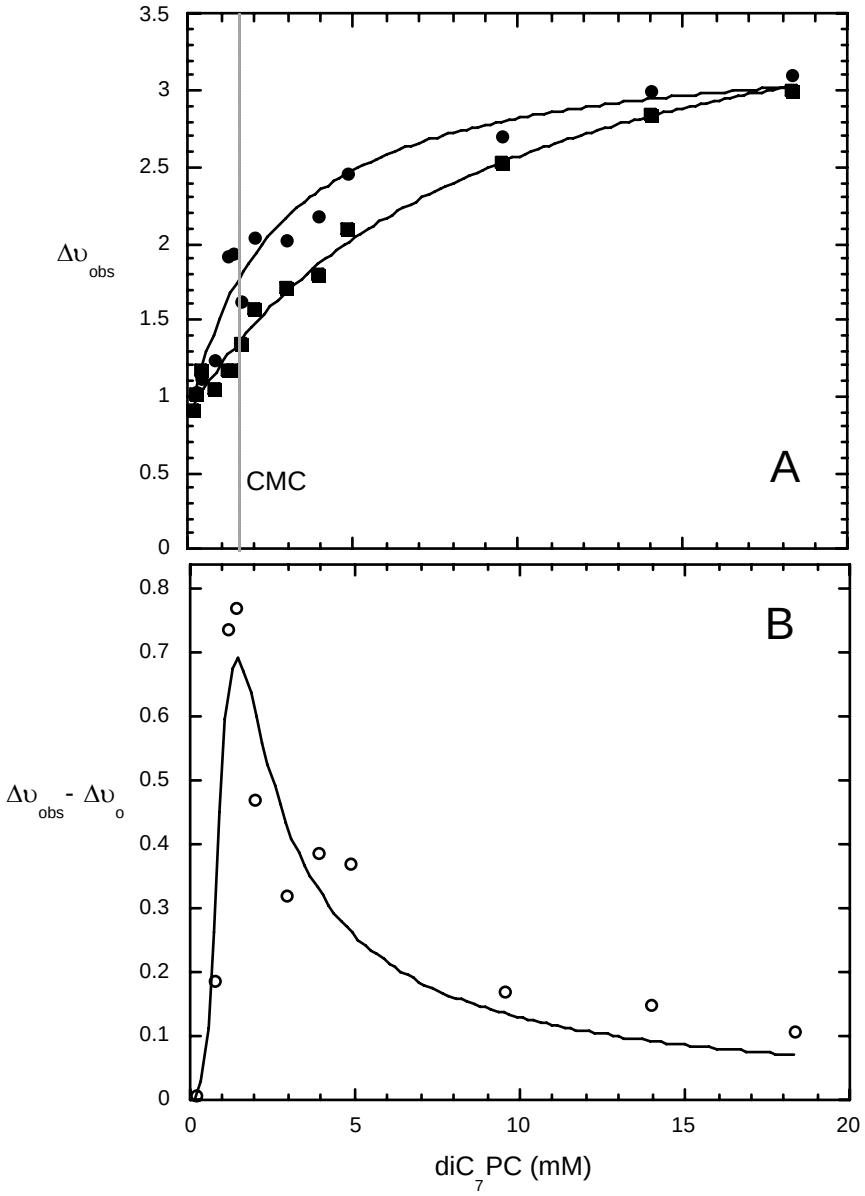

the 'K_D' describing the interaction was essentially at the CMC of the short-chain PC. The linewidth for bound PC would suggest significant mobility consistent with a small aggregate or mini-micelle interacting loosely with the protein.

L. monocytogenes PI-PLC binding to SUVs of POPC or DOPMe was also examined using a filtration / centrifugation binding assay (Wehbi et al., 2003b). As shown in Figure 4-11A, *L. monocytogenes* PI-PLC (30 μg/ml or 0.9 μM) had weak affinity for POPC SUVs – essentially >90% of the protein was eluted through the filter upon centrifugation even after incubation with 5 mM POPC SUVs. In contrast, this bacterial PI-PLC bound very tightly to anionic phospholipid SUVs regardless of headgroup. For DOPMe concentrations above 10 μM, essentially all the protein was bound to the phospholipids and none passed through the filter upon centrifugation. Thus, *L. monocytogenes* PI-PLC binds very tightly to anionic bilayers (PMe, PG, and by inference substrate PI); the interaction of this concentration of *L. monocytogenes* PI-PLC with PC bilayers was much weaker (too weak to quantify an apparent K_d by this vesicle binding assay). Yet low concentrations of POPC SUVs (0.5 mM) do activate the enzyme toward cIP. At higher protein and anionic phospholipid concentration, we observed an anionic lipid-induced precipitation of protein (Figure 4-11B). POPG vesicles (0.5 mM) precipitated all the protein in this experiment (1.2 mg/ml or 36 μM). If using PC SUVs, very little protein was present in the SDS-PAGE gel of precipitate. This very small amount of *L. monocytogenes* PI-PLC could just come from the solution (precipitates were dissolved in the same tube used to mix vesicles and enzyme) instead of the precipitate

Figure 4-11 Binding of *L. monocytogenes* PI-PLC to SUVs checked by SDS-PAGE. (A) Free enzyme (30 μg/ml) in filtrate through 100 KDa cut-off filter. (B) PG induced precipitation of enzyme (1.2 mg/ml, 36 μM). The numbers below each lane indicate mM concentration of PG or PC in SUVs added to the sample.

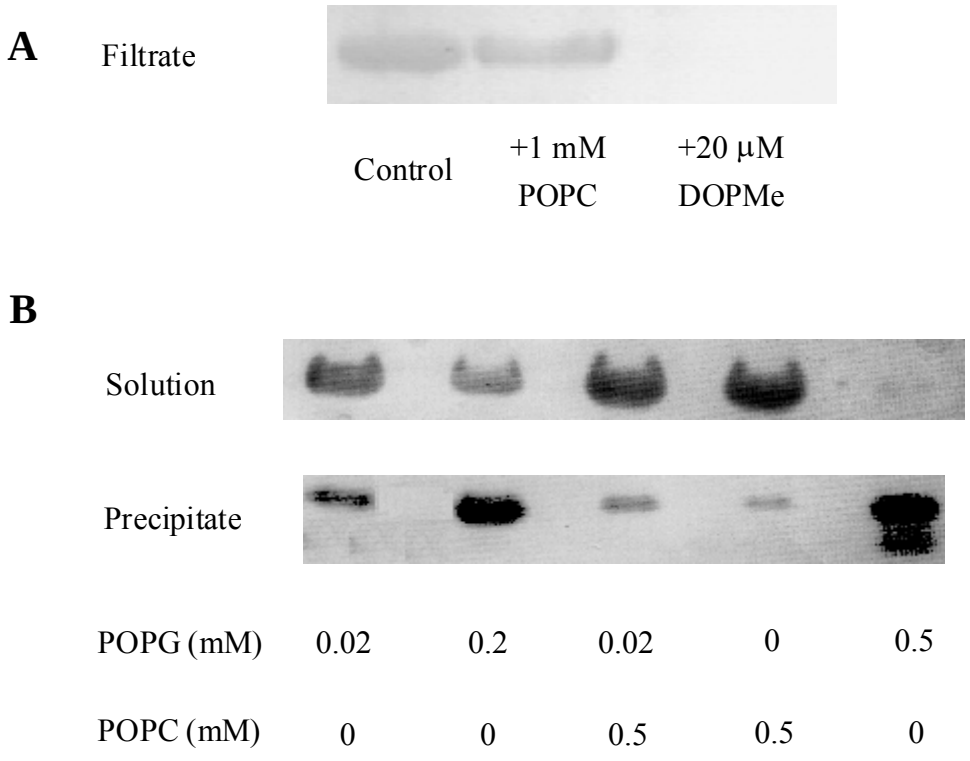

since the optical density at 350 nm (OD_{350}) of the PC solution was unchanged upon the addition of enzyme. With 0.02 mM POPG and this higher concentration of protein, protein was found in both the filtrate and the precipitate. Increasing the concentration of POPG SUVs increased the fraction of PI-PLC in the precipitate. If the SUVs used had an excess of POPC (0.02 mM POPG/0.5 mM POPC), precipitation of the protein was dramatically reduced. If micelles as opposed to vesicles were examined, more PG was needed to precipitate the protein. The amount of each lipid in the precipitate (extracted with methanol/chloroform) was measured with ^{31}P NMR, and the lipid composition in the precipitate for PG/PC SUVs or micelles was very similar to that in solution. Therefore, increasing PI-PLC specific activity as detergent or PC in SUV system is increased is likely to reflect (at least in part) disruption of this large, nonproductive aggregated complex that sequesters the enzyme from the bulk of the substrate.

The progress of precipitation was monitored by looking at OD_{350} with continuously stirring (Figure 4-12A). After adding *L. monocytogenes* PI-PLC to DOPMe/POPC (1:3.6) SUVs, an instant and very dramatic increase in optical density, corresponding to the formation of the precipitate, was observed. Similar behavior was also observed for POPG/POPC SUVs, but not for pure PC vesicles. The initial large structures eventually reorganize to smaller ones, but they are still larger than SUVs since the limiting OD_{350} was greater than the OD_{350} of the SUVs in the absence of protein. Since the precipitation could be dispersed by salt (at concentrations comparable to those used in the kinetics), it can not be related to vesicle fusion.

The release of vesicle-entrapped carboxyfluorescein upon the addition of protein was monitored to check the stability of vesicles in the presence of PI-PLC (Figure 4-12B). *L. monocytogenes* PI-PLC caused <25% carboxyfluorescein leakage (compared to total leakage from TX-100) within 2 hours (the reaction time course used for most assays) for three vesicle systems (POPC, POPC with KCl, and DOPMe). The initial release rate of carboxyfluorescein increased in the order of the affinity of enzyme for the interface (DOPMe > POPC > POPC+KCl), but the total carboxyfluorescein leakage level increased in the reverse order (POPC+KCl > POPC > DOPMe). These results indicate that the carboxyfluorescein released from SUVs is most likely related to perturbing the interface upon binding of enzyme, not pore formation or vesicle lysis. The higher the binding affinity, the faster the enzyme finds the interface, which in turn, leads to a higher initial rate of release rate of carboxyfluorescein. The more tightly the enzyme binds to a given vesicle surface, the longer the enzyme stays on that structure and less chance it will dissociate and bind to another vesicle.

The fluorescence spectrum of Pyr-PG is characterized by an excimer band at 480 nm and monomer bands at 375-395 nm (Figure 4-13A). By introducing a small amount of pyrene labeled PC to POPG / diC_7PC micelles or POPG/POPC SUVs, the ratio of intensity of monomer at 385 nm to that of excimer at 480 nm should be changed upon the addition of enzyme if *L. monocytogenes* PI-PLC perturbs the lateral distribution of Pyr-PG. As shown in Figure 4-13B, no such perturbation was oberserved. Clearly, *L. monocytogenes* PI-PLC does not induce the lateral distribution change of anionic lipids in micelles or vesicles if the surface concentration is sufficiently dilute.

Figure 4-12 (A) Turbidity changes of 0.86 mM DOPMe / 3.1 mM POPC co-sonicated SUVs upon the addition (at 10 min) of 0.15 mg/ml (o), 0.75 mg/ml (●), and 1.5 mg/ml (Δ) PI-PLC measured at OD_{350}. (B) Carboxyfluorescein released from 20 mM POPC (o), 20 mM POPC+150 mM KCl (●), and 20 mM DOPMe (Δ) vesicles mediated by *L. monocytogenes* PI-PLC (0.5 mg/ml). TX-100 was used to release all entrapped carboxyfluorescein.

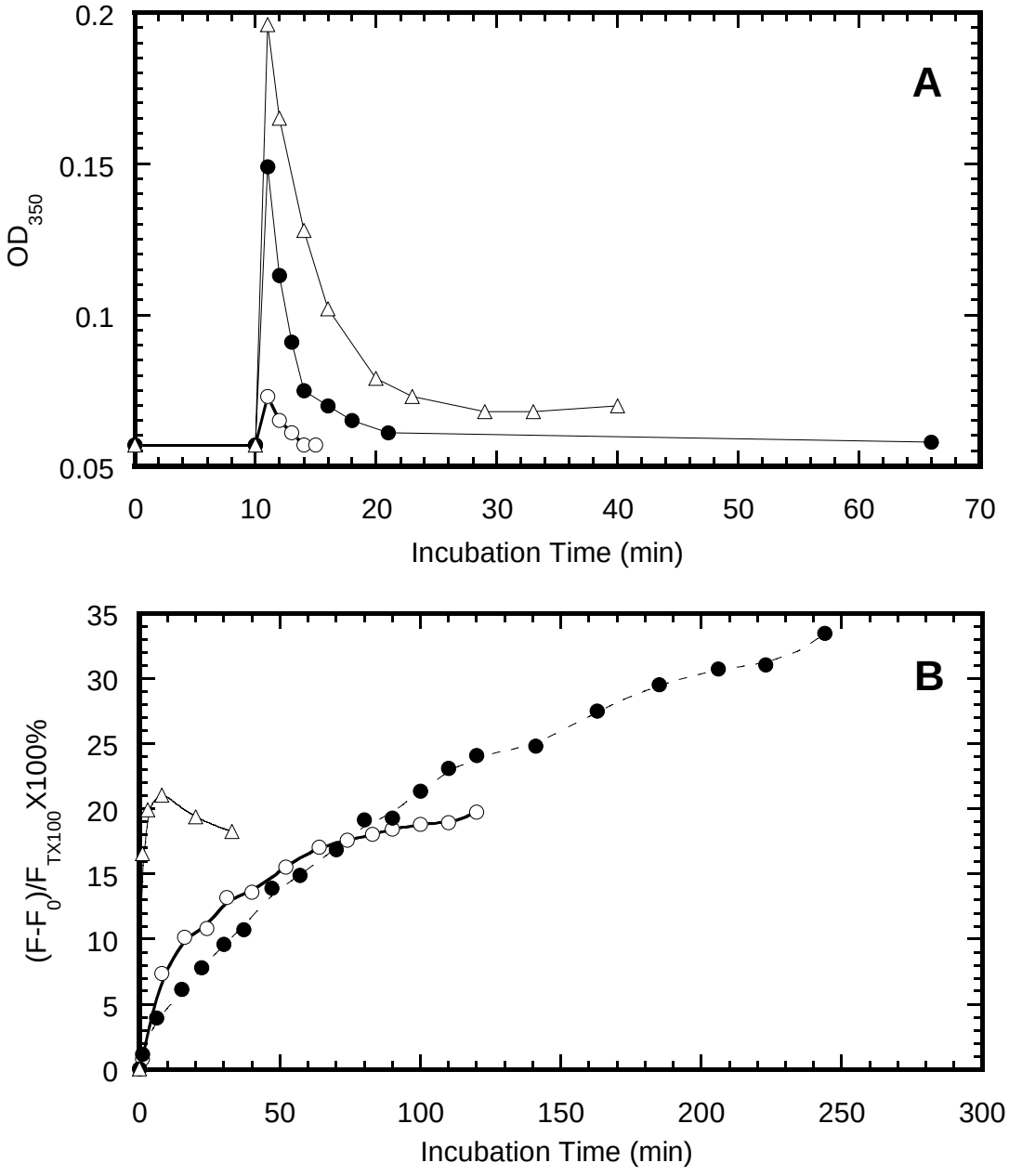

Figure 4-13 (A) Fluorescence emission spectrum of pyrene-labeled PG. (B) Effect of *L. monocytogenes* PI-PLC on the ratio of monomer (385 nm) and excimer band (480 nm) of (o) 20 μM pyrene-labeled PG / 3 mM diC_7PC micelles and (□) 100 μM pyrene-labeled PG with 100 μM unlabeled POPG / 2 mM POPC SUVs.

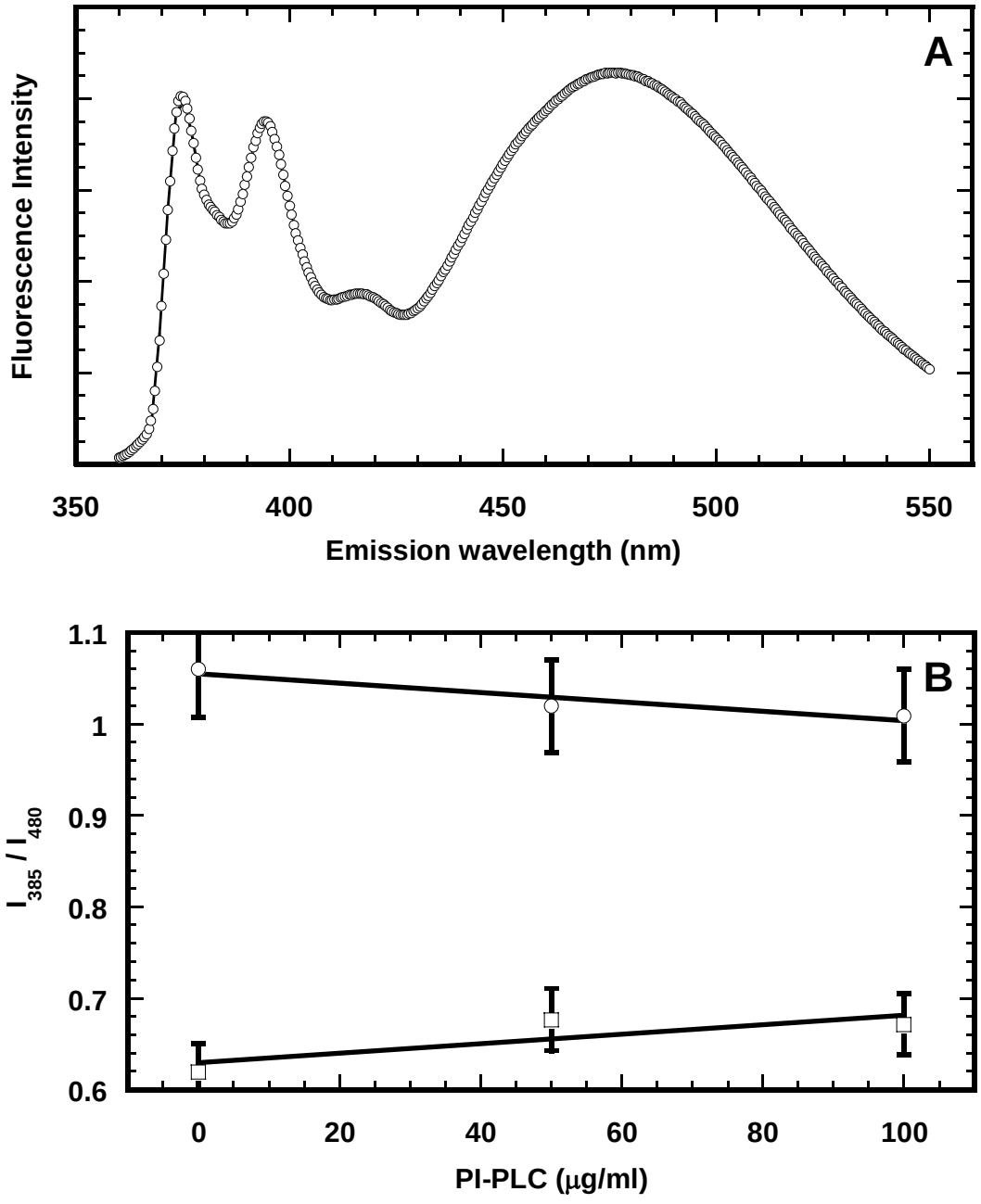

Monolayer studies provide more insight into how PC (and likely other neutral amphiphiles) contributes to the kinetic activation of the enzyme. *L. monocytogenes* PI-PLC binds tightly to anionic monolayers of DOPMe (Figure 4-14A), and π_C, the threshold pressure above which the enzyme cannot insert into the membrane, is high (46 dyne/cm) for this protein under these conditions. The strong interaction with an anionic surface may not be surprising given the high pI for this protein and the potent inhibition of cIP hydrolysis by anionic phospholipids vesicles (Table 4-1). The addition of KCl at a concentration comparable to the K_D observed for KCl kinetic activation (0.16 M) had little effect on π_C for the enzyme binding to a DOPMe monolayer, indicating binding and insertion in the anionic interface were not dramatically affected by this concentration of salt (Table 4-4 and Figure 4-14B). The slope of the plot decreased suggesting that the portion of protein maximally inserted into a membrane had decreased in the higher ionic salt solution (Table 4-4 and Figure 4-14). Binding of *L. monocytogenes* PI-PLC to POPC membranes was characterized by a considerably smaller π_C (31 dyne/cm) that was further reduced in the presence of 0.16 M KCl (to 23 dyne/cm), confirming that the binding of *L. monocytogenes* PI-PLC to PC interfaces has a smaller electrostatic component compared to binding to anionic phospholipid bilayers. Binding of *L. monocytogenes* PI-PLC to a mixed monolayer of 70 mol% PC and 30 mol % DOPMe in the absence of KCl resembled the binding curve to a pure DOPMe monolayer (Figure 4-14A, Table 4-4); π_C was unaltered while the maximum $\Delta\pi$ extrapolated decreased reflecting the PC content (24 versus 32 dyne/cm). The addition of 0.16 M KCl to this mixed monolayer had a

Figure 4-14 Effect of *L. monocytogenes* PI-PLC on the surface pressure of DOPMe (o), POPC (•), and POPC/DOPMe (7:3) (■) monolayers in the (A) absence and (B) presence of 0.16 M KCl.

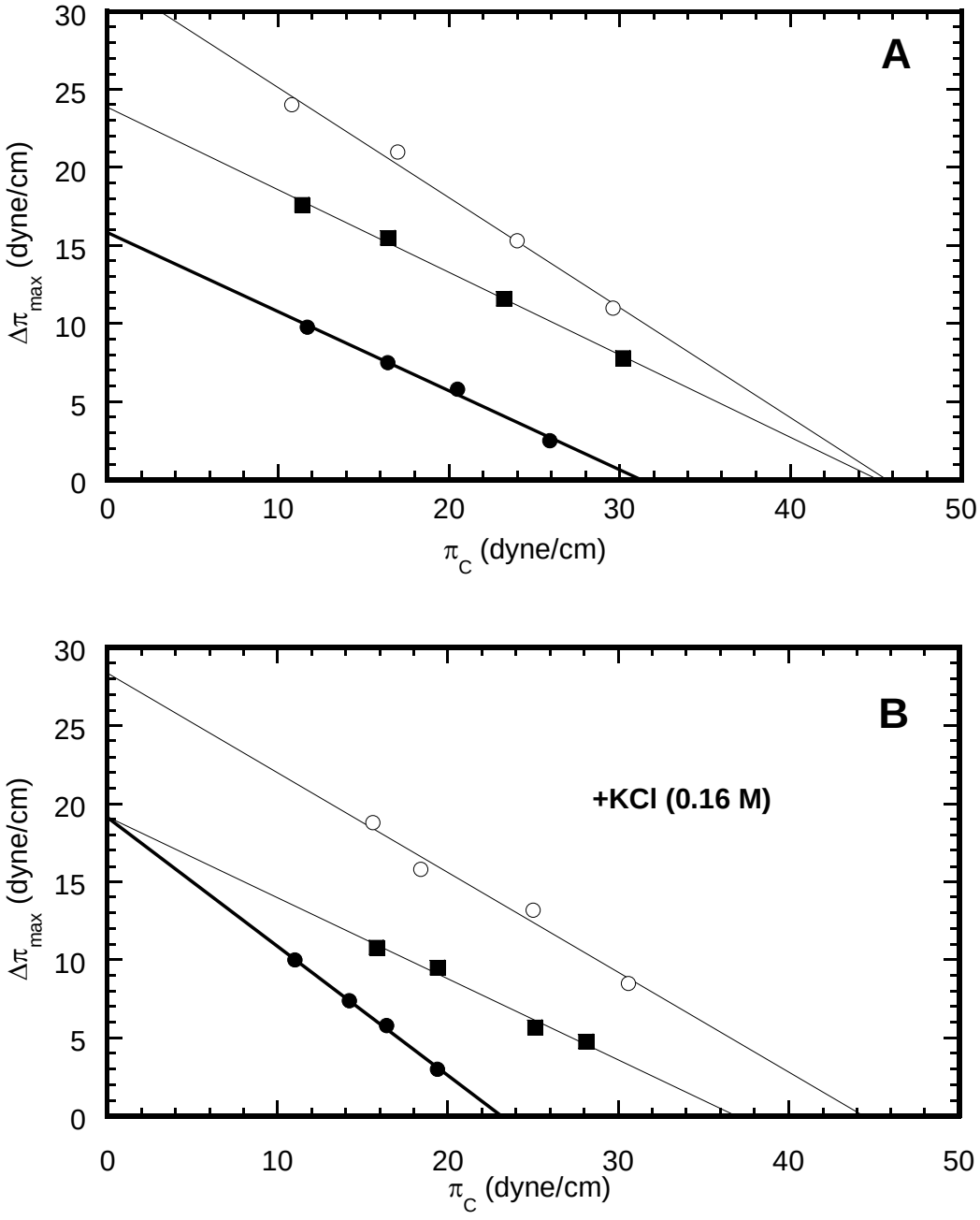

Table 4-4 Effect of KCl on the ability of *L. monocytogenes* PI-PLC to penetrate DOPMe and POPC monolayers.

Phospholipid	KCl (M)	π_c (dyne/cm)	$\Delta\pi_{max}$
DOPMe	0	45	32
DOPMe	0.16	44	28
POPC	0	31	16
POPC	0.16	23	19
DOPMe/POPC (3:7)	0	46	24
DOPMe/POPC (3:7)	0.16	37	19

pronounced effect on *L. monocytogenes* PI-PLC binding. π_C was decreased to 37 dyne/cm while $\Delta\pi$ was the same as that extrapolated from *L. monocytogenes* PI-PLC binding to a PC monolayer. When the KCl in the solution was increased to 0.5 M, the protein showed very minimal binding irrespective of any lipid composition indicating the driving force for the *L. monocytogenes* PI-PLC to bind to the lipid surface has a large electrostatic component. The presence of PC in an interface together with 0.16 M KCl reduced enzyme penetration of the monolayer. The synergistic effect of PC and KCl in reducing the interaction of *L. monocytogenes* PI-PLC with the monolayer correlates with higher enzymatic activity observed with PI/PC SUVs upon the addition of KCl (Table 4-3).

IV. Carbamylation of PI-PLC

The high pI for *L. monocytogenes* PI-PLC coupled with the monolayer results suggested that strong interactions with anionic phospholipids can be detrimental to enzyme action. Citraconic anhydride was used to modify a portion of the Lys residues on the protein surface (Figure 2-6) to see if surface charge had a dominant effect on the kinetic behavior. This reagent converts surface Lys residues to amides with a terminal carboxylate. For each Lys modified the charge is decreased by 2. The pI of two separate batches of modified enzyme were checked by 2D gel (Figure 4-15). Two distinct spots were detected with the pI between pH 7 and 9. Given the 28 Lys in the protein this shift is consistent with ~5-7 Lys modified (estimated by changing the Lys to a Glu and computing the pI). A kinetic analysis of PI cleavage in the TX-100 mixed micelle system (Table 4-5) showed that modified enzyme still could be activated by salt and amphiphiles.

Figure 4-15 2D gel of (A) unmodified *L. monocytogenes* PI-PLC migrated as a single peak at pH 9-10 region (note the high pI ~10), and (B) citraconic anhydride modified *L. monocytogenes* PI-PLC migrated as two distinct peaks between pH 7-9.

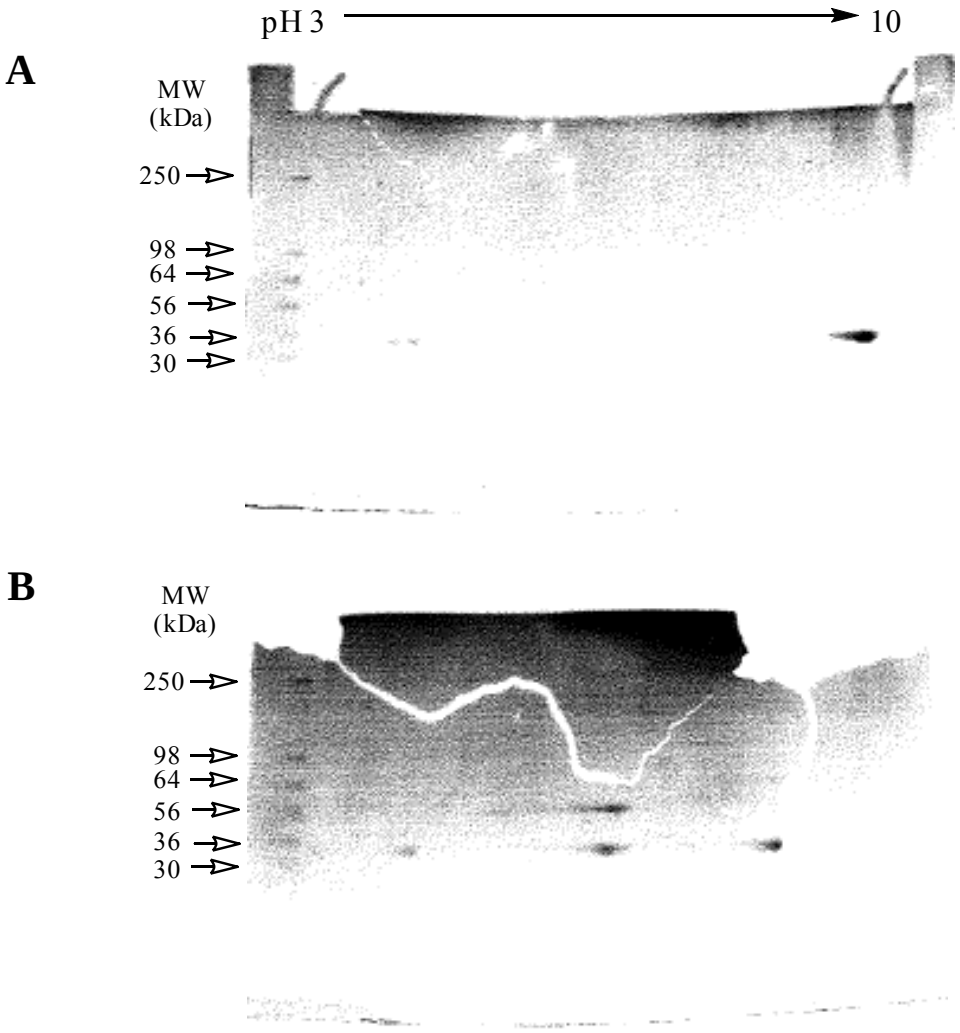

Table 4-5 Effect of citraconic anhydride modification on the kinetic activity.

	Relative activity [b]		
	Unmodified	Modified-1[c]	Modified-2[c]
Control [a]	1	1	1
8-fold increase in [E]	0.2	0.5	0.3
3-fold increase in TX-100	3.8	0.8	4.9
+150 mM KCl	3.4	6.0	3.7

[a] Control condition is 0.2 μg/ml enzyme, 8 mM PI in 32 mM TX-100.

[b] The control activity is 303 $\mu mol \cdot min^{-1} \cdot mg^{-1}$ for unmodified enzyme, 165 $\mu mol \cdot min^{-1} \cdot mg^{-1}$ for modified-1, 109 $\mu mol \cdot min^{-1} \cdot mg^{-1}$ for modified-2.

[c] Same amount of citraconic anhydride were used for Modified-1 and Modified-2, ~5-7 lysine residues were modified according to 2D gels.

However, the effect of protein concentration was diminished compared to the control enzyme suggesting that the high cationic character of the protein is a major factor in the unusual dependence of specific activity on enzyme concentration. The smaller effect on salt and amphiphile activation indicates that either (i) Arg and/or remaining unmodified Lys residues account for this kinetic activation, or (ii) a hydrophobic interaction with the *L. monocytogenes* PI-PLC is also a major component of the activation by salts and amphiphiles.

V. Discussion

A. Model for the activation of *L. monocytogenes* PI-PLC

Activation of the *B. thuringiensis* PI-PLC by phosphatidylcholine interfaces has been studied in detail (Zhou et al., 1997a, Zhou et al., 1997b; Zhou and Roberts, 1998; Feng et al., 2002; Wehbi et al., 2003a; Wehbi et al., 2003b). In the case of *B. thuringiensis* PI-PLC, the binding to PC interfaces, which appears to have a strong hydrophobic component (Wehbi et al., 2003b), alters the enzyme conformation so that it is a better catalyst in both phosphotransferase and cyclic phosphodiesterase reactions. The activation is relatively specific for zwitterionic phospholipids (Zhou et al., 1997a). The *L. monocytogenes* PI-PLC has a similar structure to the *B. cereus* enzyme (Moser et al., 1997), which might suggest very similar catalytic and possibly regulatory behavior. While the catalytic mechanism may be essentially the same (Bannam and Goldfine, 1999), the regulation of activity by amphiphiles and ionic strength is quite different for this more cationic protein.

Activators for *L. monocytogenes* PI-PLC exist in two classes: (i) neutral amphiphiles (PC and TX-100) and (ii) moderate salt concentrations. The first of these directly bind to the enzyme (e.g., diC_7PC binding to *L. monocytogenes* PI-PLC as monitored by ^{31}P linewidth changes) and alter the enzyme conformation so that it clearly becomes a more efficient catalyst for diC_4PI cleavage and cIP hydrolysis. As with *B. thuringiensis* PI-PLC, a micellar activator is more effective than a monomeric activator (Lewis et al., 1993). However, unlike *B. thuringiensis* PI-PLC, the mechanism for activation of *L. monocytogenes* PI-PLC could have a contribution from shifting the monomer/aggregate equilibrium (which itself appear to depend on the presence of substrates) towards monomeric protein. A major difference between *L. monocytogenes* PI-PLC and *B. thuringiensis* PI-PLC is that the binding affinity of the former is high to anionic lipids, but very low to zwitterionic lipids. Furthermore, the *L. monocytogenes* PI-PLC tends to form large aggregates with anionic lipids. As revealed from its crystal structure (Moser et al., 1997), there are many basic residues clustered on the sides and bottom side of the TIM-barrel which are far away from the rather hydrophobic opening to the positively charged active site. With PI dispersed in a variety of aggregates (mixed micelles or vesicles), the electrostatic interaction between the positive residues of enzyme and anionic substrate drives the enzyme to the interface where it can bind tightly in an unproductive orientation (A in Figure 4-16). Even if the protein is in the 'right' orientation, the basic residues on the opposite face of the protein will cause the clustering of nearby negatively charge lipid surfaces, forming a precipitate - in essence sequestering

Figure 4-16 Proposed model for diverse interactions of *L. monocytogenes* PI-PLC with mixed phospholipid interfaces (red is an anionic phospholipid such as PI substrate, yellow is a neutral lipid).

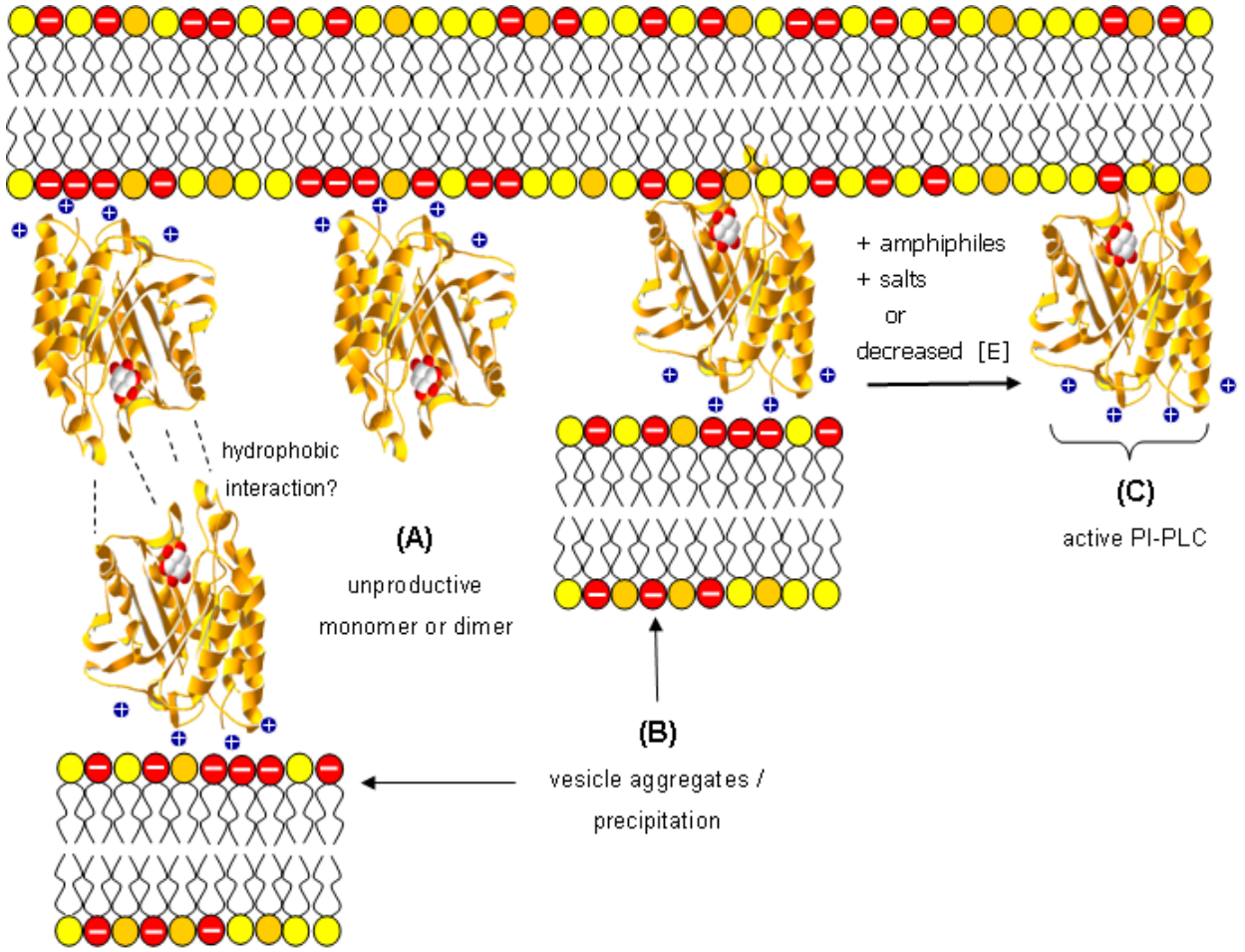

enzyme from interacting with other substrate particles and dramatically decreasing specific activity (B in Figure 4-16). An increased surface concentration of zwitterionic / neutral amphiphiles along with the salt disperses the anionic substrate, and shields charges on the protein and lipid surface. It also appears to reduce the hydrophobic interaction between enzyme and anionic surface. This enhances productive encounters of the protein with substrate molecules and hence the increases in activity (C in Figure 4-16). However, in the experiments presented, the contribution of an activator-induced conformational change separate from enzyme aggregates dissociation is difficult to quantify.

While PI/detergent micelle and cIP kinetics could be consistent with an explanation where diC_7PC and Triton X-100 primarily activate *L. monocytogenes* PI-PLC by promoting enzyme to a more active state (both conformational change and preventing formation of the aggregate complex), the kinetics with diC_4PI as a monomeric substrate for the phosphotransferase reaction are not consistent with this explanation at first glance. DiC_4PI cleavage is not dramatically enhanced by *L. monocytogenes* PI-PLC binding to the same concentration of diC_6PC or TX-100 micelles as used in cIP assays. A large increase in the enzyme specific activity is only observed with both an amphiphile and moderate (0.075 M) KCl. The difference between diC_4PI and cIP is that the first has acyl chains, short but with some hydrophobic character. There are multiple cationic sites on the enzyme that could bind this anionic phospholipid leading to inhibited enzyme. cIP, with no acyl chains, may have a much weaker affinity for these secondary sites. Amphiphile alone may not compete well at these secondary sites, so that activation by

amphiphile at low ionic strength is small. Increased salt alone (0.1-0.2 M) may not displace these molecules from the protein if there is a moderate hydrophobic interaction. However, the presence of an activating amphiphile and added salt might be more effective at weakening the interactions of diC_4PI with secondary sites and allowing the enzyme with bound substrate to bind to the activating amphiphile surface. This would lead to high specific activity toward diC_4PI only observed in the presence of both amphiphile and salt. In contrast, the enzyme would be adequately activated by amphiphile toward cIP because this molecule does not interact with other sites on the enzyme. As for long-chain PI cleavage, this is consistent with PI molecules acting to promote/stabilize *L. monocytogenes* PI-PLC aggregation.

The kinetic and biophysical studies presented here show that increased ionic strength alters the way *L. monocytogenes* PI-PLC binds to interfaces. Increased KCl (or other salts) could (i) enhance PLC binding to surfaces if the driving force is hydrophobic (and possibly promote scooting mode kinetics), (ii) weaken electrostatic interactions of the enzyme with the surface (which might enhance productive binding of substrate to the enzyme or might enhance product release), (iii) alter substrate partitioning, conformation, or dynamics in the bilayer (for example, PI lateral diffusion could be reduced when the enzyme is present but this could be overcome with high salt). The monolayer studies strongly rule out the first possibility and support the idea that KCl weakens the interaction of the protein with surfaces. Increased ionic strength reduces the maximum penetration ($\Delta\pi$) of the enzyme and π_C to a greater extent when PC is present in the interface. These results are critical in explaining the synergistic effects of POPC and KCl

on PI-PLC cleavage of PI in vesicles. KCl at moderate concentration (100-150 mM) had little effect on *L. monocytogenes* PI-PLC cleavage of PI in pure PI vesicles but was a strong activator for cleavage of the substrate in mixed PI/PC vesicles. PI-PLC binding to the POPC/DOPMe (7:3) monolayer exhibited a π_C similar to a pure DOPMe monolayer. However, the addition of KCl lowered this value dramatically as well as reduced $\Delta\pi$ to the value seen with a pure POPC monolayer. Clearly, a high π_C and $\Delta\pi$ correlate with lower activity of *L. monocytogenes* PI-PLC. The significant activation in activity toward PI SUVs by high salt concentration is consistent with the reduced binding of enzyme to the surface at 0.5 M KCl. The inhibition of salts on the hydrolysis of cIP is likely due to weakened electrostatic interactions between the enzyme and monomeric cIP in the presence of salts.

B. Biological relevance of amphiphile regulation of *L. monocytogenes* PI-PLC activity?

Several bacteria, both pathogenic and non-pathogenic, secrete PI-PLC enzymes into the media. The biological role of this enzyme, along with other nonspecific phospholipases, is to aid in survival of the organism, particularly as it infects mammalian cells. Those PI-PLC that cleave GPI-anchored proteins, such as the PI-PLC secreted by *B. thuringiensis*, *B. cereus*, and *Staphylococcus aureus*, are well poised to target those membrane components in the extracellular leaflet of the plasma membrane, which is rich in the zwitterionic lipids PC and sphingomyelin. However, secreted PI-PLC enzymes whose targets are PI and not GPI-anchors, must have a different role in bacterial survival

since PI is not found in the external leaflet of most organisms. *L. monocytogenes* is capable of hydrolyzing PI from outside mammalian cells. It appears to gain access to intracellular PI by means of pores produced by listeriolysin O (Goldfine et al., 1995; Sibelius et al., 1996a; Sibelius et al., 1996b; Sibelius et al., 1999; Wadsworth and Goldfine, 1999; Goldfine et al., 2000; Wadsworth and Goldfine, 2002). In macrophages, *L. monocytogenes* is internalized and both listeriolysin O and *L. monocytogenes* PI-PLC expression are upregulated in the phagosome (Vazquez-Boland et al., 2001). From the phagosome, *L. monocytogenes* PI-PLC presumably gains access to host PI by means of phagosomal permeabilization and eventual destruction. Activation of host PKCβ by means of DAG generated from intracellular PI and elevated intracellular calcium appears to play a significant role in escape from the phagosome (Wadsworth and Goldfine, 1999; Wadsworth and Goldfine, 2002). The inner leaflet of the vacuole membrane is presumably like the external leaflet of the plasma membrane – rich in PC or sphingomyelin with a low content of anionic phospholipids. If the *L. monocytogenes* PI-PLC has weak affinity for PC (and presumably for sphingomyelin and PE as well) under the moderate ionic strengths in cells, it will stay in the vacuolar fluid and be easily dispersed into the cytoplasm. Once there it will partition with the negatively charged components of the target membrane. It should be noted that intracellular concentrations of a typical mammalian cell are 5 to 15 mM NaCl, 140 mM KCl, 0.5 mM Mg^{2+}, and 0.1 mM Ca^{2+} (Alberts et al., 2002), an ionic strength similar to what optimally activates *L. monocytogenes* PI-PLC. As long as there are some zwitterionic / neutral lipids around, it

is likely the enzyme can bind and partially insert into the bilayer in a way that allows it to effectively hydrolyze PI and generate DAG.

Chapter 5:

L. monocytogenes PI-PLC surface mutants – testing the model

I. Introduction

For PI-PLCs, both phosphotransferase and phosphodiesterase activities are affected by the presence of non-substrate surfaces, exploring the interfacial binding should be important to understanding the regulation of their activities. In the previous chapter, binding of *L. monocytogenes* PI-PLC to interfaces was investigated. The binding behavior of *L. monocytogenes* PI-PLC to interfaces, as that of the homologous *B. thuringiensis* enzyme, is consistent with a two-stage binding model (Wallace and Janes, 1999; Stahelin and Cho, 2001; Wehbi et al., 2003b), where PI-PLC would first be driven to the lipid surface by electrostatic forces followed by formation of tight membrane-protein complexes that are stabilized by hydrophobic and/or electrostatic interactions and hydrogen bondings. However, there is a clear distinction in the binding patterns to interfaces of the two bacterial PI-PLC enzymes. *L. monocytogenes* PI-PLC binds more tightly to inhibitory anionic surfaces but more loosely to activating zwitterionic surfaces while *B. thuringiensis* PI-PLC exhibits the reverse behavior. Monolayer studies also showed that *L. monocytogenes* PI-PLC penetrated deeper into both anionic and zwitterionic surfaces than *B. thuringiensis* enzyme. Moreover, *L. monocytogenes* PI-PLC, in contrast to *B. thuringiensis* enzyme, exhibited more insertion into anionic versus zwitterionic surfaces. These differences in the interfacial binding, induced by both electrostatic and hydrophobic interactions, may contribute to the unusual kinetics of *L. monocytogenes* PI-PLC.

Chemical modification of lysine residues in *L. monocytogenes* PI-PLC with citraconic anhydride did affect enzyme activity, but the dependence of activity on the

enzyme concentration, amphiphiles and salts was still persisted. As there are 37 total basic residues (Arg + Lys), it would be time consuming to screen out the effect of electrostatic interactions. The crystal structure of PI-PLC from *L. monocytogenes* shows a close topological similarity to PI-PLC from *B. thuringiensis*, despite a low level of sequence homology (~24% sequence identity) (Moser et al., 1997). The similarity in tertiary structures between *L. monocytogenes* and *B. cereus* PI-PLCs enable us to target specific regions for the hydrophobic contribution to the interfacial binding based on what we know about the *Bacillus sp.* enzymes (98% sequence identity among *Bacillus sp.* PI-PLCs).

Both *L. monocytogenes* and *Bacillus sp.* PI-PLCs are composed of a single distorted $(\beta\alpha)_8$-barrel domain with the active site located at the C-terminal side of the β–barrel (Heinz et al., 1996; Moser et al., 1997). For *Bacillus sp.* PI-PLCs, several hydrophobic amino acid residues from short α-helix B and some loops, arranged in a semicircle around the active site cleft, form a relatively mobile hydrophobic ridge fully exposed to solvent. Among the exposed residues, two tryptophans, Trp-47 in α-helix B (PIKQV<u>W</u>G) and Trp-242 in one particular loop (SGGTA<u>W</u>N), were reported important for the enzyme to bind to both activating zwitterionic and substrate anionic interfaces (Feng et al., 2002). The structure of *L. monocytogenes* PI-PLC also consists of α-helix B and an analogous loop. Although the sequence similarity is low for these two regions, the structure-based sequence alignment of *L. monocytogenes* versus *B. cereus* PI-PLC did provide us two candidates, Trp-49 in α-helix B (IT<u>W</u>TLTKP) and Phe-237 in the loop (SATSLT<u>F</u>), to start with. Other residues in each structural feature were also mutated to

assess their contributions to surface binding and PI-PLC kinetics (Figure 5-1). The results suggest both α-helix B and the loop are kinetically important. Removal of just a single hydrophobic residue in these regions (Leu-51, Leu-235, and Phe-237) altered the unusual kinetic profile of *L. monocytogenes* PI-PLC in that none of the mutant enzymes showed the dramatically increased specific activity with decreasing enzyme concentration or increasing TX-100 above X_{det}=0.8 as did the wild type recombinant PI-PLC.

II. Trp-49 and Phe-237 mutants

A. Intrinsic fluorescence of wild type and mutant *L. monocytogenes* PI-PLCs

Protein fluorescence is a mixture of the fluorescence from two aromatic amino acids - tryptophan and tyrosine. With relatively (compared to tyrosine) high quantum yield, short lifetime, low content in most proteins, and sensitivity to environmental factors, tryptophan is the most extensively used amino acid for intrinsic fluorescence analysis of protein. When both fluorescent amino acids are present in a protein, pure emission from tryptophan can be obtained by excitation at wavelengths above 295 nm (Eftink, 1991).

Compared to seven tryptophan residues in *B. thuringiensis* enzyme, *L. monocytogenes* PI-PLC has only three tryptophan residues, Trp-6 (too flexible to be traced in the electron density map), Trp-19 in α-helix A (comparable to Trp-13 of *B. thuringiensis* PI-PLC), and Trp-49 at α-helix B (comparable to Trp-47 of *B. thuringiensis* PI-PLC) (Figure 5-2). The excitation wavelength chosen was 290 nm in an attempt to

Figure 5-1 Model of *L. monocytogenes* PI-PLC showing the location of the mutants with bound *myo*-inositol (labeled as INS).

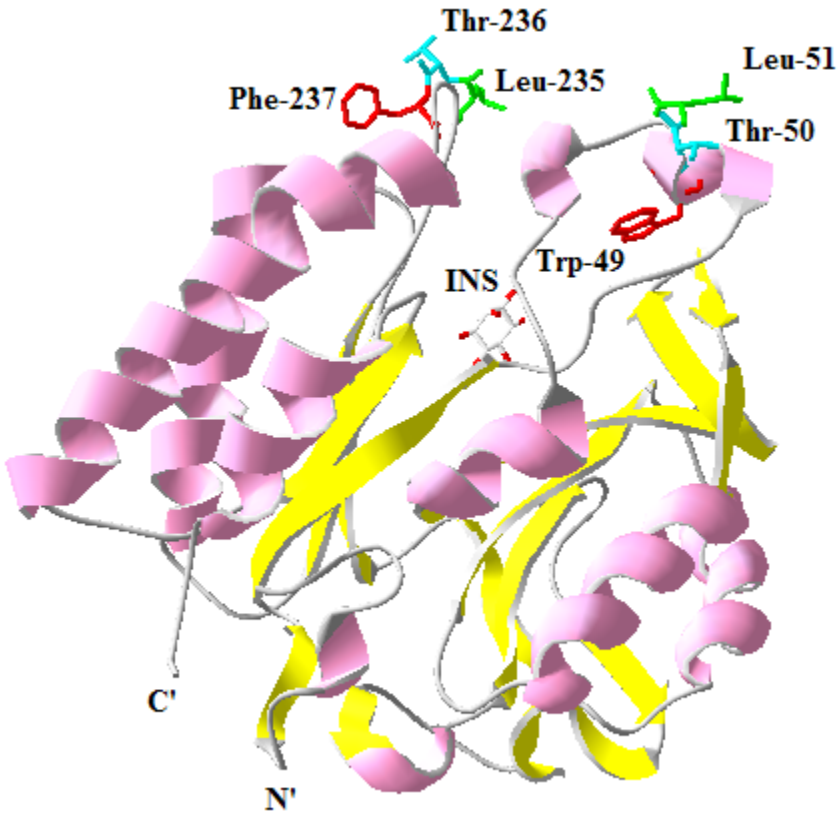

Figure 5-2 The location of Trp-19 and Trp-49 in *L. monocytogenes* PI-PLC. The side chains of both residues are in red. The bound *myo*-inositol is labeled as INS. Trp-6 at N terminal is too flexible to be traced in the electron density map**.**

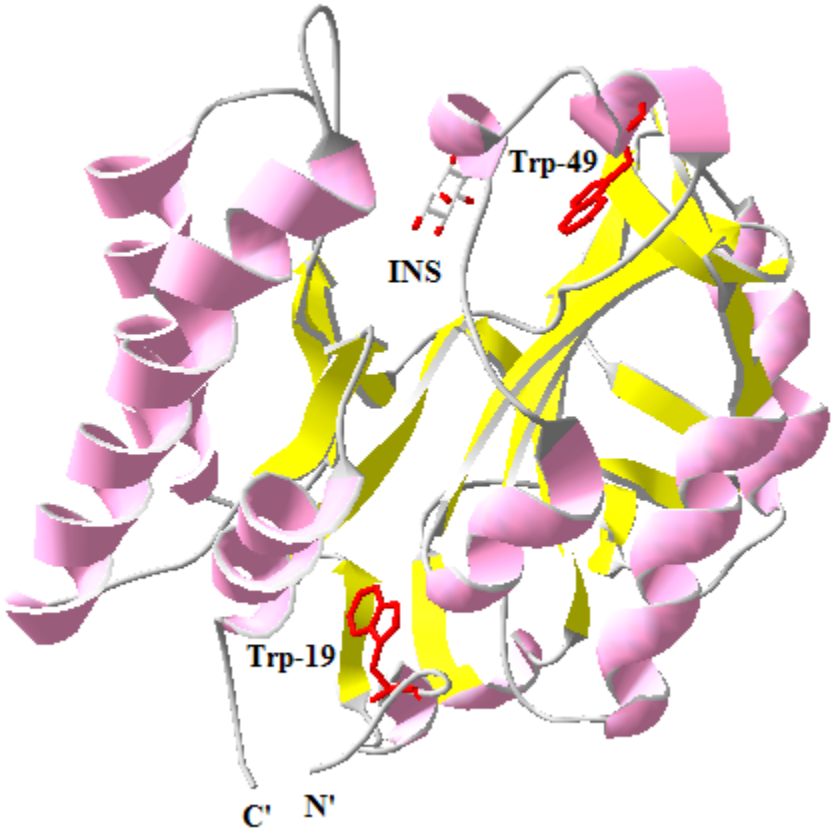

primarily excite tryptophan residues with a smaller effect on the many tyrosine residues of the protein. The *L. monocytogenes* PI-PLC fluorescence emission appeared as a broad spectrum with a shoulder at 337 nm in addition to the 323 nm main peak (Figure 5-3). The intensity of shoulder peak was about 93% that of the 323 nm peak. There are two discrete transition bands for the indole ring that contribute to the tryptophan fluorescence and can give rise to this type of spectral profile if the major fluorophore(s) is in a hydrophobic environment (Callis, 1997). For *B. thuringiensis* enzymes (both WT and Trp mutants), only one single peak with a fluorescence maximum ~340 nm peak was observed (Volwerk et al., 1994; Feng et al., 2002). Trp-242 of *B. thuringiensis* PI-PLC was reported as the major fluorophore responding to micelle binding (Feng et al., 2002). Thus, the unusual intrinsic fluorescence spectrum for the *L. monocytogenes* PI-PLC is likely to reflect a different environment from that in the *B. thuringiensis* homologue.

Of the three Trp residues in the *L. monocytogenes* PI-PLC, only Trp-19 and Trp-49 might be in hydrophobic environments. Trp-19 is buried in the protein while Trp-49 is closer to the surface. We changed Trp-49 to an alanine to see whether this residue had a significant contribution to the protein intrinsic fluorescence in solution. Substitution of Trp-49 with alanine did not change the 323 nm fluorescence emission maximum wavelength of WT, but significantly decreased the overall intensity, about 43-48% at both 323 nm and 337 nm (Figure 5-3). There might be some tyrosine residues excited at 290 nm, however the reduction in emission suggests that Trp-49 must be contributing to the overall the emission spectrum. W49A fluorescence allows us to separate any effects on this fluorophore from WT which has both Trp-19 as well as Trp-49.

The differences in the intrinsic fluorescence spectrum of the two bacterial PI-PLC enzymes motivated us to introduce a Trp in the surface loop to see if it would be sensitive to the protein binding to different surfaces as is the *B. thuringiensis* enzyme. We thus replaced the Phe-237, which aligns well with *B. thuringiensis* Trp-242. For F237W in solution, the intrinsic fluorescence profile (λ_{ex}=290 nm) changed significantly in both shape and intensity so that the maximum was now shifted to ~340 nm, indicative of a moderately polar environment (Figure 5-3). The fluorescence emission maximum of F237W was now closer to that of *B. thuringiensis* PI-PLC, although a shoulder at 237 still remained. The intensity increased 6% and 28% at 323 nm and 337 nm, respectively. Those changes in the fluorescence of F237W suggested that Trp-237 is a major contributor to the fluorescence spectrum at 340 nm.

Several other mutants were made to use for fluorescence experiments: F237A (to see if removing a hydrophobic group at this position affected surface binding), and W49A/F237A (which we originally thought would emulate W47A/W242A of *B. thuringiensis* PI-PLC and bind very poorly to surfaces). The emission spectra of F237A and W49A/F237A were comparable to WT and W49A, respectively (Figure 5-3). What the intrinsic fluorescence spectra of these mutants suggest is that F237W may be a good probe of interfacial binding by the *L. monocytogenes* PI-PLC while comparing WT and W49A may provide information on differentiating effects on Trp-19 versus Trp-49.

Figure 5-3 Intrinsic fluorescence profiles of *L. monocytogenes* PI-PLC Trp-49 and Phe-237 mutants: WT (+), F237W (•), F237A (o), W49A (Δ), and W49A/F237A (▲).

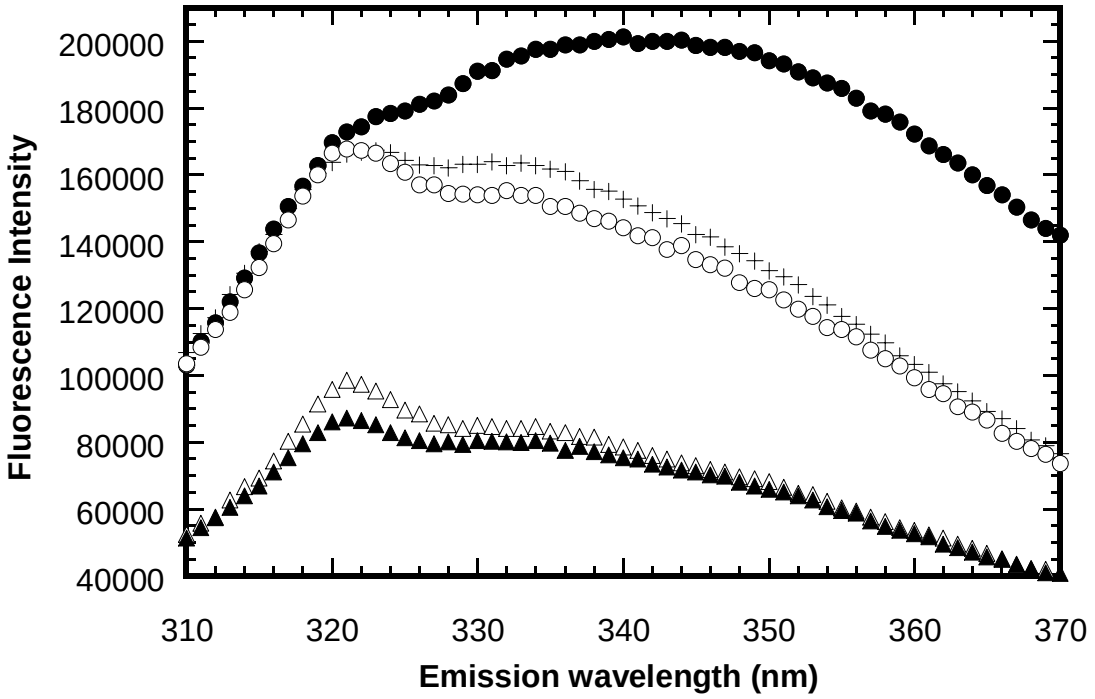

Table 5-1 Comparison of secondary structure content of WT, W49 mutants, and F237 mutants calculated from 200-260 nm CD spectra. In wavelength scan experiments, 0.2-0.3 mg/ml protein in 10 mM borate buffer (pH 7.0) was used to collect CD spectrum. Thermal stability of protein (0.02 mg/ml) was assessed using CD by following ellipticity changes at 222 nm.

Enzyme	% Secondary structure				
	α-helix	β-sheet	β-turn	Random coil	Tm (°C)
WT	30.3	18.9	17.6	33.2	44.2
F237W	30.2	19.0	17.6	33.1	43.8
F237A	29.0	19.8	18.0	33.2	44.0
W49A	29.2	19.7	17.9	33.2	43.4
W49A/F237A	29.6	19.4	17.8	33.2	42.0

B. Secondary structure and thermal stability of wild type and mutant *L. monocytogenes* PI-PLCs

CD spectra of WT and mutant PI-PLC proteins were acquired to check for overall structural elements. As shown in Table 5-1, estimates of WT secondary structure calculated from the CD wavelength spectra by CDNN (Böhm et al., 1992; Andrade et al., 1993; Waterhous and Johnson, 1994) agreed moderately well with the secondary structure elements in the crystal structure (Moser et al., 1997). All the mutants had essentially the same proportion of secondary structure elements as WT (29.7±0.6 % α-helix, 19.4±0.4 % β-sheet, 17.8±0.2 % β-turn, and 33.2±0.1 % random coil). They also had very similar thermal denaturation temperatures (43.8±0.3^{o}C for WT and the single mutant proteins with a slightly lower value, 42^{o}C, for W49A/F237A) measured by monitoring the loss of secondary structure with temperature.

C. Effect of PC, PMe, and *myo*-inositol on the intrinsic fluorescence of wild type and mutant *L. monocytogenes* PI-PLCs

As with recombinant PI-PLC (WT), interfacial binding of these *L. monocytogenes* PI-PLC mutants, either too tight to the anionic surfaces or too weak to the activators, could not be quantified with the filtration / centrifugation / SDS-PAGE assay. Previous studies have shown that intrinsic fluorescence spectrum of *Bacillus sp*. PI-PLC is sensitive to the interfacial binding, with intensity increasing upon the binding of PC activator micelles or vesicles (Hendrickson et al., 1992; Volwerk et al., 1994; Zhou et al., 1997b) and decreasing upon the binding of molecules to the active site (PA, PMe, PG) (Volwerk et

al., 1994; Zhou and Roberts, 1998). Replacing the tryptophan that is responsible for spectral change upon interfacial binding with alanine removed this fluorescence sensitivity (Feng et al., 2002). We thus examined the intrinsic fluorescence of F237W, F237A, W49A, W49A/F237A as a function of added PC, PMe, *myo*-inositol and compared with that of WT PI-PLC. The emission maximum, 337 nm for F237W and 323 nm for others, was unshifted by those additives (up to 5 mM diC_7PC, or 35 mM diC_6PC, or 1 mM SUVs, or 100 mM *myo*-inositol). However, intensity changes were observed. The relative intensity changes for each mutant were similar to WT suggesting that interfacial binding was more or less the same for these mutants.

For *B. thuringiensis* PI-PLC, short-chain PCs (diC_7PC and diC_6PC) had similar effects on the fluorescence intensities of WT and W47A, a small increase in emission (5-10%) with monomeric PC and much larger increase (30-35%) with micellar PC. This sensitivity to micelle PC binding was reduced significantly for W242A, indicating that the 242 position was much more sensitive to surface binding (Feng et al., 2002). For *L. monocytogenes* PI-PLCs, the response to PC monomer and micelle binding depended on the mutant. As shown in Figure 5-4A, the fluorescence intensity of F237W increased slightly (~5%) with monomer diC_7PC, and showed an additional ~4% increase upon binding diC_7PC micelles. For WT and F237A, any initial increase in the intensities with monomer diC_7PC was abolished. Instead, F237A showed a 5% decrease in the intensity. If Trp-19 is the major contributor to the emission maximum at 323 nm in WT, then its lack of response to monomeric diC_7PC suggests that monomer binding does not perturb the environment of that residue or Trp49. The decrease in fluorescence for F237A is

interesting and could suggest that monomeric PC binds differently to this mutant compared to WT – perhaps it binds at or near the active site. Both of these PI-PLC mutant proteins still showed an increase in fluorescence intensities once diC_7PC micelles were added. It is interesting that ~8% drop in fluorescence intensity was observed for W49A/F237A at the presence of diC_7PC micelles (Figure 5-4B). Comparing the changes in fluorescence intensity of F237W to that of F237A and WT, clearly indicates that Trp-237 is the major fluorophore and, in particular, that it must be proximal to 'monomeric' diC_7PC binding (i.e., when monomer PC is added, although small aggregates of the PC could form with this region of the protein). Trp-49, on the contrary, showed no sensitivity to monomeric diC_7PC binding. All mutants showed an increase in fluorescence with micellar diC_7PC added (i.e., comparing 1 mM to 3 mM) or roughly the same magnitude (4-5%).

DiC_6PC had a more pronounced effect on the fluorescence intensities of *L. monocytogenes* PI-PLCs than diC_7PC (Figure 5-5). As with diC_7PC, monomeric PC had little effect at concentrations well below the CMC (which may be reduced by the presence of the protein) on F237A or W49A/F237A fluorescence. There is a more gradual increase in fluorescence as the CMC is approached, particularly for F237A and W49A. If 'monomer' diC_6PC does bind to the proteins its binding is associated with nearing the CMC. This might indeed suggest that small PC aggregates are needed for

Figure 5-4 Fluorescence intensities of *L. monocytogenes* PI-PLCs as a function of added diC_7PC: (A) wild type recombinant PI-PLC (+), F237A (o), and F237W (•) mutant proteins; (B) W49A (Δ) and W49A/F237A (▲) compared to wild type PI-PLC (+).

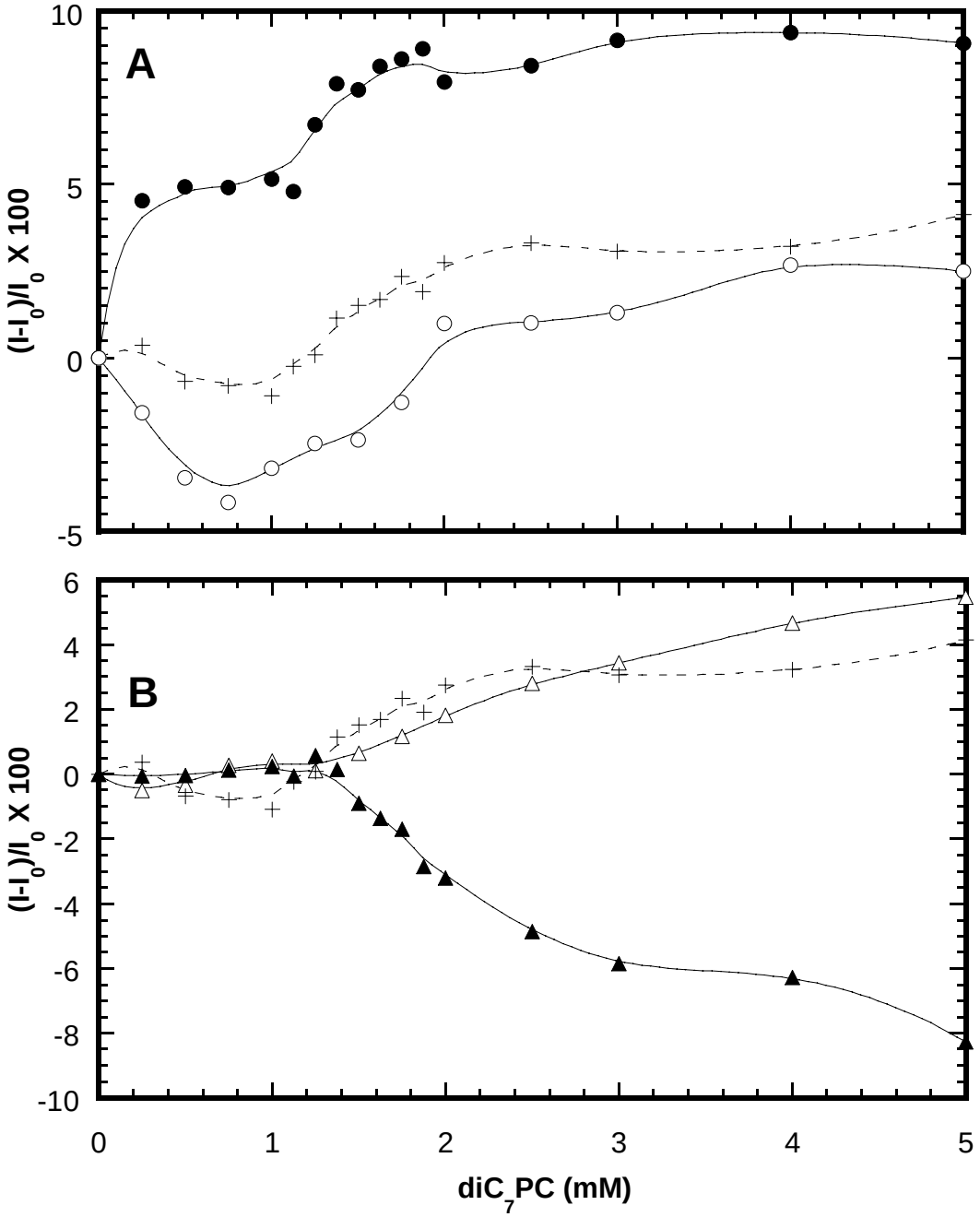

Figure 5-5 Fluorescence intensities of *L. monocytogenes* PI-PLCs as a function of added diC_6PC: (A) wild type recombinant PI-PLC (+), F237A (o), and F237W (•) mutant proteins; (B) W49A (Δ) and W49A/F237A (▲) compared to wild type PI-PLC (+).

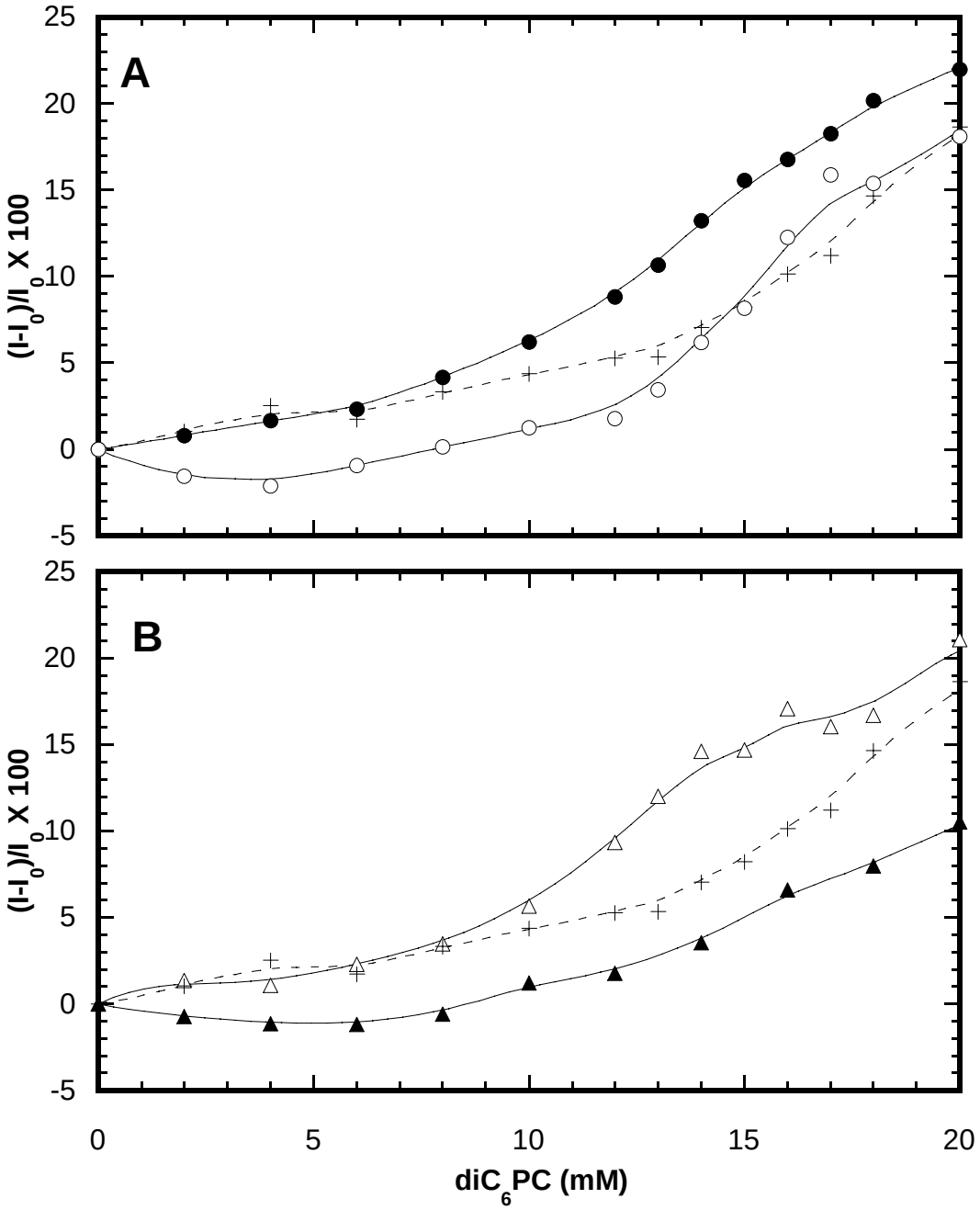

appreciable binding to the *L. monocytogenes* PI-PLC. It is hard to quantify the extent of increase with diC_6PC micelle binding, but the overall intensity increase appears larger than for diC_7PC binding.

Considering the salt activation of the phosphotransferase step with detergent present, the effects of diC_7PC on the fluorescence intensity of WT and F237W were also checked with KCl present. As shown in Figure 5-6, 0.16 M KCl did perturb their responses to diC_7PC in the similar way in that the fluorescence intensities of both enzymes were less sensitive to diC_7PC, particularly as the CMC was approached. For F237W, the fluorescence intensity increase below 1 mM diC_7PC in the absence of KCl could be fit with a hyperbolic binding equation; the second increase in fluorescence as micelles form followed a second hyperbolic profile. This treatment generated a K_d=0.04±0.01 mM for monomeric diC_7PC and an apparent K_d=1.19±0.04 mM for micellar diC_7PC which is right around the CMC of the lipid. With KCl present, there is a reproducible decrease as the CMC is approached. Since this behavior is also seen with WT in the presence of KCl, it suggests that the salt (generic ionic interactions since salt identity is not important) must alter the protein conformation such that a different fluorophore from Trp237, possibly Trp19 is affected. Micellar PC binding still results in an increase in fluorescence. What the salt results do is emphasize that there must be a discrete conformational change in the protein when moderate salt is present. This change may be weakening the interaction of the protein with monomeric PC such that micelle formation competes favorably with the protein for PC monomers. It is this change that is linked to enhanced activity when amphiphiles are present as well.

Figure 5-6 Changes in the intrinsic fluorescence of *L. monocytogenes* PI-PLC wild type (■,□) and F237W (♦,◊) binding to diC_7PC in the absence (filled symbols) or presence (open symbols) of 0.16 M KCl.

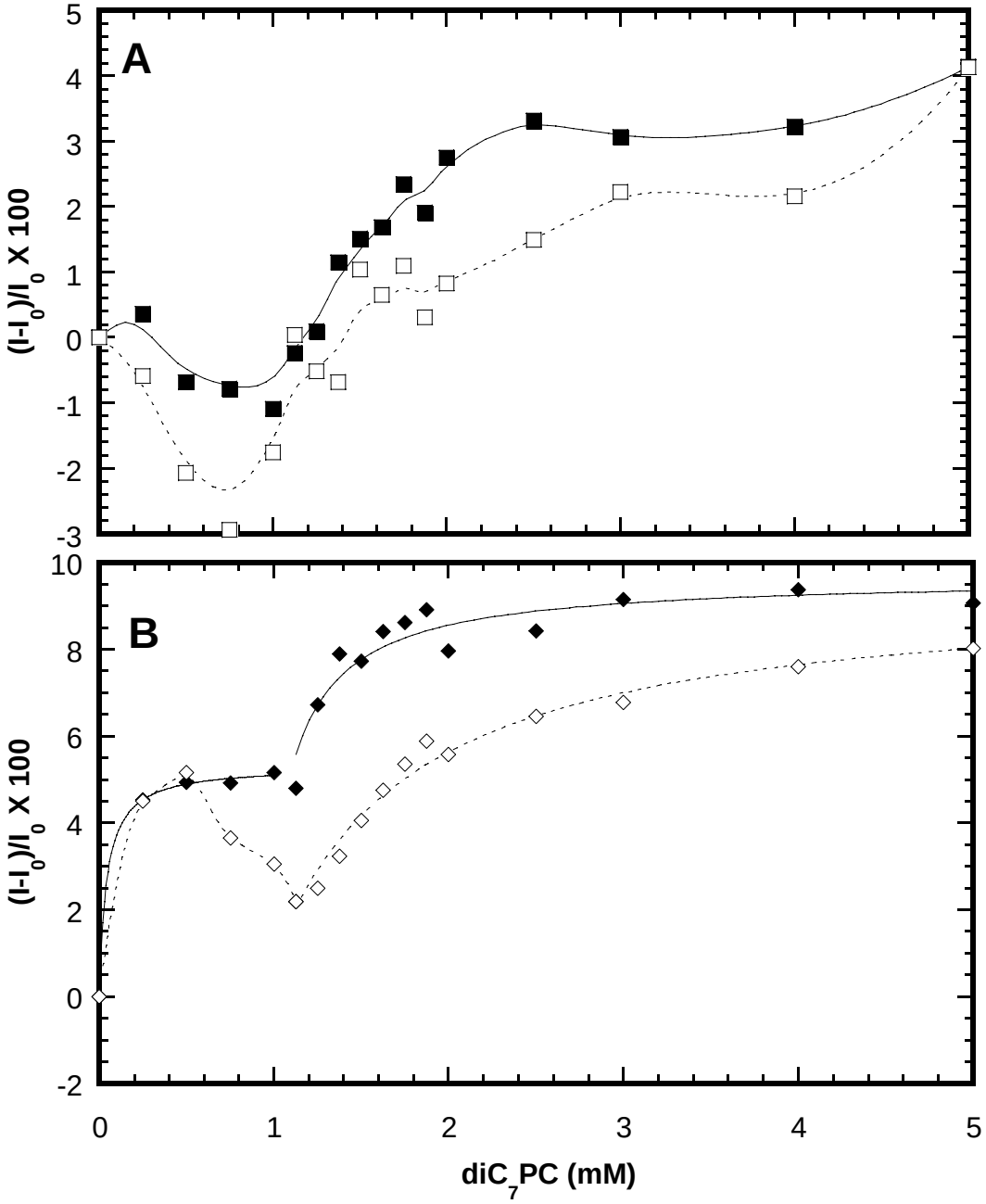

Myo-inositol, a poor competitive inhibitor of PI-PLC (Shashidhar et al., 1990), was reported to cause a decrease in fluorescence intensity of *B. thuringiensis* PI-PLC when binding to the PI-PLC active site (Feng et al., 2002). As shown in Figure 5-7, *myo*-inositol caused 4-6% decrease in the fluorescence intensity of *L. monocytogenes* PI-PLC WT and F237W, a much smaller decrease (~ 2%) for F237A, basically no change for W49A, or W49A/F237A (the 2-3% increase is likely caused by a weakly fluorescing impurity in the protein solution). Because *myo*-inositol has no tendency to form interfaces, the decrease in protein intrinsic fluorescence is correlated with binding of this molecule to the active site. For those mutants that do not exhibit the decrease shown in WT it would suggest that inositol affinity has been altered, unless the fluorophore sensing this change has been removed. The interesting mutant here is W49A since it is basically insensitive to *myo*-inositol. Either this residue is a key reporter of substrate binding, or this mutant is impaired in binding substrate-like molecules.

DOPMe SUVs inhibit PI-PLC in both cleavage of PI and hydrolysis of cIP. Binding of DOPMe at low concentration (<20 μM in our conditions) induced ~25% increase in WT, F237W and F237A fluorescence; when higher concentrations of DOPMe SUVs were present, the intrinsic fluorescence decreased (Figure 5-8). The initial steep increase in fluorescence intensity of WT and Phe-237 mutants is consistent with the observed tight binding of proteins to anionic interfaces. The smaller fluorescence increase for W49A may correspond to an impaired ability to bind anionic substrate or reduced sensitivity, consistent with the fluorescence results with *myo*-inositol. For comparison,

Figure 5-7 Intrinsic fluorescence intensities of *L. monocytogenes* PI-PLC proteins as a function of added *myo*-inositol: WT (+), F237A (o), F237W (•), W49A (Δ) and W49A/F237A (▲).

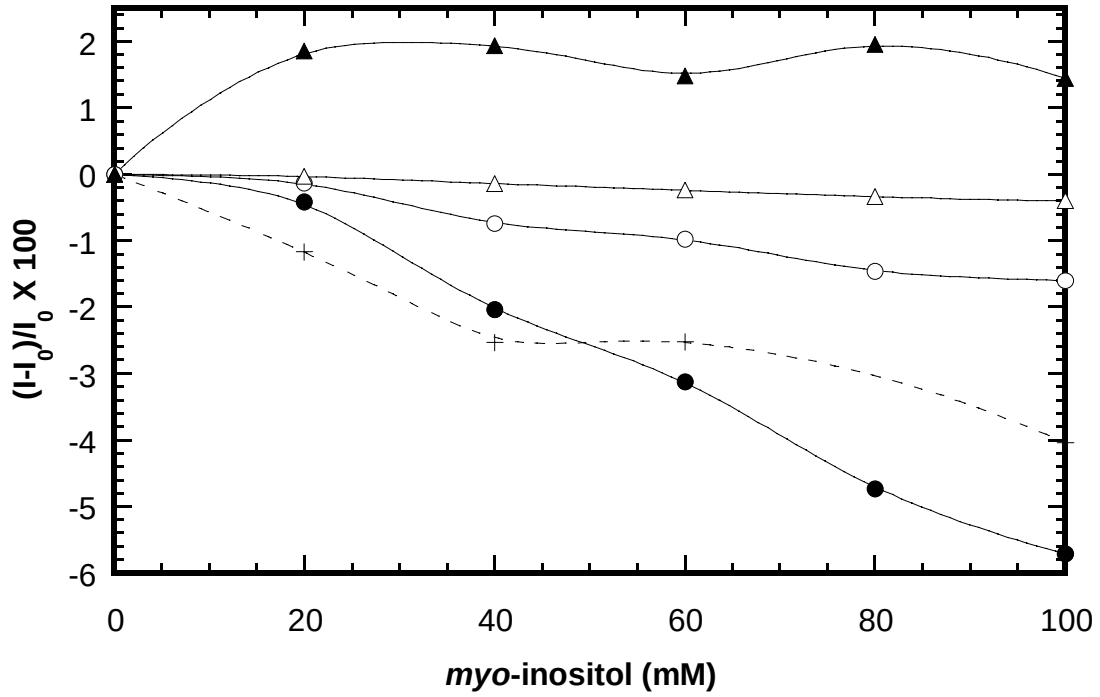

Figure 5-8 Fluorescence intensities of *L. monocytogenes* PI-PLCs as a function of added SUVs: wild type recombinant PI-PLC (+), F237A (o), F237W (•), W49A (Δ) and W49A/F237A (▲) with the addition of DOPMe; F237W (X) with the addition of POPC SUVs.

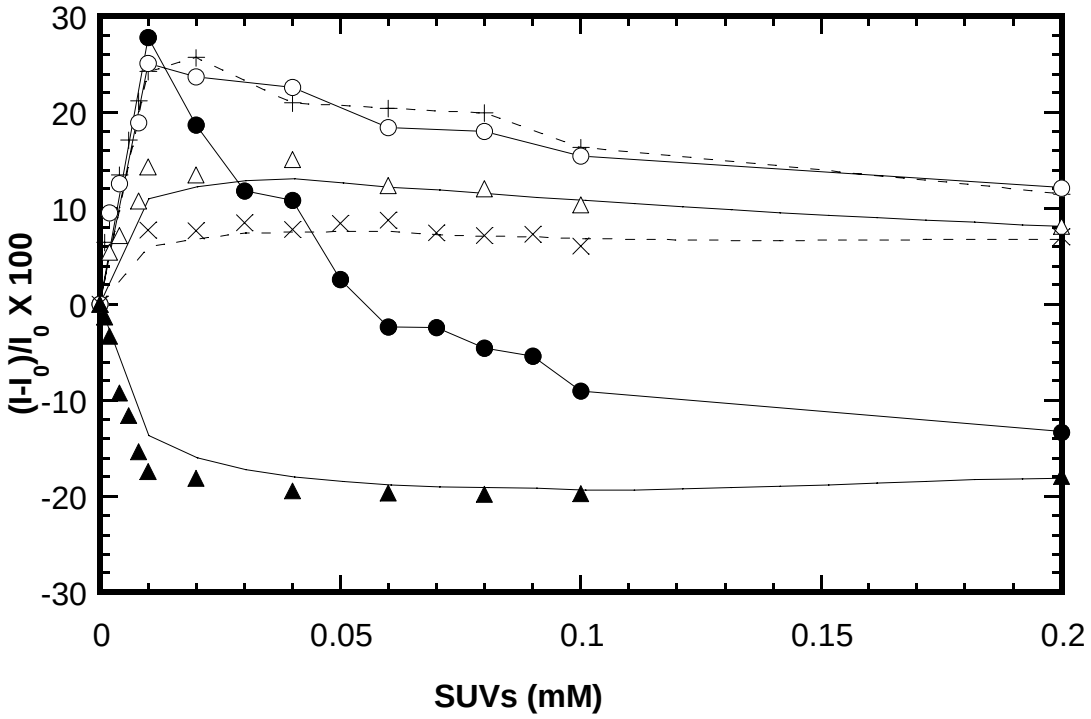

POPC SUVs, binding loosely to *L. monocytogenes* PI-PLCs, lead to a smaller increase (~8%) in intensity of F237W and no subsequent decrease. Since the response of the protein to POPC was stable, the decrease in intensity from a maximum with anionic phospholipid vesicles is likely to result from aggregation of a large PMe/PI-PLC complex that is no longer soluble. The different mutants might have different time scales for aggregation and precipitation. With this small amount protein we would not easily be able to detect aggregation, so this aspect of the interaction can not be easily examined.

D. Catalytic properties of Trp-49 and Phe-237 mutants

The potential roles of Trp-49 and Phe-237 in the kinetic behavior of *L. monocytogenes* PI-PLC were examined. As summarized in Table 5-2, no significant cyclic phosphodiesterase activity was observed for Trp-49 mutants. Even in the presence of 5 mM TX-100, incubating 7.2 μg/ml W49A or W49A/F237A with 10 mM cIP for 24 h did not generate any I-1-P detectable in the ^{31}P NMR spectrum. Removal of Trp-49 also dramatically decreased the phosphotransferase activity. At a concentration of 0.82 μg/ml, the specific activity of W49A toward PI was only 2% that of WT. With this low activity, high protein concentrations were used to check the effect of enzyme concentration, amphiphile, and salt on the PI cleavage. No WT data was available for comparison at this high enzyme concentration. The phosphotransferase activities of both Trp-49 mutants were slightly affected by enzyme concentrations, but specific activities *decreased* as the protein concentrations decreased, in contrast to WT enzyme. At a concentration of 7.2 μg/ml, increasing the amount of TX-100 had no effect on either mutant enzyme, whereas

Table 5-2 Kinetic behavior of W49A and W49A/F237A mutants.

Effect of enzyme concentration on phosphotransferase activity				
PI-PLC (μg/ml)	Mole fraction of TX-100	Salt	W49A	W49A/F237A
0.21	0.80	-	N/A	N/A
0.82			1.68	
3.60			2.07	1.85
7.20			4.09	1.95
14.90			5.30	3.35
29.80				3.31
Effect of detergent mole fraction on phosphotransferase activity				
PI-PLC (μg/ml)	Mole fraction of TX-100	Salt	W49A	W49A/F237A
7.2	0.80	-	4.09	1.95
	0.92		4.54	1.84
Effect of salt on phosphotransferase activity				
PI-PLC (μg/ml)	Mole fraction of TX-100	KCl (150 mM)	W49A	W49A/F237A
7.2	0.80	-	4.09	1.95
		+	7.26	1.88
phosphodiesterase activity				
PI-PLC (μg/ml)			W49A	W49A/F237A
7.2			N/A	N/A

this has a large effect on WT. Adding KCl to the PI/TX-100 assay system slightly increased W49A specific activity, but not that of W49A/F237A. At 0.21 μg/ml W49A/F237A, generation of cIP was not detected with ^{31}P NMR under the control assay condition (8 mM PI, 32 mM TX-100, 20 h), but a small amount of cIP was generated if KCl or TX-100 were increased (200 mM KCl or 64 mM TX-100). In any case, the specific activity of these two mutants was very low.

Unlike the Trp-49 mutant proteins, Phe-237 mutant proteins were active and comparisons with WT show interesting trends (Table 5-3). Substitution of Phe-237 with alanine reduced the PI-PLC specific activity toward cIP to 19% of WT. Although it is a less efficient enzyme, F237A can still be activated by amphiphiles. The ratio of specific activity of F237A for cIP hydrolysis with and without 3 mM TX-100, 13:1, is essentially comparable to that of WT PI-PLC (14.8:1). F237W showed similar phosphodiesterase activity as WT, but with a higher increase in activity (25-fold) than WT (15-fold) upon the addition of 3 mM TX-100.

Under the control phosphotransferase assay condition (0.21 μg/ml enzyme, 8 mM PI, 32 mM TX-100), the activities of F237A and F237W toward PI cleavage were 97% and 400% of WT, respectively. Compared to WT, both Phe-237 mutants lost the steep increase in phosphotransferase activity as enzyme concentration decreased from 0.82 to 0.02 μg/ml. Instead, F237W specific activity decreased ~30% when comparing assays with 0.02 versus 0.2 μg/ml enzyme added. F237A exhibited a 1.7-fold increase in specific activity with that 10-fold dilution, still very different from the 3.9-fold increase

Table 5-3 Comparison of specific activity behavior of *L. monocytogenes* PI-PLC WT versus Phe-237 mutants.

Effect of enzyme concentration on phosphotransferase activity					
PI-PLC (μg/ml)	Mole fraction of TX-100	Salt	WT	F237W	F237A
0.02	0.80	-	1068.79	713.30	446.02
0.21			274.27	1097.00	264.90
0.41			147.72		193.99
0.82			90.21	1099.20	170.96
Effect of detergent mole fraction on phosphotransferase activity					
PI-PLC (μg/ml)	Mole fraction of TX-100	Salt	WT	F237W	F237A
0.21	0.67	-		37.70	2.17
	0.75			563.30	42.40
	0.80		274.27	1097.00	264.90
	0.89		368.30	1113.00	257.50
	0.92		1155.30	1201.85	267.74
	0.94				180.08
Effect of salt on phosphotransferase activity					
PI-PLC (μg/ml)	Mole fraction of TX-100	KCl (150 mM)	WT	F237W	F237A
0.21	0.80	-	274.27	1097.00	264.90
		+	1033.54	2788.70	983.46
Effect of TX-100 on phosphodiesterase activity					
PI-PLC (μg/ml)	TX-100 (3 mM)		WT	F237W	F237A
7.2	-		0.16	0.18	0.03
	+		2.37	4.52	0.39

exhibited by WT. The surface dilution behavior of these mutant enzymes was also significantly altered. At the concentration of 0.21 μg/ml, WT specific activity increased 4.2-fold as the TX-100 increased from 32 to 96 mM (X_{det} increasing from 0.80 to 0.92). F237A in the same range showed constant specific activity (Table 5-3), while F237W showed a 1.1-fold increase (likely within the errors in determining activity). Both Phe-237 mutants still exhibited activation of PI cleavage by salt. Under the assay conditions used, the optimal phosphotransferase activity of F237A responding to enzyme concentration or amphiphiles was slightly lower than that of WT. Adding KCl significantly enhanced the specific activity of F237W so that it was much higher than for WT under the same assay conditions.

III. Other possible interfacial mutants of PI-PLC

Modification of either Trp-49 or Phe-237 in *L. monocytogenes* PI-PLC had very pronounced effects on the unusual kinetic behavior (increases upon dilution of the enzyme, increased mole fraction of detergent, or addition of moderate salt) of this enzyme. Since these are two positions where a hydrophobic side chain is at/near the surface of the protein, we decided to alter other residues in this region. Both helix B and the surface loop each have a leucine residue that could be involved in interfacial effects, and so each was mutated to alanine. The two surface structural elements also have a threonine residue. Each of these were also chosen for mutation, initially as a way of potentially introducing an extrinsic fluorophore for more detailed and site-specific fluorescence studies.

A. Catalytic properties of L51A and L235A

Mutation of Phe-237 and Trp-49 was originally undertaken to explore the interfacial binding behavior of *L. monocytogenes* PI-PLC. Our results showed that while Phe-237 is likely to contribute to surface binding of this PI-PLC, Trp-49 would appear to be more involved with catalysis. Two hydrophobic residues near each of the first mutagenesis targets, Leu-51 in α-helix B and Leu-235 in the loop, were mutated to alanine. Unlike W49A or F237A, both L51A and L235A retained activities toward water-soluble cIP substrate in the absence and presence of TX-100 that were comparable to WT enzyme (Table 5-4). Detergent enhanced cIP hydrolysis to the same extent as for WT. However, modulating enzyme or amphiphile concentration had a much smaller impact on the phosphotransferase activities of both L51A and L235A (Table 5-4). No dramatic changes in activity were observed for both mutants within the enzyme concentration range examined (0.02-3.60 μg/ml). As the mole fraction of TX-100 in TX-100/PI micelles increased from 0.80 to 0.92, L51A displayed no surface dilution inhibition while L235A showed a decrease in activity. The activities of both mutants toward PI cleavage could also be activated by salts, but not to the extent of WT. Clearly, removal of either hydrophobic residue Leu-51 or Leu-235 altered the unusual kinetic profile of this PI-PLC.

B. Catalytic properties of T50C and T236C

According to the Wimley and White hydrophobic scale (Wimley et al., 1996; Wimley and White, 1996; White, 2003), amino acids containing moderately polar side

Table 5-4 Comparison of specific activity behavior of *L. monocytogenes* PI-PLC WT versus L51A and L235A mutants.

Effect of enzyme concentration on phosphotransferase activity					
PI-PLC (μg/ml)	Mole fraction of TX-100	Salt	WT	L51A	L235A
0.02	0.80	-	1068.79	196.23	195.49
0.21			274.27	265.01	427.03
0.82			90.21	244.40	258.69
3.60			54.38	254.51	253.12
Effect of detergent mole fraction on phosphotransferase activity					
PI-PLC (μg/ml)	Mole fraction of TX-100	Salt	WT	L51A	L235A
0.21	0.67	-		23.33	18.32
	0.75			80.51	385.97
	0.80		274.27	265.01	427.03
	0.89		368.30		
	0.92		1155.30	238.21	179.18
Effect of salt on phosphotransferase activity					
PI-PLC (μg/ml)	Mole fraction of TX-100	KCl (150 mM)	WT	L51A	L235A
0.21	0.80	-	274.27	265.01	427.03
		+	1033.54	412.12	586.50
Effect of TX-100 on phosphodiesterase activity					
PI-PLC (μg/ml)	TX-100 (3 mM)		WT	L51A	L235A
7.2	-		0.16	0.11	0.14
	+		2.37	2.12	2.45

chains, like threonine, serine, and cysteine, prefer the interfacial region of membrane. There are several polar residues (Thr+Ser) in α-helix B (ITWTLTKP) and the loop (SATSLTF) of *L. monocytogenes* PI-PLC. From the previous results, Trp-49, Leu-51, Leu-235, and Phe-237 are involved in regulating the unusual kinetic behavior of this enzyme. It is likely that Thr-50 and Thr-236, which are flanked by those residues, also play roles. We thus replaced Thr-50 or Thr-236 with cysteine to enable the introduction of a thio-reactive probe as there are no other cysteine residues in the enzyme.

As shown in Table 5-5, cysteine substitution at Thr-50 or Thr-236 had unexpected and dramatic effects on the enzyme activities. Compared to WT, the phosphodiesterase activity was higher (2-fold and 3-fold for T50C and T236C, respectively) but exhibited about the same specific activity as WT when diC_7PC was added. Most strikingly, both enzymes were much more active than WT under standard conditions (0.21 μg/ml enzyme, 8 mM PI, 32 mM TX-100, no added KCl). The enzyme specific activities no decreased with protein dilution and increased mole fraction of detergent at high and low protein concentrations. At the lowest PI-PLC concentration (0.02 μg/ml) and 0.8 mole fraction TX-100, the specific activities of both mutants were comparable to that of WT. Both T50C and T236C exhibited obvious surface dilution inhibition at high TX-100 mole fraction (0.80 versus 0.92). Salt could enhance the phosphotransferase activity of both mutants except when extremely high activity was already achieved.

One possible rationale for the very high activity of the cysteine mutants is that

Table 5-5 Comparison of specific activity behavior of *L. monocytogenes* PI-PLC WT versus T50C and T236C mutants.

Effect of enzyme concentration on phosphotransferase activity					
PI-PLC (μg/ml)	Mole fraction of TX-100	Salt	WT	T50C	T236C
0.02	0.80	-	1068.79	910.47	748.66
0.21			274.27	8347.96	4806.39
Effect of detergent mole fraction on phosphotransferase activity					
PI-PLC (μg/ml)	Mole fraction of TX-100	Salt	WT	T50C	T236C
0.02	0.80	-	1068.79	910.47	748.66
	0.92		301.23	410.47	280.11
0.21	0.80	-	274.27	8347.96	4806.39
	0.92		1155.30	3416.12	2461.03
Effect of salt on phosphotransferase activity					
PI-PLC (μg/ml)	Mole fraction of TX-100	KCl (150 mM)	WT	T50C	T236C
0.02	0.80	-	1068.79	910.47	748.66
		+	1718.01	3598.70	2547.90
0.21		-	274.27	8347.96	4806.39
		+	1033.54	7334.12	7302.92
Effect of TX-100 on phosphodiesterase activity					
PI-PLC (μg/ml)	TX-100 (3 mM)		WT	T50C	T236C
7.2	-		0.16	0.31	0.41
	+		2.37	1.90	1.93

covalent dimmers might for at PI –containing interfaces. However, the proteins were stored with DTT in the buffer and upon dilution into the assay mixture there was still DTT present. Also given the short incubation times for these assays, disulfide formation is highly unlikely. There must be another cause of the very high specific activities of these mutant enzymes.

C. Use of coumarin/BODIPY FRET to probe the interfacial binding of T50C and T236C to POPG/POPC SUVs

The *L. monocytogenes* PI-PLC T50C and T236C enzymes were used to explore the binding of the protein to POPG/POPC SUVs via a coumarin/BODIPY FRET pair. BODIPY-labeled lipid was used as the acceptor with CPM attached to the cysteine residue of T50C or T236C via a maleimide as the donor (Keller et al., 1995). BODIPY FL is relatively environment insensitive and is fluorescent in both aqueous and lipid environment. The Förster energy transfer radius (R_o) was reported ~50Å for coumarin-β-BODIPY FL C_{12}-HPC pair. PC labeled with BODIPY connected to a shorter acyl chain (C5) instead of C12 was used in our experiments to keep the BODIPY label in the hydrophobic region of vesicles but not too far from the interface. In the absence of POPG in the vesicle, there was no quenching of coumarin fluorescence indicating that the protein did not bind to the vesicles under these conditions (10 μg/ml labeled protein and 100 μM POPC containing 2.5% BODIPY labeled PC). The filtration/centrifugation binding studies with PI-PLC and POPC SUVs (Chapter 4) suggested that most of the protein would be free in solution under these conditions. As shown in Figure 5-9, the fluorescence of CPM-T50C and CPM-T236C was increasingly quenched upon the

addition of vesicles containing β-BODIPY FL C_5-HPC as the POPG mole fraction increased, confirming that the presence of anionic surface induced the insertion of enzyme into the membrane. The fluorophore at T236C is more effectively quenched than that at T50C by binding to SUVs containing low amounts of PG. For T236C-CPM the mole fraction PI for half of the maximum quenching (57±3%) is 0.007±0.002. Quenching of T50C-CPM was much less efficient – at X_{PG} = 0.5, only 20% of the CPM fluorescence was quenched. The BODIPY-PC in these experiments shows behavior that is not quite complementary. For T236C-CPM binding, the BODIPY probe intensity increases by 16±2% and reaches half of this value at X_{PG} = 0.08±0.03; for T50C-CPM, the BODIPY emission increases a comparable amount (by 13±1%) but requiring more PG (X_{PG} = 0.19±0.01 for half the increase). The similarly increased BODIPY fluorescence suggests by X_{PG} = 0.5 all the protein is bound under these conditions. The more dramatic loss of fluorescence by the T236C-CPM compared to T50C-CPM implies that the smaller amount of quenching of the T50C-CPM could suggest that the T236-CPM site is closer to the BODIPY on the phospholipids. Perhaps, the coumarin attached to T236C inserts into the bilayer while the probe on T50C does not.

The quenching of CPM fluorescence and the increase of β-BODIPY FL C_5-HPC fluorescence with vesicles containing 0.5 mole fraction POPG were also checked at various KCl concentrations. As shown in Figure 5-10, the observation that FRET between the coumarin/BODIPY pair decreased (meaning the CPM fluorescence increased) as the concentration of KCl increased. This observation is in agreement with

Figure 5-9 (A) Quenching of CPM fluorescence or (B) increasement of β-BODIPY FL C_5-HPC fluorescence due to FRET between coumarin labeled protein, T50C-CPM (•) or T236C-CPM (o), and BODIPY labeled lipid. 10 μg/ml labeled protein and 100 μM total phospholipids (containing 2.5% BODIPY labeled lipids) were used.

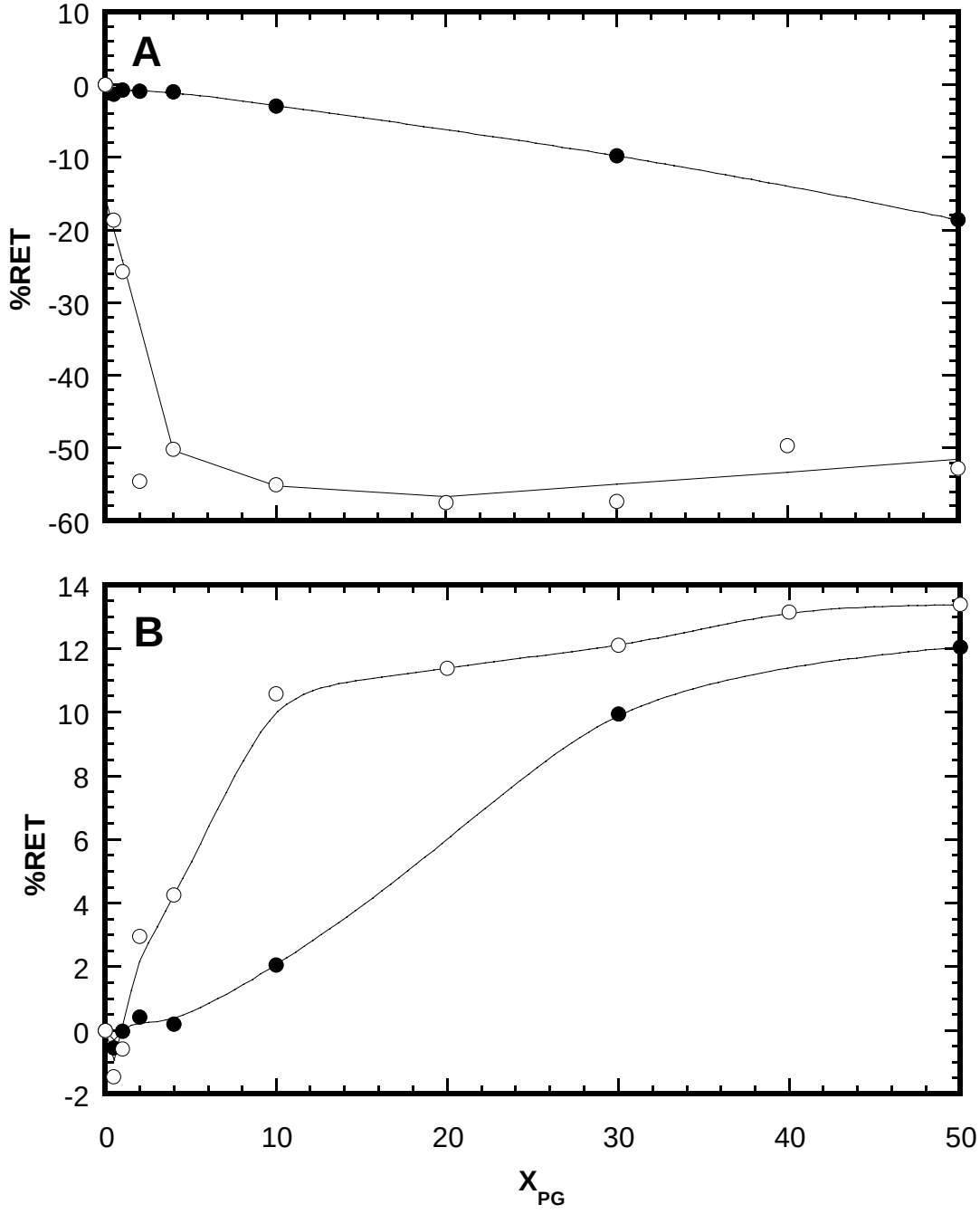

Figure 5-10 The effect of increasing KCl on the FRET between PI-PLC-CPM and β-BODIPY FL C_5-HPC initially bound to SUVs containing PC (0.05 mM) / PG (0.05 mM). (A) Increase in Donor (PI-PLC-CPM) fluorescence with added salt; (B) decrease in Acceptor (β-BODIPY FL C_5-HPC) fluorescence with added KCl. The labeled enzymes are T50C (•) and T236C (o).

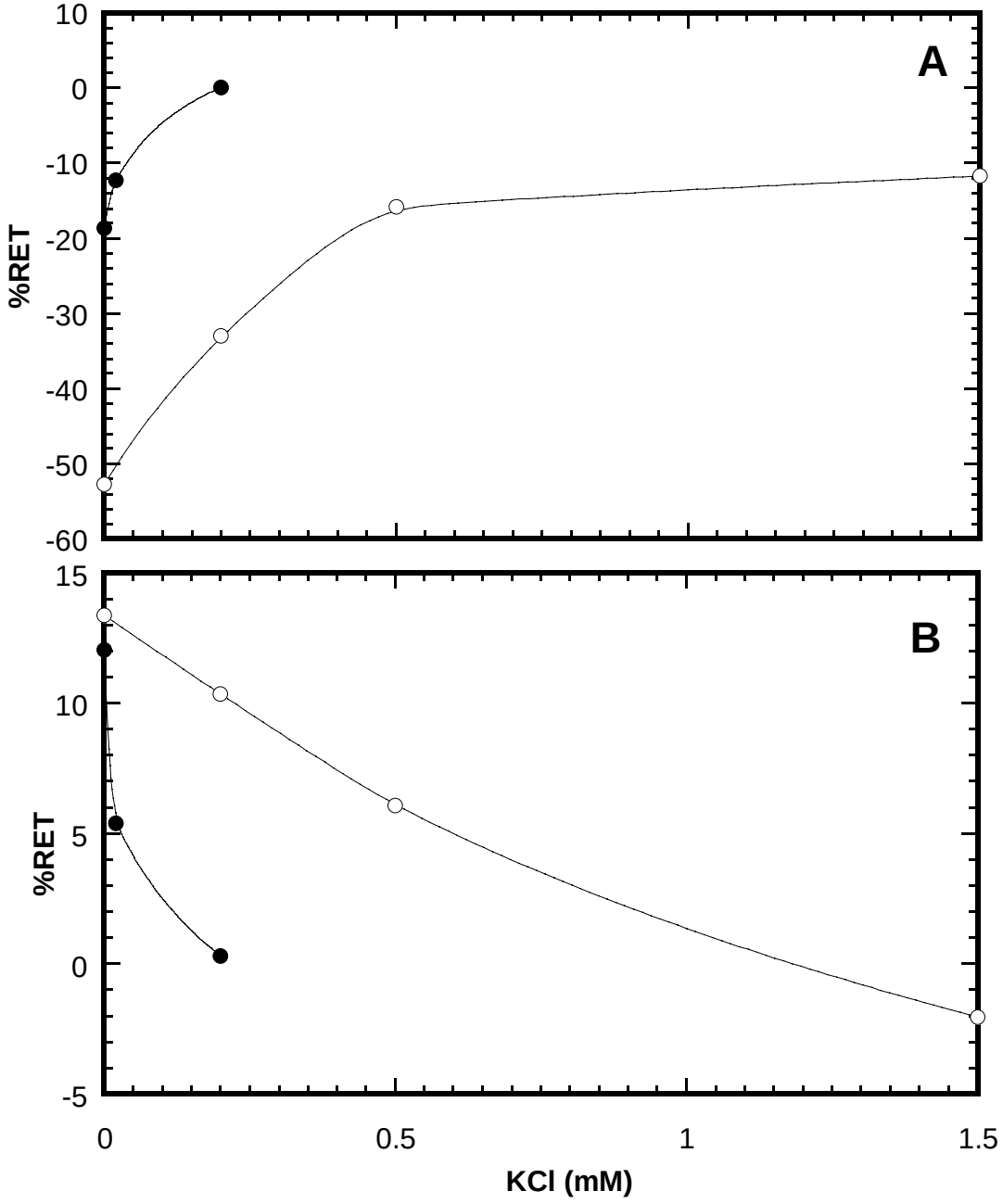

the monolayer penetration result that the driving force for the *L. monocytogenes* PI-PLC to bind to the lipid surface has a large electrostatic component. The binding of T50C-CPM to the vesicles is considerably weaker than T236C-CPM since it can be washed off with 200 mM KCl. Compared to the cysteine in α-helix B, the CPM on Cys-236 is less sensitive to the effect of KCl. Assuming the addition of the CPM does not dramatically alter the activity of the PI-PLC, these FRET results, consistent with the kinetic data, suggest that weaker interfacial binding of T50C may be the key to its higher activity as compared to T236C.

IV. The effect of F237W on plaque formation

All the PI-PLC mutants exhibit some type of altered kinetics, and vesicle binding and kinetics do not necessarily show simple connections. However, the activities of F237W are comparable to that of WT, but the response of this mutant enzyme to amphiphiles and ionic strength is radically different from WT (Table 5-3). Therefore, we decided to check if these different kinetic behaviors affect the biological activity of *L. monocytogenes*. For this we monitored, using the plaque assay, the cell-to-cell spread of *L. monocytogenes* in L2 fibroblasts. The gene for WT or F237W PI-PLC was inserted into the *p*AM401 plasmid which contains the *plc*A gene promoter with the *L. monocytogenes* PI-PLC original signal peptide sequence. These *p*AM401 plasmids containing either WT or F237W genes were electroporated into strain DP-L1552 (*Δplc*A, no *L. monocytogenes* PI-PLC expression). The modified *L. monocytogenes* strains were then used to infect monolayer cultures of mouse fibroblast L2 cells. As shown in Figure 5-11, infection with DP-L1559, *L. monocytogenes* containing no chromosomal PI-PLC

gene but with the plasmid containing the WT gene, results in decreased plaque size as reported previously (Camilli et al., 1993) when compared to 10403S (the *L. monocytogenes* WT strain where the PI-PLC gene is chromosomal) (Bishop and Hinrichs, 1987). The bigger the plaque the more effective the *L. monocytogenes* was at colonizing the fibroblasts. Interestingly, the *L. monocytogenes* strain containing the plasmid with the F237W gene produced even smaller plaques than those by *L. monocytogenes* with the WT PI-PLC gene located on the plasmid. This result indicates that PI-PLC with the F237W mutation had a negative effect over WT for cell-to-cell spread.

V. Discussion

A. Trp-49 and Phe-237 may play dual roles in adopting 'active' PI-PLC conformation and keeping PI-PLC in the 'right' orientation on the membrane

Although the secondary structures of Trp-49 and Phe-237 mutants calculated from their CD spectra are similar to that of WT, Trp-49 and Phe-237 clearly play roles in helping enzyme to adopt an 'active' conformation because the cyclic phosphodiesterase activities of both W49A and F237A toward water soluble cIP at the absence of amphiphiles are significantly lower than that of WT (Table 5-2 and Table 5-3). In the crystal structure of *B. thuringiensis* W47A/W242A, an interfacially impaired mutant, α-helix B has switched to a loop structure, presumably due to loss of hydrophobic stacking interaction between Ile-43 and Trp-47 (Shao et al., 2007). This hydrophobic stacking partner is not found for *L. monocytogenes* PI-PLC. Instead the side chain of Trp-49 in α-

Figure 5-11 Cell-to-cell spread in murine L2 fibroblasts, as indicated by plaque size. 10403S is the *L. monocytogenes* WT strain where the PI-PLC gene is chromosomal. DP-L1559 (pAM401::*plc*A) and F237W (pAM401::F237W) were inserted into the DP-L1552 (Δ*plc*A, no *L. monocytogenes* PI-PLC expression) background.

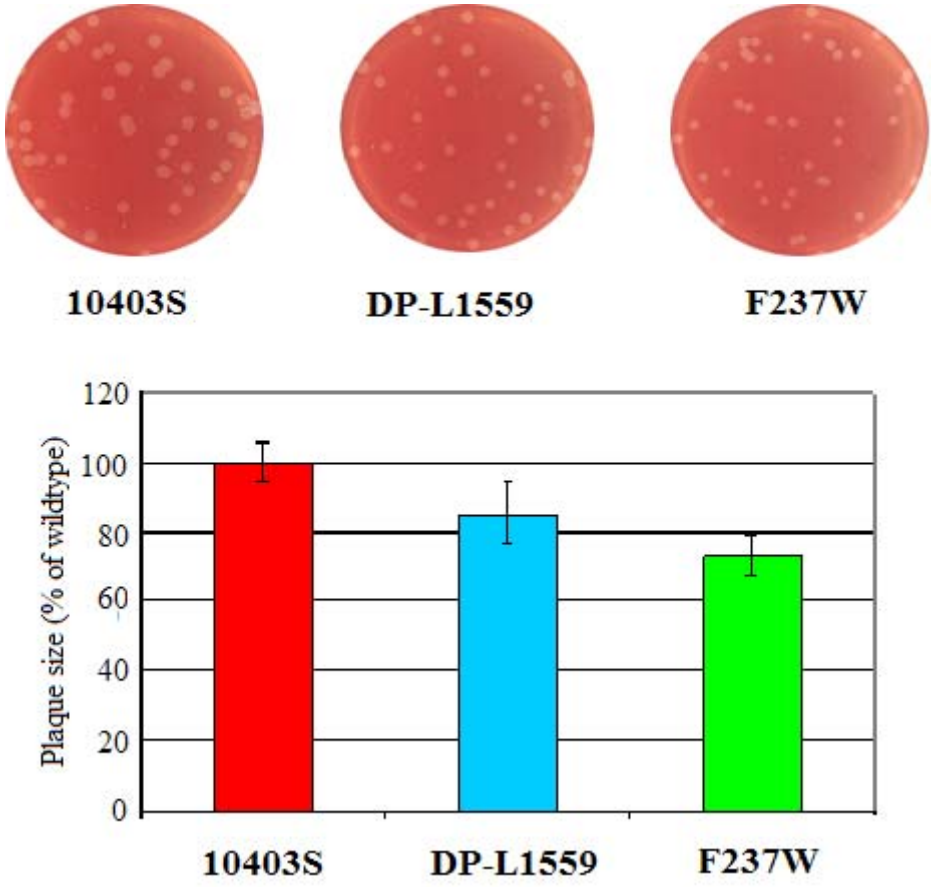

helix B points inward (Figure 5-1) where it may be involved in interacting with substrates. Replacement of the bulky, hydrophobic tryptophan side chain with a methyl group may disorder this short helix and impair both phosphotransferase and phosphodiesterase activities. Substitution of Phe-237 in the surface the loop with alanine still shows reduced activities but not to the same extent as W49A. The specific activities of F237A for cIP hydrolysis and PI cleavage (0.21 μg/ml enzyme, 8 mM PI, 32 mM TX-100) are 19% and 97% that of WT. However, a hydrophobic group located at residue 237 appears important for the 'active' conformation that leads to optimal PI-PLC specific activity. F237W, but not F237A, has maximum phosphodiesterase activity comparable to WT enzyme.

Mutant intrinsic fluorescence and FRET assays between β-BODIPY FL C_5-HPC and CPM labeled T50C or T236C further explore these regions of the protein. The larger changes in the intrinsic fluorescence intensity of F237W upon binding to PC micelles compared to the other mutant proteins suggests that the side chain at 237 is likely to insert into the phospholipid aggregate. A fluorophore at this position is also sensitive to 'monomeric' PC binding. The changes in F237W intrinsic fluorescence with diC_7PC are reminiscent of what has been observed with the *B. thuringiensis* PI-PLC (Feng et al., 2002), except that the increase with monomeric PC is much larger for F237W. The differences between WT and F237A intrinsic fluorescent profiles are also notable. Replacement of Phe-237 with alanine does not alter the number or placement of fluorophores in these experiments. However, what it does is generate a protein whose fluorophores are now sensitive to monomer PC binding. Not only does this mutant exhibit changes in intensity below 1 mM diC_7PC (while WT and W49A, containing the

same fluorophores, do not), but the *decrease* in fluorescence detected is consistent with what is seen with a molecule, *myo*-inositol, that binds to the active site. F237A is not as active as WT or F237W and the lower activity could be reflected in the altered fluorescence behavior of Trp-19 or Trp-49 observed with monomeric PC.

Both W49A and W49A/F237A are poor PI-PLC enzymes containing the same two Trp residues. The difference in intrinsic fluorescence with micellar diC_7PC (Figure 5-3B) suggests that when both these hydrophobic side chains are removed, the remaining fluorophores sense a very different conformational change. In the crystal structure of *L. monocytogenes* PI-PLC, there are many solvent accessible basic residues as well as several tyrosine and phenylalanine residues at the bottom and side of the TIM-barrel. These may provide some non-productive interfacial binding sites competing with α-helix B and the loop for lipids. By removing both Trp-49 and Phe-237, the chances for enzyme binding to those regions may greatly increase. The tryptophan residues of W49A/F237A, Trp-6 and Trp-19, are located at the N-terminus of the enzyme. Trp-19 in α-helix A has limited solvent accessibility while Trp-6 is thought to be flexible. Perhaps the latter segment is involved in "non-productive" interfacial binding with micellar diC_7PC. Trp-6 and "non-productive" interfacial binding could also account for the monotonic increases in the intrinsic fluorescence changes of *L. monocytogenes* PI-PLCs upon binding micellar diC_6PC above 20 mM.

B. *L. monocytogenes* PI-PLC – could it dimerize on surfaces?

PI-PLC dimerization on phospholipid interfaces, mediated by helix B residues, the 240's loop and a strip of tyrosine residues on the surface of the barrel, has been

suggested as a major factor in enhancing the activity of that enzyme. Given the overall structural similarity of the *L. monocytogenes* to that PI-PLC, it is worth examining evidence for similar dimerization. In *B. thuringiensis* PI-PLC, α-helix B tilts at a small angle relative to the axis of TIM-barrel, and Trp-47, at the C-terminus of α-helix B, points outward into solution. For the *B. thuringiensis* enzyme, the interaction of Trp-47 with the membrane is critical for dimerization. Trp-47 and helix B form a sort of plug that prevents the close approach of Tyr-246, Tyr-247, Tyr-248, and Tyr-251, residues that form the core of the homodimer. The flexibility of the 240's loop also places Trp-242 near Trp-47 upon binding to interfaces in the homodimer model of the activated enzyme. In the *L. monocytogenes* PI-PLC, helix B is almost perpendicular to the axis of TIM-barrel, and Trp-49, in the middle of the α-helix, points inward (not into solution). This orientational change makes it difficult to see how Trp-49 might initiate tight membrane binding by inserting into a PC rich bilayer. It also makes it impossible to place Phe-237 near Trp-49. This change in the orientation of helix B may be the reason for much weaker binding of the Listeria enzyme to PC interfaces compared to the *B. thuringiensis* PI-PLC. Furthermore, there are no counterparts to the residues that form the dimer in the *B. thuringiensis* PI-PLC. There is no region rich in Tyr residues to form the herringbone pattern observed in the W47A/W242A dimmer (Shao et al., 2007). If the *L. monocytogenes* PI-PLC were to dimerize on membrane surfaces it would need a radically different dimer interface.

C. Residues in helix B and the rim loop are important in regulating the enzyme kinetic behavior

In our model, the binding pattern of *L. monocytogenes* PI-PLC, tight to anionic surfaces but weaker to zwitterionic surfaces, is correlated with the unusual kinetics of the enzyme. If this is the case, any perturbation of the binding behavior should moderate the unusual kinetics. We constructed several mutants at α-helix B and the loop to test their catalytic properties. Substitution of Leu-51, Phe-237, and Leu-235 with the less hydrophobic alanine residue does moderate the unusual kinetics of WT. Replacing Phe-237 with tryptophan also has a similar effect on the kinetic behavior as the alanine substitution. The results of F237W, at first glance, conflict with that of F237A because tryptophan is more hydrophobic than phenylalanine according to the Wimley and White hydrophobic scale (Wimley et al., 1996; Wimley and White, 1996; White, 2003). Transfer free energies measured with small peptides indicate that tryptophan favors inserting into the interfacial region of the bilayer over aqueous solvent – this orientation is favored more strongly than for any other natural amino acid (White and Wimley, 1999). In contrast, insertion of phenylalanine into a bilayer would favor interior regions over the interface. Studies of benzene partitioning in bilayers indicate it is distributed throughout the lipid bilayer, with the hydrocarbon core as the most stable position (Norman and Nymeyer, 2006). Phenylalanine, instead of tryptophan at residue 237, may facilitate deep penetration of WT PI-PLC into the bilayer. This tight anchoring of the protein might keep the protein anchored on a surface and minimize release into solution where it might surface denature at the air-water interface. Tight binding of this PI-PLC to an anion-rich

membrane would also promote aggregation of vesicles at high protein concentrations, given the very high cationic character of the protein. That such a mechanism is operational might be supported by the surface dilution kinetics with the F237W mutant where very dilute protein leads to lower specific activity. A major problem with understanding these results is that we do not have a good assay for quantitative surface binding of the different mutants, in part because of the aggregation of the protein bound to vesicles to generate a precipitate. A better method to quantify *L. monocytogenes* PI-PLC binding to vesicles as a function of composition is needed. FCS, fluorescence correlation spectroscopy, may be such a technique since it can use very low protein concentrations (3-4 nM, which translates to 0.1-0.2 μg/ml and is the amount used in kinetics for this PI-PLC) (Pu et al., 2008a; Pu et al., 2008b). This will require attaching a fluorophore to the protein on a segment far away form the surface binding regions. However, it would allow us a better handle on the protein/vesicles aggregation and what happens as the vesicle composition changes.

It was unexpected by us that replacement of Thr-50 and Thr-236 with cysteine also dramatically changed the kinetic behavior of WT. This may suggest that hydrogen bonding also contributes to the complex kinetics of *L. monocytogenes* PI-PLC. Lacking a way to quantify the interfacial binding affinities of mutants to various lipid surfaces prevents us from looking further into this issue at this time. However, another interpretation of the kinetics for these mutants is possible. These two mutant enzymes are much more active at higher protein concentrations than WT, while at the lowest enzyme concentration, 0.02 μg/ml, they are comparable to WT. It is possible that the Cys residues

on the surface of these proteins form disulfides when proteins are bound to vesicles. Covalent dimers might increase specific activity because scooting mode catalysis is enhanced. This very high activity is only observed in the phosphotransferase step.

Chapter 6:

Effect of deoxy-PI compounds on activities of PI-PLC and PI3K enzymes

I. Introduction

The phosphatidylinositol 3-kinase (PI3K) / Akt (or PKB) signaling pathway is crucial to many aspects of cell growth, survival and apoptosis (Brazil et al., 2004; Hanada et al., 2004) and upregulated in a variety of human cancer cell lines (Vivanco and Sawyers, 2002) and solid tumors (Seufferlein, 2002; Ghosh et al., 2003; Barnett et al., 2005). A key step in this pathway is the specific phosphorylation of the 3-hydroxyl group of the inositol ring in phosphoinositides by PI3K enzymes (Qiao et al., 1998; Kandel and Hay, 1999; Meuillet et al., 2003).

Attempts to inhibit the PI3K/Akt pathway led to the synthesis of D-3-deoxy-phosphatidylinositol molecules that can no longer be phosphorylated by PI3K (Gills and Dennis, 2004). Many of these molecules have antiproliferative properties (Kozikowski et al., 1995; Kozikowski et al., 2003). The first of these, 3-deoxy-dipalmitoyl-PI, was shown to inhibit cancer cell (HT-29 human colon carcinoma) growth in vitro with an IC_{50} of 35 μM (Kozikowski et al., 1995). Recent syntheses of ether linked rather than ester linked alkyl chains, e.g., D-3-deoxy-myo-inositol 1-[(R)-3-(hexadecyloxy)-2-hydroxypropyl hydrogen phosphate], have generated a newer class of PI analogues that should have higher stability in vivo and may also have slightly better delivery properties since they are more like lyso-phospholipids (Andresen et al., 2004). 3-Deoxy-PIs have also been shown to reduce drug resistance in human leukemia cell lines (Tabellini et al., 2004). Thus, these PI analogues may have a future in treatment of a variety of cancers.

A series of 3-deoxy-dioctanoyl phosphatidylinositol (3-deoxy-diC_8PI) derivatives (Figure 6-1) that can exist as monomers below 0.5 mM were synthesized by

the group of Scott Miller. We decided to explore the interactions of these lipids with different enzymes in the PI3K/Akt pathway. Part of this study was to examine the susceptibility of these short-chain PIs to phospholipase C cleavage and their effects on the catalytic activity of PI3K. Under the assay conditions, these compounds were poor substrates and not inhibitors of the PLC. There was also little inhibition of PI3K observed except for 3-deoxy-diC_8PI enantiomers, suggesting that the 3-deoxy-diC_8PI molecules are unlikely to have a significant effect on PI3K in vivo.

II. Results and Discussion

A. Effect of phospholipase C enzymes on 3-deoxy-diC_8PI molecules

PI-PLC plays a key role in the metabolism of membrane phospholipids by hydrolyzing PI(4,5)P_2 to second messengers, I (1,4,5)P_3 and DAG (Berridge and Irvine, 1989). The initial 3-deoxy-PI studied as a cell growth inhibitor, D-3-deoxy-dipalmitoyl-PI, did not appear to be a substrate for PLC (although in vivo potency of the drug was dramatically improved when the acyl linkages were replaced by ether linkages). However, that phospholipid has a high gel-to-liquid-crystalline phase transition temperature and may not have been presented in structures accessible to phospholipases. By using D-diC_8PI as the standard substrate, we can quantify the relative cleavage of the 3-deoxy-diC_8PIs substrates as well as examine their ability to inhibit the enzyme, which reflects their ability to bind to PLC active sites.

We examined the 3-deoxy-PI molecules as substrates and inhibitors of two

Figure 6-1 Structures of 3-deoxy-dioctanoylphosphatidylinositol (3-deoxy-diC_8PI) compounds synthesized.

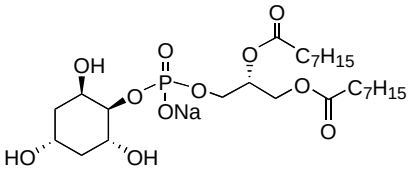

D-3,5-dideoxy-diC_8PI

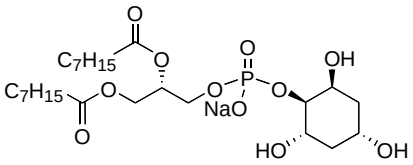

***ent*-3,5-dideoxy-diC_8PI = L-3,5-dideoxy-diC_8PI**

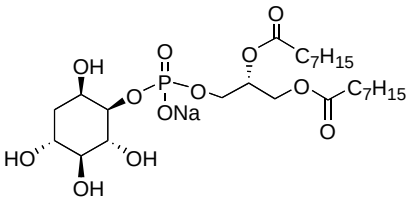

D-3-deoxy-diC_8PI

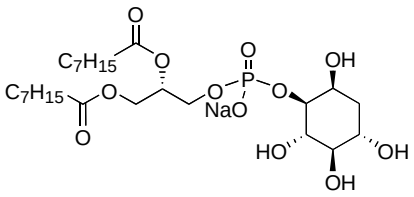

***ent*-3-deoxy-diC_8PI = L-3-deoxy-diC_8PI**

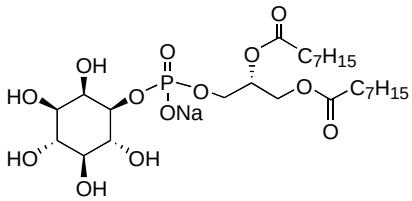

D-diC_8PI

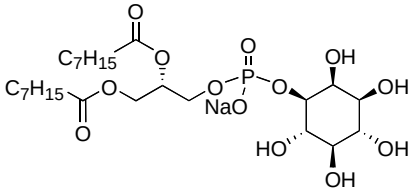

***ent*-diC_8PI = L-diC_8PI**

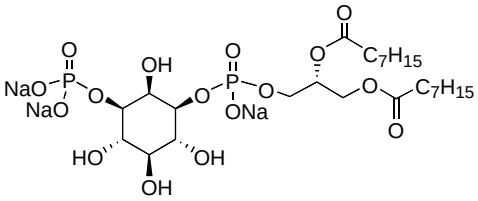

D-diC_8PI (3) P

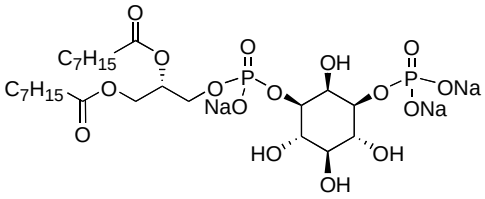

***ent*-diC_8PI (3) P = L-diC_8PI (3) P**

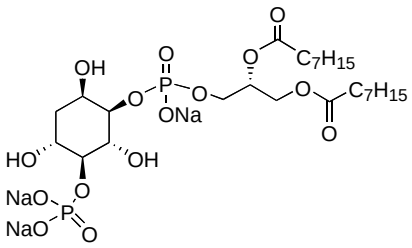

D-3-deoxy-diC_8PI (5) P

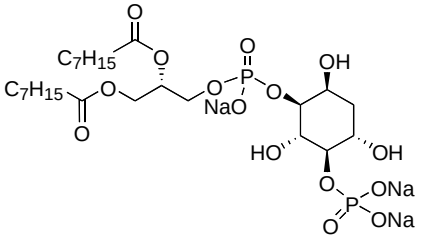

***ent*-D-3-deoxy-diC_8PI (5) P**
= L-3-deoxy-diC_8PI (5) P

different phosphatidylinositol-specific PLC enzymes – a Ca^{2+}-dependent mammalian PLCδ1 (this is a chimera of the –δ1 catalytic domain and the –β1 PH domain and was chosen because it has moderately high activity in vitro (Barnett et al., 1995)) and a Ca^{2+}-independent bacterial PLC. Mechanistically, PI cleavage occurs in a similar fashion in both types of enzymes except that an Arg replaces the active site Ca^{2+} in the bacterial enzyme (Bian and Roberts, 1992; Lewis et al., 1993). As seen in Table 6-1, removal of the hydroxyl group at C3 generated a very poor substrate for the PLCδ1 enzyme with PI cleavage occurring at 0.5 to 1% that of diC_8PI. However, in the context of a cell and over the time course of several days, these lipids are likely to be hydrolyzed by the endogenous PLC enzymes.

These compounds were also not very good inhibitors of this PLCδ1. The ratio of cIP to the final water-soluble product I-1-P reflects how well the intermediate is bound to the enzyme. A tighter binding cIP generated in situ translates to a lower ratio of cIP/I-1-P (Lowry et al., 1951, Shi et al., 2007). As hydroxyl groups are removed from the inositol ring, the intermediate cIP analogue becomes more hydrophobic and its release is slow compared to attack by water and production of I-1-P (Table 6-1). With D-3,5-dideoxy-diC_8PI, no cIP was observed suggesting that the enzyme must hold the cyclic intermediate sufficiently long that it is always hydrolyzed (but very slowly). Addition of a phosphate to C(5) to produce D-3-deoxy-diC_8PI(5)P did not generate a better substrate but it did bias the enzyme so that now cIP was the dominant product. This is an interesting contrast to how the enzyme hydrolyzed phosphorylated glycerol-

Table 6-1 Recombinant PLC-δ1 activity toward diC_8PI and deoxy-diC_8PI lipids

Substrate [a]	Inhibitor (mM) [b]	$\frac{cIP}{I-1-P}$	Specific Activity [c] ($\mu mol \cdot min^{-1} \cdot mg^{-1}$)	Relative Activity
D-diC_8PI		0.93	3.68	1.00
D-3-deoxy-diC_8PI		0.22	0.039	0.011
D-3,5-dideoxy-diC_8PI		0.00	0.018	0.005
D-3-deoxy- $diC_8PI(5)P$		3.01	0.022	0.006
D-diC_8PI	D-3-deoxy-diC_8PI (2)	1.99	3.01	0.82
D-diC_8PI	D-3-deoxy-diC_8PI5P (6)	1.29	4.81	1.31
D-diC_8PI	D-3,5-dideoxy-diC_8PI (2)	1.77	3.25	0.88
D-diC_8PI	D-3,5-dideoxy-diC_8PI (6)	0.99	3.93	1.07
D-diC_8PI	L-diC_8PI (2)	1.02	3.08	0.84

[a]Substrates present at 2 mM.

[b]The value in parentheses represents the concentration of inhibitor used in these assays.

[c]Errors in specific activity typically <20%.

phosphoinositols (Lowry et al., 1951), where a phosphorylated substrate was more efficiently hydrolyzed and I-1-P became the major product. It strongly indicates that the 3-hydroxy group of the inositol ring must make important hydrogen bond contacts with the enzyme that stabilize binding of PI analogues to the protein but not in an optimal configuration for PI cleavage.

Mammalian PLC enzymes have multiple domains that could complicate / mask effects of the deoxy-diC_8PI compounds. Therefore, for comparison we also examined the effect of these compounds on the PLC from *L. monocytogenes*. This bacterial PLC is essentially the catalytic domain of the mammalian enzymes and serves to assess the effects of the deoxy-PI compounds on catalysis only. The 3-deoxy-diC_8PI compounds were also poor substrates and poor inhibitors for *L. monocytogenes* PLC (Table 6-2). The specific activities toward D-3-deoxy-diC_8PI and D-3,5-dideoxy-diC_8PI were 1.3 and 0.037% that toward diC_8PI, respectively. Addition of 2 to 6 mM deoxy-PI compounds had only minor effects on the activity of *L. monocytogenes* PLC toward 2 mM D-diC_8PI. For all the deoxy-compounds, the decrease in specific activity was less than 10%, comparable to the effect of L-diC_8PI. As with the mammalian enzyme, removal of the 3-hydroxyl group generates a compound that binds very poorly to PLC and does not compete well with substrate.

B. Effect of 3-deoxy-diC_8PI molecules on PI3K activity

Removal of the 3-hydroxyl group from PI generates a molecule that should inhibit PI3K. Previous work (Meuillet et al., 2003) has suggested that the 3-deoxy-PI

Table 6-2 Recombinant *L. monocytogenes*. PI-PLC activity toward 1D-diC_8PI and deoxy-diC_8PI lipids.

Substrate [a]	Inhibitor (mM)	Specific Activity [b] (μmol min^{-1} mg^{-1})	Relative Activity
D-diC_8PI		489	1.00
D-3-deoxy-diC_8PI		6.44	0.013
D-3,5-dideoxy-diC_8PI		0.18	$3.7x10^{-4}$
D-diC_8PI	D-3-deoxy-diC_8PI (2)	522	1.07
D-diC_8PI	D-3-deoxy-diC_8PI(5)P (6)	452	0.92
D-diC_8PI	D-3,5-dideoxy-diC_8PI (2)	522	1.07
D-diC_8PI	D-3,5-dideoxy-diC_8PI (6)	539	1.10
D-diC_8PI	L-diC_8PI (2)	441	0.90

[a]Substrates present at 2 mM with the indicated concentration of inhibitor molecule.

[b]The value in parentheses represents the concentration of inhibitor used in these assays.

[c]Errors in specific activity were ≤15%.

species are not very potent inhibitors of PI3K, although this can be misleading if substrate and inhibitor have different chain lengths or solubilities. In an attempt to keep substrate and inhibitors in the same physical state we investigated the activity of the p110α/p85α complex towards 1 mM D-diC_8PI in the absence and presence of 1 or 3 mM 3-deoxy-diC_8PI analogs. Since PI3K prefers interfacial PI substrate (Wu et al., 1997), the concentrations of PIs were chosen so that substrate was micellar. As shown in Table 6-3, only 3-deoxy-diC_8PI inhibited the phosphorylation of diC_8PI; removing a second hydroxyl group (data not shown) or adding a phosphate to the 5-hydroxyl group reduced the potency of these compounds as inhibitors so that no inhibition was observed under these conditions. Interestingly, both 3-deoxy-diC_8PI enantiomers were equally effective at inhibiting PI3K. Assuming the 3-deoxy-diC_8PI compound is a competitive inhibitor of diC_8PI and the K_m<3 mM (likely given kinetics with longer chain substrates), the K_i/K_m is likely to be 0.5 for D-3-deoxy-diC_8PI and 0.6 for L-3-deoxy-diC_8PI. For comparison, we also examined the inhibitory effect of L-diC_8PI on p110α/p85α activity toward D-diC_8PI. The substrate enantiomer had no effect on D-diC_8PI phosphorylation. The replacement of the 3-hydroxyl of inositol ring of diC_8PI with hydrogen not only improved the binding of 3-deoxy-diC_8PI compounds to PI3K (compared to diC_8PI) but also eliminated the inositol ring stereoisomer selectivity for ligand binding. A phosphorylated 3-deoxy-diC_8PI (D-3-diC_8PI(5)P at 1 and 3 mM) was also examined for inhibition of diC_8PI phosphorylation by PI3K. Enzyme activity increased slightly with 1:1 substrate/inhibitor and decreased only 20% with an excess of D-3-diC_8PI(5)P. Adding

Table 6-3 Recombinant PI3K (P110α/ P85α) activity toward 1 mM diC_8PI and inhibition by deoxy-diC_8PI lipids.[a]

Inhibitor	(mM)	Specific Activity [b] ($\mu mol\ min^{-1}\ mg^{-1}$)	Relative Activity
–		0.60	1.00
D-3-deoxy-diC_8PI	3	0.09	0.15
D-3-deoxy-$diC_8PI(5)P$	1	0.66	1.10
	3	0.49	0.81
L-diC_8PI	3	0.60	1.00
L-3-deoxy-diC_8PI	3	0.11	0.18

[a]Assay conditions included 1 mM D-diC8PI and 2 mM ATP as substrates, 5 mM Mg^{2+}, in 50 mM Tris-HCl, pH 7.5, with 3 mM of the deoxy-PI analogs.

[b]For several of the samples run in duplicate, the error in determining the specific activity was <10%

a phosphate to the C5 of inositol did not improve the ability of this compound to interact with the enzyme, although this could also reflect the fact that the CMC for this phospholipid is notably higher than for the 3-deoxy-diC_8PI compounds. These in vitro assays suggest that the 3-deoxy-diC_8PI molecules are unlikely to have a significant effect on PI3K in vivo. They also suggest that if PI3K is involved, both D- and L-3-deoxy-diC_8PI should have similar effects.

Our results of PLC and PI3K suggested that removal of the 3-hydroxyl group generates a serious of compounds unlikely to have a significant effect on both PLC and PI3K in vivo. Under the assay conditions, these compounds were poor substrates and not inhibitors of the PLC. There was also little inhibition of PI3K observed except for 3-deoxy-diC_8PI enantiomers.

Chapter 7:

Future studies

The work in this thesis aimed to explore the kinetic profile of *L. monocytogenes* PI-PLC and its biological relevance. Compared to its *Bacillus* sp. PI-PLC counterpart, *L. monocytogenes* PI-PLC exhibits several different kinetic properties, including dependence of activity on enzyme concentration, lacking of surface dilution inhibition at high mole fraction of amphiphiles, and salt activation. Our results indicate those kinetic behaviors are tuned by the distinct binding abilities of this enzyme to anionic substrates versus zwitterionic or neutral amphiphiles. The binding assays used for *Bacillus* sp. PI-PLC (centrifugation, gel filtration, fluorescence, and NMR), however, are not sensitive enough to quantify surface binding of *L. monocytogenes* PI-PLC (binding either too loosely to zwitterionic or neutral amphiphiles or too tightly to anionic substrates). The protein/vesicle aggregation induced by *L. monocytogenes* PI-PLC in the presence of anionic lipids complicates the binding studies. Therefore, a good assay for quantitative surface binding of *L. monocytogenes* PI-PLC is needed to further understand these results. Fluorescence correlation spectroscopy (FCS) may be such a technique. In contrast to other fluorescence techniques, FCS monitors minute spontaneous intensity fluctuations for information rather than just the steady-state emission intensity. To obtain good signal-to-noise, researchers use femtoliter detection volume and nanomolar protein concentration (comparable to the amount used in kinetics for PI-PLC) for optimal FCS measurements. With a fluorophore attached to a region far away from the surface binding areas (it is easy to introduce a fluorophore at a specific position since there is no Cys for wild type *L. monocytogenes* PI-PLC), fluorescence cross-correlation spectroscopy (FCCS) may allow us a better handle on the protein/vesicles aggregation and what happens under

different conditions (vesicle composition, salt, enzyme mutants). By introducing a fluorophore at different regions of enzyme, FRET-FCS may also be helpful to probe the binding of these regions to the interface (non-productive binding).

Some of the interesting surface mutants we already have generated should also be checked for their effect on plaque formation when *L. monocytogenes* infects fibroblasts. Almost all the mutant proteins we generated have kinetic parameters more like the *B. thuringiensis* PI-PLC. For instance, the two surface Cys mutants, T50C and T236C, were extremely active in our in vitro assays. However, these enzymes show little kinetic sensitivity to decreasing protein concentration or increasing X_{det}. It would be particularly interesting to see how these affect L. monocytogenes infection. The enhanced catalytic activity might lead to enhanced infection. Alternatively, if the high activity if the wild type PI-PLC at very low concentrations is really critical, perhaps these mutant enzymes will be less infective.

The results obtained in this first round of mutagenesis suggest we should examine surface regions for other interesting changes in kinetics. In particular, the helix B moiety has other residues that may aid in surface binding of the PI-PLC. Thr-48 is certainly worth examining (either converting it to Cys or to Ala). In the same vein, we need to prepare T50A and T236A to see if the high activity is solely associated with the cysteine side chain. If it is, the question becomes what causes this change? Also the lone cationic residue in this structural unit, Lys-53, may be important in binding to anionic surfaces. It would be interesting to convert it to Ala or to reverse the charge to Glu to see how binding and enzyme kinetics are affected.

Once we have a better idea of how the enzyme binds to surfaces, we may have a better chance at developing selective inhibitors that could be used to reduce *L. monocytogenes* infections.

References

Alberti-Segui, C., Goeden, K.R., and Higgins, D.E. (2007) *Cell* 9, 179-195.

Alberts, B., Johnson, A., Lewis, J., Raff, M., Roberts, K., and Walter, P. (2002). Molecular Biology of the Cell. New York, Garland Science.

Ames, G.F. (1968) *J. Bacteriol.* 95, 833-843.

Andrade, M.A., Chacon, P., Merelo, J.J., and Moran, F. (1993) *Protein Eng.* 6, 383-390.

Andresen, T.L., Skytte, D.M., and Madsen, R. (2004) *Org. Biomol. Chem.* 2, 2951-2957.

Arechaga, I., Miroux, B., Runswick, M.J., and Walker, J.E. (2003) *FEBS Lett.* 547, 97-100.

Bae, Y.S., Cantley, L.G., Chen, C.S., Kim, S.R., Kwon, K.S., and Rhee, S.G. (1998) *J. Biol. Chem.* 273, 4465-4469.

Bagatolli, L.A., Parasassi, T., and Gratton, E. (2000) *Chem. Phys. Lipids* 105, 135-147.

Balsinde, J., Winstead, M.V., and Dennis, E.A. (2002) *FEBS Lett.* 531, 2-6.

Bangham, A.D., Standish, M.M., and Watkins, J.C. (1965) *J. Mol. Biol.* 13, 238-252.

Bannam, T., and Goldfine, H. (1999) *Infect. Immun.* 67, 182-186.

Barnett, S.F., Bilodeau, M.T., and Lindsley, C.W. (2005) *Curr. Top. Med. Chem.* 5, 109-125.

Barnett, S.F., Ledder, L.M., Stirdivant, S.M., Ahern, J., Conroy, R.R., and Heimbrook, D.C. (1995) *Biochemistry* 34, 14254-14262.

Batenburg, J.J. (1992) *Am. J. Physiol. Lung Cell Mol. Physiol.* 262, L367-385.

Becker, G.W., and Lester, R.L. (1980) *J. Bacteriol.* 142, 747-754.

Bennett, D.E., McCreary, C.E., and Coleman, D.C. (1998) *Microbiology* 144, 55-72.

Berg, O.G., and Jain, M.K. (2002). Interfacial Enzyme Kinetic, Wiley.

Berg, O.G., Rogers, J., Yu, B.Z., Yao, J., Romsted, L.S., and Jain, M.K. (1997) *Biochemistry* 36, 14512 -14530.

Berg, O.G., Yu, B.Z., Rogers, J., and Jain, M.K. (1991) *Biochemistry* 30, 7283-7297.

Berridge, M.J. (1993) *Nature* 361, 315-325.

Berridge, M.J., and Irvine, R.F. (1987) *Annu. Rev. Biochem.* 56, 159-193.

Berridge, M.J., and Irvine, R.F. (1989) *Nature* 341, 197-205.

Beyer, D., Elender, G., Knoll, W., Kühner, M., Maus, S., Ringsdorf, H., and Sackmann, E. (1996) *Angew. Chem. Int. Ed. Engl.* 35, 1682-1685.

Bian, J., and Roberts, M.F. (1992) *J. Colloid Interface Sci.* 153, 420-428.

Bielecki, J., Youngman, P., Connelly, P., and Portnoy, D.A. (1990) *Nature* 345, 175-176.

Bishop, D.K., and Hinrichs, D.J. (1987) *J. Immunol.* 139, 2005-2009.

Bishop, R.E., Gibbons, H.S., Guina, T., Trent, M.S., Miller, S.I., and Raetz, C.R. (2000) *EMBO J.* 19, 5071-5080.

Bogdanov, M., and Dowhan, W. (1999) *J. Biol. Chem.* 274, 36827-36830.

Bogdanov, M., Heacock, P.N., and Dowhan, W. (2002) *EMBO J.* 21, 2107-2116.

Bogdanov, M., Sun, J., Kaback, H.R., and Dowhan, W. (1996) *J. Biol. Chem.* 271, 11615-11618.

Böhm, G., Muhr, R., and Jaenicke, R. (1992) *Protein Eng.* 5, 191-195.

Braman, J., Papworth, C., and Greener, A. (1996) *Methods Mol. Biol.* 57, 31-44.
Braun, L., and Cossart, P. (2000) *Microbes Infect.* 2, 803-811.
Brazil, D.P., Yang, Z.Z., and Hemmings, B.A. (2004) *Trends Biochem. Sci.* 29, 233-242.
Brian, A.A., and McConnell, H.M. (1984) *Proc. Natl. Acad. Sci. U.S.A.* 81, 6159-6163.
Brunner, J., Skrabal, P., and Hauser, H. (1976) *Biochim. Biophys. Acta* 455, 322-331.
Bruzik, K.S., Hakeem, A.A., and Tsai, M.D. (1994) *Biochemistry* 33, 8367-8374.
Bruzik, K.S., Morocho, A.M., Jhon, D.Y., Rhee, S.G., and Tsai, M.D. (1992) *Biochemistry* 31, 5183-5193.
Bruzik, K.S., and Tsai, M.D. (1994) *Bioorg. Med. Chem.* 2, 49-72.
Byun, H.M., Kang, S.G., and Kang, H.M. (2002) *Mol. Cells* 14, 16-23.
Callegan, M.C., Cochran, D.C., Kane, S.T., Gilmore, M.S., Gominet, M., and Lereclus, D. (2002) *Infect. Immun.* 70, 5381-5389.
Callis, P.R. (1997) *Meth. Enzymol.* 278, 113-150.
Cameron, L.A., Giardini, P.A., Soo, F.S., and Theriot, J.A. (2000) *Nat. Rev. Mol. Cell Biol.* 1, 110-119.
Camilli, A., Tilney, L.G., and Portnoy, D.A. (1993) *Mol. Microbiol.* 8, 143-157.
Carman, G.M., Deems, R.A., and Dennis, E.A. (1995) *J. Biol. Chem.* 270, 18711-18714.
Carrière, F., Thirstrup, K., Hjorth, S., Ferrato, F., Nielsen, P.F., Withers-Martinez, C., Cambillau, C., Boel, E., Thim, L., and Verger, R. (1997) *Biochemistry* 36, 239-248.
Cevc, G., and Marsh, D. (1987). Phospholipid Bilayers - Physical Principles and Models, John Wiley & Sons.
Chandler, D. (2005) *Nature* 437, 640-647.
Chang, J.S., Seok, H., Kwon, T.K., Min, D.S., Ahn, B.H., Lee, Y.H., Suh, J.W., Kim, J.W., Iwashita, S., Omori, A., et al. (2002) *J. Biol. Chem.* 277, 19697-19702.
Cho, W., Bittova, L., and Stahelin, R.V. (2001a) *Anal. Biochem.* 296, 153-161.
Chong, S., Shao, Y., Paulus, H., Benner, J., Perler, F.B., and Xu, M.-Q. (1996) *J. Biol. Chem.* 271, 22159-22168.
Chong, S., Williams, K.S., Wotkowicz, C., and Xu, M.-Q. (1998) *J. Biol. Chem.* 273, 10567-10577.
Clapham, D.E. (2003) *Nature* 426, 517-524.
Cockcroft, S., and De Matteis, M.A. (2001) *J. Membr. Biol.* 180, 187-194.
Cossart, P. (2001) *Trends Microbiol.* 9, 105-107.
Cronan, J.E., Jr., and Vagelos, P.R. (1972) *Biochim. Biophys. Acta* 265, 25-60.
Cullis, P.R., and de Kruijff, B. (1979) *Biochim. Biophys. Acta* 559, 399-420.
Daugherty, S., and Low, M.G. (1993) *Infect. Immun.* 61, 5078-5089.
Davis, G.D., Elisee, C., Newham, D.M., and Harrison, R.G. (1999) *Biotechnol. Bioeng.* 65, 382-388.
Davletov, B.A., and Südhof, T.C. (1993) *J. Biol. Chem.* 268, 26386-26390.
Dennis, E.A. (1973) *Arch. Biochem. Biophys.* 158, 485-493.
Derewenda, U., Brzozowski, A.M., Lawson, D.M., and Derewenda, Z.S. (1992) *Biochemistry* 31, 1532-1541.
Dowhan, W., Mileykovskaya, E., and Bogdanov, M. (2004) *Biochim. Biophys. Acta* 1666, 19-39.

Duncan, R.S., Hwang, S.Y., and Koulen, P. (2007) *Int. J. Biochem. Cell Biol.* 39, 1852-1862.
Eftink, M.R. (1991) *Methods Biochem. Anal.* 35, 127-205.
Essen, L.O., Perisic, O., Cheung, R., Katan, M., and Williams, R.L. (1996) *Nature* 380, 595-602.
Essen, L.O., Perisic, O., Lynch, D.E., Katan, M., and Williams, R.L. (1997) *Biochemistry* 36, 2753-2762.
Exton, J.H. (1994) *Biochim. Biophys. Acta* 1212, 26-42.
Falasca, M., Logan, S.K., Lehto, V.P., Baccante, G., Lemmon, M.A., and Schlessinger, J. (1998) *EMBO J.* 17, 414-422.
Fankhauser, C., Homans, S.W., Thomas-Oates, J.E., McConville, M.J., Desponds, C., Conzelmann, A., and Ferguson, M.A. (1993) *J. Biol. Chem.* 268, 26365-26374.
Feng, J., Hania, W., and Roberts, M.F. (2002) *J. Biol. Chem.* 277, 19867-19875.
Ferguson, K.M., Lemmon, M.A., Sigler, P.B., and Schlessinger, J. (1995) *Nat. Struct. Biol.* 2, 715-718.
Flick, J.S., and Thorner, J. (1993) *Mol. Cell. Biol.* 13, 5861-5876.
Folta-Stogniew, E., and Williams, K.R. (1999) *J. Biomol. Tech.* 10, 51-63.
Garcia, P., Gupta, R., Shan, S., Morris, A.J., Rudge, S.A., Scarlata, S., Petrova, V., Mclaughlin, S., and Rebecchi, M.J. (1995) *Biochemistry* 34, 16228-16234.
Garigapati, V.R., and Roberts, M.F. (1993) *Tetrahedron Lett.* 34, 769-772.
Gässler, C.S., Ryan, M., Liu, T., Griffith, O.H., and Heinz, D.W. (1997) *Biochemistry* 36, 12802-12813.
Gelb, M.H., Min, J.H., and Jain, M.K. (2000) *Biochim. Biophys. Acta* 1488, 20-27.
Gennis, R.B. (1989). Biomembranes: Molecular Structure and Function, Springer-Verlag.
Georgiou, G., and Valax, P. (1996) *Curr. Opin. Biotechnol.* 7, 190-197.
Ghannoum, M.A. (2000) *Clin. Microbiol. Rev.* 13, 122-143.
Ghosh, P.M., Malik, S., Bedolla, R., and Kreisberg, J.I. (2003) *Curr. Drug Metab.* 4, 487-496.
Gills, J.J., and Dennis, P.A. (2004) *Expert Opin. Investig. Drugs* 13, 787-797.
Gliozzi, A., Relini, A., and Chong, P.-G. (2002) *J. Memb. Sci.* 206, 131-147.
Goldfine (1984) *J. Lipid Res.* 25, 1501-1507.
Goldfine, H., and Knob, C. (1992) *Infect. Immun.* 60, 4059-4067.
Goldfine, H., Knob, C., Alford, D., and Bentz, J. (1995) *Proc. Natl. Acad. Sci. U.S.A.* 92, 2979-2983.
Goldfine, H., and Wadsworth, S.J. (2002) *Microbes Infect.* 4, 1335-1343.
Goldfine, H., Wadsworth, S.J., and Johnston, N.C. (2000) *Infect. Immun.* 68, 5735-5741.
Görg, A. (1998). "Two-Dimensional Electrophoresis with Immobilized pH Gradients for Proteome Analysis." from http://www.weihenstephan.de/blm/deg/2D-Manual.pdf.
Görg, A., Postel, W., and Günther, S. (1988) *Electrophoresis* 9, 531-546.
Griffith, O.H., and Ryan, M. (1999) *Biochim. Biophys. Acta* 1441, 237-254.
Griner, E.M., and Kazanietz, M.G. (2007) *Nat. Rev. Cancer* 7, 281-294.
Grobler, J.A., and Hurley, J.H. (1998) *Biochemistry* 37, 5020-5028.
Guther, M.L., de Almeida, M.L., Rosenberry, T.L., and Ferguson, M.A. (1994) *Anal. Biochem.* 219, 249-255.

Hanada, M., Feng, J., and Hemmings, B.A. (2004) *Biochim. Biophys. Acta* 1697, 3-16.
Hannig, G., and Makrides, S.C. (1998) *Trends Biotechnol.* 16, 54-60.
Harrison, R.G. (2000) *inNovations* 11, 4-7.
Hatfield, D., and Diamond, A. (1993) *Trends Genet.* 9, 69-70.
Hauser, H., and Gains, N. (1982) *Proc. Natl. Acad. Sci. U.S.A.* 79, 1683-1687.
Heinz, D.W., Essen, L.O., and Williams, R.L. (1998) *J. Mol. Biol.* 275, 635-650.
Heinz, D.W., Ryan, M., Smith, M.P., Weaver, L.H., Keana, J.F., and Griffith, O.H. (1995) *Biochemistry* 35, 3855-3863.
Heinz, D.W., Ryan, M., Smith, M.P., Weaver, L.H., Keana, J.F., and Griffith, O.H. (1996) *Biochemistry* 35, 9496-9504.
Hendrickson, H.S., Hendrickson, E.K., Johnson, J.L., Khan, T.H., and Chial, H.J. (1992) *Biochemistry* 31, 12169-12172.
Higgins, D.E., Shastri, N., and Portnoy, D.A. (1999) *Mol. Microbiol.* 31, 1631-1641.
Horváth, C., Melander, W., and Molnár, I. (1976) *J. Chromatogr. A* 125, 129-156.
Hwang, J.I., Oh, Y.S., Shin, K.J., Kim, H., Ryu, S.H., and Suh, P.G. (2005) *Biochem. J.* 389, 181-186.
Ichimura, Y., Kirisako, T., Takao, T., Satomi, Y., Shimonishi, Y., Ishihara, N., Mizushima, N., Tanida, I., Kominami, E., Ohsumi, M., et al. (2000) *Nature* 408, 488-492.
Ikezawa, H. (2004) *J. Toxicol. Toxin. Rev.* 23, 479-508.
Ikezawa, H., Yamanegi, M., Taguchi, R., Miyashita, T., and Ohyabu, T. (1976) *Biochim. Biophys. Acta* 450, 154-164.
Ilkaeva, O., Kinch, L.N., Paulssen, R.H., and Ross, E.M. (2002) *J. Biol. Chem.* 277, 4294-4300.
Irino, Y., Cho, H., Nakamura, Y., Nakahara, M., M., F., Suh, P.G., Takenawa, T., and Fukami, K. (2004) *Biochem. Biophys. Res. Commun.* 320, 537-543.
Irvine, R.F. (2003) *Nat. Rev. Mol. Cell Biol.* 4, 349-360.
Israelachvili, J.N., Marcelja, S., and Horn, R.G. (1980) *Q. Rev. Biophys.* 13, 121-200.
Jacquet, A., Daminet, V., Haumount, M., Garcia, L., Chaudoir, S., Bollen, A., and Biemans, R. (1999) *Protein Expr. Purif.* 17, 392-400.
Jain, M.K. (1988). Introduction to Biological Membranes, John Wiley & Sons Inc.
Jain, M.K., and Berg, O.G. (1989) *Biochim. Biophys. Acta* 1002, 127-156.
Jain, M.K., and Berg, O.G. (2006) *Curr. Opin. Chem. Biol.* 10, 473-479.
Jang, I.H., Lee, S., Park, J.B., Kim, J.H., Lee, C.S., Hur, E.M., Kim, I.S., Kim, K.T., Yagisawa, H., Suh, P.G., et al. (2003) *J. Biol. Chem.* 278, 18184-18190.
Jenkins, G.M., and Frohman, M.A. (2005) *Cell. Mol. Life Sci.* 62, 2305-2316.
Johnson, S.M., Bangham, A.D., Hill, M.W., and Korn, E.D. (1971) *Biochim. Biophys. Acta* 233, 820-826.
Jones, M.N., and Chapman, D. (1995). Micelles, monolayers and biomembranes, Wiley-Liss.
Kalb, E., Frey, S., and Tamm, L.K. (1992) *Biochim. Biophys. Acta* 1103, 307-316.
Kandel, E.S., and Hay, N. (1999) *Exp. Cell Res.* 253, 210-229.
Kane, J.F. (1995) *Curr. Opin. Biotechnol.* 6, 494-500.
Kapust, R.B., and Waugh, D.S. (1999) *Protein Sci.* 8, 1668-1674.

Katan, M. (2005) *Biochem. J.* 391, e7-e9.
Keller, R.C., Silvius, J.R., and De Kruijff, B. (1995) *Biochem. Biophys. Res. Commun.* 207, 508-514.
Kelley, G.G., Reks, S.E., Ondrako, J.M., and Smrcka, A.V. (2001) *EMBO J.* 20, 743-754.
Kemp, P., Hubscher, G., and Hawthorne, J.N. (1959) *Biochim. Biophys. Acta* 31, 585-586.
Kim, C.G., Park, D., and Rhee, S.G. (1996) *J. Biol. Chem.* 271, 21187-21192.
Klichko, V.I., Miller, J., Wu, A., Popov, S.G., and Alibek, K. (2003) *Biochem. Biophys. Res. Commun.* 303, 855-862.
Koke, J.A., Yang, M., Henner, D.J., Volwerk, J.J., and Griffith, O.H. (1991) *Protein Expr. Purif.* 2, 51-58.
Kominami, T., Miki, A., and Ikehara, Y. (1985) *Biochem. J.* 227, 183-189.
Kouchi, Z., Shikano, T., Nakamura, Y., Shirakawa, H., Fukami, K., and Miyazaki, S. (2005) *J. Biol. Chem.* 280, 21015-21021.
Kozikowski, A.P., Kiddle, J.J., Frew, T., Berggren, M., and Powis, G. (1995) *J. Med. Chem.* 38, 1053-1056.
Kozikowski, A.P., Sun, H., Brognard, J., and Dennis, P.A. (2003) *J. Am. Chem. Soc.* 125, 1144-1145.
Kozloff, L.M., Turner, M.A., Arellano, F., and Lute, M. (1991) *J. Bacteriol.* 173, 2053-2060.
Kubiak, R.J., Yue, X., Hondal, R.J., Mihai, C., Tsai, M.D., and Bruzik, K.S. (2001) *Biochemistry* 40, 5422-5432.
Kuhner, M., Tampe, R., and Sackmann, E. (1994) *Biophys. J.* 67, 217-226.
Larijani, B., and Dufourc, E.J. (2006) *Lipids* 41, 925-932.
Lechevalier, M.P. (1977) *CRC Crit. Rev. Microbiol.* 5, 109-210.
Leigh, A.J., Volwerk, J.J., Griffith, O.H., and Keana, J.F. (1992) *Biochemistry* 31, 8978-8983.
Leimeister-Wächter, M., Domann, E., and Chakraborty, T. (1991) *Mol. Microbiol.* 5, 361-366.
Leimeister-Wächter, M., Domann, E., and Chakraborty, T. (1992) *J. Bacteriol.* 174, 947-952.
Lennartz, M.R. (1999) *The international journal of biochemistry & cell biology* 31, 415-430.
Lester, R.L., and Dickson, R.C. (1993) *Adv. Lipid Res.* 26, 253-274.
Lewis, K.A., Garigapati, V.R., Zhou, C., and Roberts, M.F. (1993) *Biochemistry* 32, 8836-8841.
Lichtenberg, D., Robson, R.J., and Dennis, E.A. (1983) *Biochim. Biophys. Acta* 737, 285-304.
Lin, G.L., Bennett, C.F., and Tsai, M.D. (1990) *Biochemistry* 29, 2747-2757.
Lin, T.L., Chen, S.H., Gabriel, N.E., and Roberts, M.F. (1986) *J. Am. Chem. Soc.* 108, 3499-3507.
Lomasney, J.W., Cheng, H.F., Roffler, S.R., and King, K. (1999) *J. Biol. Chem.* 274, 21995-22001.
Lomasney, J.W., Cheng, H.F., Wang, L.P., Kuan, Y., Liu, S., Fesik, S.W., and King, K. (1996) *J. Biol. Chem.* 271, 25316-25326.

Lopez, I., Mak, E.C., Ding, J., Hamm, H.E., and Lomasney, J.W. (2001) *J. Biol. Chem.* 276, 2758-2765.
Low, M.G. (1981) *Meth. Enzymol.* 71, 741-746.
Low, M.G., and Finean, J.B. (1977) *Biochem. J.* 162, 235-240.
Low, M.G., Stiernberg, J., Waneck, G.L., Flavell, R.A., and Kincade, P.W. (1988) *J. Immunol. Methods* 113, 101-111.
Lowry, O.H., Rosebrough, N.J., Farr, A.L., and Randall, R.J. (1951) *J. Biol. Chem.* 193, 265-275.
Martin, T.F. (2001) *Curr. Opin. Cell Biol.* 13, 493-499.
Martinez, A., Knappskog, P.M., Olafsdottir, S., Doskeland, A.P., Eiken, H.G., Svebak, R.M., Bozzini, M., Apold, J., and Flatmark, T. (1995) *Biochem. J.* 306, 589-597.
Massimelli, M.J., Beassoni, P.R., Forrellad, M.A., Barra, J.L., Garrido, M.N., Domenech, C.E., and Lisa, A.T. (2005) *Curr. Microbiol.* 50, 251-256.
Mayer, L.D., Hope, M.J., and Cullis, P.R. (1986) *Biochim. Biophys. Acta* 858, 161-168.
Medkova, M., and Cho, W. (1998) *Biochemistry* 37, 4892-4900.
Mengaud, J., Braun-Breton, C., and Cossart, P. (1991) *Mol. Microbiol.* 5, 367-372.
Mengaud, J., Dramsi, S., Gouin, E., vazquez-Boland, J.A., Milon, G., and Cossart, P. (1991) *Mol. Microbiol.* 5, 2273-2283.
Mengaud, J., Vicente, M.F., and Cossart, P. (1989) *Infect. Immun.* 57, 3695-3701.
Menger, F.M., and Keiper, J.S. (1998) *Curr. Opin. Chem. Biol.* 2, 726-732.
Menon, A.K., and Stevens, V.L. (1992) *J. Biol. Chem.* 267, 15277-15280.
Meuillet, E.J., Mahadevan, D., Vankayalapati, H., Berggren, M., Williams, R., Coon, A., Kozikowski, A.P., and Powis, G. (2003) *Mol. Cancer Ther.* 2, 389-399.
Michell, R.H. (1975) *Biochim. Biophys. Acta* 415, 81-147.
Middelberg, A. (2002) *Trends Biotechnol.* 20, 437-443.
Moser, J., Gerstel, B., Meyer, J.E., Chakraborty, T., Wehland, J., and Heinz, D.W. (1997) *J. Mol. Biol.* 273, 269-282.
Murray, E.G.D., Webb, R.E., and Swann, M.B.R. (1926) *J. Pathol. Bacteriol.* 29, 407-439.
Nakahara, M., Shimozawa, M., Nakamura, Y., Irino, Y., Morita, M., Kiudo, Y., and Fukami, K. (2005) *J. Biol. Chem.* 280, 29128-29134.
Nayar, R., Hope, M.J., and Cullis, P.R. (1989) *Biochim. Biophys. Acta* 986, 200-206.
Nelson, M., and McClelland, M. (1992) *Meth. Enzymol.* 216, 279-303.
Nielsen, H., Engelbrecht, J., Brunak, S., and von Heijine, G. (1997a) *Protein Eng.* 10, 1-6.
Nielsen, H., Engelbrecht, J., Brunak, S., and Von Heijine, G. (1997b) *Int. J. Neural. Syst.* 8, 581-599.
Nishizuka, Y. (1992) *Science* 258, 607-614.
Norman, K.E., and Nymeyer, H. (2006) *Biophys. J.* 91, 2046-2054.
Nozaki, T., Toh-e, A., Fujii, M., Yagisawa, H., M., N., and T., T. (1999) *Mol. Biochem. Parasitol.* 102, 283-295.
Ohyabu, T., Taguchi, R., and Ikezawa, H. (1978) *Arch. Biochem. Biophys.* 190, 1-7.
Olson, F., Hunt, C.A., Szoka, F.C., Vail, W.J., and Papahadjopoulos, D. (1979) *Biochim. Biophys. Acta* 557, 9-23.
Palmer, M. (2001) *Toxicon* 39, 1681-1689.

Pamer, E.G. (2004) *Nat. Rev. Immunol.* 4, 812-823.
Pan, Y.Y., Wang, X., Ma, L.G., and Sun, D.Y. (2005) *Plant Cell Physiol.* 46, 1657-1665.
Paoli, G.C., Bhunia, A., and Bayles, D.O. (2005). Foodborne Pathogens: Microbiology and Molecular Biology, Caister Academic Press.
Perler, F.B., Davis, E.O., Dean, G.E., Gimble, F.S., Jack, W.E., Neff, N., Noren, C.J., Thorner, J., and Belfort, M. (1994) *Nucleic Acids Res.* 22, 1125-1127.
Perlman, D., and Halvorson, H.O. (1983) *J. Mol. Biol.* 167, 391-409.
Portnoy, D.A., Auerbuch, V., and Glomski, I. (2002) *J. Cell Biol.* 158, 409-414.
Portnoy, D.A., Jacks, P.S., and Hinrichs, D.J. (1988) *J. Exp. Med.* 167, 1459-1471.
Pu, M.M., Fang, X.M., Redfield, A.G., Gershenson, A., and Roberts, M.F. (2008a) submitted.
Pu, M.M., Roberts, M.F., and Gershenson, A. (2008b) in preparation.
Qiao, L., Nan, F., Kunkel, M., Gallegos, A., Powis, G., and Kozikowski, A.P. (1998) *J. Med. Chem.* 41, 3303-3306.
Ravoo, B.J., Weringa, W.D., and Engberts, J.B.F.N. (1999) *Biophys. J.* 76, 374-386.
Raynaud, C., and Charbit, A. (2005) *Microbiology* 151, 3769-3776.
Read, T.D., Peterson, S.N., Tourasse, N., Baillie, L.W., Paulsen, I.T., Nelson, K.E., Tettelin, H., Fouts, D.E., Eisen, J.A., Gill, S.R., et al. (2003) *Nature* 423, 81-86.
Rebecchi, M.J., and Pentyala, S.N. (2000) *Physiol. Rev.* 80, 1291-1335.
Rebecchi, M.J., and Scarlata, S. (1998) *Annu. Rev. Biophys. Biomol. Struct.* 27, 503-528.
Redfern, D.A., and Gericke, A. (2004) *Biophys. J.* 86, 2980-2992.
Repp, H., Pamukci, Z., Koschinski, A., Domann, E., Darji, A., Birringer, J., Brockmeier, D., Chakraborty, T., and Dreyer, F. (2002) *Cell. Microbiol.* 4, 483-491.
Rhee, S.G., and Bae, Y.S. (1997) *J. Biol. Chem.* 272, 15045-15048.
Roberts, M.F. (1991) *Meth. Enzymol.* 197, 95-112.
Rodriguez, A.V., Baigori, M.D., Alvarez, S., Castro, G.R., and Oliver, G. (2001) *FEMS Microbiol. Lett.* 204, 33-38.
Rosenberg, A.H., Lade, B.N., Chui, D.S., Lin, S.W., Dunn, J.J., and Studier, F.W. (1987) *Gene* 56, 125-135.
Ross, E.M., and Wilkie, T.M. (2000) *Annu. Rev. Biochem.* 69, 795-827.
Ryan, M., Liu, T., Dahlquist, F.W., and Griffith, O.H. (2001) *Biochemistry* 40, 9743-9750.
Ryan, M., Zaikova, T.O., Keana, J.F., Goldfine, H., and Griffith, O.H. (2002) *Biophys. Chem.* 101-102, 347-358.
Sackmann, E. (1996) *Science* 271, 43-48.
Saunders, C.M., Larman, M.G., Parrington, J., Cox, L.J., Royse, J., Blayney, L.M., Swann, K., and Lai, F.A. (2002) *Development* 129, 3533-3544.
Seufferlein, T. (2002) *Int. J. Gastrointest. Cancer* 31, 15-21.
Shao, C., Shi, X., Wehbi, H., Zambonelli, C., Head, J.F., Seaton, B.A., and Roberts, M.F. (2007) *J. Biol. Chem.* 282, 9228-9235.
Sharp, P.M., and Bulmer, M. (1988) *Gene* 63, 141-145.
Shashidhar, M.S., Volwerk, J.J., Keana, J.F., and Griffith, O.H. (1990) *Biochim. Biophys. Acta* 1042, 410-412.

Shi, X., Shao, C., Zhang, X., Zambonelli, C., Redfield, A.G., Head, J.F., Seaton, B.A., and Roberts, M.F. (2007) *J. Biol. Chem.* in press.
Shoemaker, S.D., and Vanderlick, T.K. (2002) *Biophys. J.* 83, 2007-2014.
Sibelius, U., Chakraborty, T., Krögel, B., Wolf, J., Rose, F., Schmidt, R., Wehland, J., Seeger, W., and Grimminger, F. (1996b) *J. Immunol.* 157, 4055-4060.
Sibelius, U., Rose, F., Chakraborty, T., Darji, A., Wehland, J., Weiss, S., Seeger, W., and Grimminger, F. (1996a) *Infect. Immun.* 64, 674-676.
Sibelius, U., Schulz, E.C., Rose, F., Hattar, K., Jacobs, T., Weiss, S., Chakraborty, T., Seeger, W., and Grimminger, F. (1999) *Infect. Immun.* 67, 1125-1130.
Singer, A.U., Waldo, G.L., Harden, T.K., and Sondek, J. (2002) *Nat. Struct. Biol.* 9, 32-36.
Singer, S.J., and Nicolson, G.L. (1972) *Science* 175, 720-731.
Smith, G.A., Marquis, H., Jones, S., Johnston, N.C., Portnoy, D.A., and Goldfine, H. (1995) *Infect. Immun.* 63, 4231-4237.
Song, C., Hu, C.D., Masago, M., Kariyai, K., Yamawaki-Kataoka, Y., Shibatohge, M., Wu, D., Satoh, T., and Kataoka, T. (2001) *J. Biol. Chem.* 276, 2752-2757.
Songer, J.G. (1997) *Trends Microbiol.* 5, 156-161.
Sørensen, H.P., and Mortensen, K.K. (2005) *J. Biotechnol.* 115, 113-128.
Stahelin, R.V., and Cho, W. (2001) *Biochem. J.* 359, 679-685.
Stevens, R.C. (2000) *Structure* 8, R177-R185.
Stewart, A.J., Mukherjee, J., Roberts, S.L., Lester, D., and Farquharson, C. (2005) *Int. J. Mol. Med.* 15, 117-121.
Stieglitz, K., Seaton, B., and Roberts, M.F. (1999) *J. Biol. Chem.* 274, 35367-35374.
Stieglitz, K.A., Seaton, B.A., and Roberts, M.F. (2001) *Biochemistry* 40, 13954-13963.
Stossel, T.P., J., C., Cooley, L., Hartwig, J.H., Noegel, A., Schleicher, M., Shapiro, S.S., Stossel, T.P., Condeelis, J., Cooley, L., et al. (2001) *Nat. Rev. Mol. Cell Biol.* 2, 138-145.
Studier, F.W., and Moffatt, B.A. (1986) *J. Mol. Biol.* 189, 113-130.
Studier, F.W., Rosenberg, A.H., Dunn, J.J., and Dubendorff, J.W. (1990) *Meth. Enzymol.* 185, 60-89.
Suh, P.G., Hwang, J.I., Ryu, S.H., Donowitz, M., and Kim, J.H. (2001) *Biochem. Biophys. Res. Commun.* 288, 1-7.
Sun, A.N., Camilli, A., and Portnoy, D.A. (1990) *Infect. Immun.* 58, 3770-3778.
Szoka, F.J., and Papahadjopoulos, D. (1980) *Annu. Rev. Biophys. Bioeng.* 9, 467-508.
Szweda, P., Pladzyk, R., Kotlowski, R., and Kur, J. (2001) *Protein Expr. Purif.* 22, 467-471.
Tabellini, G., Tazzari, P.L., Bortul, R., Billi, A.M., Conte, R., Manzoli, L., Cocco, L., and Martelli, A.M. (2004) *Br. J. Haematol.* 126, 574-582.
Taguehi, R., Asahi, Y., and Ikezawa, H. (1980) *Biochim. Biophys. Acta* 619, 48-57.
Uhumwangho, M.U., and Okor, R.S. (2005) *J. Med. Bio. Res.* 4, 9-21.
Uji, A., Matsuda, M., Maeda, K., Kanematsu, T., and Hirata, M. (2002) *Life Sci.* 72, 443-453.
van Erpecum, K.J., Petruzzelli, M., Groen, A.K., and Moschetta , A. (2007) *Eur. J. Lipid Sci. Technol.* 109, 982-986.

van Klompenburg, W., Nilsson, I., von Heijne, G., and de Kruijff, B. (1997) *EMBO J.* 16, 4261-4266.
Vazquez-Boland, J.A., Kuhn, M., Berche, P., Chakraborty, T., Dominguez-Bernal, G., Goebel, W., Gonzalez-Zorn, B., Wehland, J., and Kreft, J. (2001) *Clin. Microbiol. Rev.* 14, 584-640.
Verger, R., Mieras, M.C.E., and De Haas, G.H. (1973) *J. Biol. Chem.* 248, 4023-4034.
Verger, R., and Pattus, F. (1982) *Chem. Phys. Lipids* 30, 189-227.
Verheij, H.M., Slotboom, A.J., and de Haas, G.H. (1981) *Rev. Physiol. Biochem. Pharmacol.* 91, 91-203.
Vivanco, I., and Sawyers, C.L. (2002) *Nat. Rev. Cancer* 2, 489-501.
Volwerk, J.J., Filthuth, E., Griffith, O.H., and Jain, M.K. (1994) *Biochemistry* 33, 3464-3474.
Volwerk, J.J., Koke, J.A., Wetherwax, P.B., and Griffith, O.H. (1989) *FEMS Microbiol. Lett.* 52, 237-241.
Volwerk, J.J., Shashidhar, M.S., Kuppe, A., and Griffith, O.H. (1990) *Biochemistry* 29, 8056-8062.
von Heijine, G. (1983) *Eur. J. Biochem.* 133, 17-21.
von Heijine, G. (1985) *J. Mol. Biol.* 184, 99-105.
von Heijine, G., and Abrahmsen, L. (1989) *FEBS Lett.* 244, 439-446.
Wadsworth, S.J., and Goldfine, H. (1999) *Infect. Immun.* 67, 1770-1778.
Wadsworth, S.J., and Goldfine, H. (2002) *Infect. Immun.* 70, 4650-4660.
Waldo, G.S., Standish, B.M., Berendzen, J., and Terwilliger, T.C. (1999) *Nat. Biotechnol.* 17, 691-695.
Wallace, B.A., and Janes, R.W. (1999) *Adv. Exp. Med. Biol.* 467, 789-799.
Wang, A., and Dennis, E.A. (1999) *Biochim. Biophys. Acta* 1439, 1-16.
Wang, T., Pentyala, S., Elliott, J.T., Dowal, L., Gupta, E., Rebecchi, M.J., and Scarlata, S. (1999) *Proc. Natl. Acad. Sci. U.S.A.* 96, 7843-7846.
Wang, T., Pentyala, S., Rebecchi, M.J., and Scarlata, S. (1999) *Biochemistry* 38, 1517-1524.
Wang, X. (2001) *Annu. Rev. Plant Physiol. Plant Mol. Biol.* 52, 211-231.
Wang, X., Devaiah, S.P., Zhang, W., and Welti, R. (2006) *Prog. Lipid Res.* 45, 250-278.
Wang, Z.X. (1999) *Eur. J. Biochem.* 259, 609-617.
Waterhous, D.V., and Johnson, W.C. (1994) *Biochemistry* 33, 2121-2128.
Weerninka, P.A.O., Hana, L., Jakobsa, K.H., and Schmidtb, M. (2007) *Biochim. Biophys. Acta* 1768, 888-900.
Wehbi, H., Feng, J., Kolbeck, J., Ananthanarayanan, B., Cho, W., and Roberts, M.F. (2003b) *Biochemistry* 42, 9374-9382.
Wehbi, H., Feng, J., and Roberts, M.F. (2003a) *Biochim. Biophys. Acta* 1613, 15-27.
Wei, Z., Zenewicz, L.A., and Goldfine, H. (2005) *Proc. Natl. Acad. Sci. U.S.A.* 102, 12927-12931.
Wenzl, P., Fringeli, M., Goette, J., and Fringeli, U.P. (1994) *Langmuir* 10, 4253-4264.
White, S.H. (2003) *FEBS Lett.* 555, 116-121.
White, S.H., and Wimley, W.C. (1999) *Annu. Rev. Biophys. Biomol. Struct.* 28, 319-365.
Wilkinson, D.L., and Harrison, R.G. (1991) *Biotechnology (N. Y.)* 9, 443-448.

Wimley, W.C., Creamer, T.P., and White, S.H. (1996) *Biochemistry* 35, 5109 -5124.
Wimley, W.C., and White, S.H. (1996) *Nat. Struct. Biol.* 3, 842-848.
Wing, M.R., Bourdon, D.M., and Harden, T.K. (2003) *Mol. Interv.* 3, 273-280.
Wirth, R., An, F.Y., and Clewell, D.B. (1986) *J. Bacteriol.* 165, 831-836.
Wu, Y., Perisic, O., Williams, R.L., Katan, M., and Roberts, M.F. (1997) *Biochemistry* 36, 11223-11233.
Wyatt, P.J. (1993) *Anal. Chim. Acta* 272, 1-40.
Xu, M.-Q., and Perler, F.B. (1996) *EMBO J.* 15, 5146-5153.
Xu, M.-Q., Southworth, M.W., Mersha, F.B., Hornstra, L.J., and Perler, F.B. (1993) *Cell* 75, 1371-1377.
Ye, K., Aghdasi, B., Luo, H.R., Moriarity, J.L., Wu, F.Y., Hong, J.J., Hurt, K.J., Bae, S.S., Suh, P.G., and Snyder, S.H. (2002) *Nature* 415, 541-544.
Zenewicz, L.A., Wei, Z., Goldfine, H., and Shen, H. (2005) *J. Immunol.* 174, 8011-8016.
Zhang, W., Bogdanov, M., Pi, J., Pittard, A.J., and Dowhan, W. (2003) *J. Biol. Chem.* 278, 50128-50135.
Zhang, W., Campbell, H.A., Kingll, S.C., and Dowhan, W. (2005) *J. Biol. Chem.* 280, 26032-26038.
Zhang, W., and Neer, E.J. (2001) *J. Biol. Chem.* 276, 2503-2508.
Zhou, C., Qian, X., and Roberts, M.F. (1997b) *Biochemistry* 36, 10089-10097.
Zhou, C., and Roberts, M.F. (1998) *Biochemistry* 37, 16430-16439.
Zhou, C., Wu, Y., and Roberts, M.F. (1997a) *Biochemistry* 36, 347-355.
Zhou, J.S., Shu, Q., Rutherfurd, K.J., Prasad, J., Birtles, M.J., Gopal, P.K., and Gill, H.S. (2000) *Int. J. Food Microbiol.* 56, 87-96.
Zhou, Y., Wing, M.R., Sondek, J., and Harden, T.K. (2005) *Biochem. J.* 391, 667-676.